Fouling Study in Ultrafiltration:
Mechanism and Control via Membrane Surface Modification

(Untersuchung zum Fouling in der Ultrafiltration:
Mechanismen und Kontrolle durch Oberflächenmodifizierung von Membranen)

by
Heru Susanto

Thesis submitted to the Department of Chemistry of
Universität Duisburg-Essen, in partial fulfilment of
the requirements of the degree of
Dr. rer. nat.

Approved by the examining committee on July 17, 2007:

Chair : Prof. Dr. Thomas Schrader

Advisor : Prof. Dr. Mathias Ulbricht

Reviewer : Prof. Dr. Axel Schönbucher

Essen, 2007

ABSTRACT

Two important issues in application of ultrafiltration (UF) membrane, i.e. study of fouling mechanism and synthesis of low fouling membrane have been performed. Study on fouling mechanism was done by investigation of membrane–solute interactions (static adsorption) and membrane–solute–solute interactions (UF) using dextran and myoglobin as the model for polysaccharide and protein, respectively. Low fouling UF membranes have been synthesized by photograft copolymerization of water soluble monomers, poly(ethylene glycol) methacrylate (PEGMA) and N,N-dimethyl-N-(2-methacryloyloxyethyl-N-(3-sulfopropyl) ammonium betaine (SPE), onto polyethersulfone (PES) membrane with and without cross-linker monomer N,N'-methylene bisacrylamide (MBAA). Commercial polyethersulfone (PES) and cellulose–based UF membranes were used during fouling mechanism study whereas two commercial PES UF membranes with different nominal cut–off were used as the base membrane upon surface modification.

In both studies, the membranes were characterized with respect to the membrane chemistry (by IR–ATR spectroscopy and elemental analysis), surface wettability (by contact angle), surface charge (by zeta potential) and pure water permeability, pore structure and surface morphology (by hydraulic permeability and rejection measurements, scanning electron microscopy, and atomic force microscopy). In addition, in the fouling mechanism study, quantification of solute attached on the membrane surface was performed by simultaneously diffusion adsorption measurements (SDAM).

The results obtained from fouling mechanism study showed that significant changes in membrane characteristics and water permeability were observed for PES membranes after static adsorption using dextran. However, such changes were not observed for cellulose–based membrane. Good correlations were obtained between the water flux reduction (RFR) caused by dextran adsorption and the quantitative data for bound dextran on the PES membranes. Further, a pronounced effect of dextran size on adsorptive membrane fouling was identified. Contact angle and zeta potential measurements with non–porous films, where solute entrapment in pores can be ruled out, gave additional clear evidence for dextran binding on the PES surface. Complementary data for adsorption and fouling of PES membranes and non–porous films by the protein myoglobin indicate that the larger fouling tendency for protein than for dextran is due to a higher surface coverage

of PES by the adsorbed biomacromolecule layer. Data for UF confirmed the conclusions from the static contact experiments because significant fouling was observed for PES membranes (more severe for myoglobin than for dextrans), while no fouling was observed for a cellulose–based UF membrane with the same nominal cut–off. Finally, two mechanisms for the attractive PES–dextran interaction – multiple hydrogen bonding involving the SO_2 groups of PES and "surface dehydration" of the relatively hydrophobic PES – are discussed. Study on the synthesis of low fouling UF membrane suggests that PEGMA/SPE–modified membranes showed much higher fouling resistance evaluated by using protein, sugarcane juice, dextran and humic acid solutions than unmodified membranes having similar and larger nominal cut–off. However, contribution of membrane pore structure on membrane–solute interactions was still clearly observed. In some cases, the presence of cross-linker could improve both flux permeate and rejection during ultrafiltration. Modified membranes prepared using "period 2" for the first batch and PEGMA–modified membrane (PES-g-PEGMA) and PEGMA–modified with low concentration of cross-linker (PES-g-PEGMA/MBAA) for the second batch showed the best performance during evaluation. Furthermore, modified membranes prepared with an "old generation" non fouling material, PEGMA, showed better performances than modified membrane prepared with a "new generation" non fouling material, zwitterionic SPE. The surface chemistry as well as surface wettability of modified membranes did not change after incubating in sodium hypochlorite solution for a period of 8 days. Finally, their combined high fouling resistance and high rejection supported by chemical stability by cleaning suggest that those modified membranes were very attractive as new generation of thin layer composite low fouling UF membranes.

This thesis is dedicated with love to my wife (Titik) and my children (Qori and Ihdina) both for the support, love and tolerance provided over three years during my doctorate study.

PREFACE

All the praises and thanks be to Allah. This work would not have finished without help from him. This work was performed in the time from April 2004 up to March 2007 to fulfill the requirements of doctoral program (Dr. rer. net) at the Institute of Technical Chemistry (Lehrstuhl für Technische Chemie II), Department of Chemistry, Universität Duisburg-Essen under the supervision of Prof. Dr. Mathias Ulbricht. Basically, this work concerns on fouling study of ultrafiltration membranes and surface modification via photograft copolymerization for control of fouling.

This thesis is composed of six chapters. Chapter 1 focuses on the background and state of the research problem. Chapter 2 provides briefly the fundamental theories for ultrafiltration and surface modification. Further, recent developments in surface modification for control of fouling are also described. Material and method used during experimental works are written in Chapter 3. Chapter 4 presents the results obtained from this study. The results are classified into four main parts, i.e. (i) commercial membrane characterization, (ii) study on dextran fouling of UF membrane, (iii) membrane surface modification, and (iv) evaluation of modified membranes performance. Chapter 5 discusses the phenomena behind the obtained results and tries to correlate each other. Chapter 6 presents the conclusions of this work.

Upon finishing this work I would like to take the chance to thank many people who have supported and helped me to perform this project. First of all, I would like to express my hearty thank for the supervision and the support provided by my advisor Prof. Dr. Mathias Ulbricht. He has supervised me not only to think critically and to conduct a comprehensive research but also to trust with my own opinion. Moreover, he also paid attention to my private life where I lived in Germany with my family during the study. I would like to thank my reviewer Prof. Dr. Axel Schönbucher for his advice and support.

I would like to give special thanks to DAAD (Deutscher Akademischer Austauschdienst) for providing my doctoral scholarship. I am grateful to the all members of membrane research group at Lehrstuhl für Technische Chemie II, Universität Duisburg-Essen, i.e. Mehmet, Inge, Danuta, Halim, Abdus, Christian, Dongming, Melvy, Claudia, Frank, Alex, Jun, Uwe, Dimitrios, Rafael, Frau Steffens and Frau Nordmann for good discussion and environment. In particular I would thank Diete Jacobi for his contribution in GPC analysis, Tim Leimer for conducting the ATR–IR analysis, Dr. Stefen Franzka for

AFM observation, Smail Boukercha for SEM visualization and Veronika Hiltenkamp and Kerstin Brauner for the elemental analysis. I would also like to thank Sartorius (Germany), Alfa Laval (Nakskov, Denmark), and Microdyn-Nadir (Germany) for donation of the membranes. The donation of the SPE monomer by Raschig GmbH (Germany) is also very much acknowledged.

Finally, this thesis would not have been possible without contribution from my parents. Even though they stay far away (in Indonesia), they have supported and prayed for me to finish this work. Their pray and care were part of critical points of my work.

The main parts of this thesis have been published in the following publications:

H. Susanto, M. Ulbricht, Photo-grafted thin polymer hydrogel layers on PES ultrafiltration membranes: Characterization, stability and influence on separation performance, Langmuir 2007, 23, 7818.

H. Susanto, S. Franzka, M. Ulbricht, Dextran fouling of polyethersulfone ultrafiltration membranes–Causes, extent and consequences, J. Membr. Sci. 296 (2007) 147.

H. Susanto, M. Balakrishnan, M. Ulbricht, Via surface functionalization by photograft copolymerization to low-fouling polyethersulfone-based ultrafiltration membranes, J. Membr. Sci. 288 (2007) 157.

H. Susanto, M. Ulbricht, Influence of ultrafiltration membrane characteristics on adsorptive fouling with dextrans, J. Membr. Sci. 266 (2005) 132.

Other publications including submitted and conference papers during doctoral study are attached in Appendix-1.

CONTENTS

LIST OF TABLES

LIST OF FIGURES

Chapter 1
INTRODUCTION

1.2. Background

Nowadays, ultrafiltration (UF) is generally recognized as a promising separation tool in many technical processes. UF has replaced not only the conventional separation techniques but it has also successfully been utilized to solve mass separation problems. The applications of UF include fractionation or concentration step in the food, pharmaceutical and biotechnological industries, pure water production and water and wastewater treatments [1-6]. Along with those increasing demands, concentration polarization and fouling – causing significant loss of performance with respect to flux and often selectivity – are still two severe problems during its application. Concentration polarization can facilitate irreversible membrane fouling by altering interactions among solvent, solute and membrane. Eventually, these limitations not only prevent a more widespread commercial applicability of UF but also shorten the membrane life due to chemical cleaning.

Since fouling significantly worsens UF membrane performance, efforts to overcome this problem have drawn more and more attention in the UF research. Basically, those studies included identification/characterization of foulant, investigation of fouling mechanism and minimizing or control of fouling. In these regards, two important issues are observed, i.e. (i) basic knowledge of the fouling mechanism is important in order to improve the UF performance and (ii) synthesis of low fouling membrane is strongly needed. Even though process conditions have been remarkably engineered in order to achieve a better control of membrane fouling, in most cases, the permeate fluxes are clearly determined by membrane itself. Therefore, in this project, study of fouling mechanism and synthesis of low fouling membrane are performed.

Most of previous studies of mechanism of UF fouling (including characterization) had been concerned with proteins and humic substances (humic and vulvic acids) as potential foulants (e.g., [7-15]). Along with the increasing number and scale for applications of UF, studies of polysaccharide fouling of polymeric membranes have become an important issue from various points of view. Such investigations were concerned with extracellular polysaccharides (EPS) [16,17], wine polysaccharides [18] or sugarcane juice polysaccharides [19]. In all the previously mentioned examples, it is probable that the interactions between the polysaccharide and the polymeric membrane were driven by "sticky" charged or hydrophobic groups conjugated with the carbohydrate.

Considering dextran as a model polysaccharide in this study, it turned out that dextran does play a major role in real feed streams, for example in sugar beet or sugarcane processing [20,21] and in medical application [22]. More importantly, dextrans are extensively used for characterizing the rejection of UF membranes including the nominal cut-off [1,2]. Previously reported studies showed that there has been uncertainty regarding the extent of membrane–dextran interactions. Nobrega *et al.* [23,24] showed that dextran molecules did not foul the polysulfone UF membrane. Different results were reported by Gekas and co-workers [25]. They observed that the water flux decreased after UF of dextran for both polysulfone and cellulose triacetate membranes indicating fouling had occurred. This observation is supported by study of Reddy *et al*. [26]. Under some conditions, dextran can form a deposit on the upper surface of the membrane as had been reported by Mochizuki and Zydney [27]. Mulherkar and van Reis [28] implied that there were significant interactions between a neutral composite regenerated cellulose (CRC) membrane and a positively charged fluorescent-labelled dextran and between a modified positively charged CRC membrane and a neutral fluorescent-labelled dextran, with a reduced permeability and a changed retention of the membranes as consequences. Along

with execution of this Ph.D. project, more specific studies on dextran fouling in UF membrane were reported by Kweon and Lawler [29,30]. It was found that dextran clearly fouled the polysulfone UF membrane. However, the mechanism of fouling was not clearly understood. Furthermore, quantifications of the amounts of dextran attached to the membrane and of the factors affecting the fouling are also still missing. In this project, such conditions are studied with emphasis on membrane-solute interactions (adsorptive fouling). Studies were performed through investigation of membrane-solute and membrane-solute-solute interactions. Thus, the fundamental understanding of the fouling mechanism can be well developed.

In case of synthesis of low fouling membrane, cellulose−based membranes such as regenerated cellulose, are the state-of-the-art. However, the chemical stability and relatively low porosity (compared to polyethersulfone, PES) are the significant limitations of those membranes. Blending of the membrane polymer (e.g., PES) with a hydrophilic modifier might in some cases improve the fouling resistance [31,32]. However, membrane manufacturing from a polymer blend will yield a different pore structure (cut−off) and hence flux and selectivity, and the stability of the modification may be another problem. Therefore, surface modification of commercial membranes, while preserving their chemical resistance and mechanical strength, is of great interest in producing low fouling UF membrane (e.g., [33-40]). Overall, two approaches for low fouling surface modification have been essentially proposed, i.e. increasing membrane surface charge to promote electrostatic repulsion and hydrophilization to increase water−surface interaction [33]. As most promising strategies, polyethylene glycol and zwitterionic moieties have been proposed as the basis for non fouling polymeric materials.

In general, surface modification by grafting the functional polymer has proven as the promising technique to create low fouling membrane or at least drastically depress the

fouling tendency of the base membrane. Nevertheless, to be practically useful, the resulting membrane performance must further be improved with respect to hydraulic permeability after modification as well as solute rejection in relation to the fouling resistance, and stability in the chemical cleaning solutions. In this project, efforts to increase the modified membrane performance are presented. Evidences showed that the permeability of the modified membranes decreased after modification. Moreover, the performance of modified membranes for long-term applications largely depends on the stability of the grafted polymer layer in the chemical cleaning solutions. Even though efforts to reduce the chemical cleaning have been intensively proposed, chemical cleaning is still required [41]. Therefore, such stability is an important parameter to be evaluated. To the best of my knowledge, attention to the chemical stability of the grafted polymer layer on the membrane is still very rare.

1.2. State of the Problem

In the development and application of UF membranes, understanding of the fouling mechanism and synthesis of low fouling membrane are important and attractive issues. Less attention has been devoted to the polysaccharides (compared to protein and humic substances) as a foulant during UF fouling study. Therefore, in this project, fouling mechanism study is performed using dextran as model for polysaccharides.

To be practically useful, current proposed work to synthesis low fouling membrane via surface modification must further be improved with respect to the membrane permeability as well as rejection in relation to the fouling resistance and stability. In this effort, surface modification was performed by UV−assisted graft copolymerization of two hydrogel monomers, poly(ethylene glycol) methacrylate (PEGMA) and N,N-dimethyl-N-(2-methacryloyloxyethyl-N-(3-sulfopropyl) ammonium betaine (SPE), onto PES UF

membrane. The effects of addition of cross-linker on modification and the stability study of grafted polymer layer in the chemical cleaning solution were also investigated.

1.3. Objective of the Research

In general, the objectives of this research project are (i) study on mechanism of polysaccharide fouling in UF membrane and (ii) synthesis of low fouling PES–based UF membrane via surface modification by UV–assisted graft copolymerization. More specific, the research objectives include:

(i) characterization of commercial membranes used in this study.

(ii) characterization and mechanism studies of dextran fouling of UF membranes by membrane–solute and membrane–solute–solute interactions.

(iii) study on the effects of process parameters, i.e. UV irradiation time, monomer concentration and monomer type on the flux and selectivity of modified membrane.

(iv) study on the effect of cross-linker on the flux and selectivity of modified membrane.

(v) evaluation of the stability of grafted polymer layer in the chemical cleaning solution.

(vi) anti–fouling and ultrafiltration performance test of modified membranes for potential practical applications.

1.4. Scope of the Research

The study on mechanism of polysaccharides fouling was performed by using neutral dextran as model for polysaccharides. Commercial PES and cellulose–based UF membranes were used. The membrane nominal cut-offs (also called nominal molecular

weight cut−off, NMWCO) were 10, 30 and 100 kg/mol. The structure and property of the membranes used were firstly investigated in detail. Study on fouling mechanism was carried out by investigation of membrane−solute and membrane−solute−solute interactions. The effects of dextran concentration, adsorption time and dextran molar mass on adsorptive fouling were then investigated. In addition, the effects of dextran (adsorptive) fouling on apparent pore size, contact angle, surface charge, surface chemistry and surface morphology were studied. The amount of dextran bound onto the membrane was quantified by using simultaneous diffusion−adsorption measurements (SDAM) experiment (cf. Section 3.3.2, Chapter 3). Further, myoglobin was used for comparison study in order to understand the extent and consequences of dextran fouling. Additional experiments with non−porous PES films where solute entrapment in the pores could be ruled out were conducted in order to explain the mechanism of interactions. Finally, possible mechanisms of membrane−dextran interaction were discussed.

Two different commercial PES UF membranes with nominal cut−off 50 (PES-050H) and 100 (PES-SG100) kg/mol were used as the base membrane during surface modification experiments. The modifications were firstly done by using PES-050H (called first batch modification). Modification using PES-SG100 (called second batch modification) was then conducted to improve the performance of modified membrane resulting from the first batch. The modification has been done by photograft copolymerization of water soluble monomers, PEGMA and SPE, onto the base membranes with and without cross-linker. Hydrophilic cross-linker, N,N'-methylenbisacrylamide (MBAA), was used. The effects of monomer concentration, UV-irradiation time and cross-linker concentration on the grafting efficiency and membrane characteristics (membrane chemistry, membrane wettability, surface charge, surface morphology, hydraulic

permeability and apparent pore size) and flux and selectivity were investigated in detail. Stability of grafted polymer layer was evaluated by incubating in sodium hypochlorite solution. The anti-fouling and ultrafiltration performances were then evaluated by using protein, sugarcane juice polysaccharides, humic acid and dextran solutions.

All preceding studies were supported by a comprehensive characterization with respect to the membrane chemistry (by IR-ATR spectroscopy and elemental analysis), surface wettability (by contact angle), surface charge (by zeta potential) and pure water permeability, pore structure and surface morphology (by hydraulic permeability and rejection measurements, scanning electron microscopy and atomic force microscopy).

Chapter 2
THEORY

2.1. Ultrafiltration

Ultrafiltration (UF) is a pressure–driven membrane–based separation process in which particles and dissolved macromolecules smaller than 0.1 μm and larger than about 2 nm are rejected [42]. The membranes usually have a pore size ranging from 1 nm to 0.1 μm. Nevertheless, many definitions and even pore size criteria are found in different literature. As an example, Cheryan [1] gave the size of component retained by UF larger than about 1 nm to 0.02 μm. UF is normally used for purifying, concentrating and fractionating macromolecules or fine particle suspensions. The nature of UF lies between nanofiltration (NF) and microfiltration (MF). However, the membrane structure for UF is more asymmetric than for MF with the top layer (skin layer) that has smaller pore size as well as porosity than supporting layer. The pressure used in UF is up to 1 MPa. It should be noted that UF membrane is normally characterized in term of molar mass (molecular weight) cut–off (limit) instead of particle size (pore size in microns). Nominal cut–off is usually defined as the molar mass of a test molecule that would be retained to > 90% by the membrane.

As UF is now well established technique for macromolecular separation, it is supported by large scale production of membrane materials with type–specific cut–off in the range of about 5 to 200 kg/mol. Among several polymer materials, polysulfone (PS), polyethersulfone (PES), polyacrylonitrile (PAN) and cellulose–based polymers (mostly from cellulose acetate) are usually used for UF membranes. Cellulose–based membranes such as regenerated cellulose are the state-of-the-art for low fouling UF membranes. However, the chemical

stability, temperature stability and relatively low porosity (e.g., compared to PES) are the significant limitations of those membranes. Thus, due to their mechanical strength, thermal and chemical stability as well as excellence film forming properties, PS and PES are frequently used as materials for high performance UF or MF membranes [43]. Nevertheless, the hydrophobicity of those materials can cause more severe fouling problem (cf. Section 2.3). In addition to the organic polymers, inorganic materials such as ceramic are nowadays also used as UF membrane material.

2.2. Mass Transport in Ultrafiltration Membrane

Due to the complexity of the mass transfer phenomena during UF process, many phenomenological approaches and mathematical models were proposed. Basically, the mass transport was visualized as a sieve filtration. The reason for this approach is due to relatively large pore size of UF compared to the solution diffusion based membrane processes. One of the classifications for mass transfer in UF is [44-46]: (i) model based on a phenomenological description of transport trough finely porous structure without taking into account any boundary effects, (ii) model based on irreversible thermodynamics and also neglecting boundary effect, and (iii) model using a phenomenological approach where concentration polarization as boundary effect is involved. In fact, to the best of our knowledge, none of them is adequate to explain mass transfer phenomena for all UF cases and conditions. Thus, combining two models or even more has often been done to minimize the deviation from experimental data.

2.2.1. Models based on transport through finely porous material

Transport of solute and solvent through the porous material can be determined by hydrodynamic model, which is evaluated by directly solving the equations of motion for a well–defined solute (typically assumed to be spherical) in a well–defined (typically cylindrical) pore [2]. The transport of pure solvent (flux), J_v, is described by Darcy's law where the solvent flux is proportional to the applied pressure.

$$J_v = K\frac{\Delta P}{\mu \delta_m} \tag{2.1}$$

where J_v is volumetric filtrate flux (solvent) through the membrane, $K/(\mu\delta_m)$ is the hydraulic permeability of the membrane, and equal to L_p in the Kedem-Katchalski equation [2], ΔP is transmembrane pressure, μ is viscosity and δ_m is the membrane thickness.

In simplistic models, it is assumed that membranes are composed of a parallel array of uniform nonintersecting cylindrical pores. In such case, it is generally believed that the best description of fluid flow (solvent) through the membrane is given by Hagen-Poiseuille's law:

$$J_v = \frac{\varepsilon r_p^2 \Delta P}{8\mu\delta_m} \tag{2.2}$$

where r_p is the (mean) pore radius, ε is the surface porosity of the membrane. It should be noted that Darcy's and Hagen Poiseuille laws are only valid for describing the pure solvent flux in an ideal condition, e.g., in the absence of osmotic pressure or concentration polarization caused by solutes, where no fouling occurs and for a membrane with uniformly distributed and evenly shaped and sized pores in the membrane. In fact, most membranes have irregular pore structure (size and shape), pores interconnectivity, pore tortuosity, etc.

Solute separation in UF occurs either because the size is larger than membrane pore size or because the interaction between solute and membrane/pores. In fact, in many cases, UF membranes work not only on the basis of sieving mechanism but also on the basis of membrane–solute interactions. Factors such as the shape, deformation and dissociation of the macromolecules should also be considered in solute retention study. Ferry–Faxén equation describes the effect of steric hindrance and frictional resistance on the transport of solute [46]:

$$\frac{A_i}{A_p} = \left[2\left(1-\frac{a_i}{d_p}\right)^2 - \left(1-\frac{a_i}{d_p}\right)^4 \right]\left[1-2.104\frac{a_i}{d_p} + 2.09\left(\frac{a_i}{d_p}\right)^3 - 0.95\left(\frac{a_i}{d_p}\right)^5 \right] \qquad (2.3)$$

where A_i is the effective pore area for transport of solute and A_p is the total pore area, a_i is the diameter of component i and dp is the pore diameter. This equation describes the total restriction to UF due to steric effect (first bracket derived by Ferry) and frictional interaction with pore walls (second bracket, derived by Faxen). As the retention is determined relative to water, the maximum retention can be calculated using Eq. (2.4).

$$R_{max} = 1-\frac{A_i}{A_w} = 1-\frac{A_i/A_p}{A_w/A_p} \qquad (2.4)$$

where A_w is the effective pore area for transport of water.

2.2.2. Models based on irreversible thermodynamics

In irreversible thermodynamics models, membrane is considered as a black box. As a consequence, there is no information obtained or required about the structure of the membrane. The models view permeation through the membrane as a result from the force–flux relations comprising different transport systems. Kedem–Katchalsky and Spiegler–Kedem models are well known as mass transport models based on this approach.

Kedem-Katchalsky described the transport of solvent (mostly water) and solute in isothermal membrane systems as follow [47]:

$$J_v = L_p (\Delta P - \sigma \Delta \pi) \tag{2.5}$$

$$J_s = \omega \Delta \pi + (1 - \sigma) J_v C \tag{2.6}$$

where J_v and J_s are volumetric flux for solvent and solute, respectively, L_p is the membrane hydraulic permeability, ω is the solute permeability, σ is reflection coefficient, which indicates the solute rejection property of the membrane ($\sigma = 0$ means there is no rejection, $\sigma = 1$ means rejection is 100%), C is the logarithmic average of C_m (concentration at the membrane surface) and C_p (concentration of permeate), and $\Delta\pi$ is osmotic difference between permeate and membrane surface. Thus, L_p, ω and σ are the figures–of–merit for the membrane. This model assumes that the system is close to the equilibrium. For large volume flow and high concentration gradient the influence of J_v on J_s will not be adequately represented by the last term in Eq. (2.6). Therefore, for UF membranes, this condition may not be well satisfied. Thus, the non linear model (Eqs. (2.7), (2.8) and (2.9)) proposed by Spiegler-Kedem [47] is more adequate to describe such condition.

$$J_v = -\wp_I \left(\frac{dp}{dx} - \sigma \frac{d\pi}{dx} \right) \tag{2.7}$$

$$J_s = -\psi \frac{dc_s}{dx} + (1 - \sigma) c_s J_v \tag{2.8}$$

$$\frac{1}{R} = \frac{\exp[J_v (1 - \sigma)/\omega] - \sigma}{\sigma \{\exp[J_v (1 - \sigma)/\omega] - 1\}} \tag{2.9}$$

where $\wp$ is the specific hydraulic permeability or intrinsic membrane permeability, ψ is the local solute permeability coefficient, R is the solute rejection. In this context, p (pressure), c

(solute concentration in bulk) and π (osmotic pressure) refer to the average parameter measured in the solutions on both sides of a differential membrane–element and not to the membrane phase itself.

2.2.3. Models based on boundary layer which incorporate bulk mass transport

In this section, most of the discussions are taken from Zeman and Zydney's book [2] due to the comprehensive structure and analysis. One of the important factors, which had not been considered in the previous models determining the overall mass transport during UF is the rate of solute or particle transport in the bulk solution adjacent to the membrane. Other factor is the transport of permeate through the membrane itself. Figure 2.1 shows schematically the convective and diffusive solute transports of pressure–driven membrane processes.

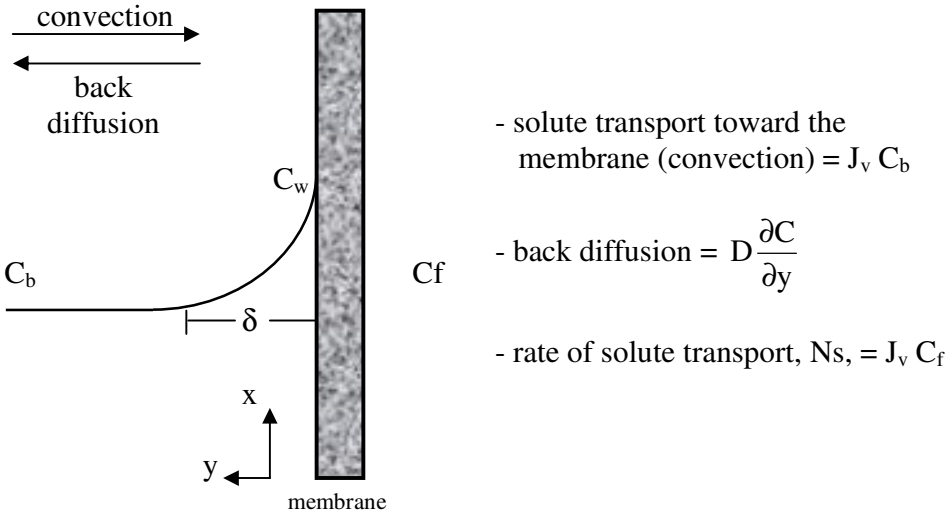

Figure 2.1. Schematic representation of mass transport within concentration polarization boundary layer of thickness δ_{bl}.

Concentration polarization (CP) is accumulation of retained solutes at the upstream surface of the membrane generating a concentration gradient across the boundary layer thickness, δ_{bl}, near the membrane surface (ranging from C_b to C_w). The CP can affect the filtrate flux in three distinct ways [2]. First, the accumulation can generate an osmotically driven fluid flow back across the membrane, thereby reducing the net rate of solvent transport by reducing the net transmembrane pressure. In addition, the reduction of flux due to CP is caused by a back transport of the solute into the bulk side because of diffusion. Second, the accumulated solutes can provide an additional hydraulic resistance to the solvent flow in series with that provided by membrane. Third, the accumulation of solutes can also irreversibly foul the membrane, thereby altering its hydraulic permeability as well as its sieving characteristics.

Other impact of CP can be observed by plotting the filtrate flux versus transmembrane pressure, i.e. a pressure–independent limiting flux is obtained. Howell and Velicangil [48] reported that the steady state conditions are rapidly attained and CP is formed in no more than 5 seconds. However, CP layer is assumed to be dynamic (unlike fouling). Changing the operating conditions, such as lowering pressure or feed concentration, or increasing the feed velocity, should revert the system back to the pressure controlled regime [1].

In order to evaluate the solute concentration profiles, it is necessary to solve the following governing equations describing solute mass transfer in the feed (bulk) solution:

$$J_v = L_p(\Delta P - \sigma\Delta\pi) \tag{2.10}$$

$$N_s = J_v C_f = J_v C_w S_a \tag{2.11}$$

where N_s is solute flux, C_f and C_w are the solute concentration at the permeate and at membrane surface, respectively, S_a is actual membrane sieving coefficient. A number of

different approaches had been proposed to obtain solutions to these governing equations, Eqs. (2.10) and (2.11).

Generally speaking, models based on the boundary layer involve film–theory model, osmotic pressure model and gel polarization model, which will be explained in more detail below.

Film–theory (mass transfer) model. At steady state condition, the rate of solute transport toward the membrane due to the pressure–driven flow is balanced by the rate of solute transport through the membrane plus the diffusive solute flux back into bulk solution (cf. Figure 2.1). The rate of solute diffusion in the *x* direction has been assumed to be negligible relative to the rate of solute convection. Equation (2.12) describes the classical equation for stagnant film model.

$$VC - D\frac{\partial C}{\partial y} = -N_s \tag{2.12}$$

$$\text{with } V = -J_v \; ; \; Ns = J_v \, C_f \tag{2.13}$$

It should be noted that the negative sign on the right–hand side of Eqs. (2.12) and (2.13) reflects the fact that the transmembrane velocity V is in the negative *y* direction, but the filtrate flux, J_v, and solute flux, N_s, are traditionally taken as having positive values (cf. Figure 2.1). Integration of Eq. (2.12) from 0 to y and from C_w to C yields the following equation:

$$\frac{C - C_f}{C_w - C_f} = \exp\left(-\frac{J_v y}{D}\right) \tag{2.14}$$

Eq. (2.14) is only valid within the concentration boundary layer. Thus, application of boundary conditions (at y = 0, C = C_w and at y = δ_{bl}, C = C_b) yields the following expression

for the filtrate flux in terms of the solute concentration, the solute diffusivity and the concentration boundary layer thickness:

$$J_v = \frac{D}{\delta_{bl}} \ln\left(\frac{C_w - C_f}{C_b - C_f}\right) \tag{2.15}$$

In this context, if the mass transfer coefficient is defined as the ratio of the diffusion coefficient to the thickness of boundary layer, $k = D/\delta$, Eq. (2.15) can thus be written in terms of the solute mass transfer coefficient (Eq. (2.16)).

$$J_v = k \ln\left(\frac{C_w - C_f}{C_b - C_f}\right) \tag{2.16}$$

Eq (2.16) is the classical stagnant film resulting for the filtrate flux in terms of solute mass transfer coefficient driving force. The mass transfer coefficient is basically obtained from Sherwood's equation.

Osmotic pressure model. In the film theory model, the osmotic pressure is not included to determine the filtrate flux. This approach is based on the fact that the osmotic pressure of macromolecular solutions seems to be very small as compared to the applied pressure. However, at high concentration, the osmotic pressure increases sharply as reported by Vilker *et al*. [49] and Jonsson [50]. Therefore, the osmotic pressure should be included for determining the mass transport. Some critics have been addressed to the stagnant film model with respect to the actual mechanism by which the accumulated solute limited the filtrate flux (e.g., [51,52]). Osmotic pressure model assumes that the filtrate flux is determined entirely by the difference between the applied transmembrane pressure and the osmotic pressure difference associated with the retained solutes. Membrane fouling and hydraulic resistance

provided by any particles or cakes or gels layers are assumed to be negligible. The filtrate flux in the osmotic model is thus evaluated by simultaneous solution of Eqs. (2.17) and (2.18).

$$J_v = L_p (\Delta P - \sigma \Delta \pi) \tag{2.17}$$

$$J_v = k \ln\left(\frac{C_w - C_f}{C_b - C_f}\right) \tag{2.18}$$

where $\Delta\pi = \pi (C_w) - \pi (C_f)$. The osmotic pressure ($\pi$) itself is evaluated by virial equation (Eq. (2.19)). The membrane properties L_p (hydraulic membrane permeability) and σ (retention) are assumed to be known and filtrate concentration is evaluated in term of C_w using actual sieving coefficient, that is, $C_f = S_a C_w$, where S_a is a known function of J_v given by Eq. (2.11).

$$\pi = A_1 C_s + A_2 C_s^2 + A_3 C_s^3 \tag{2.19}$$

where A_1, A_2 and A_3, are the osmotic – A_1 is the van't Hoff equation coefficient, which is applicable for very dilute concentration. A_2 and A_3 represent the non–ideality of the solution.

At low transmembrane pressure and low feed concentration, the osmotic pressure has small value and consequently does not influence the filtrate flux. However, as the transmembrane pressure is increased, the solute concentration on the membrane surface increases, causing an increase in osmotic pressure and a corresponding decrease in the filtrate flux. Such phenomena were well described by Opong and Zydney [53]. It is important to note that the filtrate flux predicted by the osmotic pressure model never actually attains a true pressure–independent plateau unless the boundary layer undergoes a phase transition causing osmotic pressure to increase without bound. Bhattacharjee *et al*. [54] also reported the effect of osmotic pressure including solute–solute interactions on the permeate flux decline.

Gel polarization model. The key assumption in the gel polarization model is that at high transmembrane pressure, ΔP, the solute concentration on the membrane surface, C_w, attains a

constant (maximum) value determined by the physical characteristics of the particular macromolecules. It is assumed that this maximum concentration reflects the point of gelation, precipitation, and/or aggregation of the macrosolute at the membrane surface. The gel layer formed at the membrane surface yields an additional hydraulic resistance to the filtrate flow. In this model, the filtrate flux is described by the following equation:

$$J_v = \left(\frac{\Delta P}{R_m + R_c} \right) \tag{2.20}$$

where $R_m = 1/L_p$ is the hydraulic resistance provided by the membrane and R_c is the resistance of the gel (or cake) layer. Initially, the filtrate flux increases with increasing the transmembrane pressure, then at very high ΔP, the gel layer resistance is assumed to become proportional to ΔP. Under these conditions, the filtrate flux attains a maximum pressure–independent value. If the permeate concentration, $C_f = 0$ meaning that all solute is retained by the membrane, the pressure independent flux is given by Eq. (2.21).

$$J_v = k \ln\left(\frac{C_g}{C_b} \right) \tag{2.21}$$

where C_g is the "gel" concentration. Further increase in the applied pressure causes a corresponding increase in the hydraulic resistance provided by the gel layer. It is also possible an increase in the hydraulic resistance of the macrosolutes in the liquid boundary layer or in the osmotic pressure of the retained solutes. The net result is that the filtrate flux remains independent of ΔP. Plotting of J_v as function of log (C_b) is often used to estimate both gel concentration (from the intercept) and the mass transfer coefficient (from the slope) for particular module.

One of the primary disadvantages of the gel polarization model is that it can only be used to evaluate the pressure−independent filtrate flux. In addition, the gel concentration appears to depend on the specific device and membrane under consideration, making it difficult to obtain quantitative a priori prediction of $C_{g.}$

2.3. Ultrafiltration Fouling

Flux decline over time and often changing in selectivity due CP and fouling are generally observed during UF operation. Fouling is defined as a process resulting in loss of performance of a membrane due to the deposition of suspended or dissolved substances on external surfaces, at the pore openings or within its pores [42], whereas CP is the buildup of the solute concentration at the membrane surface due to selectivity of the membrane. Even though CP is reversible process (cf. Section 2.2 in more detail for CP) it can facilitates irreversible membrane fouling by altering interactions among solvent, solute and membrane.

2.3.1. Mechanism and characteristic of fouling

Essentially, membrane surface chemistry, membrane−solute interactions and solute−solute interactions are the key to understanding the fouling phenomena. Membrane−solute interactions will determine fouling through adsorption of solute on the membrane surface (in certain cases also in the membrane pores). This interaction had been proposed as the important parameter in a fouling study by Mathiasson [7] using bovine serum albumin as a model solute. Furthermore, this interaction will enhance or modify the particle deposition and the pore blocking processes. The solute−solute interactions will facilitate fouling by solute aggregation in solution and/or on the surface preadsorbed with solutes [55].

It is interesting to note that due to slow kinetics, certain colloids may not form fouling during a period of laboratory study but may form fouling during plant operation.

The ways in which solute or particle fouls the membrane depend on the solute or particle property, membrane property and hydrodynamic condition used during operation. Bacchin *et al*. [56] classified the solute or particle fouling in the following forms:

(i) Adsorption: occurs when attractive interactions between the membrane and the solutes or particles exist. A monolayer of particles and solutes can grow even in the absence of permeation flux leading to an additional hydraulic resistance. If the degree of adsorption is concentration dependent then concentration polarization exacerbates the amount of adsorption.

(ii) Pore blockage: when filtering, pore blockage can occur leading to a reduction of flux due to the closure (or partial closure) of pores.

(iii) Deposit: a deposit of the particle can grow layer by layer at the membrane surface leading to an additional hydraulic resistance. This is often referred to as a cake resistance.

(iv) Gel: the level of concentration polarization may lead to gel formation for certain macromolecules.

The effects of such fouling types on the membrane pore sizes distribution as well as membrane flux are schematically described in Figure 2.2 [57]. With this regard, many models have been proposed to describe the fouling phenomena (e.g., [58,59]).

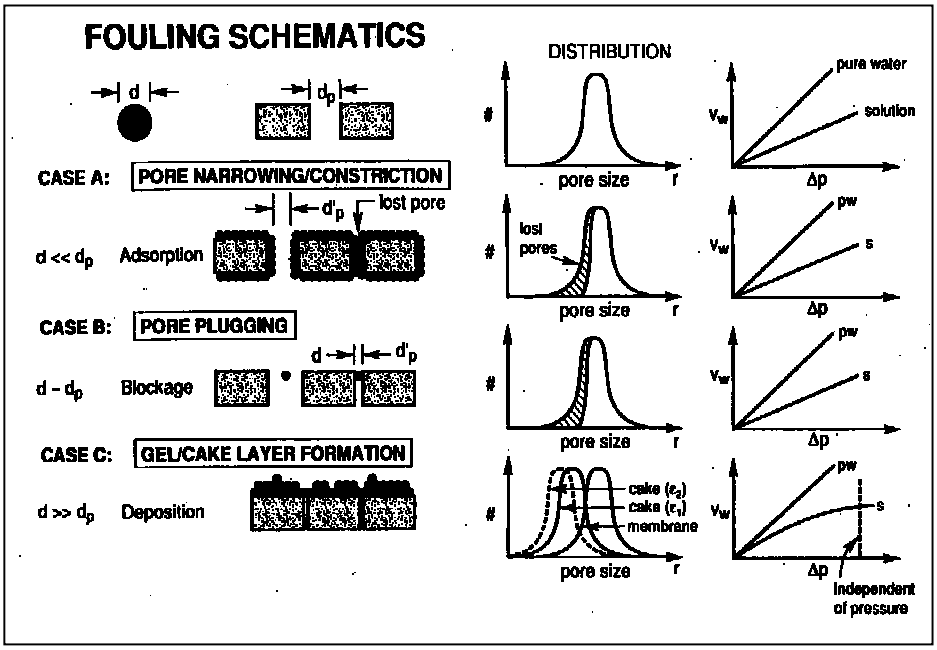

Figure 2.2. Schematics of fouling with typical pore size distribution as well as membrane flux: pore narrowing/constriction (case A), pore plugging (case B) and solute deposition and gel and cake formation [57].

Other analyses of the effects of different fouling scenarios on membrane filtration process are given by many other authors. UF of bovine serum albumin (BSA) at various feed pH through different molecular weight cut–off membranes indicated that initial fouling is controlled by protein–membrane interactions while protein-protein interactions dominate in the later stages [9,10]. It was also explained that pore blocking will increase the membrane resistance while cake formation creates an additional layer of resistance to the membrane to the permeation flow [60]. Pore narrowing can increase both the membrane resistance and the cake formation. Therefore, pore blocking and cake formation are the essential mechanisms in membrane fouling. Other factors, such as solute adsorption, particle deposition within the membrane pores and characteristic change in the cake layer can affect membrane fouling by

enhancing or modification of pore blocking and cake formation. Marshall *et al*. [61] reported that fouling in UF occurred mainly by surface pore blocking and cake formation. Further, the rapid initial drop of the flux is attributed to the quick blocking of the membrane pores. The degree of pore blockage depends on the shape and the size of the pores and particles.

Fouling can also be classified with respect to the flux decline over filtration time. De *et al*. [62] categorized the flux decline in UF into short and long terms. The short term decline is an osmotic pressure limited and the long term decline is controlled by growth of polarized layer. Different classification was given by Song [60]. The profile of flux decline over time can be classified into three regions as shown in Figure 2.3: (i) started by a rapid initial drop from the flux of pure water filtration, (ii) followed by a long term gradual flux decrease, and (iii) ended with a steady state flux.

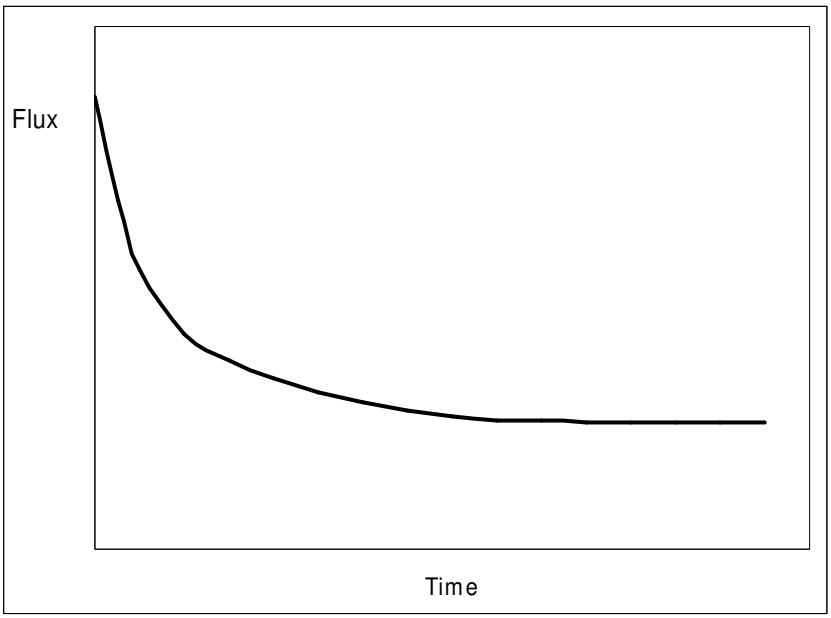

Figure 2.3. Profile of the time-dependent flux.

The "standard" classical fouling model proposed by Hermia is normally used to analyze the flux over time data in order to determine the fouling mechanism [63],

$$\frac{d^2t}{dV^2} = k\left(\frac{dt}{dV}\right)^n \tag{2.22}$$

where t is the filtration time, V is total filtered volume, k is a fouling coefficient and n is a dimensionless filtration constant reflecting the mode of fouling. Basically, that model describes three possible fouling mechanisms, i.e. pore blocking, pore constriction and cake formation (cf. Figure 2.2). Cake formation corresponds to the value of n = 0, whereas complete pore blocking correspond to n = 2. Pore constriction (standard blocking) is represented by the value of n = 3/2 (cf. Ref. [63,64] in more detail). The filtrate flux over time data is plotted as d^2t/dV^2 versus dt/dV as described by Eq. (2.22). The required derivatives are evaluated in terms of the filtrate flux [59,65]:

$$\frac{dt}{dV} = \frac{1}{JA} \tag{2.23}$$

$$\frac{d^2t}{dV^2} = -\frac{1}{J^3A^2}\frac{dJ}{dt} \tag{2.24}$$

with dJ/dt was evaluated by differentiating the adjusting polynomials that gave the best fitting for experimental data.

With respect to the characterization method, several innovative experimental techniques such as X-ray diffraction [66], infra red internal reflection spectroscopy [67,68] contact angle [69,70], atomic force microscopy [71] and small angle neutron scattering [72] have been explored for membrane fouling characterization. A recent review of characterization methods for membrane fouling with protein can be found in reference [73].

2.3.2. Factors affecting fouling

It is known that fouling is a complex process as a result from the interactions between the membrane (including pores) and solute(s) in the feed and perhaps between the adsorbed solute and other solutes in the feed stream. Basically, fouling is influenced by three factors namely the membrane properties, solute (solution) properties, and operating parameters [1]. Those factors can interact with each other and give rise to quite different effects in combination than if these factors were studied individually or with model systems.

Membrane properties. The membrane properties affecting the fouling include hydrophilicity, surface topography, charge on the membrane surface, and pore structure [1]. It is generally known that membranes made of hydrophilic material show less fouling than those made of hydrophobic material. Membrane that has smooth and uniform surface tends to foul less than membrane with high surface roughness. However, contradictory result was also reported in another publication. Bowen *et al*. [71] reported that membrane with higher surface roughness gave a lower area of contact between the probe and the membrane surface and hence a lower adhesive force. Correlated with fouling, surface charge of the membrane is also important character especially for processing charged particles/macromolecules. It is important to note that most membranes and colloids have a negative charge under usual aqueous conditions. In this case, electrostatic attraction should be minimized in order to reduce the fouling. The ratio between pore size and solute size is very important. Marshall *et al*. [61] reported that membranes with larger pores will initially have higher flux than tighter membranes but will eventually have lower flux. It should be kept in mind that (complete) pore blocking reduces the flux more pronounce than pore narrowing [16,74]. However, if the pores are much smaller than particles to be separated, the particles will not get caught within the

pores but will roll off the surface under the shear forces generated by flow. Thus, although it may seem logical to use membranes with pore sizes that are the same or slightly smaller than the particle size, the short−term advantage of higher initial flux will be outweighed by the long−term problems associated with higher fouling rate. A better rule of thumb is particle size to pore size of 10, i.e. select a membrane with pores that are one−tenth the particle size (on average), at least as a starting point for testing [1]. The pore structure and morphology such as porosity and pore connectivity also influenced the fouling behavior [75].

Solute (solution) properties. The solute (solution) properties affecting the fouling include functional group content, solute charge (density), hydrophobicity, and the physical structure. As consequences of these solute properties, the following solution properties: salt (ionic strength), pH and cation content also influence the extent and the behavior of fouling. Minerals salts can precipitate on the membrane surface because of poor solubility or bind to the membrane directly by charge interactions [1]. In addition, salts can increase the ionic strength, which in turn affects solute−solute and solute−membrane interactions. As examples, Babu and Gaikar [76] reported that the protein layer resistance increased with an increase in salt concentration. Increasing salt concentration reduced electrostatic repulsion between like-charged materials (increasing adsorption tendency) and decreased electrostatic attraction between oppositely charged materials (decreasing adsorption tendency) [77]. The adhesion energy between ionic EPS and polymeric membranes was critically determined by the ionic strength of the aqueous solution [17]. Many researchers studied the effect of pH on the membrane fouling (e.g., [10,55,78]). In general, pH influences the fouling by weak electrolyte colloids through the charge (electrostatic) interaction. It is well known that the lowest flux is obtained at the isoelectric point (IEP) of the colloid due to hydrophobic interaction and then,

flux become higher as the pH is moved away from the IEP. In addition, the change in pH affects solubility and conformation of feed component. An example, the solubility of protein is generally lowest at the IEP.

Operating parameters. In addition to the membrane and solute (solution) properties, fouling is strongly influenced by process parameters including temperature, flow rate (stirring rate), pressure and feed concentration as well as overall equipment design. Increasing temperature can either decrease or increase the fouling of UF. This will depend on the effects of temperature on the solubility of feed components, viscosity, diffusivity or denaturation of solute. As an example, Babu and Gaikar [76] showed that the increase in temperature decreased the fouling during UF of BSA using cellulose triacetate and regenerated cellulose. Generally, at the high flow rate or stirring rate the accumulated solutes (particles) on the membrane surface tend to be swept from the membrane surface and thus the fouling layer is reduced. However, higher fouling at higher flow rate was also observed by other researchers [79,80]. The flux during UF will increase as transmembrane pressure is increased. However, after CP reaches maximal point where gel layer has been formed then the flux does not increase any more (cf. Section 2.2.3). In some cases, further increase in transmembrane pressure yields even decreasing in flux [2].

2.3.3. Fouling control in ultrafiltration

To our knowledge, there is no method of fouling control that can be successfully used in all applications. The most effective method to minimize and control the fouling will depend on the nature of the fouling process. Many attempts have been devoted to control and counteract

the fouling. In general, control of fouling during UF could be done by three different ways namely hydrodynamic, physical and chemical methods.

Most of the developed methods to reduce and control the fouling are hydrodynamic ways. Basically, hydrodynamic methods are performed by manipulating pressure and/or cross flow velocity during operation. In addition, development of module design focused on improving the mass transfer at the membrane surface and the back−migration of retained species away from the membrane−solution−interface. This method includes enhancing the turbulence of feed flow, uniform transmembrane pressure (co−current permeate flow), backflushing (-pulsing, -shocking, -washing, -pressure), intermittent jets and pulsatile flow [1]. Based on the back−migration process, Drew and coworkers [81] developed strategies to minimize particle capture through inertial lift. Unsteady fluid instabilities resulting from the surfaces roughness, pulsation of the feed stream and centrifugal instabilities could increase significantly the permeation rate [82]. Model based on the concept of particle adhesion for calculating the accumulation of retained particle on the membrane surface and predicting the time−dependent flux had also been developed [83]. Further, low fouling or high flux could be achieved by operating at high feed velocity and low transmembrane pressure [84] and by allowing work in a turbulent regime and at high temperature [85].

Physical methods for fouling control include the addition of particles and the use of electric fields. The aims of the addition of particles are to attract dissolved macromolecules and to drag them away from the membrane whereas the use of electric field is to move charged molecules away from the membrane surface depending on the electrical field strength applied, thus reducing the extent of concentration polarization and increasing flux [86]. Pulse electric fields, where the field is switched on and off at regular intervals has also been

proposed. This method gave a greater benefit on flux with less of the problems of continuously applied electric field [87]. The use of electrical based method in the control of fouling is well reviewed by Bowen [88].

Fouling can be chemically controlled via modification of the membrane surface chemistry directed to reduce the attractive forces or increase the repulsive forces between solute and membrane. Steuck [89] modified membranes by heterogeneous chemical method to reduce the fouling process. He coated a cross-linked polymer (hydroxyalkyl acrylate) on porous PVDF membrane. Surface modification of polymers via irradiation methods and low temperature plasma has also been proposed [90,91]. Further, adsorption of hydrophilic polymers was used as pretreatment process to reduce fouling (e.g., [92]). Detailed discussion on membrane modification will be described in the Section 2.3.4. In addition to the membrane surface modification, fouling can also be chemically controlled via adjusting the feed solution chemistry, mainly pH and ionic strength (note that in most cases, the property of proteins, fatty acids and natural organic matters foulants are strongly influenced by pH and ionic strength).

Overall, previously literature showed that membrane fouling during UF of aqueous system can be controlled by process optimization, physical method and chemical method (cf. [93] for recent review of methods employed for control of fouling). However, in most cases, the permeate flux is clearly determined by the membrane itself. Therefore, control of fouling via surface modification seems to be promising technique.

2.3.4. Control of fouling through membrane modification

Control of fouling through membrane (post) modification is basically directed to prevent undesired adsorption or adhesion processes on the surface of membrane, because this

will prevent or at least slow down the subsequent accumulation of colloids, e.g., denaturation and aggregation of protein [33]. This modification can be an efficient approach towards UF fouling–resistant membranes. However, both rational strategies and careful selections of mild conditions in order to preserve the membrane's pore structure (cut–off) are strongly required. Experimental evidences showed that the permeability of the modified membranes often decreased after modification.

In several applications, the charged membranes could dramatically reduce the fouling (e.g., [1,2,94]). Therefore, introduction of charge may be the first choice. However, the performance of membrane synthesized by this approach will strongly depend on the pH and ionic strength of the feed solution leading to high electrostatic repulsion between solute and membrane. In addition, this approach will be difficult to be practically applied for multi solutes in the feed solution. Hydrophilic membranes, on the other hand, have also shown low adsorptive as well as ultrafiltration fouling with protein (e.g., [9,55,95,96]). Even though in some applications the charged membrane could have higher performance, the performance of hydrophilic membrane should be not influenced by the physico-chemistry of the feed solution.

Furthermore, with self assembled monolayers (SAMs), structure property relationships for non–adsorptive and non–adhesive surface have been identified on molecular level by Whitesides *et al*. [97-99]. They concluded that the characteristics of materials that resist the adsorption of protein should be: (i) hydrophilic/polar, (ii) overall electrically neutral, (iii) hydrogen bond acceptors, and (iv) not hydrogen bond donors. In these regards, polyethylene glycol (PEG), zwitterionic moieties and material that display "kosmotropes" were identified as the non fouling materials that resist protein adsorption.

A permanent functionalization, i.e. stable anchoring of modifying species to membrane, is required for long–term membrane applications including repeating cleaning cycles. For UF membranes with selective pore sizes between 2 and 10 nm, this is rather complicated task, while several surface modifications of MF membranes, due to the more robust morphology and larger pore sizes, had been established commercially. Nevertheless, several approaches have been tried for UF membranes (cf. Section 2.4)

2.4. Membrane Surface Modification

In this section, a recent comprehensive feature article written by Ulbricht [33] is used as the main reference. Basically, polymer surface modification can be done by using chemical and physical processes [100]. Physical processes take advantage of e.g., surface segregation, radiation of electromagnetic waves, while chemical modifications uses wet–treatment, blending, coating and metallization. In this section, the discussion is focused on the chemical modification. Generally speaking, chemically control surface modification can be done through (pure) physical process and chemical reaction (with physical activation).

A membrane surface modification is aimed either to minimize undesired (secondary) interactions (adsorption or adhesion), which reduce the performance (membrane fouling), or to introduce additional interactions (affinity, responsive or catalytic properties) for improving the selectivity or creating an entirely novel separation function [33]. Figure 2.4 describes the improvement of membrane performance via surface modification. A key feature of a successful (i.e. “tailored”) surface functionalization is a synergy between the useful properties of the base membrane and the novel functional (layer).

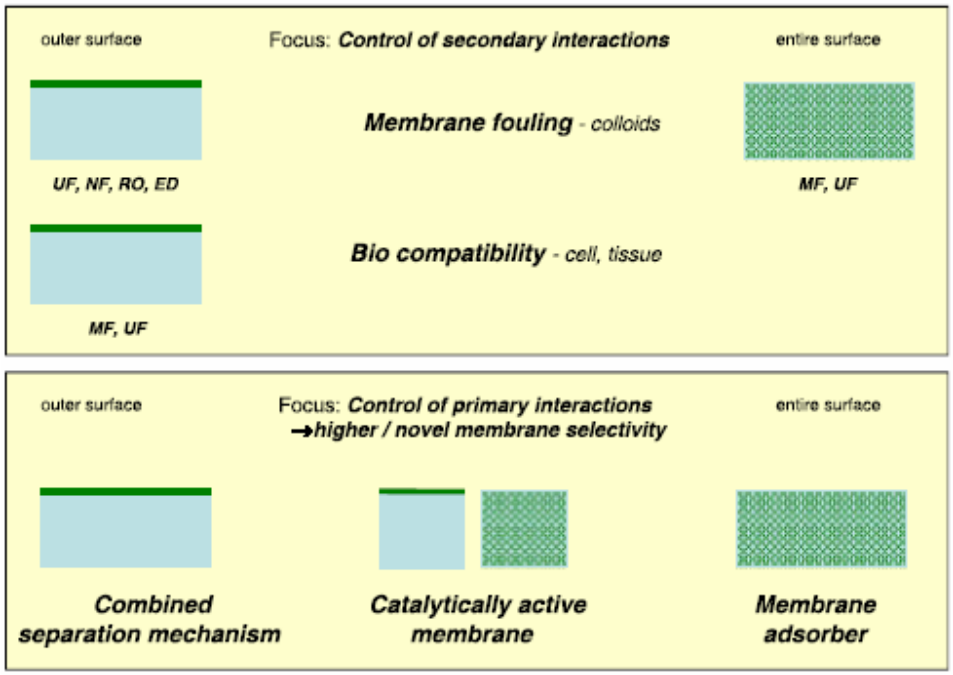

Figure 2.4. Improvement of membrane performance via membrane surface modification: a thin functional layer (green) – depending on pore structure and separation function either on the outer or the entire surface – leads to effective solutions for problems or to novel principles. 'Secondary' interactions (occurring also without a separation) should be controlled without sacrifying the separation function of the membrane. Controlling "primary" interactions can be used to tailor the separation function of a membrane or to 'integrate' them with other processes [33].

2.4.1. Chemical surface modification by physical methods

In the physical method, membrane surface is modified by exploiting physical mechanisms. Attachment of functional monomer onto a membrane surface could be done via the following ways [33]: (a) adsorption/adhesion – the functional layer is only physically fixed on the base material. The binding strength can be increased via multiple interactions between functional groups in the macromolecular layer and on the solid surface, (b) interpenetration via mixing between the added functional polymer and the base polymer in an interphase, (c)

mechanical interpenetration (macroscopic entanglement) of an added polymer layer and the pore structure of a membrane.

The stability of the functional layer or “coat” is dependent on the (ir)reversibility of the adsorption or more generally of the non−covalent attachment, with the thickness of the layers depends on the selected strategy. Many surface modification efforts have been performed by using this method [26,92,101-104]. It has been shown that chemical cross-linking of a hydrophilic polymer can yield "thin−layer hydrogel" composite membrane for UF separation without fouling [105,106]; however, pore blocking of the UF membrane support should be minimized.

Overall, in this way, the modification is simple and could improve the membrane performance with respect to the fouling resistance. However, loss of permeability after modification was also observed. More importantly, the stability of the coating/functional layer and incomplete surface coverage leading to the heterogeneity were other significant limitations.

In the last decade, layer by layer (LBL) adsorption was proposed as a new method to modify a solid surface [107]. An example for membrane modification using this technique was reported by Bruening and Sullivan [108]. It was reported that the composite membrane with selective ultrathin polyelectrolyte skin was formed. This membrane allowed highly separation of ions according to the charge, size, or hydration energy. In general, the particular advantage of LBL technique is the vertical organization and stabilization of the layers in combination with the potential to design both outer surface and internal layer structures on a wide range of base materials. As a precondition for the use of LBL technique is that the base material must be able to adsorb the first polyelectrolyte layer via (multiple) ionic bonds. However, the

required density of charged functional groups on the surface is moderate (see reference [33] for more detail review).

2.4.2. Surface modification by chemical reactions

In the chemical modification, the chemistry of polymeric membrane surface is modified either by direct chemical reaction or by the covalent bonding of suitable macromolecular chains onto the membrane surface (grafting) with physical activation. In order to achieve the ultimate aim of a membrane surface modification, the following methods have been proposed [33]: (i) heterogeneous reactions of the membrane polymer, (ii) "grafting–to" reaction, and (iii) "grafting–from" reaction.

Heterogeneous reactions of the membrane polymer. Chemical reactions on the surface of the membrane material could be classified into following two ways [33]:

(a) derivatization of or grafting onto the membrane polymer via reaction of intrinsic functional groups without material degradation (no polymer chain scission or change in bulk morphology). Basically, this method is more possible to modify the membrane based on biopolymer such as cellulose, but application for other polymer membrane had also been reported [109]. In this case, controlled heterogeneous functionalizations are complicated or even impossible due to chemical stability of the base membrane polymer. By this approach, introducing charge groups on the membrane surface could also be done (e.g., [110]). They prepared UF membrane from PAN homopolymer and copolymer with methyl acrylate.

(b) controlled degradation of the membrane material for the activation of derivatization or grafting reactions (at minimized polymer chain scission or change of bulk

morphology). The “oxidative hydrolysis” of polyethylene terephthalate, which had been established for a surface functionalization of track−etched membranes without significant changes of their pore structure, is an example for functionalizaition using this approach [111].

Overall, polymer−analogous reactions of the membrane polymer depend very much on the chemical structure of the polymer and their application is thus limited, for example, a large variety of chemistries have been explored for PS but the conditions caused membrane damage along with the desired chemical functionalization [112]. Nevertheless, some improvements to avoid changing in morphology of the base membrane have been proposed (e.g. [111]).

“Grafting–to” reaction. **“**Grafting−to” reaction is performed by coupling polymer molecules to surface. Introducing macromolecular functional layers to the surface of membranes could be done via the following strategies [33]: (a) direct coupling on reactive side groups or end groups of the membrane, (b) primary functionalization of the membrane − introduction of amino, aldehyde, epoxide, carboxyl or other reactive groups on the surface − and subsequent coupling, (c) adsorption on the membrane surface and subsequent physically activated coupling.

Functionalizations of UF or MF membrane with hydrophilic macromolecule [113,114] or other functional polymers (e.g., [115]) using “grafting−to” reaction had been reported. This method has a potential advantage that the structure of the polymer to be used for surface modification can be well controlled (very selective) by synthesis also characterized in detail. However, the grafting density on the surface, which may be achieved are limited (surface coverage is rather low) and the coupling reactions typically require special effort.

"Grafting–from" reaction. During "grafting–from" reaction, monomers are polymerized using an initiation at the surface. Until now, synthesis of macromolecular layers via "grafting–from" a polymer membrane surface is done by radical polymerization. Figure 2.5 shows the different ways for initiation during "grafting–from" reaction.

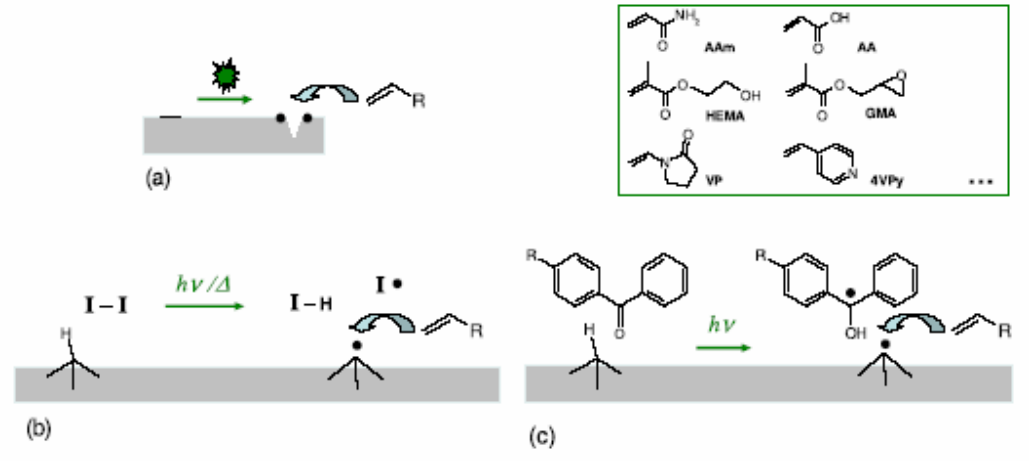

Figure 2.5. Initiation (formation of starter radicals) during heterogeneous radical graft copolymerization ("grafting–from") of functional monomers on membrane polymers: (a) degradation of the membrane polymer (main chain scission or cleavage of side groups), via physical excitation with radiation or plasma, (b) decomposition of an initiator in solution and radical transfer (here hydrogen abstraction); radicals in solution may initiate a homopolymerization as a side reaction or leading to grafting via radical recombination, (c) adsorption of a type II photoiniator (e.g., benzophenone derivative) on the surface and selective UV excitation [33].

In the "grafting–from" method, physical activation (cf. below) is usually needed to create free radicals [100,116]. As consequences, unwanted changes in membrane morphology and/or an even modification in the interior of porous membrane are the side effects of this approach. The extent of these side effects depends on the sensitivity of the membrane material and the excitation used. Via a direct UV excitation, it is possible to functionalize UV–sensitive

membrane polymers, such as PES, also under ‘simultaneous’ conditions, i.e. in direct contact with the monomer; the starter radicals are formed via scission of the main chain of the membrane polymer (cf. Figure 2.5 (a)). The research group of Belfort has intensively explored this method to modify PES and PS membranes with respect to minimize the fouling [34-38,117,118].

Via decomposition of peroxides in a solution in contact with the membrane, the radicals transfer to the membrane material can also form the starter radicals (cf. Figure 2.5 (b)). Such “grafting–from” functionalizations without additional activation by external means could also be applied for the modification of membranes in modules.

The use of UV–assisted methods for a heterogeneous graft copolymerization, mainly with the intention to improve the ‘decoupling’ effects of the activation and the grafting reactions had been developed by Ulbricht *et al.* [39,40,42,111,119-122]. Additional photoinitiators, which can be selectively excited by certain UV energies, were used. An especially easy and effective two–step approach is based on (i) the adsorption of a ‘type II’ photoinitiator (e.g., benzophenone, BP) on the membrane surface and (ii) the subsequent UV initiated hydrogen abstraction reaction to yield polymer radicals on the surface of the membrane in the presence of monomer [119] (cf. Figure 2.5 (c)). Recently, another option to improve the surface selectivity by confining the initiator had been demonstrated: The photoinitiator BP had been ‘entrapped’ in the surface layer of polypropylene (PP) by using a solvent, which can swell the PP in the coating step (i). By selecting suited BP concentration and time the uptake in the surface layer of the PP can be adjusted, and after change to a more polar solvent such as water or alcohol a fraction of the BP is immobilized but can still initiate a graft copolymerization [122].

Physical activation, especially via controlled degradation of polymer is possible by high energy radiation (e.g., γ-or electron beam), plasma or corona and UV irradiation [33,116]. In fact, those physical activations could be used (alone) to modify the membrane (such modification is not discussed in this report).

Activation by high energy radiation/ionization radiation. One of activation methods during photochemical modifications is high energy radiation/ionization radiation. To generate free radicals for graft polymerization, the membrane can be exposed to the high energy radiation using electron beam or γ-ray irradiation. In the presence of monomer, irradiation of polymer with ionization radiation can cause several chemical effects such as cross-linking, degradation, grafting and polymerization [116]. Many reported surface modification efforts especially the preparation of either ion exchange membrane or polymer electrolyte membrane (PEM) fuel cell membrane are initiated using electron beam or high energy radiation (cf. [123,124] in detail review). In addition, the use of this activation method was also reported for cellulose and PES membrane modifications [125,126]. Overall, the excitation with high energy irradiation yields a low selectivity and a bond scission in the volume of a membrane material can not be avoided. This condition is due to high energy is delivered not only to the membrane surface but also to the whole bulk of membrane. As the results, this modification is not a surface selective membrane modification and pore enlargement via bond cleavage also occurs. Decreasing in both permeability and rejection during grafting of PEG onto PES activated by gamma−ray irradiation had also been observed [126].

Activation by plasma or corona discharge. Membrane modification activated by temperature plasma (low or cold) and corona discharge treatment involves the reaction of plasma, a low pressure gas containing electrons, ions, photons and excited particle with the

polymer chains of the membrane surface [103]. Corona discharge is the name given to the atmospheric plasma produced when air is ionized by a high electric field. The membrane surface is oxidized by corona discharge forming the starter radicals. By reacting with atmospheric oxygen, these radicals form peroxide groups and then decompose to give oxygen containing functional group, such as hydroxyls, carbonyls and carboxyls. Low temperature plasma modification uses a particular gas such as O_2, N_2, Ar, He or combination of gases ionized by an applied electric field in an evacuated reactor. In this method, the following routes are possible: (i) plasma treatment, (ii) plasma treatment followed by polymer grafting and (iii) plasma polymerization

Application of plasma for membrane surface modification had been intensively studied with typical application is hydrophilization and introduction of special functional groups on the surface [33]. Ulbricht and Belfort [127,128] had modified PAN and PS using helium and a mixture of helium and water plasma alone or followed by graft polymerization to increase the membrane hydrophilicity. The results showed that the modified membranes had higher protein fouling resistance than unmodified membrane. Chen and Belfort [129] modified the PES UF membrane with plasma treatment alone and followed by the grafting of NVP. Both modifications could improve the membrane performance with respect to the permeability and fouling resistance (without loss of rejection). However, no significant difference in membrane performance as well as membrane characteristic between modified membrane treated by plasma alone and modified membrane treated by plasma and grafting. For UF membranes, it is possible to modify exclusively the outer surface, but a degradation of the micro- and mesoporous structure of the skin layer with consequences for the separation selectivity of the membrane can usually not be avoided [33]. PAN UF membranes can be an exception, because

under well defined plasma conditions a hydrophilization occurs in parallel to a stabilization of the membrane material via an intramacromolecular cyclization of the PAN [127].

Overall, chemical surface modification activated by plasma is flexible because of the variety of gases that can be used. Modification is surface selective and is restricted to the top several nanometers of the surface, so the bulk polymer properties are usually unaffected. Further, homogeneity of surface modification can be achieved due to under vacuum operation [33]. However, the ablation tendency of the base polymer may be significant [127] and the complexity of the process including using vacuum equipment is the limitations. Then, the change in pore structure or pore etching leading to the retention loss, significant loss of membrane permeability were also observed. Modifications in small pores (diameter < 100 nm) are complicated because the dimension is smaller than the average free path length of the active species in the plasma [33].

Activation by UV irradiation. Ultraviolet (UV) irradiation is generally considered as a radiation that has a wave length ranging from 100 to 450 nm [116]. In this technique, the membrane is modified by growing polymer chains through free radical polymerization (cf. above for the mechanism, Figure 2.5). Membrane surface modification for the purpose of decreasing both adsorptive fouling and ultrafiltration fouling has intensely investigated with photoinitiator [40,113,119] and without photoinitiator (cf. Section 2.4.3).

Overall, the excitation with UV irradiation has the great advantage that the wavelength can be adjusted selectively to the reaction to be initiated, and, hence, undesired side reactions can be avoided or at least reduced very much [33]. Photoinitiation can be used without problems also in small pores. The UV technology can be integrated into continuous manufacturing processes simply and cost–efficiently. Photo–initiated processes have their

largest potential when surface–selective functionalizations of complex polymer morphologies shall be performed with minimal degradation of the base membrane, and when they are used to create macromolecular layers via "grafting–to" or "grafting–from" (cf. above).

2.4.3. Strategy of this project

In this project, PES UF membranes were photo–chemically modified using UV light in order to minimize the membrane fouling (cf. above for the advantages of the photochemical method). Yamagishi *et al*. [34,117] developed direct modification of PS and PES UF membranes without the use of photoinitiator. This method was based on the intrinsic photoactivity of PES and PS to create radicals site on the membrane surface after exposing to UV light. They reported that the UV light directly cleaved the sulfur–carbon bonds in the PS and PES polymer chain and created radical site (Figure 2.6). After this finding, further works were then reported [35-40,117,118,130-132]. Simultaneous and sequential modification could be done in this method [36,40]. Modification using non selective radiation (λ > 220 nm) yielded lower water flux (but higher dextran rejection) than modification using selective radiation ((λ > 320 nm). This result was explained due to cross-linking process and degradation of the base membrane at higher energy wave length (λ > 220 nm).

In this modification project, two water-soluble monomers, PEGMA (poly(ethylene glycol) methacrylate) and zwitterionic SPE (N,N-dimethyl-N-(2-methacryloyloxyethyl-N-(3-sulfopropyl)), are used as the functional monomers (Scheme 2.1). The use of PEGMA is based on the fact that PEG (PEG-derivative) has been well known as a non fouling material (e.g., [40,133-136]), whereas zwitterionic has been reported as a new generation of non fouling material in the non porous surface technology field [137-140]. Although the use of

zwitterionic polymers to synthesis a low fouling UF membrane via a phase inversion method has been proposed [141,142], very few study until now has been reported to investigate the post−grafting of zwitterionic monomer onto UF membrane, which is expected more promising to be practically applied than synthesis based blending. Grafting of phospholipids zwitterionic polymer has been done on cellulose hemodialysis membrane [143]. Recently, Xu *et al*. [144] reported the photografting of phospholipid analogous polymers using benzophenone onto polypropylene microfiltration membrane. Therefore, feasibility of the zwitterionic monomer for UF membrane modification is interesting to be evaluated.

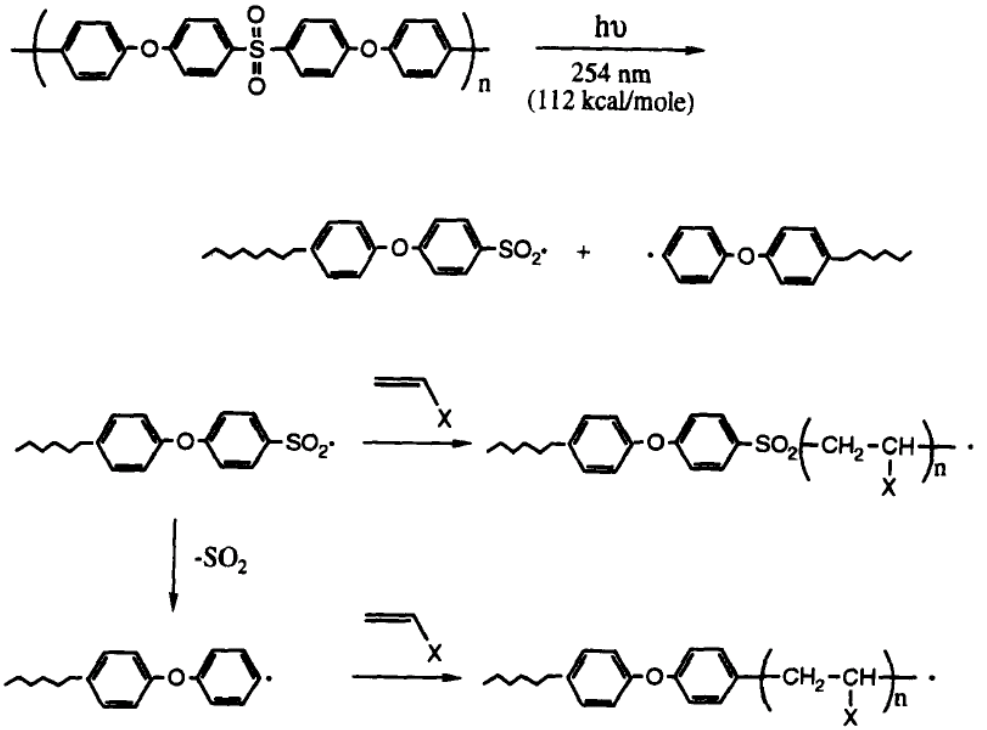

Figure 2.6. Mechanism of photograft polymerization of poly(ether sulfone) membranes [34].

Hydrophilic cross-linker, MBAA, was used to improve the fouling resistance via reducing the membrane−solute interactions. The use of cross-linker was directed towards

increasing the size exclusion effect of solute from the membrane surface and as a result we expect that the solute (e.g., protein) will not easily reach the substrate surface to be adsorbed. Yang *et al*. [145] reported that the protein adsorption could significantly be diminished by highly cross-linked layer. Beside its good performance to resist protein adsorption, PEG may be susceptible to oxidative degradation and chain cleavage like other polyether or hydrophilic polymers when exposed to aqueous system. Further, it was reported that PEG has some limitations like it could decompose in the presence of oxygen and transition metal ions (relatively low stable) [138] and loosed its resistance to fouling beyond 35^{o}C [139]. It is important to note that the target of this works is to obtain modified membranes having nominal cut−off of ~10 kg/mol and fouling resistance better than commercial membrane with similar water permeability and nominal membrane cut-off.

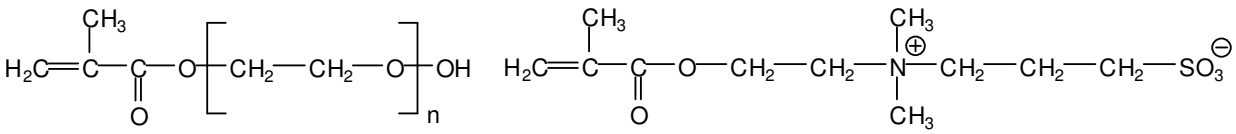

(a) (b)

Scheme 2.1. Chemical structure of the monomer used for modification:
(a) PEGMA (n~9), (b) SPE.

Chapter 3
EXPERIMENTS

3.1. Materials

Commercial ultrafiltration (UF) membranes were used for both fouling mechanism study and membrane surface modification. The use of commercial membranes is because the consistency of membrane properties manufactured industrially is typically much better than from lab-made membranes.

Study on fouling mechanism of polysaccharides was performed by using polyethersulfone (PES) UF membranes with nominal cut–off (also called nominal molecular weight cut off, NMWCO) of 10 kg/mol (type 146.30), 30 kg/mol (type 146.59) and 100 kg/mol (type 146.68) obtained from Sartorius, Germany, and PES UF membrane with nominal cut–off of 10 kg/mol (GR81PP) obtained from Alfa Laval, Denmark. In addition, two cellulose–based membranes having nominal cut-off of 10 kg/mol (RC70PP from Alfa Laval, and Hydrosart 144.39 from Sartorius) were used. For simplicity reason, in further discussions the membranes from Sartorius are called PES-SG10, PES-SG30, PES-SG100 and SC-10 instead of 146.30, type 146.59, type 146.68 and type 144.39, respectively, whereas the membranes from Alfa Laval are called PES-GR10 and RC-10 instead of GR81PP and RC70PP, respectively. Prior to use for experiments, the membranes were initially washed by soaking overnight in water to remove impurities left over from the manufacturing process or additives used for stabilization.

Two PES UF membranes, i.e. 100 kg/mol (type 146.68 (PES-SG100), from Sartorius) and 50 kg/mol (UF-PES-050H called PES-050H, from Microdyn–Nadir, Germany) were used as the base membranes during surface modification experiments. In addition, two PES UF membranes having nominal cut–off of 10 kg/mol (P010F from

Microdyn-Nadir and PES-SG10 from Sartorius) were also used for performance comparison study. Before use for modification, the membranes were initially washed with ethanol and shaking at 100 rpm on the mechanical shaker for 1.5–2 h and then equilibrated with water.

The heterogeneity of membrane properties is a common problem in membrane technology field in particular for experiments with a small membrane sample area. Therefore, preliminary experiments were done in order to avoid an influence of initial membrane properties on experimental results. Table 3.1 shows an example of the variation in initial membrane permeability and the corresponding variations of relative water flux reduction, RFR, (cf. Eq. (3.1)) after adsorptive fouling with dextran T-4 (10 g/L). It was observed that a membrane having higher initial water permeability yielded a smaller RFR. In order to minimize this effect, selection criteria for the membrane samples were specified. Hence, for all fouling mechanism study experiments, only membranes that have the initial water permeability (L/(m^2hkPa) in the range of $\pm$ 10% relative to the average values, i.e. 0.892 $\pm$ 0.089, 0.077 $\pm$ 0.008, 0.414 $\pm$ 0.041 and 0.483 $\pm$ 0.048 for PES-SG10, PES-GR10, SC-10 and RC-10 membranes, respectively, were used. Due to much higher permeability (compared to 10 kg/mol), the selection range was broadened for membranes with higher nominal cut–off. Thus, only membrane samples that had the initial water permeability in the range $\pm$ 15% relative to the average values, i.e. 5.71 $\pm$ 0.86 for PES-SG100 and 5.51 $\pm$ 0.83 for PES-050H were used for surface modification experiments.

Table 3.1. Initial pure water permeability (L/m^{2}hkPa) and RFR of membranes (data from preliminary experiments)

Sample no	SG-PES membrane		GR-PES membrane		SC membrane	
	J/p	RFR* (%)	J/p	RFR* (%)	J/p	RFR* (%)
1	0.819	4.6	0.065	14.1	0.384	-1.3
2	0.800	5.6	0.052	14.2	0.395	-1.5
3	0.844	4.7	0.073	12.9	0.390	-1.3
4	0.933	2.5	0.108	7.7	0.367	-1.1
5	0.867	3.5	0.083	9.8	0.400	-1.8
6	0.900	3.1	0.080	9.1	0.377	-1.4
7	1.291	1.2	0.054	14.3	0.448	1.1
8	0.598	6.6	0.087	8.6	0.470	0.8
9	0.755	2.2	0.102	8.0	0.465	-1.1
10	1.109	1.4	0.070	13.8	0.439	1.2
Average[1]	0.892 ± 0.192	3.5 ± 1.8	0.077 ± 0.019	11.3 ± 2.8	0.414 ± 0.038	-0. 65 ± 1.1
Average [2]	0.861 ± 0.050	4.0 ± 1.2	0.078± 0.009	11.4 ± 2.5	-	-

* were measured using dextran T-4 (10g/L)
Average[1]: used the all data obtained, ± standard deviation; Average[2]: excluded extreme values (labeled grey) based on the permeability criteria (cf. Experimental), ± standard deviation

Dextran T-4, T-15, T-35, T-100 and T-200 (the number indicates molar mass in kg/mol) from Serva Feinbiochemica GmbH&Co, Heidelberg, Germany, and dextran T-10, T-70 from Pharmacia Fine Chemicals, Uppsala, Sweden, were used. Characteristics of dextrans as given by the manufacturers and determined experimentally are summarized in Table 3.2. Polyethylene glycols (PEG 1.5, PEG 3, PEG 6, PEG 12 and PEG 35, the number indicates molar mass in kg/mol) were purchased from Fluka Chemica GmbH whereas PEG 100 and PEG 200 were purchased from Acros Geel, Belgium. Poly(ethylene glycol) methacrylate (PEGMA 400, the number indicates PEG molar mass in g/mol)

purchased from Polysciences Inc. Warrington and N,N-dimethyl-N-(2-methacryloyloxyethyl-N-(3-sulfopropyl) ammonium betaine (SPE 279, the number indicating monomer molar mass in g/mol) obtained from Raschig GmbH, Germany, were used as the functional monomers. N,N'-methylenbisacrylamide (MBAA) as cross-linker, myoglobin (Myo) from horse skeletal muscle (95-100% purity), humic acid and sodium hypochlorite were purchased from Sigma-Aldrich Chemie GmbH, Steinheim, Germany. Bovine serum albumin (BSA) was purchased from ICN Biomedicals, Inc. (California, US). Potassium dihydrogen phosphate (KH_2PO_4), disodium hydrogen phosphate dihydrate ($Na_2HPO_4.2H_2O$) and calcium chloride dihydrate ($CaCl_2.2H_2O$) were purchased from Fluka Chemie AG (Buchs, Germany). Potassium chloride (KCl), potassium hydroxide (KOH), and hydrochloric acid (HCl), all of p.a. quality, were purchased from Bernd Kraft GmbH, Duisburg, Germany. Sulfuric acid was from J.T. Baker, Holland. Potassium acid phthalate and ferroin indicator solution were purchased from Acros Organics, Geel, Belgium. Potassium dichromate was reagent grade. Ferrous ammonium sulfate (FAS) was purchased from Fluka Chemica GmbH. Nitrogen gas purchased from Messer Griesheim GmbH, Krefeld, Germany, was of ultrahigh purity. Water purified with a Milli-Q system from Millipore was used for all experiments.

Table 3.2. Characteristics of dextrans used in this study.

Dextran Type	M [a] (kg/mol)	M_n [b] (kg/mol)	M_w [b] (kg/mol)	$D = Mw/Mn$ [b]
T4	4 – 6	1.72	3.79	2.20
T10	~10	7.21	10.17	1.41
T15	15 – 20	11.10	15.32	1.38
T35	35 – 50	13.76	33.00	2.40
T70	~70	46.48	71.16	1.53
T100	100 - 200	61.57	130.61	2.12
T200	200 - 300	297.02	334.09	1.12

[a] Given by manufacturer
[b] Data were obtained from gel permeation chromatography (GPC)

3.2. Sugarcane Juice Polysaccharides (SJP) Preparation

Clarified sugarcane juice was obtained from a sugar mill in Uttar Pradesh, India. The feed preparation for sugarcane juice polysaccharides was described in detail [19]. Briefly, treated sugarcane juice was stored at −70°C. Thereafter, the juice was thawed and precipitated by addition of HCl followed by ethanol. The sample was then left overnight at ambient temperature to allow the precipitate to settle. The supernatant was decanted and the precipitate was filtered. Thereafter, the sample was dried at 45−50°C till constant weight was reached. The soluble fraction was obtained by dissolving the sample in pure water (1 mg/1 ml water) and filtering through a 0.45 μm cellulose acetate filter (Sartorius AG, Germany). The filtrate was frozen and then lyophilized. All experiments were conducted using 1.5 g/L freshly reconstituted solution of the freeze dried fraction.

3.3. Analyses

Before use for experiments, myoglobin (in phosphate buffer solution pH 7), BSA (in phosphate buffer solution pH 7.2) and humic acid solution (in water at different pHs) were pre-filtered through a 0.45 μm microfiltration membrane (Sartorius, Germany) to remove suspended material.

Gel permeation chromatography (GPC) was used to analyze the molar mass distribution of PEGs, dextrans and reconstituted SJP. All analyses using GPC were conducted in sodium azide solution (0.01 M). PEGs were analyzed using a MZ Hema Bio column (MZ Analytik, Mainz, Germany) coupled with a Waters refractive index detector. Calibration curves for the correlation of retention volume and molar mass were obtained using different PEG molar mass standards. A PSS Suprema (PSS, Mainz, Germany) and a MZ Hema 40 (MZ Analytik, Mainz Germany) column in series were used to analyze dextran. Calibration was performed using different dextran molar mass standards. In

addition to the GPC, in some cases, the “chemical oxygen demand” method was also used to analyze dextran concentrations in water solution. This method is based on the dextran oxidation using a known amount of potassium dichromate under acidic conditions followed by the titration of the unreacted excess of potassium dichromate with ferrous ammonium sulfate (FAS) using ferroin indicator. This method can be used for dextran concentrations down to 5 mg/L. BSA concentration was analyzed using the bicinchoninic acid (BCA) protein assay (from Pierce [146]). The concentration of myoglobin and humic acid were calculated from their UV absorbance at 230 and 255 nm, respectively, measured using the UV-Visible spectrophotometer CARY-50 Probe (Varian, Germany). A microbalance (ME 215P Genius, Sartorius, Germany) was used for all gravimetric determination.

3.4. Methods

3.4.1. Procedures of static adsorption, UF and sieving (rejection) characterization

Static adsorption (membrane–solute interactions), UF (membrane–solute–solute interactions) and sieving (rejection) characterization were carried out using a dead-end stirred cell filtration system. The system consisted of a filtration cell (Amicon model 8010 or 8050, Millipore) connected to a reservoir (~450 or ~1850 mL). It was pressurized by nitrogen gas. To avoid the effects of compaction process, each membrane was firstly compacted by filtration of pure water at high pressure for at least 0.5–1 hour (until the conductivity of permeate was equal to the one of the water used). Thereafter, the pressure was reduced to the desired pressure for water flux measurement. Estimation of water flux reduction due to adsorptive fouling was conducted at constant pressure of 300 kPa. Both UF and sieving experiments were conducted at constant pressure with either similar or different initial water permeability for different membranes. Table 3.3 summarizes the

experimental set-up and procedures for the static adsorption, ultrafiltration and rejection (sieving) characterization during fouling mechanism study as well as surface modification.

All fluxes of pure water were measured (by gravimetric method) until the consecutively recorded values were considered constant (i.e. differed by less than 2–4% depending on the membrane nominal cut–off). For static adsorption (membrane–solute interactions) experiments, a test solution (dextran or myoglobin or BSA or reconstituted SJP or humic acid solution) was added to the cell and the outer membrane surface was exposed for certain time (cf. Table 3.3) without any flux at a stirring rate of 300 rpm (31.416 rad/s). Then, the test solution was removed and the membrane surface was rinsed two times by filling the cell with pure water and shaking it for 30 seconds (cf. Table 3.3 for the quantity of water used). Water fluxes were measured before and after exposing to the test solution. The evaluation of membrane–solute interactions was done by calculating the relative water flux reduction as described by the following equation:

$$\text{RFR}\ (\%) = \frac{J_o - J_{ads}}{J_o} \text{x} 100 \qquad (3.1)$$

where RFR is the relative water flux reduction. J_o and J_{ads} are water fluxes before and after exposing (adsorption), respectively.

UF experiments were performed using the same test solution as in adsorptive experiments as the feeds for certain concentration and filtration time (cf. Table 3.3). Thereafter, the solution was removed, and the membrane surface was externally rinsed in similar way for adsorptive fouling (cf. Table 3.3). During experiments for investigation of flux profile over time, the balance was connected to the PC and weight of permeate flux was online recorded. Water fluxes were measured before and after ultrafiltration. Besides the RFR after UF, the solute rejection was also estimated using Eq. (3.2).

Table 3.3. The experimental set-up and procedure of experiment for static adsorption, ultrafiltration and sieving (rejection)

Comments	Study on fouling mechanism			Membrane surface modification		
	Static fouling[1]	Ultrafiltration[2]	Rejection/sieving[3]	Static fouling[1]	Ultrafiltration[2]	Rejection/sieving[3]
Filtration cell	Amicon cell 8010	Amicon cell 8050	Amicon cell 8050	Amicon cell 8010	Amicon cell 8010	Amicon cell 8050
Effective membrane area	3.14 cm^2	12.56 cm^2	12.56 cm^2	3.14 cm^2	3.14 cm^2	12.56 cm^2
Compaction	450 kPa, ~1 hour	450 kPa, ~1 hour	450 kPa, ~1 hour	450 kPa, ~0.5 hour	450 kPa, ~0.5 hour	450 kPa, ~0.5 hour
TMP[4]/Initial water flux	300 kPa	300 kPa	26±2 L/m²h (initial water flux)	300 kPa	- 100 kPa for Myo, BSA and SJP[5] - 90 ± 5 L/m^2h for HA solution	- 20 kPa - 100 kPa
Solution test/ Feed solution; adsorption (exposure) time/ filtration time/ long of filtration	- Dextran (0.2-25 g/L); adsorption time (0.5-4 h) - Myo (1 g/L); adsorption time 3 h	- Dextran (1 g/L); filtration time 3 h - Myo (0.1 g/L); filtration time 2 h	- Mixed PEGs; around 10 mL permeate was collected	- Myo (1 g/L); 2 h - BSA (1 g/L); 2.5 h - SJP[5] (1.5 g/L); 2.5 h - HA (100 mg/L); 18 h	- Myo (1 g/L); 2 h - BSA (1g/L); ~20 mL permeate was collected - SJP[5] (1.5g/L); ~20 mL permeate was collected - HA (50 mg/L); 48 h	-Mixed PEGs (1 g/L); ~10 mL permeate was collected or - Mixed dextrans (1 g/L); ~10 mL permeate was collected
Temperature	21±2 °C	21±2 °C	21±2 °C	21±2 °C	21±2 °C	21±2 °C
Stirring rate	300 rpm	300 rpm	300 rpm	300 rpm	300 rpm	300 rpm
Rinsing	2 x 5 mL	2 x 25 mL	2 x 25 mL	2 x 5 mL	2 x 5 mL	2 x 25 mL
Performance indicator	RFR[6]	Flux profile vs. time, RFR[6] and rejection	Sieving curve	RFR[6], R_f[7]	Flux profile vs. time, rejection	Rejection curve

[1]static fouling: membrane−solute interactions, [2]ultrafiltration: membrane−solute−solute interactions, [3] rejection or sieving characterization, [4]TMP: transmembrane pressure, [5]SJP: sugarcane juice polysaccharides, [6]RFR: relative flux reduction, [7]R_f: adsorptive fouling resistance

$$R\ (\%) = \left(1 - \frac{C_{downstream}}{C_{upstream}}\right) x\ 100 \qquad (3.2)$$

where $C_{downstream}$ and $C_{upstream}$ are the concentration of solute on the downstream and the upstream sides of the membrane, respectively. The feed concentrations at the beginning and at the end of the experiment were averaged to obtain the representative values of upstream concentration during ultrafiltration.

A five component mixture of PEGs with molar mass ranging either from 1.5 to 35 kg/mol (for fouling study) or from 1.5 to 200 kg/mol (for surface modification) at total concentration of 1 g/L was used for rejection/sieving characterizations including the membrane cut−off. The compositions of PEGs in the feed permeate and retentate mixtures were analyzed by using GPC. Sieving for each molar mass was determined using the following Equation:

$$S = \frac{C_{downstream}}{C_{upstream}} \qquad (3.3)$$

The feed concentrations at the beginning and at the end of the experiment were also averaged. Nominal cut-off was defined as the molar mass of a test molecule that would be retained to > 90% by the membrane (sieving < 0.1).

3.4.2. Simultaneous diffusion−adsorption measurements (SDAM)

The SDAM method was used to quantify the amount of solute bound to / in the membrane as well as the effective diffusion coefficient. As shown in Figure 3.1, the diffusion cell consisted of two half−cells, i.e. the upstream cell (high concentration) and the downstream cell (low concentration). Each cell was equipped with a stirring system. The membrane with an effective area of ~12.56 cm^2 was placed between the two cells and sealed with O-rings. The upstream and downstream cells were filled at the same time with

120 ml of a solution of either dextran (10 g/L in 0.01 M sodium azide solution) or myoglobin (400 mg/L, in phosphate buffer pH 7) and 120 ml of either 0.01 M sodium azide solution or phosphate buffer (pH 7), respectively. Even though Lebrun and Junter [147] had reported that for diffusion of dextran through porous media, the mass transfer resistances at the liquid-solid interfaces were negligible, in order to minimize the resistance of boundary layers, the two half-cells were stirred at the same stirring rate. The diffusion of dextran/myoglobin (Myo) through the membrane was monitored by measuring the concentrations of dextran/ (Myo) in both half–cells at certain times for up to four hours. The effective diffusion coefficient was calculated from the initial diffusion rates and the amount of dextran/Myo adsorbed on / in the membrane was deduced from the mass balance.

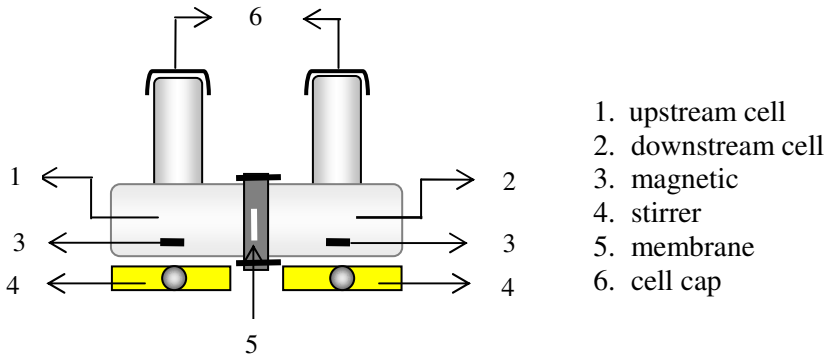

Figure 3.1. Experimental device for diffusion measurements as well as quantification of dextran/Myo adsorbed onto membrane (SDAM).

3.4.3. Membrane modification by photografting

A UVA Print system (Hoenle AG, Gräfelfing, Germany) equipped with a high–pressure mercury lamp with wavelength more than 300 nm, providing homogenous illumination of up to 100 cm^2 area was used for modification. The intensities (measured with a UVA meter, Hoenle AG) were 60 $\pm$ 10 mW/cm^2 for modification using PES-050H

as the base membrane (first batch modification) and 35 ± 5 mW/cm^2 for modification using PES-SG100 (second batch modification). Circular PES base membrane samples with a diameter either of 25 mm or of 44 mm were immersed into monomer solutions in a Petri dish (the monomer solution was degassed by bubbling with nitrogen for at least 10 min). A second smaller Petri dish was used to cover the membranes (also as the glass filter). After at least 2 min (since first contact between membrane and monomer solution), samples were subjected to UV irradiation for various time periods. Thereafter, the membranes were taken out and immediately rinsed with water and then washed with excess of water to remove any unreacted monomer or physically adsorbed polymer. The washing was sequentially done at room temperature for 30 min, at 50 ± 2^{o}C for 2 hours and again at room temperature for 30 min. In modification using UV irradiation only, water was used instead of monomer solutions. The UV absorbance spectra of the both functional monomers as well as the cross-linker and glass filters used for modification are presented in Figure 3.2.

3.4.4. Degree of grafting (DG)

DG was gravimetrically determined as the weight increase per membrane outer surface area as described by the following equation:

$$DG = \frac{m_m - m_o}{A} \tag{3.4}$$

where m_o is the initial membrane sample weight, m_m is the membrane weight after modification and A is the outer surface area of the membrane used. All membranes used for DG determination were not used for flux, fouling and sieving experiments. Control experiment for the washing process as well as gravimetric method was also performed.

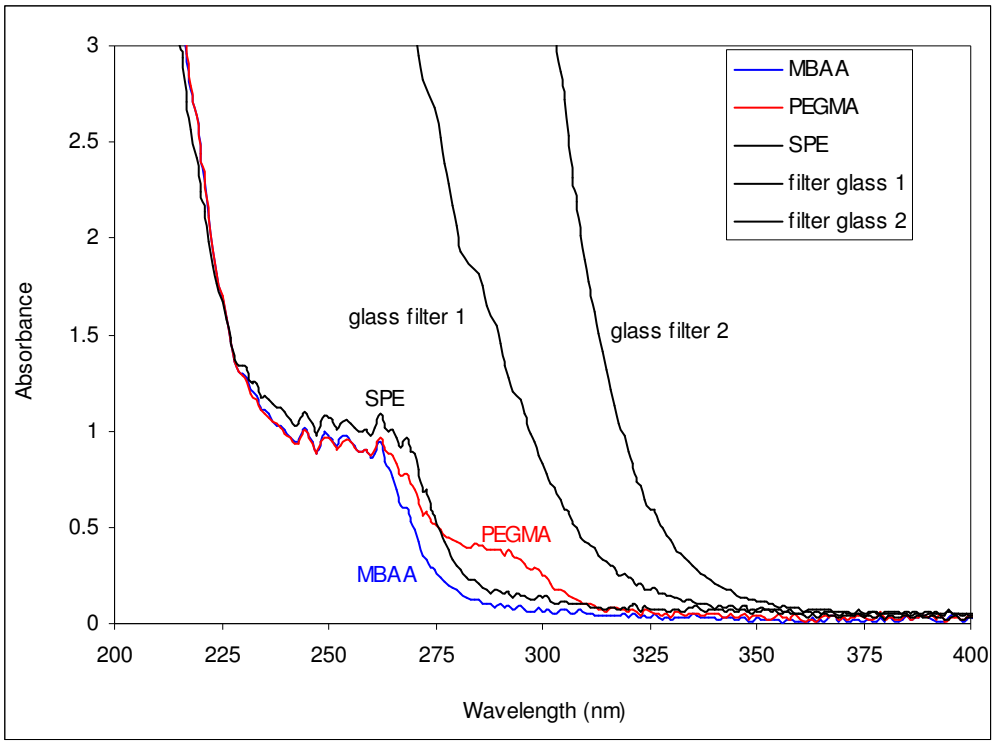

Figure 3.2. UV absorbance spectra of functional monomer, cross-linker and glass filter used for modification. Glass filter 1 was used for modification using PES-050H (first batch) whereas glass filter 2 was used during PES-SG100 modification (second batch).

3.4.5. Membrane characterization

Membrane chemistry. The membrane surface chemistry was analyzed by attenuated total reflection infrared spectroscopy (ATR-IR) using a Bruker Equinox 55 instrument (Bruker Optics Inc., Billerica, MA) equipped with a liquid nitrogen detector. A total of 64 scans were performed at a resolution of 4 cm^{-1} using a diamond crystal; the temperature was 21±1°C. A program written for the Opus software from Bruker was used to record the different spectra versus the corresponding background spectra. In addition to the (ATR-IR) spectroscopy, the elemental analysis was also used to analyze the whole membrane chemistry for several cases.

Membrane wettability. Membrane wettability was analyzed in term of contact angle (CA). CA was measured by using the static captive bubble method. This method should be

preferred for porous membrane surfaces [148]. Membranes were inverted (active layer to the bottom) in the pure water at a temperature of 21 $\pm$ 1^{o}C. An air bubble (5−10 µl) was injected from a syringe onto the sample surface water. An optical contact angle measurement system (OCA 15 plus; Dataphysics, Germany) was used, and at least seven to ten measurements of bubbles were averaged to obtain contact angle of the membrane. Static sessile drop method was used for CA measurements of nonporous PES film.

Membrane surface charge. The membrane surface charge was investigated via outer surface streaming potential measurement. Experiments were carried out in a flat−sheet tangential flow module [149]. After washing with water, the membrane was equilibrated by soaking in 0.001 mol/L KCl solution over night. Two UF membrane samples were placed above and below the spacer with both the active layers facing the flow channel. The electrolyte solution was pumped by a variable−speed pump drive by Vancouver, USA (model 120-00, Series E 221317). Pressure was measured using a pressure transducer by Setra Systems, USA (model 280 E). The membrane streaming potential was measured using 0.001 mol/L KCl solution, in the range of pH 3-10 (at pH higher than 10, the electrode is unstable and at pH lower than 3, the conductivity of the solution will be too large and disturb the measurement) and at a temperature of 25 $\pm$ 1^{o}C. The pH was measured using a pH−meter by Radiometer Copenhagen (PHM 62 Standard) and adjusted by addition of KOH and HCl solutions. The conductivity was recorded by WTW microprocessor conductivity meter LF 535. At each pH, the pressure was then step−wise increased (ranging from 65 to 100 kPa). A digital voltmeter by Voltcraft, Germany, was used to measure the streaming potential. Fouling (adsorptive) experiment was carried out by slow circulation of a test solution for certain time. A test solution was then replaced step−wise by water and 0.001 mol/L KCl solution, respectively. The zeta

potential, ζ, was determined using the Helmholtz–Smoluchowski equation as described in Eq. (3.5) [149,150].

$$\zeta = \frac{\kappa\eta}{\varepsilon_0 \varepsilon} \frac{\Delta E}{\Delta P} \tag{3.5}$$

where ΔE is the streaming potential, ΔP is the hydrodynamic pressure difference, η the viscosity of the solution, and ε, ε_0, and κ are the dielectric constant of the solvent, the permittivity of vacuum and the conductivity of the solution, respectively.

Membrane surface morphology. The morphology of membrane top surface was observed by using scanning electron microscope and atomic force microscopy (AFM). An environmental scanning electron microscope (ESEM) Quanta 400 FEG (FEI, USA) was used. A sputter coater K 550 (Emitech, UK) was used for coating of the outer surface of the scan sample with gold/palladium.

AFM topography images were obtained using a MultiMode AFM with Nanoscope IIIa controller and equipped with a 10 μm scanner from Digital Instruments, Santa Barbara, CA. The Tapping–Mode was applied using an oscillating cantilever with a silicon tip having a radius of < 10 nm. Dry membrane samples of about 25 mm^2 area were mounted on a steel disc with double sided sticky tape and subjected to analysis in air under room temperature condition. The cantilever oscillation was tuned to a frequency between 250 and 325 kHz. For the analysis of morphology, surface porosity and roughness, the AFM image processing program (NanoScope software) was used to zero out waviness of the surface topography. Average roughness (R_a) and root-mean-square roughness (R_{ms}) were obtained at surface areas of 1 μm^2.

3.4.6. Performance test of modified membranes

The modified membrane performance was evaluated with respect to the hydraulic permeability, static adsorption and ultrafiltration (cf. Section 3.4.1; Table 3.3). The effect of modification on membrane hydraulic permeability was investigated by measuring the water flux before and after modification at a constant pressure of 300 kPa. The result was expressed in term of hydraulic permeability ratio (Eq. (3.6)). The evaluation of membrane performance with respect to the adsorptive fouling was expressed in term of relative flux reduction (cf. Eq. (3.1)). In addition, the term of fouling resistance, R_f, was also introduced to evaluate the membrane performance during adsorptive fouling resistance–hydraulic permeability analysis (Eq. (3.7)). A fouling resistance of 1 means no adsorptive fouling has occurred.

$$\text{Hydraulic permeability ratio} = \frac{L_{po}}{L_{pm}} \tag{3.6}$$

$$R_f = 1 - RFR \tag{3.7}$$

where L_{po} and L_{pm} are the membrane hydraulic permeability before and after modification, respectively. Ultrafiltration experiments using test solutions were conducted at constant transmembrane pressure with either similar or different initial water flux for different membranes.

3.4.7. Stability test

Stability of the grafted polymer layer was examined by incubating in the sodium hypochlorite solution (at active chlorine of 500 mg/L) up to 8 days. This time seemed sufficient to achieve maximal effect [41]. Sodium hypochlorite was chosen because it is usually used for membrane cleaning. Samples were rinsed with pure water before

measurements. Contact angle, ATR-IR spectroscopy and elemental analysis were used to evaluate the stability of the grafted polymer layer.

3.4.8. Preparation of non−porous PES film

Glass coverslips with 24 x 24 mm^2 size (Menzel, Germany) were first cleaned with a commercial detergent−water mixture in an ultrasonic bath for 15 min. Then, it was rinsed with Milli-Q water, and etched for 15 min at approximately 40 $\pm$ 5°C in a freshly mixed 3/1 (v/v) sulphuric acid (96%)/hydrogen peroxide (30%) solution. The glass coverslips were then thoroughly rinsed with ultrapure water (Milli-Q System), and finally dried free of dust overnight at 120°C. Second, non−porous PES films were prepared by spin−coating (SCI-30 spin coater, LOT Oriel) of glass coverslips with solutions of PES (1%; w/w in methylenechloride) at 5000 rpm for 1 min and subsequent drying overnight at ~60 °C.

3.4.9. Measurement of swelling degree of functional polymer hydrogels

Method to determine the swelling degree used in this experiment was adapted from [151]. PEGMA/SPE hydrogels were prepared by free radical polymerization in aqueous solution using the following composition: 6.211 g of either PEGMA or SPE, 0.311 g of MBAA and 47.478 g of water were mixed in the glass vessel. Thereafter, 43.29 mg of ammonium peroxidisulfat and 173.2 mg of N,N,N,N'-tetramethylenediamine were added in order to initiate the polymerization. The glass vessel was then closed and kept for 24 h at room temperature. The gels were cut into small size (~ 1 cm x 1 cm x 1 cm) and washed by transferring into ultrapure water. The gels were weighed, then dried at 80^{o}C for 24 h in a vacuum oven and then weighed again. The swelling degree of the gel is defined as the mass of the swollen gel relative to the mass of the dried gel.

Chapter 4
RESULTS

The experimental results obtained are classified into four following sections: (i) membrane characterization, (ii) study on dextran fouling of UF membranes, (iii) membrane surface modification, and (iv) evaluation of modified membranes performance.

4.1. Membrane Characterization

It is well understood that the performance of an UF membrane is very much influenced by its characteristics. Hence, it is important to know the characteristics of used membranes in this study. The membranes as received from manufactures were characterized with respect to the water permeability, the sieving or rejection measurement, the surface wettability (by contact angle /CA/), the surface charge (by zeta potential /ZP/) as well as the surface morphology and pore structure (by atomic force microscopy /AFM/). Characterization was mainly focused on the membranes used for fouling study (i.e. PES-SG10, PES-GR10, SC-10 and RC-10), which have nominal cut−off of 10 kg/mol. The results are presented in Table 4.1.

It is shown in Table 4.1 that the membranes with identical nominal cut−off (from manufacturer) show different characteristics. Membranes made of PES showed that the PES-SG10 membrane had more than ten times higher water permeability than the PES-GR10 membrane, but both cellulose−based membranes had similar values. All membrane cut−offs obtained from this experiment were lower than the values given by the manufactures except for PES-050H. Significant difference in membrane cut−off was also observed. For 10 kg/mol membranes, the PES-SG10 membrane had the largest and the two cellulose−based membranes

Table 4.1. Observed characteristics of the commercial UF membranes used in this study.

Parameter	10 kg/mol Membranes				PES-SG30	PES-050H	PES-SG100
	PES-SG10	PES-GR10	SC-10	RC-10			
Water permeability (L/m^2hkPa)	0.905[a] ± 0.106	0.080[a] ± 0.016	0.468[a] ± 0.021	0.483 ± 0.012	3.62 ± 0.356	5.71 ± 0.883	5.71 ± 0.941
Contact angle (°)							
(1) captive bubble[b]	61.7 ± 2.4	68.4 ± 4.8	57.9 ± 3.8	33.7 ± 5.3	53.6 ± 3.2	61.1 ± 1.9	44.8 ± 4.2
(2) sessile drop[c]	68.6 ± 1.7	73.1 ± 1.8	< 20	spreading	not done	not done	not done
Zeta potential at pH ~9.5 (mV)	- 35.1	-35.2	-21.1	not done	not done	-26.1	-21.6
Zeta potential at pH ~3.7 (mV)	-5.7	-4.7	-3.3	not done	not done	-7.8	-9.4
Nominal cut-off [d]	10000	10000	10000	10000	30000	50000	100000
Experimental cut-off (g/mol)	~4000[e]	~3000[e]	~2000[e]	~2000[e]	~18000[e]	~220000[f]	~75000[e]
Surface porosity from AFM (%)	13.2 ± 4.4	6.4 ± 4.4	11.0 ± 5.2	not done	not done	not done	not done
Rejection of dextran (T4 / T10 / T15) (%)	7 / 78 / 83	20 / 85 / 89	28 / 92 / 96	18 / 88 / 90	not done	not done	not done

[a] different value with the value in Table 3.1 because more number of samples including different sheet was used in this Table.
[b] measured with the captive bubble technique (air) in water, [c] measured using water as liquid medium
[d] from manufacturer [e] determined with PEG mixtures (see results in more detail)
[f] determined with dextran mixtures (see results in more detail)

had the lowest cut-off values from PEG sieving (cf. Section 4.2.1 in more detail). This observation is supported by observed rejections of these membranes for various dextrans. Comparing the PES-SG100 and PES-050H showed that even though those membranes had different cut−off, they had similar water permeability.

With respect to the wettability, the PES-GR10 membrane showed higher CA than the PES-SG10. For similar membrane cut−off, PES membranes showed higher contact angle than the cellulose−based membranes. Surprisingly, the SC-10 cellulose−based membrane had a relatively high captive bubble CA (~58^{o}), which is much higher than the RC-10 membrane (~34^{o}), meaning that the latter was much more hydrophilic. Sessile drop CA measurements showed that the dry SC-10 membrane was quickly wetted by a water drop (CA < 20^{o}), while for the RC-10 membrane even a spontaneous and complete spreading was observed with the sessile water drop. The ZP values, especially at higher pH, were much larger for the PES as compared to the cellulose−based membranes (cf. 4.2.1 for more detail).

Figures 4.1 and 4.2 show the AFM topography images of the top membrane surface. Membrane pores may be identified as dark areas (the bright regions indicate the highest areas, and the dark regions indicate either depressions or pores). However, the quantification of pore size or even of pore density and surface porosity using AFM is complicated. Even though several quantifications had been proposed in the literature (e.g., [152,153]), the surface roughness in combination with the variations of pore size and pore shape cause major problems, which have not fully been solved yet. First, if the pore size is too small compared with the tip size, a pore can not be precisely “seen” in the AFM topography image (due to a “convolution effect”). Second, even for larger pores, it is difficult to differentiate between surface roughness and pores. It is clear that the surface roughness of the two PES membranes

was significantly different (cf. Figure 4.1 a & c); for the PES-SG10 membrane, R_{ms} and R_a were 0.90–1.03 nm and 0.70–0.82 nm, respectively, while for the PES-GR10 membranes, R_{ms} and R_a were 0.64–0.74 nm and 0.45–0.59 nm, respectively. Along with the pictures, this indicates that the PES-SG10 membrane had a higher density of pores and a larger average pore size than the PES-GR10 membrane; i.e. the AFM tip can access more membrane pores. For membrane made from the same material, but different cut–off (PES-SG10, PES-SG30 and PES-SG100, cf. Figure 4.2), it is clearly seen that the increase in membrane cut–off increased both the appearance of the dark region on the image (indicating larger pore size) and the roughness of the surface (for 30 kg/mol membrane, R_{ms} and R_a were 1.96 nm and 1.56 nm, respectively, while for 100 kg/mol membrane R_{ms} and R_a were 4.98 nm and 3.83 nm, respectively). Increasing surface roughness as increase in membrane cut–off was due to the fact that the larger membrane cut–off gave larger pore size; hence the tip can enter deeper into the pores and access more the pore in the surface layer. For the SC-cellulose membrane, pores on the skin surface were also observed even though not as clear as for PES membranes (cf. Figure 4.1 e). This was due to a higher surface undulation than for the PES membrane as evidenced by higher surface roughness (R_{ms}=1.15–1.30 nm, R_a=0.94–0.97 nm). After considering all the above considerations, a quantification of surface porosity yielded 13.2 $\pm$ 4.4%, 6.4 $\pm$ 4.4% and 11.0 $\pm$ 5.2% (cf. Figure 4.1 b, d, f) for PES-SG10, PES-GR10 and SC-10 membranes, respectively. However, for the cellulose–based membrane, due to the different polymer material and surface structure, the results of this quantification may be influenced by much larger systematic error (see Chapter 5).

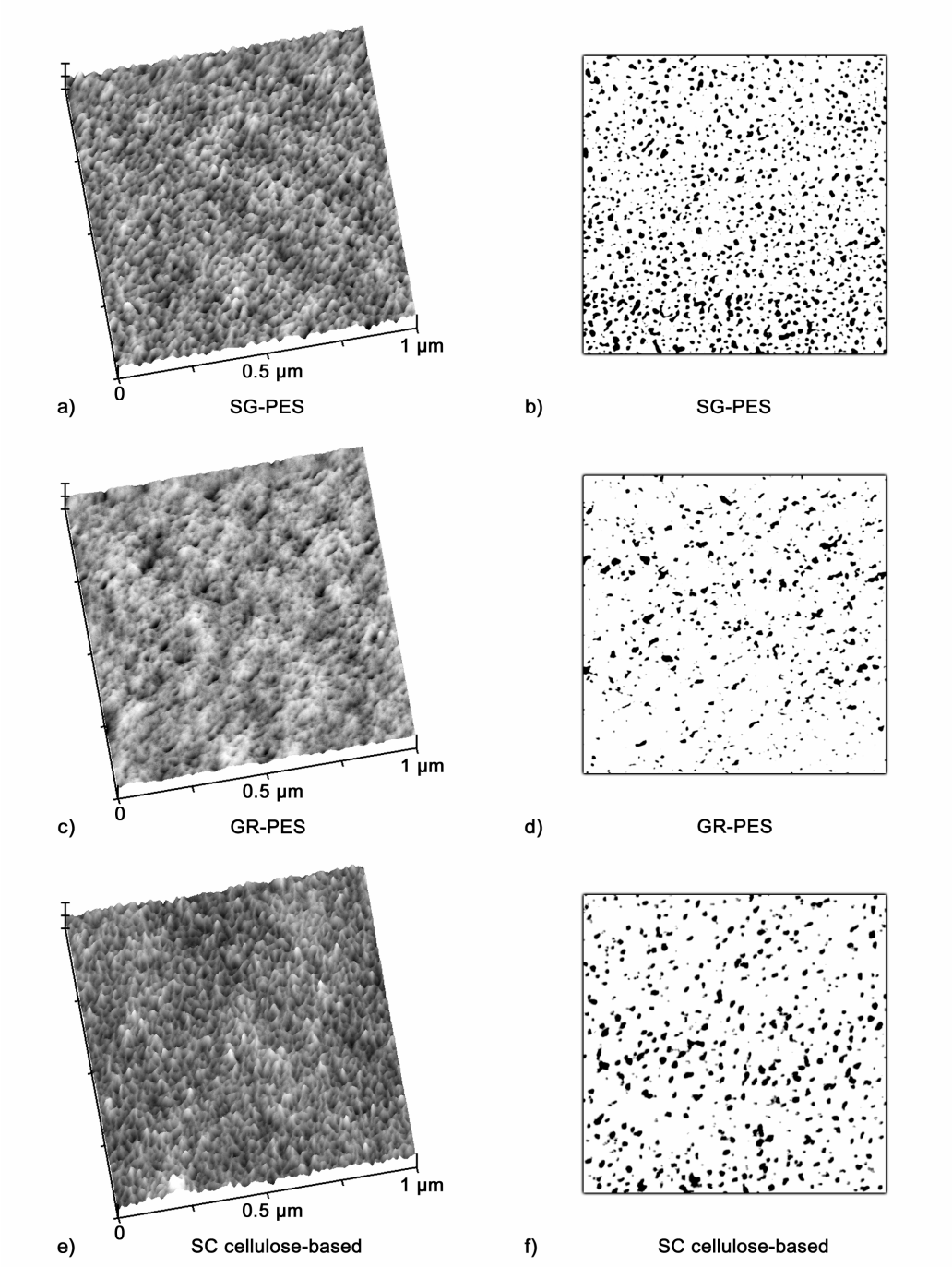

Figure 4.1. AFM topography images (left) of the top skin layer surface of 10 kg/mol UF membranes (as received from manufacturer) and visualization of pore distribution (right): (a, b) PES-SG10, (c, d) PES-GR10, (e, f) SC-10.; topography height scale: 10 nm/div; pores are identified as black regions.

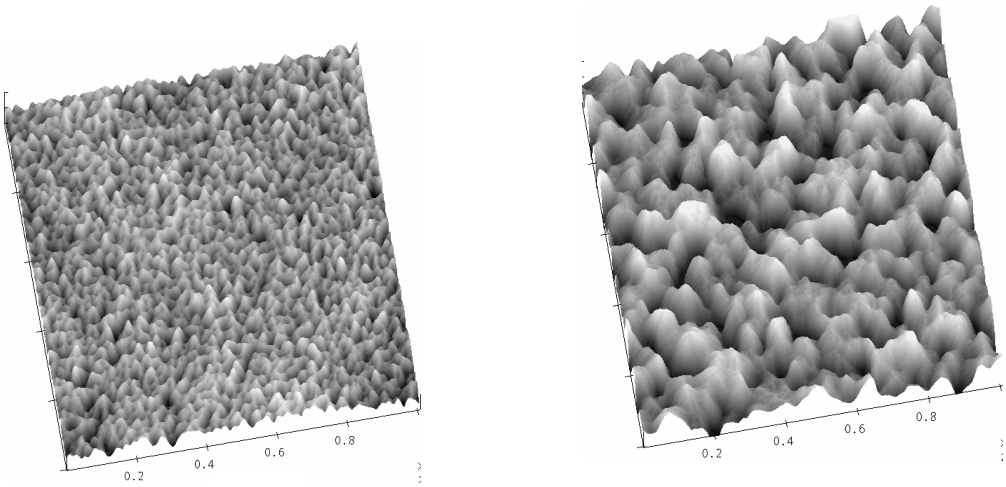

(a) (b)

Figure 4.2. AFM topography images of the top skin layer surface of PES-SG30 (a) and PES-SG100 (b) membranes (as received from manufacturer); topography height scale: 10 nm/div; pores are identified as black regions.

4.2. Study on Dextran Fouling of UF Membranes

In this study, investigation of membrane–solute interactions (fouling by static adsorption) including their impact on membrane characteristics, solute adsorption on non–porous PES film surface and membrane–solute–solute interactions (UF) are performed. The results are presented in the following subsections.

4.2.1. Membrane–solute interactions (fouling by static adsorption)

UF fouling is strongly influenced by membrane–solute interactions. Therefore, dextran–membrane interactions were firstly investigated. Membrane–solute interactions were investigated by exposing the outer membrane surface to a dextran solution without any

pressure. For simplicity reason, the membrane−solute interactions are called adsorptive fouling in further discussions.

Effect of adsorptive fouling on membrane water flux. The effect of dextran concentration on the membrane water flux was firstly studied using PES-SG10. The water flux before and after exposing to the dextran solution were measures and RFR (cf. Eq. (3.1), Chapter 3) was used as the evaluation indicator. Dextran concentration was varied from 0.2 to 25 g/L and exposure time was 3 h. Myoglobin was also used for comparison study. As clearly seen in Figure 4.3, after exposing to both dextran and myoglobin solutions, the membrane water fluxes were significantly smaller than the initial water flux as evidenced by significant value of RFR. The increase in dextran concentration from 0.2 to 5 g/L increased RFR, and beyond 8 g/L a plateau condition seemed to be reached. With myoglobin instead of dextran, the RFR was much larger and reached a plateau value at much lower concentration, i.e. around 0.5 g/L.

Assuming a correlation with the amount of adsorbed solute on the solid membrane surface, the RFR was then analyzed using the Langmuir (Model 1) and the Freundlich (Model 2) models for adsorption [154]. Fits of the experimental data gave the empirical correlations presented in Table 4.2. A good agreement between experimental results with the Langmuir model was observed at lower concentrations for both dextran and myoglobin. At higher concentrations (in the plateau region), the experimental data were somewhat higher than predicted by the Langmuir model and larger deviations were observed for protein than for dextran. However, the Freundlich model, with no limit for adsorption capacity, yielded even larger deviations from the experimental data in the range of higher concentrations.

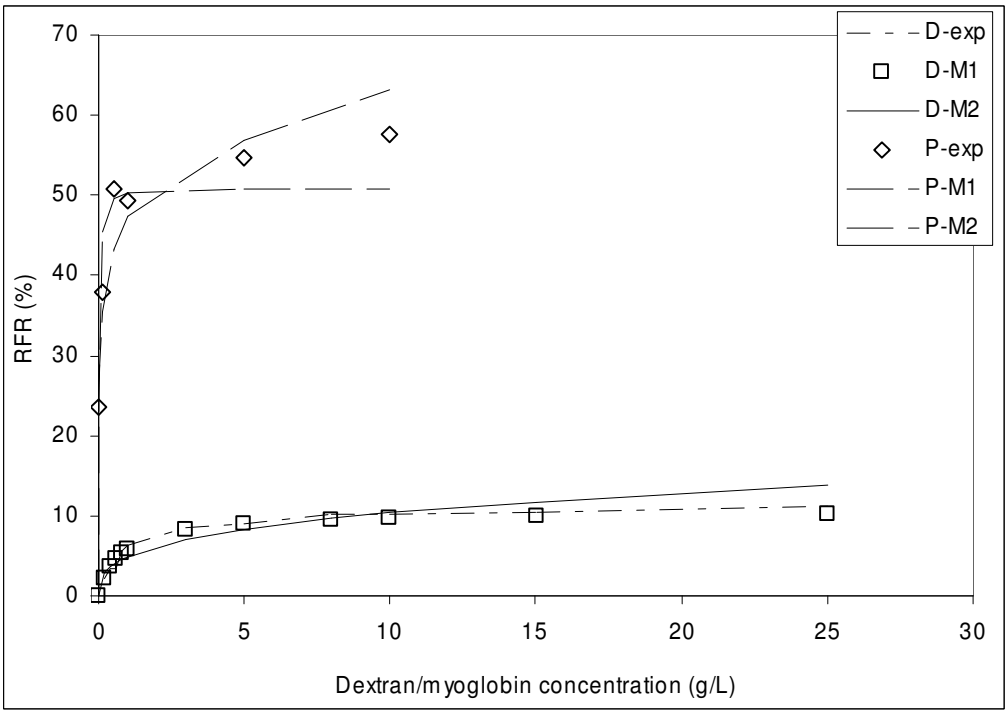

Figure 4.3. Effect of solute concentration on RFR after static adsorption (isotherm adsorption; PES-SG10 membrane, exposure time 3 hours, D: dextran T10, P: myoglobin, exp: experimental data, M1: Langmuir model, M2: Freundlich model).

Table 4.2. Empirical model of RFR as a function of solute concentration (PES-SG10 membrane).

Model	Dextran	Myoglobin
Langmuir (Model 1)	$\mathrm{RFR} = \frac{0.104\mathrm{C}}{0.774 + \mathrm{C}}$ $R^2 = 0.959$	$\mathrm{RFR} = \frac{0.508\mathrm{C}}{0.012 + \mathrm{C}}$ $R^2 = 0.942$
Freundlich (Model 2)	$\mathrm{RFR} = 0.049\mathrm{C}^{0.324}$ $R^2 = 0.895$	$\mathrm{RFR} = 0.473\mathrm{C}^{0.125}$ $R^2 = 0.896$

The effect of exposure time on RFR was then investigated using PES-SG10. The exposure time was varied from 30 to 240 min and dextran solution used was 10 g/L. Figure 4.4 shows the RFR as a function of exposure time. After an initial time delay of about 30

minutes, as exposure time was increased, the RFR would linearly increase with time, and after about 150 minutes, the RFR seemed to increase only very slightly with further increasing exposure time. Apparently, after 150 minutes the surface coverage by dextran has approximated the maximum value. Note that all adsorption experiments were done with stirring in order to minimize the boundary layer mass transfer resistance.

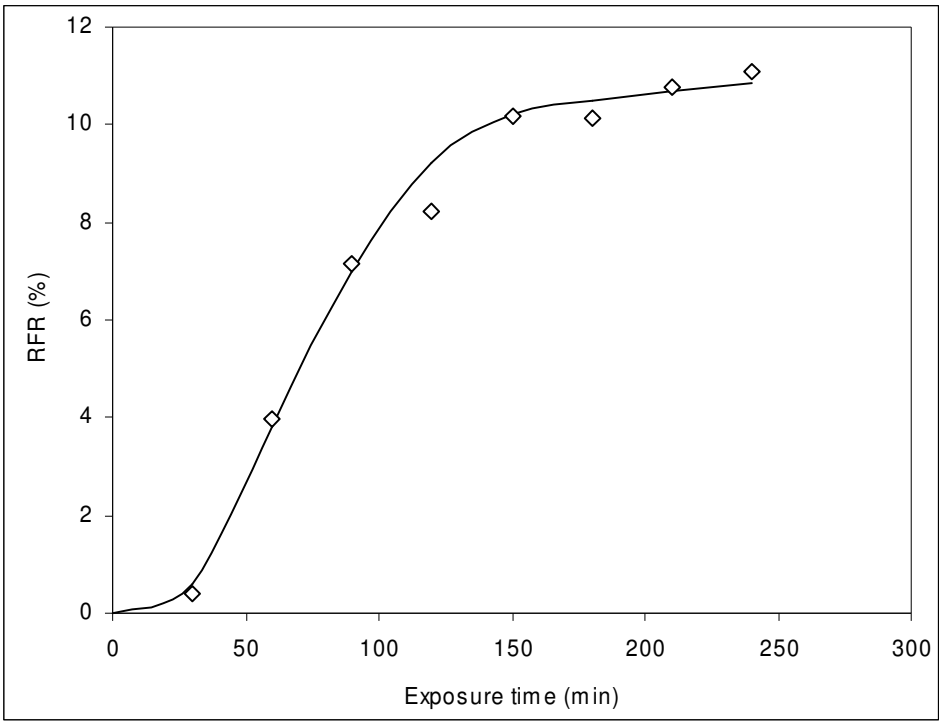

Figure 4.4. Effect of exposure time on RFR after static adsorption (adsorption kinetics, dextran T-10 (10 g/L), PES-SG10 membrane).

The effect of adsorptive fouling on RFR was also studied for various membrane types (Figure 4.5). Exposing the PES membranes to the dextran solution yielded RFR ranging from 4 to 12% and from 11 to 15% for PES-SG10 and PES-GR10 membranes, respectively. The adsorptive fouling using myoglobin on the PES membranes yielded higher flux reduction than using dextran. Then, a clear difference in RFR between PES-SG10 and PES-GR10 membranes

after exposing to the dextran as well as protein solution was observed. In contrast, no significant changes in water flux were observed for both cellulose–based membranes after exposing to the dextran solution, and only very minor flux reductions were observed after protein adsorption. Furthermore, there was also a clear effect of dextran molar mass on RFR indicating that a more effective pore blocking occurred with larger dextran molecules (cf. also Figure 4.6).

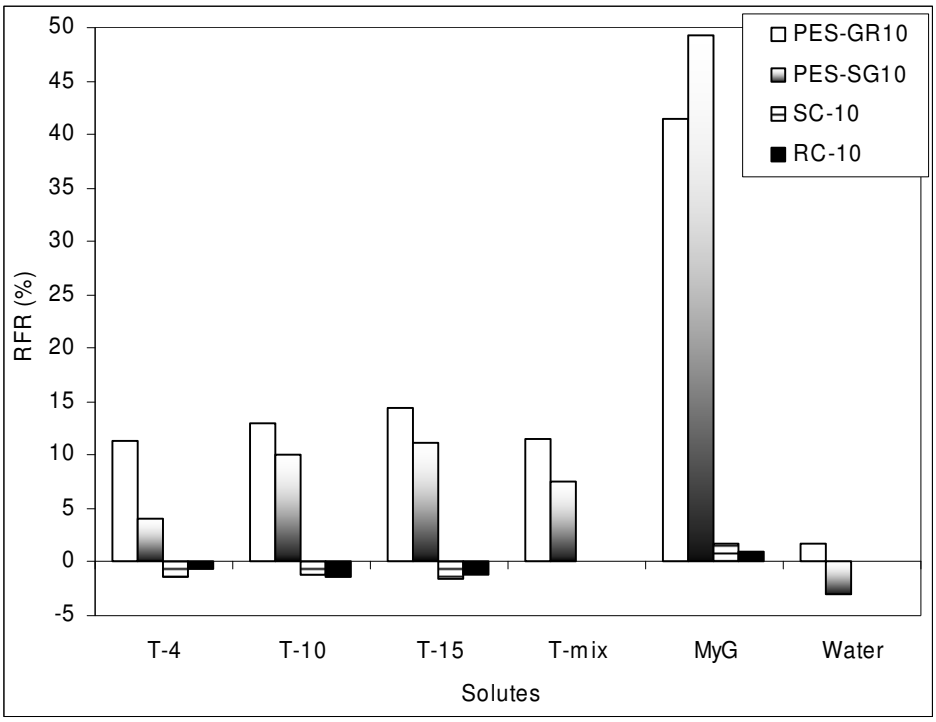

Figure 4.5. RFR after static adsorption (3 hours) of various dextrans (T-4, T-10, T-15, and T-mix; 10 g/L) and myoglobin (1 g/L, pH 7). Control experiment using water yielded no difference in water flux after exposing.

The effect of dextran molar mass (cf. Table 3.2, Chapter 3) on RFR was also investigated using PES membranes (Figure 4.6). It was clearly seen that as the molar mass of dextran was increased, the RFR would firstly increase; however, beyond ~70 kg/mol, the RFR

decreased again with further increasing molar mass of dextran. In addition, the PES-SG10 membrane showed a smaller flux reduction at low molar masses, but a larger flux reduction at high molar masses when compared to the PES-GR10 membrane.

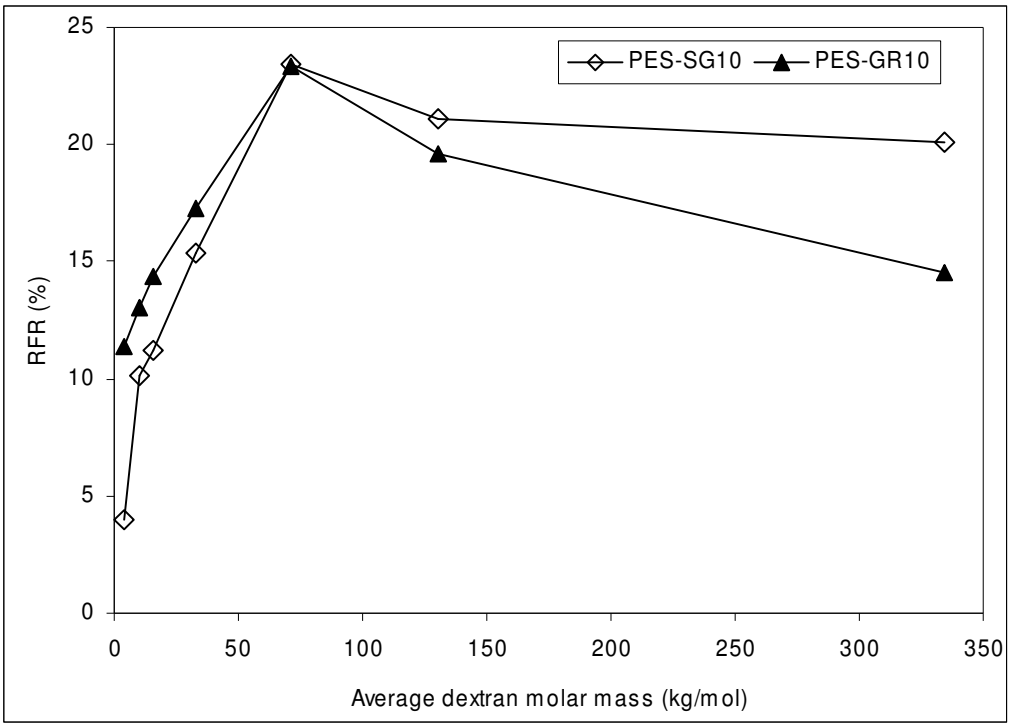

Figure 4.6. Effect of dextran molar mass on RFR for PES membranes after static adsorption (solute concentration 10 g/L, exposure time 3 hours).

Effect of adsorptive fouling on ultrafiltration sieving. Effect of adsorptive fouling on the apparent membrane pore size distribution was studied by measuring the membrane sieving before and after exposing to the dextran solution. Membrane sieving was measured using mixed PEGs as the solute (PEG was chosen because exposing the membrane to the PEG solution did not change significantly the water flux). Although during measurement hindrance of the flow of smaller molecules by large molecules could be a problem [155], this method is expected to describe the effect of adsorptive fouling on pore size of the membrane in more

details than the RFR for water. The molar masses of the PEGs used were then correlated with their Stokes-Einstein radii according to the following equation [155]:

$$\mathrm{rPEG}\left(\text{Å}\right) = 0.262\sqrt{\mathrm{M}\left(\frac{\mathrm{g}}{\mathrm{mol}}\right)} - 0.3 \qquad (4.1)$$

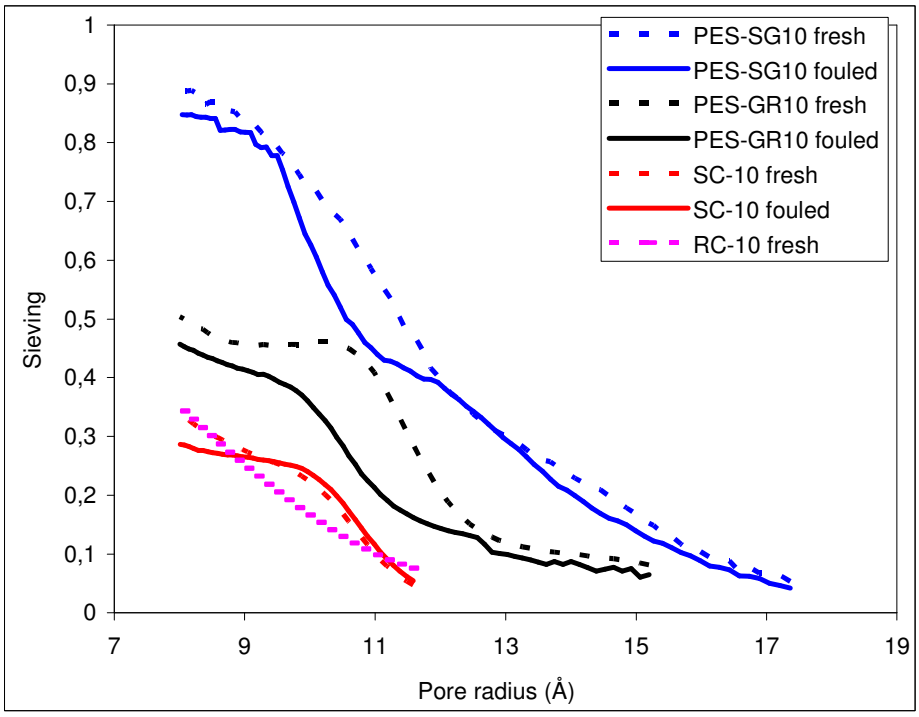

Figure 4.7. Membrane sieving curves – determined with PEG mixtures in water (1 g/L) at low initial filtrate flux (26±2 L/m^{2}h) – for fresh and fouled with dextran T-10 (10 g/L) (adsorptive) membranes. The molar mass of PEGs used were converted to PEG radii using Eq. (4.1) (e.g., pore radii of 7 and 17 Å correspond to PEG molar masses of ~ 0.78 and ~ 4.3 kg/mol, respectively).

As presented in Figure 4.7, the three different fresh UF membranes (PES-SG10, PES-GR10 and RC-10) with the same nominal cut–off (10 kg/mol) showed significantly different sieving curves under the same test conditions. Similar sieving curve was observed for both cellulose–based membranes (SC-10 and RC-10). Then, the data (nominal cut–off) obtained

from this experiment were smaller than the values given by the manufacturer (see also Table 4.1). This observation is supported by a study by Mulherkar and van Reis [28]. They had also found a significant different between nominal cut–off and experimental data based on sieving curve analysis.

For both PES membranes, adsorptive fouling caused a significant shift of the sieving curves towards lower pore radii, and it also reduced the nominal cut–off. The nominal cut–off reductions were 5% (from 16.3 to 15.5 Å) and 11% (from 14.2 to 12.6 Å) for the PES-SG10 and the PES-GR10 membranes, respectively. Also, the shifts in the lower pore size range showed the same trends, i.e. larger effects for the PES-GR10 membrane. In contrast, the sieving curves for cellulose–based membrane (SC-10) did not change significantly after exposing to dextran solution. All these effects were in qualitative agreement with results of relative water flux reduction.

Effect of adsorptive fouling on membrane contact angle (CA). CA is one of the most sensitive techniques with changing of solid surface characteristic. Thus, CA was used to evaluate dextran adsorptive fouling. Membrane CAs before and after exposing to the dextran solution were measured using captive bubble method. The results are presented in Table 4.3.

Table 4.3. Static contact angles of fresh and fouled (adsorptive) membranes[a]

Membrane	CA of fresh membrane (°)	CA of dextran-fouled membrane[b] (°)	CA of myoglobin-fouled membrane[c] (°)
PES-SG10	61.7[d] ± 2.4[e]	55.9 ± 2.9	54.2± 3.1
PES-GR10	68.4 ± 4.8	59.2 ± 4.8	n.d.
SC-10	57.9 ± 3.8	55.9 ± 3.6	n.d.

[a]measured with the captive bubble technique (air) in water (see chapter 3 for details)
[b]fouled by exposing to dextran T-10 solution (10 g/L); [c]fouled by exposing to myoglobin solution (1 g/L)
[d]measured contact angle; [e]standard deviation, [f]n.d.; not done

It is clearly seen that all membranes that had similar cut−off showed different CA (cf. Sections 4.1 and 5.1 in more detail). Exposing the membranes to the dextran solution reduced the contact angle significantly for both PES membranes. By contrast, for the cellulose−based membrane (SC-10) no change was observed. However, it should be also noted that after contact with dextran, the contact angles for all three membranes were almost equal. Furthermore, the changes in contact angle were also different for the two PES membranes (~9.5% for PES-SG10 and ~13.5% for PES-GR10), i.e. the more hydrophobic membrane did change more significantly, and this observation correlated with the larger effects onto water permeability (cf. Figure 4.5) and sieving (cf. Figure 4.7).

Effect of adsorptive fouling on surface charge of membrane (ZP). The surface charge of a membrane can be estimated by measuring the streaming potential for calculating the zeta potential. This measure can also be very sensitive to changes of the surface properties [156]. Tangential streaming potential was used because other technique, i.e. transmembrane streaming potential underestimates the ZP for UF membrane due to overlapping planes of shear [157]. The membrane surface charges were investigated before and after exposing to the dextran under the same conditions. The results are depicted in Figure 4.8.

It is clearly seen that the absolute zeta potential value for the PES membranes was large and decreased towards acidic pH values. The signs of the zeta potential for the PES membranes (indicating a negative surface charge) were the same as reported by Causserand *et al.* [158], but the absolute values were higher. Staude and co−workers [149] also reported that the zeta potential of polysulfone membrane showed similar characteristic for surfaces with no fixed charge, the surface charge was even slightly positive at pH < 4 and increasingly negative with increasing pH until it reached a plateau value. Then, it is also seen that the relatively

large zeta potential of SC membrane, which also decreased towards acidic pH values. However the values for the SC cellulose–based membrane were significantly smaller than for both PES membranes.

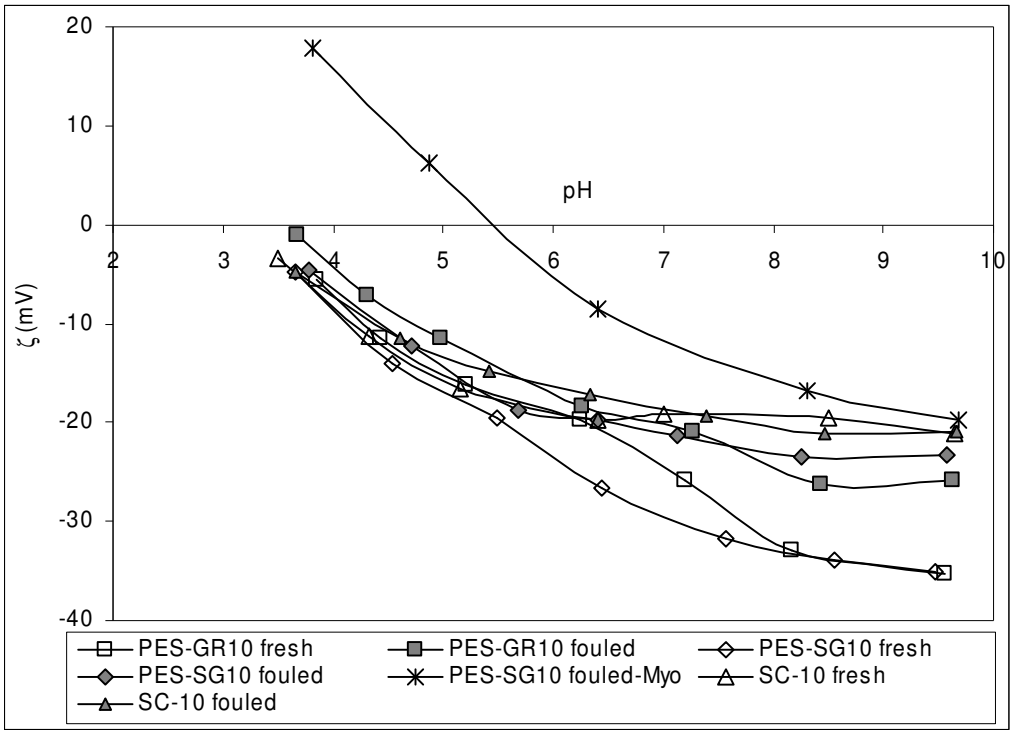

Figure 4.8. Zeta potentials, ζ, as a function of pH for fresh membranes and the same membranes after static adsorption (3 hours) of dextran T-10 (10 g/L), calculated from tangential streaming potential of outer surface of membrane (0.001 mol/L KCl, pH adjusted with KOH or HCl, 25°C). Fouled membrane by myoglobin (PES-SG10 fouled-Myo) is included for comparison.

Exposing the membranes to the dextran solution changed the zeta potential significantly for PES membranes, but not for cellulose–based membrane. In a recent study using self-assembled PEG-terminated monolayers on a gold surface, Chan *et al.* [159] had also found that the increase of amount of PEG (i.e. thickness of the PEG brush layer) decreased the

zeta potential. Furthermore, the reduction of negative ZP was larger for myoglobin than for dextran, and for pH <4.9 the membrane had positive ZP after myoglobin adsorption.

Effect of adsorptive fouling on surface morphology. Atomic force microscopy (AFM) was used to visualize the effect of dextran fouling by adsorption on surface morphology. The AFM topography images before and after exposing to either dextran or protein solution are shown in Figure 4.9.

Images of the native membranes after washing with water and drying (at room temperature) were used here in order to take into account the effect of wetting the membranes with aqueous solution and subsequent drying prior AFM onto surface morphology (see [160] for a discussion why using dry samples). Significant changes in surface morphology were observed for both PES membranes with both solutes. The average surface roughness (R_a) changed from 0.94–1.12 nm to 0.64–0.73 nm and from 1.09–1.23 nm to 1.40–1.51 nm for PES-SG10 and PES-GR10 membranes, respectively, after exposing to the dextran solution. All changes were much more pronounced for the PES-GR10 than for the PES-SG10 membrane. Surprisingly, the change in AFM topography images of PES membranes after exposing to the protein solution seemed to be not greater than after exposing to the dextran solution; again changes were more pronounced for PES-GR10 than for PES-SG10 membranes. However, protein aggregates were occasionally also observed on the PES membranes, while this observation was not the case for dextran. In contrast to the PES membrane, the surface morphology of the cellulose–based membranes did not change after exposing to the dextran solution (Figure 4.10 (a) and (b)).

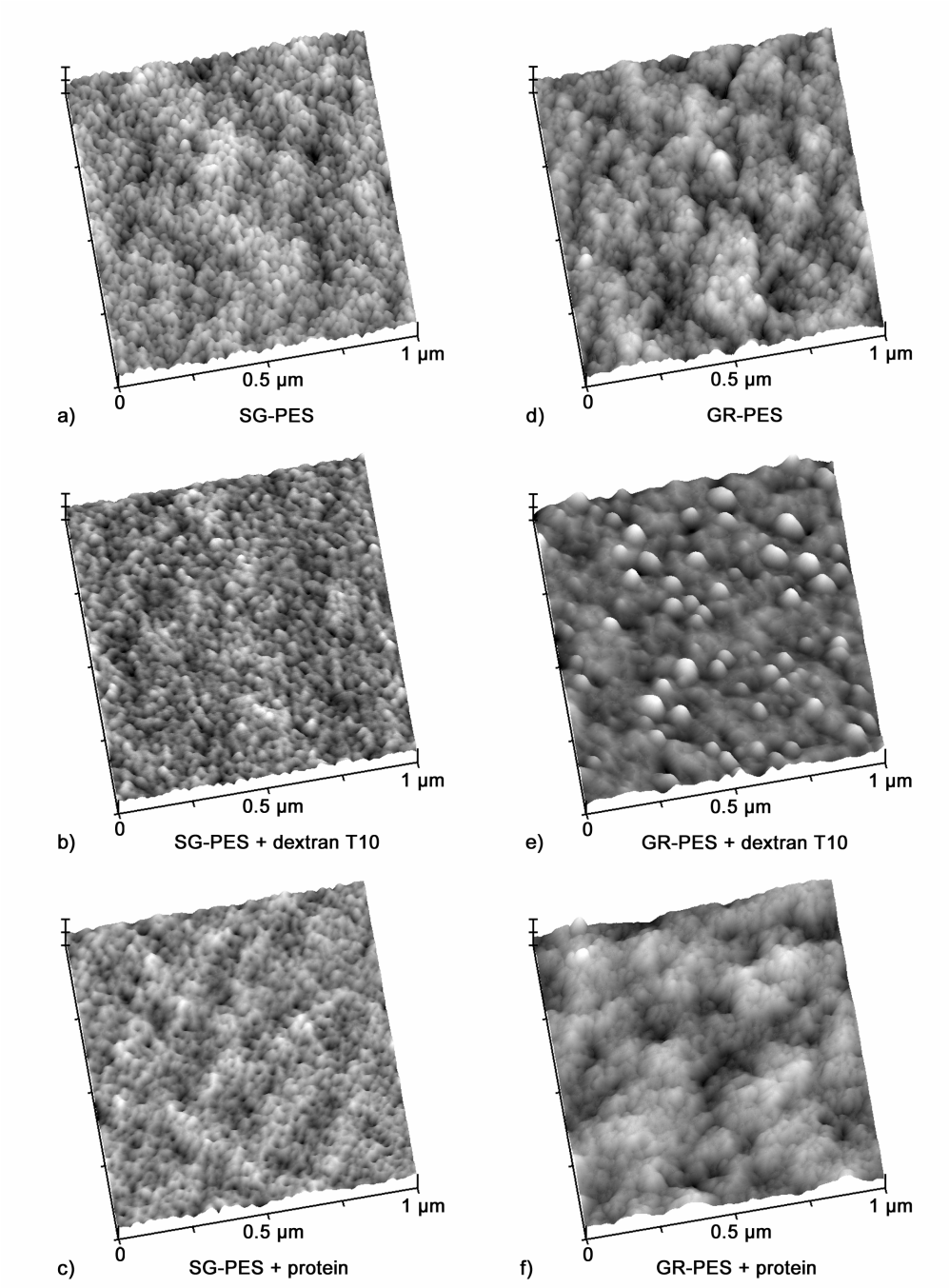

Figure 4.9. Effect of adsorptive fouling on membrane surface morphology. Left: PES-SG10; (a), (b) and (c) are fresh, after exposing to the dextran solution (T10 , 10 g/L, 3 h exposure) and after exposing to the myoglobin (1 g/L, 3 h exposure) solution, respectively, right: PES-GR10; fresh (d),(e) and (f) are fresh, after exposing to the dextran solution (T10, 10 g/L) and after exposing to the myoglobin solution (1 g/L), respectively.

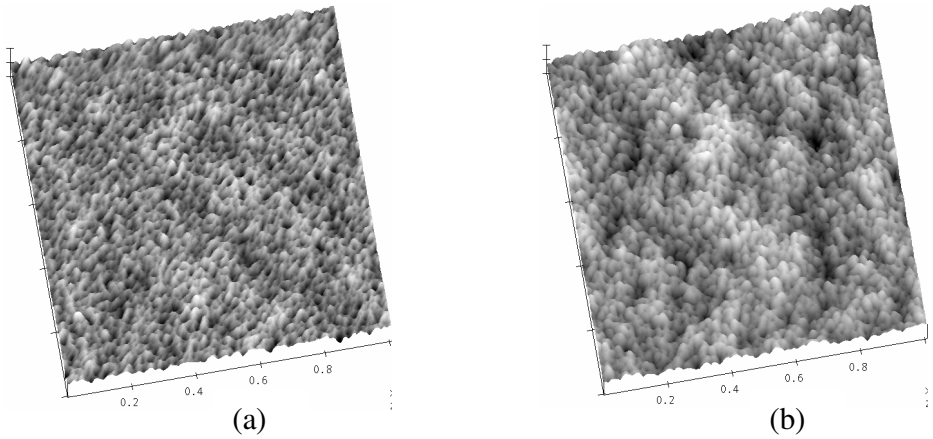

(a) (b)

Figure 4.10 Effect of adsorptive fouling on surface morphology of SC-10 cellulose–based membrane: (a) SC-10 fresh and (b) SC-10 after exposing to the dextran solution (T-10, 10 g/L, 3 h exposure).

Characterization of adsorbed dextran using ATR-IR spectroscopy. Attenuated total reflection infrared spectroscopy (ATR-IR) was used to analyze the surface chemistry of both fresh and fouled membranes. As presented in Figure 4.11, both PES membranes showed typical aromatic bands at 1578 and 1485 cm^{-1} (due to benzene ring C=C bond stretch). The aromatic ether band at around 1240 cm^{-1} was strongly observed. In addition, a significant absorbance band at ~1660 cm^{-1} was found in both PES membranes, and the assignment to a primary amide stretch (-CO-NH-) was supported by the appearance of another band at ~3360-3340 cm^{-1}. This band was presumably from polyvinylpyrrolidone (PVP), which is a well–established additive for the manufacturing of UF membranes from PES. However, after washing with water, the IR band of this additive was completely absent for the PES-GR10 membrane, but only reduced in intensity for PES-SG10 membrane (Figure 4.12). Other preservatives with bands at ~3600-3000 cm^{-1} and ~2960-2860 cm^{-1} (presumably from glycerin) were completely washed out with water for both PES membranes.

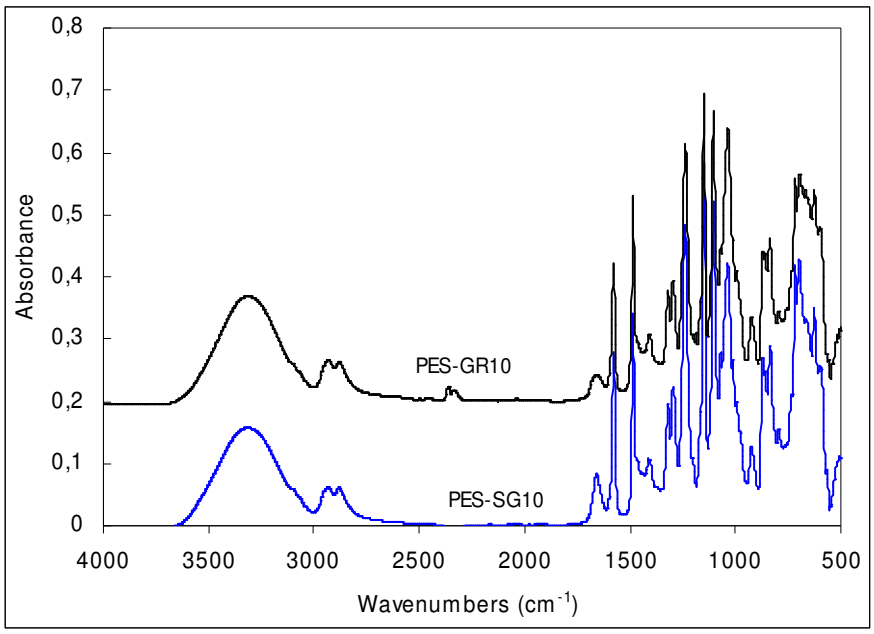

Figure 4.11. ATR–IR spectra of native PES membranes (as received from manufacture without treatment).

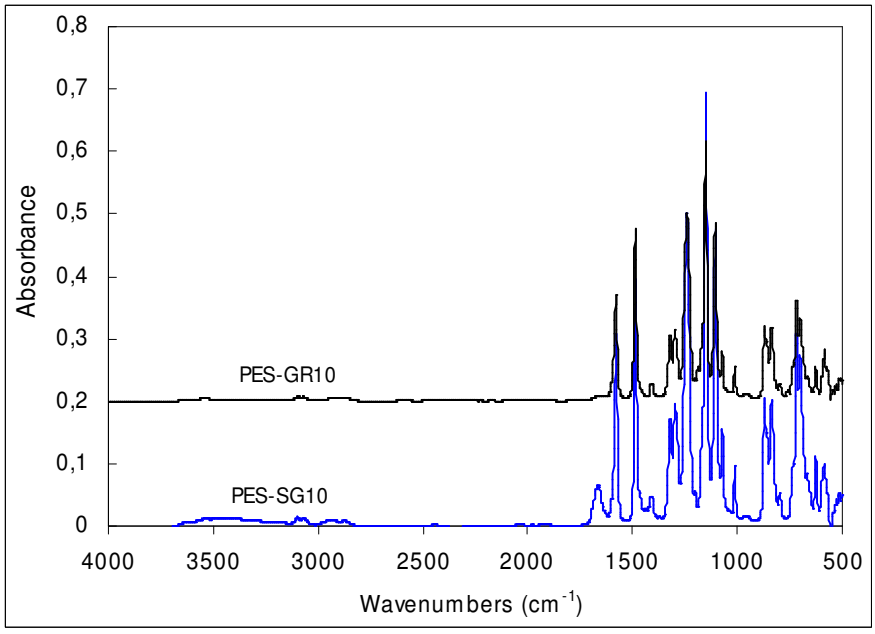

Figure 4.12. ATR–IR spectra of the surface of PES membranes after washing with water and drying at room temperature.

In case of cellulose–based membranes, as presented in Figure 4.13, SC-10 and RC-10 membranes basically had similar infrared spectra indicating that they were made of similar material. However, difference in band intensity for –CH stretching located at ~2920 cm^{-1} and ~2850 cm^{-1} was observed. Significant difference in intensity was also observed for C–O single bond stretching (belongs to ether linkage) at wave number of ~1025 cm^{-1}. No ester band at ~ 1725 cm^{-1} was observed for both cellulose–based membranes. Exposure of SC-10 and RC-10 to the dextran solution did not change the observed infrared spectra.

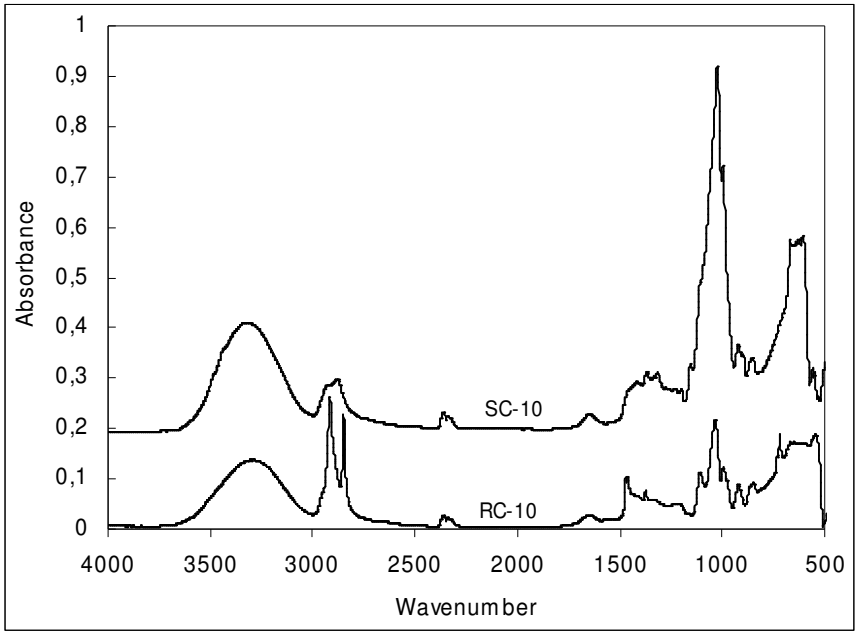

Figure 4.13. ATR–IR spectra of the surface of cellulose–based membranes (as received from manufacture without treatment).

Figure 4.14 shows an example of infrared spectra of PES membranes before and after exposing to the dextran solution. The observed changes in IR spectra – in the ranges ~3600–3130 cm^{-1} (presumably due to O–H glucosidic groups) and ~3100–2800 cm^{-1}

(presumably due to C–H glucosidic groups) – indicate the presence of dextran on the outer membrane surface or in the about 2 μm thick layer sampled by ATR-IR. Further, a quantitative analysis was done by calculating the absorbance band area (3600–3130 cm^{-1}) using an integration method and subtracting the respective absorbance band area of the fresh membrane (after washing with water).

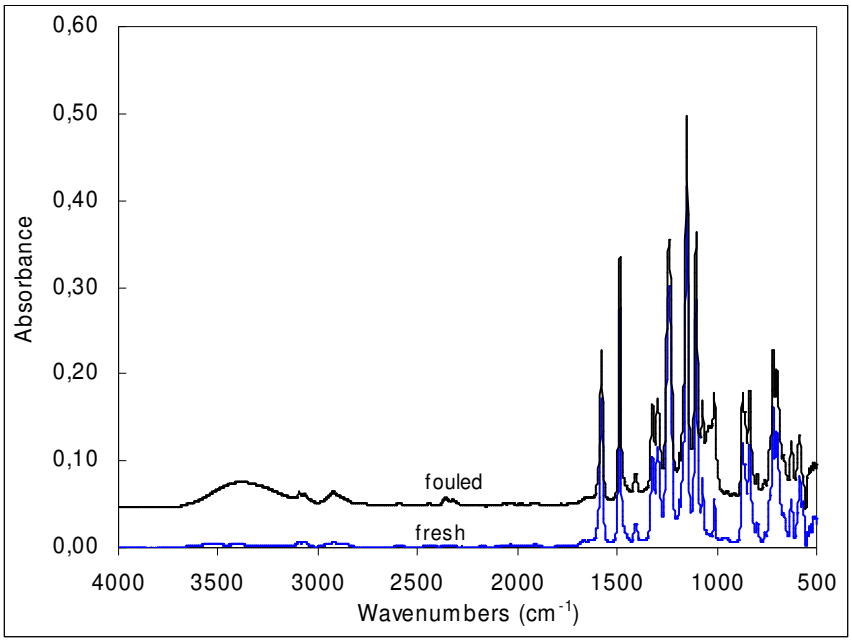

Figure 4.14. ATR–IR spectra of native and fouled PES-SG10 membranes (fresh membrane has been washed with water; fouled membrane was obtained by exposing to 10 g/L of dextran T10 solution for 3 hours).

As can be seen in Figure 4.15, increasing dextran concentration up to 5 g/L increased the IR band area for the fouled membrane. Beyond that value, a plateau condition seemed to be reached. It is also observed that the increases in band area at all dextran concentrations were larger for the PES-GR10 than for the PES-GR10 membrane.

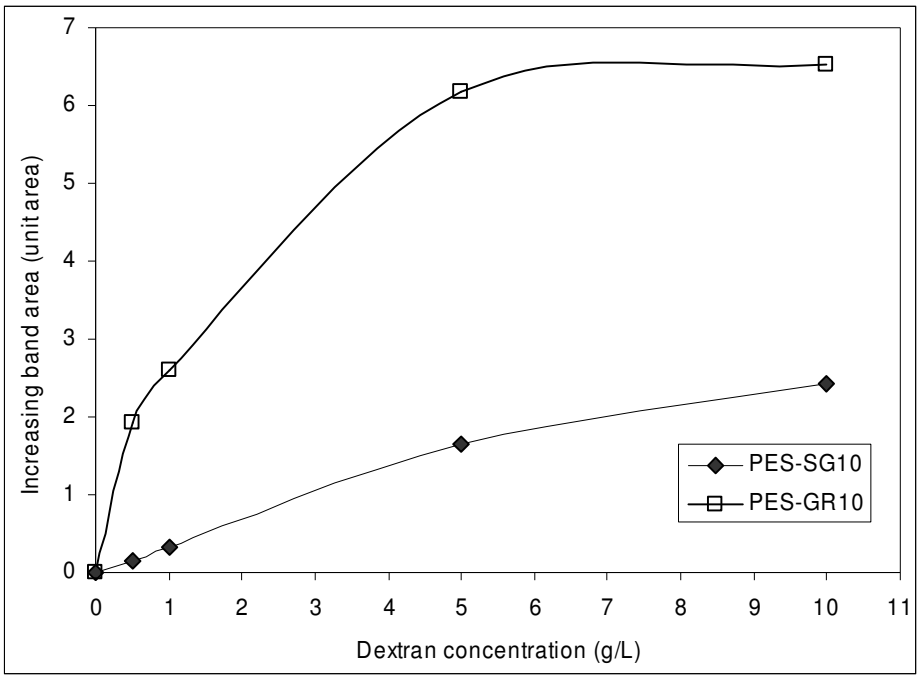

Figure 4.15. Increase in ATR–IR band area (in the range 3130 to 3600 cm^{-1}) for PES membranes after contact with solutions of different dextran T10 concentration (3 hours), relative to ATR–IR spectra for native membranes.

Quantification of adsorbed dextran by simultaneous diffusion adsorption measurements (SDAM). SDAM experiments were used to quantify the amount of dextran and myoglobin attached on the membrane as well as their ability to diffuse through the membrane barrier as expressed by the effective diffusion coefficient. In all experiments both using dextran T10 and myoglobin as the solute, the solute concentration in the high concentration (upstream) half–cell decreased with increasing time whereas the solute concentration in the downstream half–cell increased (cf. Figure 4.16 as an example). This phenomenon indicates that these solutes could penetrate through the pores in the membrane barrier. In contrast to the

dextran T10 and myoglobin, no permeation through the membranes was observed for dextran T100 as evidenced by no dextran in the downstream cell was detected.

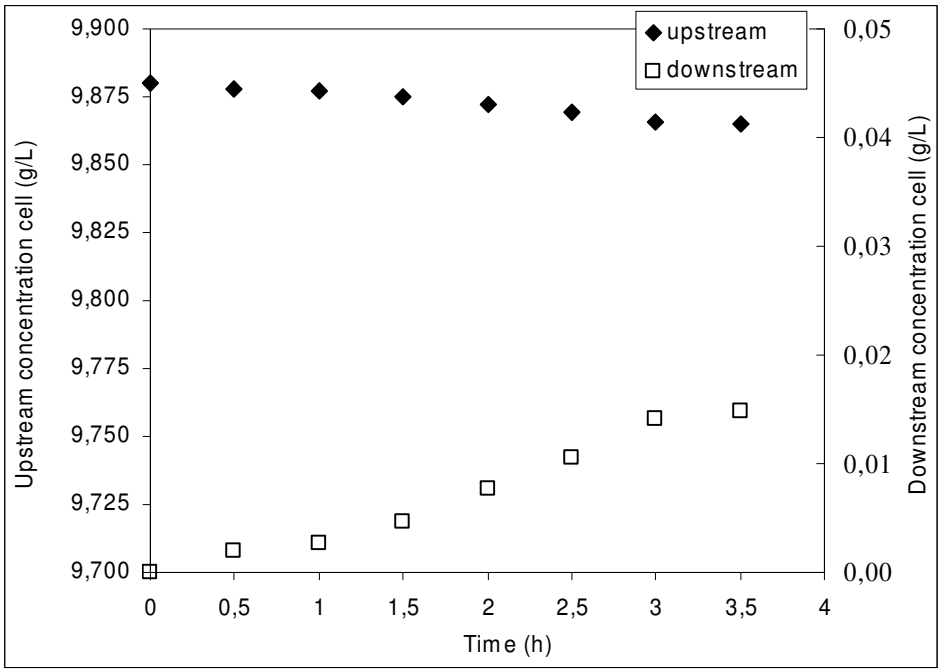

Figure 4.16. Profile of dextran (T-10) concentration during SDAM experiment over time for PES-GR10 membrane. Initial dextran concentration at upstream cell was 10 g/L (measured 9.88 g/L).

The effective diffusion coefficient for various solutes through various membranes is given in Table. 4.4. Dextran diffusion was much faster through the PES-SG10 membrane than through the PES-GR10 and the cellulose–based membrane (SC-10). Diffusion of myoglobin was much slower than diffusion of dextran (measured for the PES-SG10 membrane). Due to the smaller characteristic pore size of the membranes used in this study, the dextran diffusion coefficients obtained in this study were smaller than those obtained by Lebrun and Junter [147].

The significant difference between the amounts of solute released by the upstream half–cell and received by the downstream half–cell indicates that solute adsorption on or solute binding in the membranes also occurred. The amounts of dextran and myoglobin bound to the membranes as deduced from the mass balance are depicted in Figure 4.17. After an initial time delay, the bound amount of dextran increased significantly, but beyond a contact time of 3 hours the values seemed to approach a plateau value. No significant differences with respect to dextran accumulation on the membrane and effective diffusion coefficient were seen for the same membrane type in inverse orientation. For myoglobin, it was observed that the bound mass (on the PES-SG10 membrane) increased linearly between 0 and 1 hour whereas the further increase between 1 and 2 hours was relatively small, and beyond 2 hours a plateau condition seemed to be reached (75 mg/m^2). Assuming that the available surface area on the membranes is similar for dextran and for myoglobin, the surface coverage by myoglobin is ~5 times greater than by dextran (calculated from the ratio of bound amounts). Surprisingly, dextran binding was also observed to the cellulose–based membranes (up to 10 mg/m^2).

Table 4.4. Effective diffusion coefficients (m^2/s) of dextran and myoglobin through different UF membranes.

Membrane	Dextran T10[a]	Dextran T100[b]	Myoglobin[c]
PES-SG10	4.8 x 10^{-12}	no diffusion	9.4 x 10^{-13}
PES-SG30	9.6 x 10^{-12}	n.d.	n.d.
PES-SG100	1.2 x 10^{-11}	n.d.	n.d.
PES-SG10 inverse	5.2 x 10^{-12}	n.d.	n.d.
PES-GR10	2.4 x 10^{-12}	n.d.	n.d.
SC-10	2.0 x 10^{-12}	n.d.	n.d.

[a,b]10 g/L; [c]400 mg/L, n.d.: not done

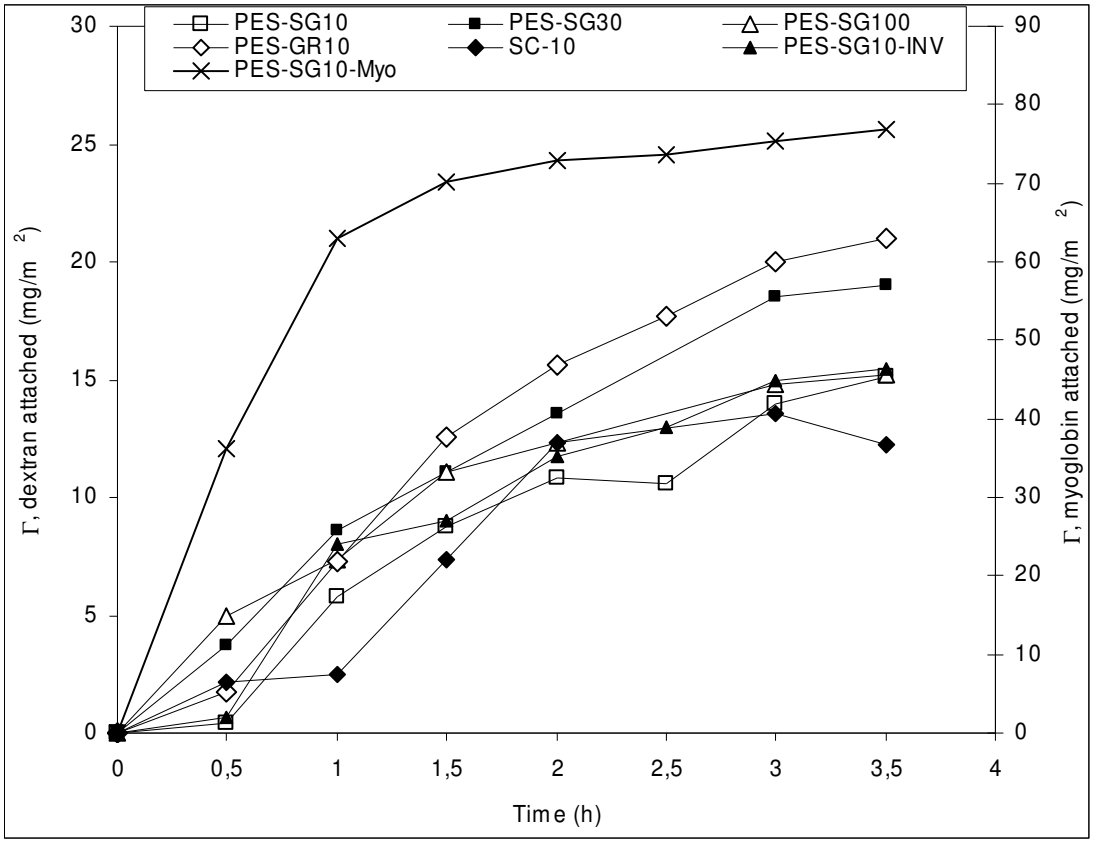

Figure 4.17. Amount of dextran or myoglobin bound on/in the PES membranes (dextran T10 concentration of 10 g/L, "SG-10-INV" … data from diffusion experiment with dextran T10 through membrane in inverted orientation; myoglobin concentration of 400 mg/L at pH 7).

4.2.2. Solute adsorption on non–porous PES film surface

To avoid the effect of pore structure on the interaction between solute and membrane surface, additional experiments were done using non–porous PES films. The effects of adsorption were evaluated by measuring contact angles (Figure 4.18) and zeta potential (Figure 4.19).

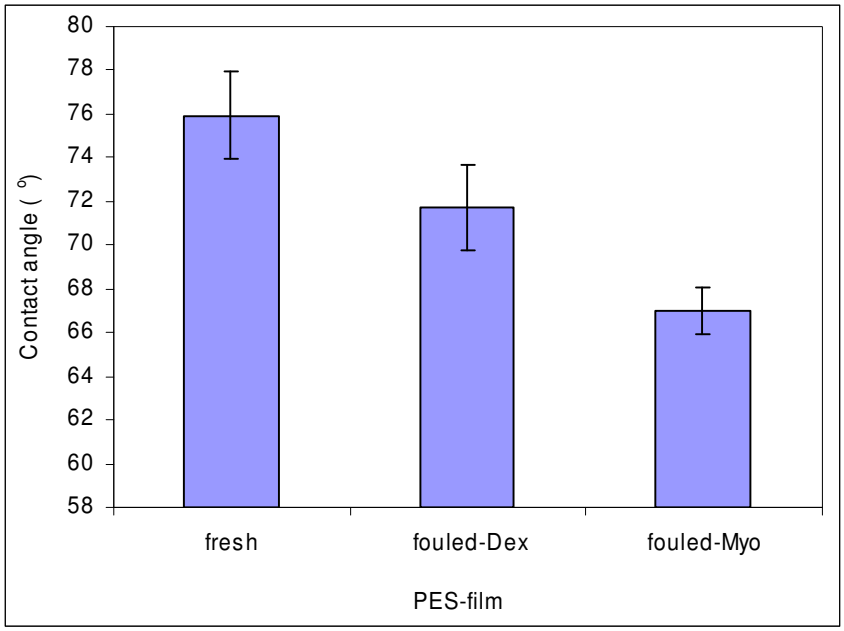

Figure 4.18. Static contact angle measured by sessile drop method using water of non–porous PES film surfaces: fresh and after exposing to either dextran solution (T10, 10 g/L) or myoglobin solution (1 g/L, pH 7) for 3 hours.

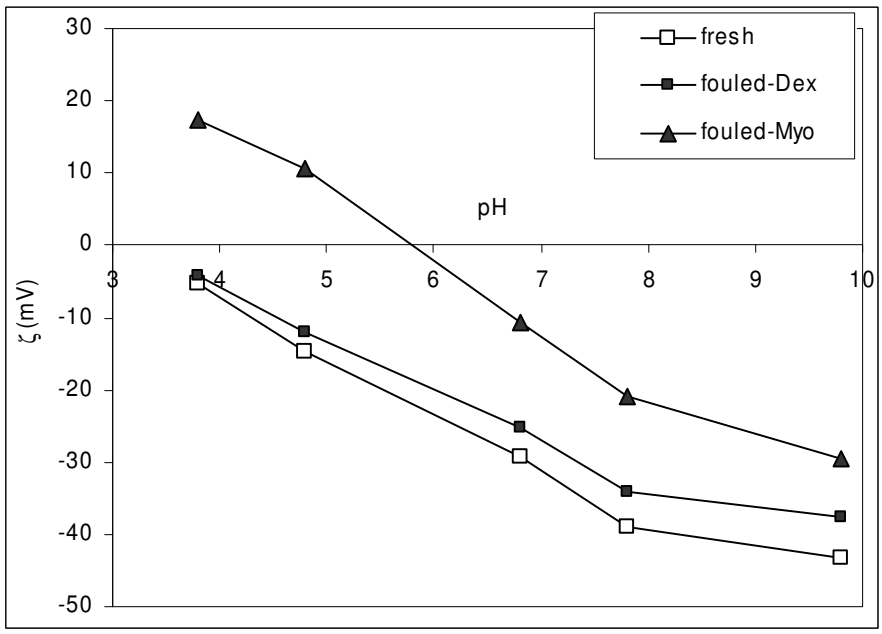

Figure 4.19. Zeta potentials,ζ, as a function of pH (at 0.001 mol/L KCl) for fresh non–porous PES film surfaces before and after exposing to either dextran solution or myoglobin.

Overall, exposing to the solutions of both dextran and protein reduced the CA and absolute ZP of the PES film surface. While the CA of PES did not change significantly (<2^{o}) after exposing to the water under identical conditions, the reduction of CA was larger after exposing to the myoglobin solution than after exposing to the dextran solution. Both biomacromolecules are hydrophilic, and therefore, the apparent hydrophilization of the PES surface strongly indicates solute adsorption. Similar phenomenon, i.e. decrease in contact angle after adsorption of a protein (BSA) had also been reported by Swerdya-Krawiec *et al*. [161]. That the change is smaller in this study may be related to the smaller protein used. The effect of solute adsorption on ZP of non porous PES agrees well with previous results using PES membrane (see Figure 4.8). Again, this observation supports that the effective surface charge of the PES membranes has been reduced by the adsorption of either dextran or protein.

4.2.3. Membrane–solute–solute–interactions (fouling during dead–end stirred UF)

To investigate the membrane–solute–solute interactions, ultrafiltration experiments using dextran were performed. It should be noted that during UF, membrane–solute interactions and solute–solute interactions usually occur. Therefore, in order to obtain also information on the solute–solute interactions in contact with the membrane surfaces, ultrafiltration experiments at a constant transmembrane pressure (300 kPa) were conducted using dextran solution (0.5 g/L). Figures 4.20 and 4.21 show the relative water flux reduction after ultrafiltration and the rejection of dextrans with varied dextran molar mass, respectively. Furthermore, flux profile over time during UF was also investigated.

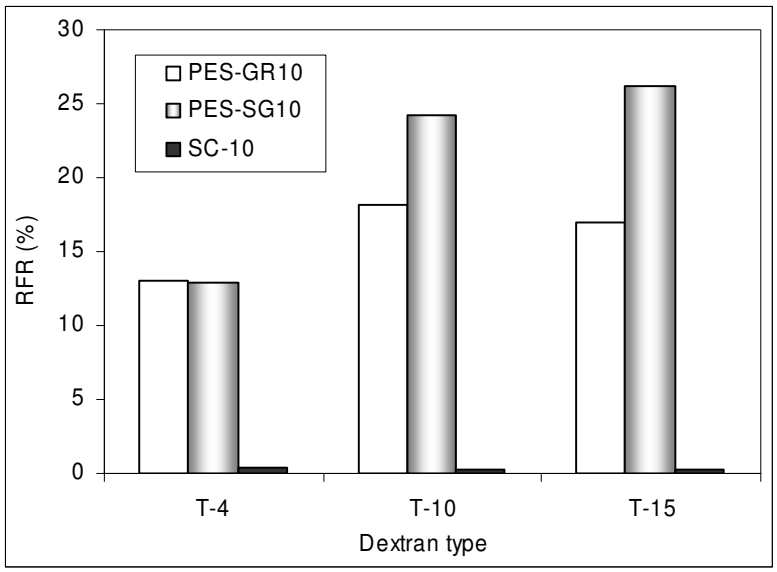

Figure 4.20. Relative water flux reduction after ultrafiltration of various dextrans (concentration of dextran used was 0.5 g/L, transmembrane pressure of 300 kPa).

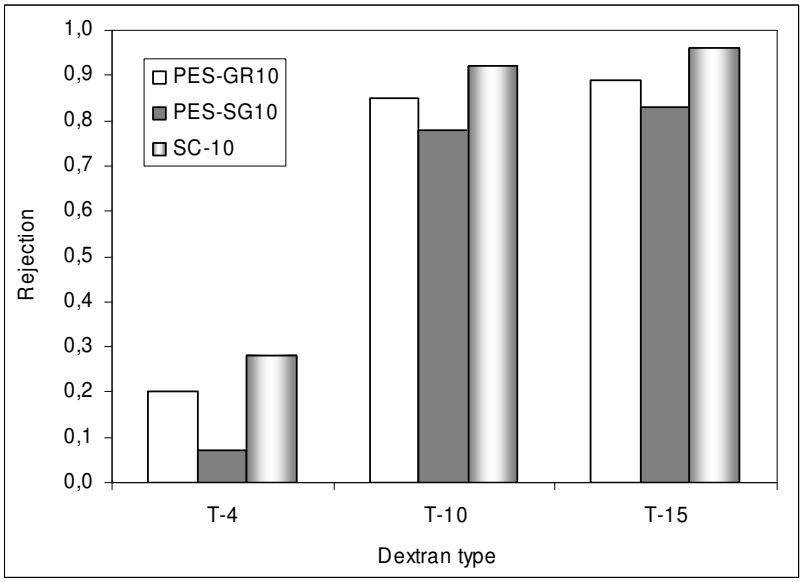

Figure 4.21. Rejection of ultrafiltration membranes with various dextrans (concentration of dextran used was 0.5 g/L, transmembrane pressure of 300 kPa).

For both PES membranes, the relative water flux reductions after ultrafiltration were clearly influenced by the molar mass of dextran. The values of RFR for the PES-SG10 membrane were 12-26%, whereas for the PES-GR10 membrane were 13-17%. It should be noted that the permeability of the PES-SG10 membrane was much higher than the one of the PES-GR10 membrane (cf. Table 4.1). Surprisingly, the water flux of the SC-10 membrane did not change for all dextran types after ultrafiltration, even though the membranes showed the highest rejection (cf. Figure 4.21). Furthermore, the dextran rejections were consistently lower for the PES-SG10 membrane than for the PES-GR10 membrane for all types of dextran. This observation is supported by the sieving results (cf. Figure 4.7). The increase in molar mass of dextran increased the membrane rejection for all membranes. In addition, the partial accessibility of the internal pore structure for dextran evoked above (cf. Table 4.4) has been confirmed. Other result shows that the internal cleaning increased the water flux after ultrafiltration of PES membranes (~6% for PES-SG10 and ~10% for PES-GR10). However, the pure water permeability was not reached again (the ratio of the flux after internal cleaning and the initial flux was ~90% and ~95%, for PES-SG10 and PES-GR10 membranes, respectively). Thus, not only reversible fouling occurred but also irreversible fouling during UF of dextran.

Flux profile over time was investigated by ultrafiltration of dextran solution (1 g/L) and myoglobin (0.1 g/L, pH 7) at constant transmembrane pressure with the same initial water flux. Only PES-SG10 and SC-10 were used. It should be noted that the experiments were performed at lower pressure than experiments presented in Figure 4.20 and using 10 times lower solute concentration compared to the conditions used in the adsorption / RFR studies. In addition, the solute rejection and the RFR after UF were also measured (Table 4.5).

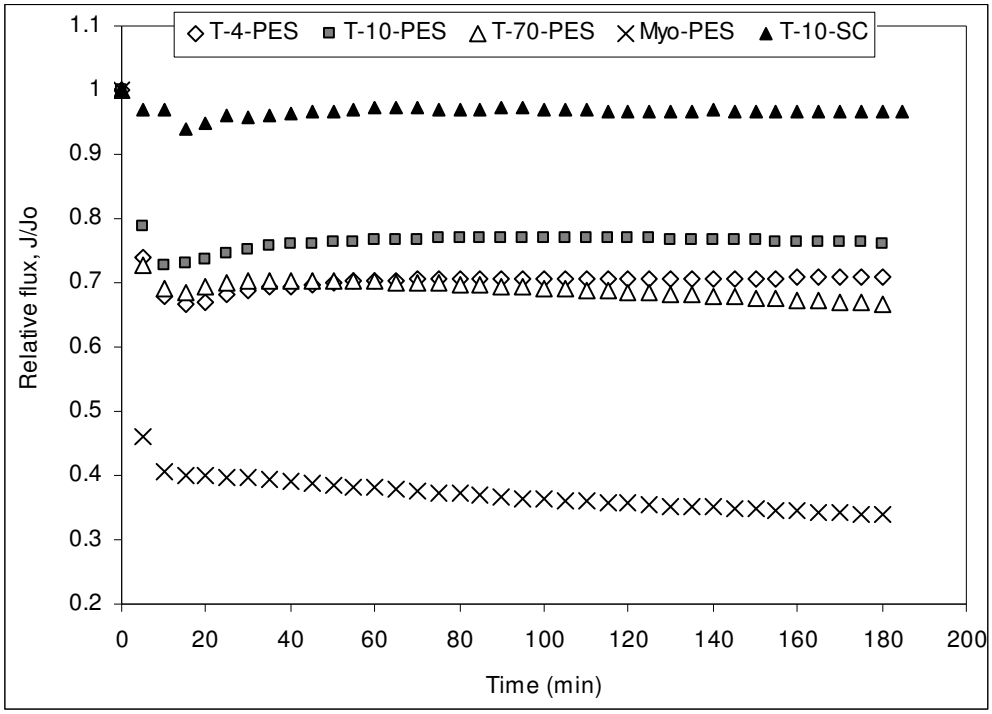

Figure 4.22. Flux profile as function of UF time for various dextrans (1 g/L) and myoglobin (0.1 g/L, pH 7) using PES-SG10 and SC-10 membranes at transmembrane pressure of 20 kPa and 40 kPa, respectively.

As clearly seen in Figure 4.22, the fluxes through the PES UF membrane dropped very rapidly in the beginning of filtration for both dextran and myoglobin. The permeate fluxes were much smaller than the water fluxes. Permeate fluxes (compared to the initial water flux) of PES membrane were in the following order: T10 > T4 > T70 >> Myo. By contrast, the permeate fluxes for dextran T10 through the SC-10 membrane were almost identical to the water flux. Further, the solute rejections during UF were consistent with the differences in (average) solute molar mass (see Table 4.5). In all cases, the water fluxes after ultrafiltration and external rinsing were significantly smaller than the initial water fluxes, and the RFR for

myoglobin was much larger than the respective values for the three dextrans. Slight differences between results in Figure 4.20, 4.21 and Table 4.5 were due to difference in operation condition for ultrafiltration.

Table 4.5. RFR after ultrafiltration and observed rejection for different solutes with PES-SG10 and SC-10 membranes.

Solute	PES-SG10 membrane		SC-cellulose–based membrane	
	RFR (%)	Rejection	RFR (%)	Rejection (%)
Dextran T4	9.2	35.3	n.d	n.d
Dextran T10	8.2	73.8	~ 0	82.32
Dextran T70	10.3	99.2	n.d	n.d
Myoglobin	47.0	76.5	n.d	n.d

n.d.: not done

Overall, ultrafiltration of both dextran and myoglobin solutions yielded greater RFR than after static adsorption. This result implies that membrane–solute–solute interactions were larger than membrane–solute interactions alone. Importantly, it is clearly shown that membrane yielding RFR after membrane–solute experiment (adsorptive fouling) also yields RFR after ultrafiltration.

4.3. Membrane Surface Modification

In this section, results obtained from surface modification of PES UF membrane by photograft copolymerization are presented. The base membranes used are PES-050H (cut−off: 50 kg/mol) and PES-SG100 (cut−off: 100 kg/mol). It is important to note that the modification was first performed using PES-050H (at intensity 60 $\pm$ 10 mW/cm^2, glass filter 1, called first batch modification). Thereafter, to increase the membrane performance, modification using PES-SG100 (at intensity 35 $\pm$ 5 mW/cm^2, glass filter 2) was then performed (second batch modification) based on the results obtained from the first batch modification.

4.3.1. Effect of UV irradiation and cross-linker (alone)

In this modification, free radicals on the PES surface as one of the key variables are created by UV irradiation; therefore, it is important to know the photosensitivity of the base membrane towards the UV light used. In addition, the effect of cross-linker availability was also investigated. The sensitivity was evaluated in term of changes in membrane hydraulic permeability as well as membrane cut−off. Figures 4.23 and 4.24 show the photosensitivity of PES-050H and PES-SG100, respectively. Control experiment was performed by washing the unmodified membrane with similar procedure for modified membrane and it was found that this did not change significantly the hydraulic permeability (~1.3%).

It was observed in Figures 4.23 and 4.24 that exposing the membrane towards UV light changed the membrane hydraulic permeability. Results from the first batch agree well (qualitatively) with results from the second batch modification. As the UV irradiation was increased, the hydraulic permeability would firstly rise and then fall. After irradiation beyond 6 min for PES-050H and 7 min for PES-SG100, the membrane hydraulic

permeability was somewhat lower than for the native one. Nevertheless, different sensitivity of PES membranes towards UV irradiation with respect to hydraulic permeability after irradiation is found in many previously reported works [38,90,162]. Further, the UV irradiation caused significant changing in membrane cut−off (Figure 4.23). The results are in good agreement with the changes in water flux, i.e. the maximum apparent pore size was observed after 6 min irradiation.

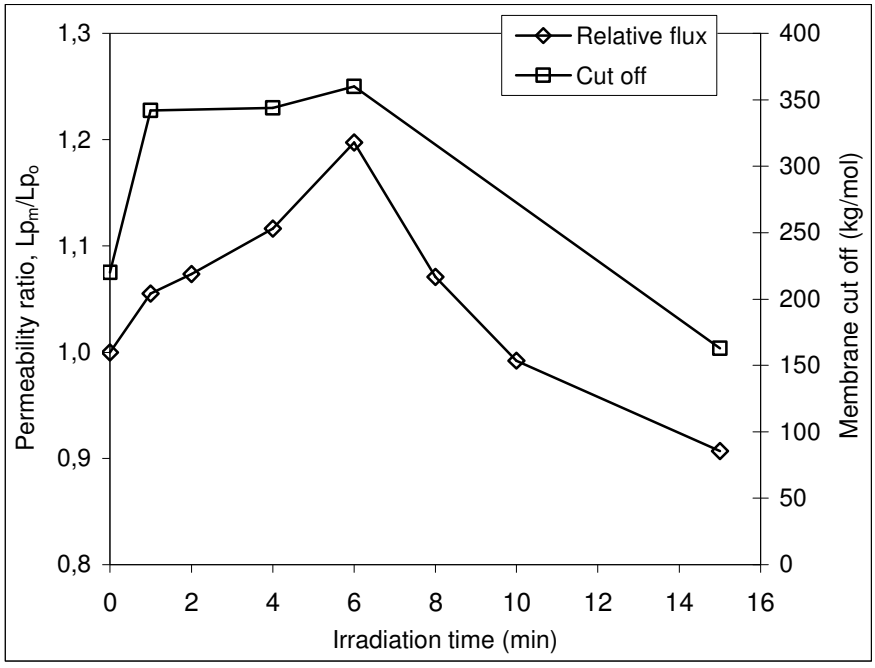

Figure 4.23. Effect of UV irradiation time (without monomer) on hydraulic permeability and membrane cut−off of PES−050H membrane (obtained from sieving test using mixed dextrans). Lp_m and Lp_o are the hydraulic permeability after and before irradiations, respectively.

Addition of cross-linker during exposing to the UV light decreased the hydraulic permeability for all UV irradiation. The reduction of hydraulic permeability increased with increasing the UV irradiation. However, increasing hydraulic permeability was observed at irradiation beyond 5 min and then a plateau values seemed to be reached (Figure 4.24).

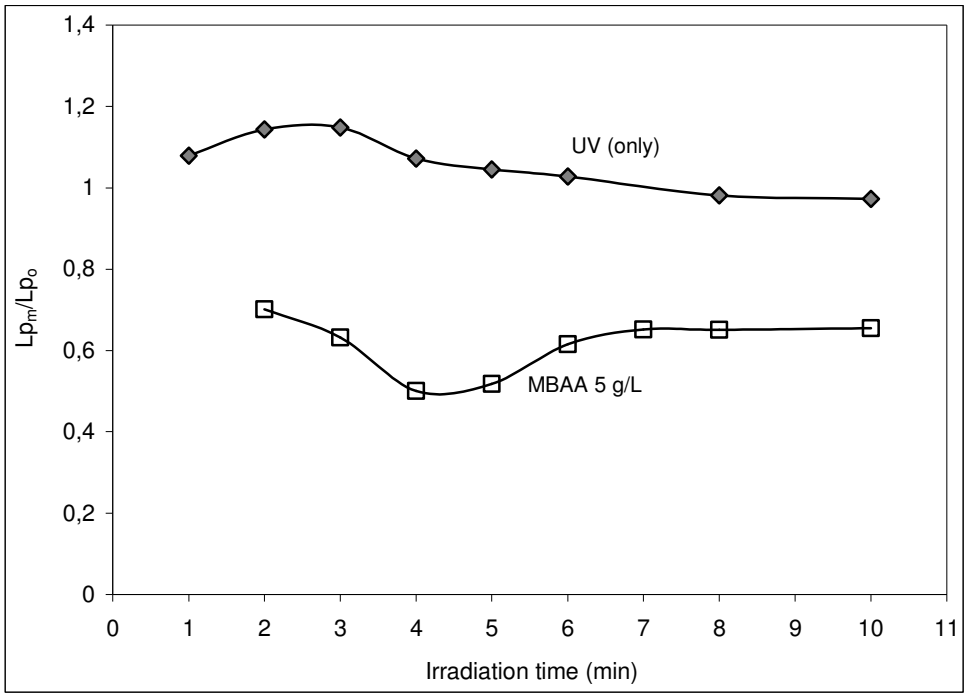

Figure 4.24. Effect of UV irradiation time on hydraulic permeability (without monomer) and photograft functionalization with cross-linker (only). Lp_m and Lp_o are the hydraulic permeability after and before irradiations, respectively.

4.3.2. Membrane surface modification by photograft copolymerization

Degree of grafting. The degree of grafting was used to quantify the amount of grafted polymer on PES membrane. The effects of irradiation time and monomer concentration on DG during first batch modification are presented in Figures 4.25 and 4.26, respectively. It is important to note that control experiment performed by washing the unmodified membrane with similar procedure for modification did not significantly change the membrane weight.

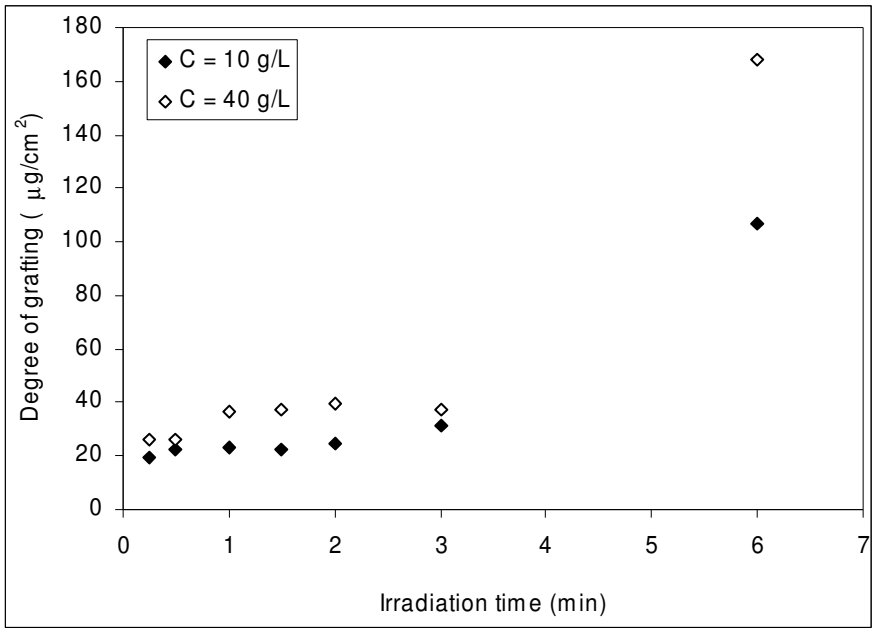

Figure 4.25. Effect of UV irradiation time on photograft functionalization of PES-050H membrane with PEGMA.

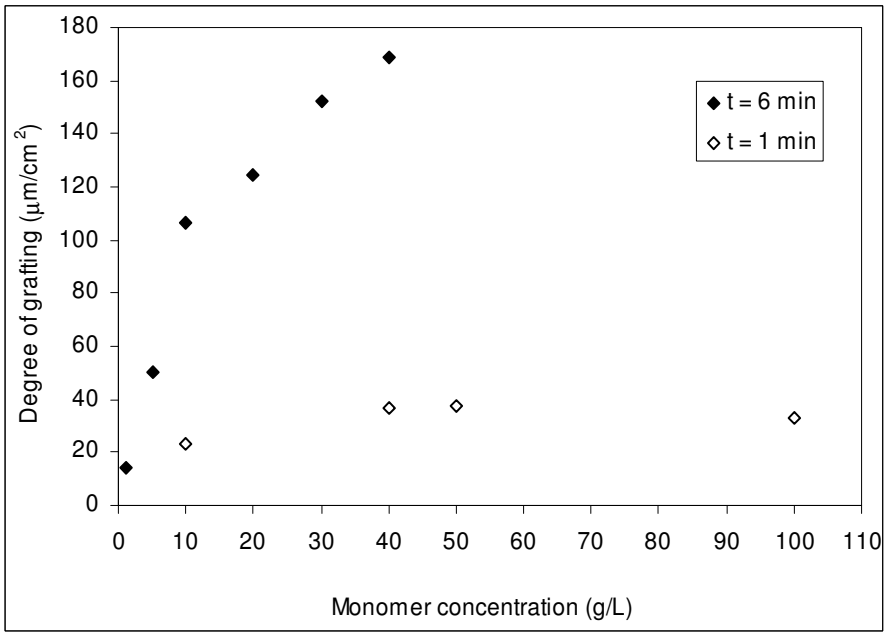

Figure 4.26. Effect of monomer concentration on photograft functionalization of PES-050H membrane with PEGMA.

For relatively short irradiation times (~1 min), the DG values were relatively low (20–40 μg/cm^2) and increased only slightly with further increasing irradiation time.

However, beyond 3 min irradiation, the DG increased strongly with UV irradiation time. At longer irradiation time (6 min) the DG values were a monotonic function of monomer concentration, while at 1 min irradiation the DG increased only slightly with increasing monomer concentration and did not significantly change beyond 40 g/L. Similar kinetic data for heterogeneous graft copolymerization had been reported by Ulbricht *et al.* [40] and Pierraci *et al.* [163].

By using this modification condition, further increase in DG is not feasible due to high flux reduction after modification (cf. Figure 4.40). Hence, in order to obtain high DG, experiments using base membrane having a higher membrane cut−off, along with UV light of lower intensity and glass filter with absorbance at higher UV energy (cf. Figure 3.2) were conducted (second batch modification). In addition to the PEGMA, zwitterionic (SPE) was used as the functional monomer. The results are depicted in Figures 4.27, 4.28, and 4.29.

It is observed in Figure 4.27 that the DG increased with increasing the monomer concentration. However, at concentration beyond 40 g/L, the increase in DG seemed only small with further increasing monomer concentration. This result implies that an "optimal" monomer concentration was 40 g/L; therefore, the experiments in the following studies were mainly conducted using monomer concentration of 40 g/L. Other important phenomena were as the UV irradiation time was increased, the DG would rise for both modifications without and with cross-linker (Figures 4.27 and 4.28). In all cases of modifications without cross-linker, the rate of grafting was lower at longer irradiation time than at shorter irradiation as evidenced by decreasing the slope of the plots at longer irradiation. Moreover, for the same concentration and UV irradiation time, modification using PEGMA yielded DG greater than modification using SPE. Converting the DG from $\mu g/cm^2$ to $\mu mol/cm^2$ also showed that the conversion (mol of grafted monomer/mol of

monomer used) of PEGMA was larger than SPE indicating the PEGMA is more reactive than SPE.

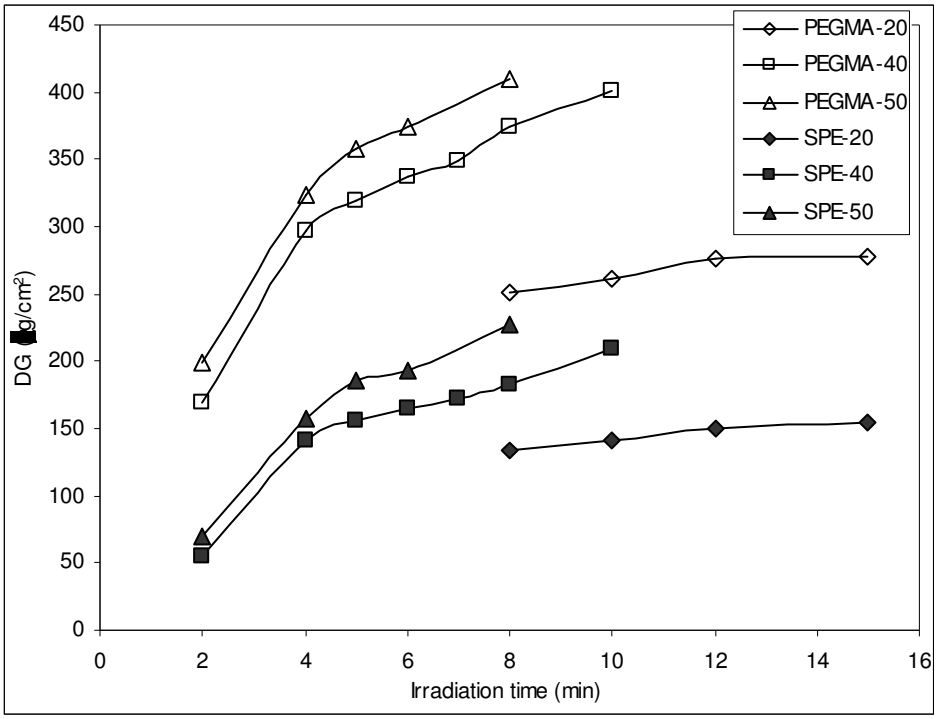

Figure 4.27. Effect of UV irradiation time and monomer concentration (without cross-linker) on DG during modification of PES-SG100. The numbers in legend indicate monomer concentration (g/L). The variation of DG data for modifications where two or three independent experiments have been performed was smaller than 10 μg/cm^2.

Figure 4.28 shows an example that the addition of cross-linker could either decrease (for PEGMA) or increase (for SPE) the DG. The reduction of DG seemed to be a function of cross-linker concentration in the bulk solution, i.e. the higher reduction was achieved at the higher cross-linker concentration. The phenomenon decreasing in DG with cross-linker addition was also observed by Kai *at al.* [164] and Gupta *et al.* [165] upon preparation of plasma-graft filling polymer membranes and cross-linking ion exchange membranes, respectively. Nevertheless, at high concentration of cross-linker, the DGs were somewhat higher than without cross-linker. By contrast, the presence of cross-linker enhanced the DG for modification using SPE. Enhancing the DG by addition of cross-linker was also found

in the previous reported literature [166,167]. Further study on the effect of cross-linker on DG showed similar phenomenon for both monomers, i.e. as the cross-linker content was increased to even larger values, the DG would first fall and then rise (Figure 4.29).

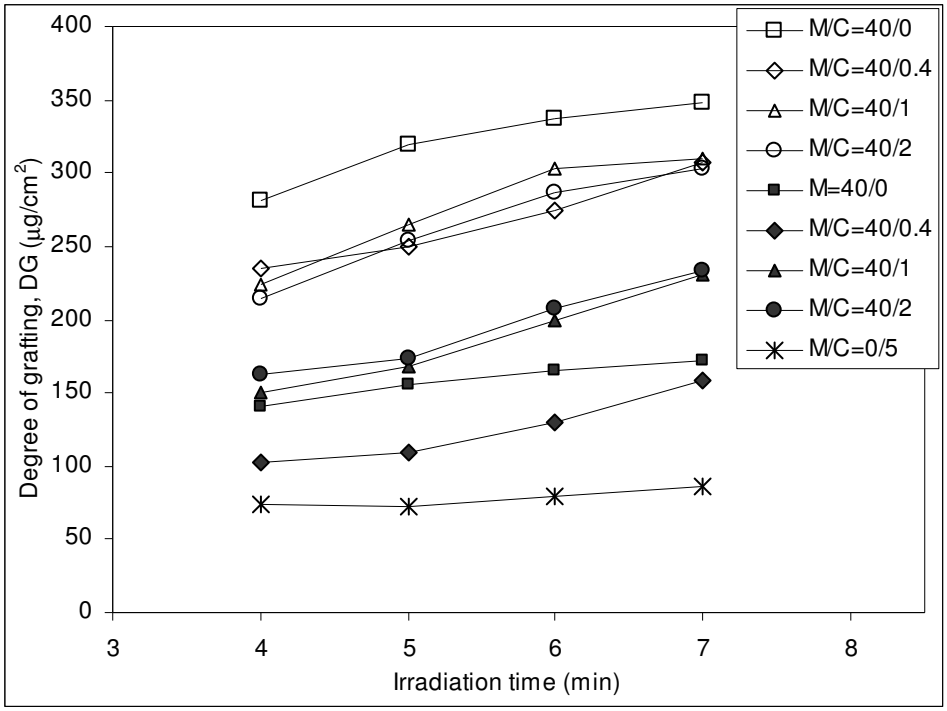

Figure 4.28. Effect of UV irradiation time on DG for modification of PES-SG100 with PEGMA and SPE (solid marker) at various cross-linker concentrations. M and C in legend are monomer and cross-linker, respectively, with the number indicating the concentration (g/L). For information about experimental error, cf. Figure 4.27.

Overall, from theses results (Figures 4.25-4.29), it is observed that DG could be adjusted by controlling the grafting time (UV irradiation time) and monomer concentration. Cross-linker content in the reaction mixture could also be used to adjust the DG. Then, it is important to note that the intensity and the wave length of UV light used also influenced the DG.

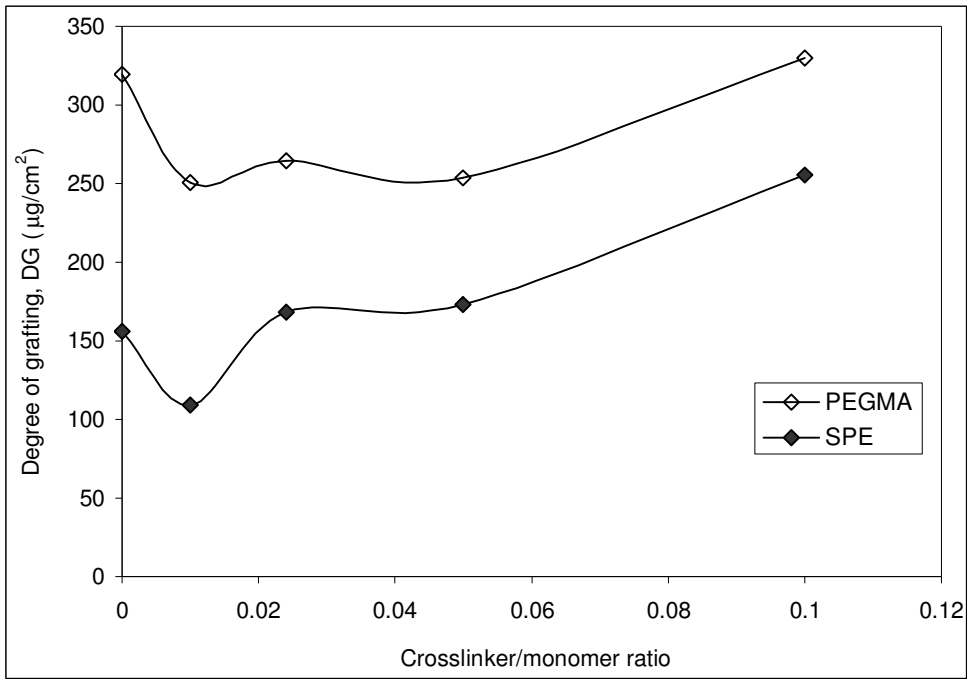

Figure 4.29. Effect of cross-linker content in the reaction mixture (40 g/L of PEGMA or SPE) on DG (at 5 min UV irradiation time) during modification of PES-SG100. For information about experimental error, cf. Figure 4.27.

***Membrane characterization*.** The membranes were characterized with respect to the membrane chemistry, surface wettability, surface charge, surface morphology, pore structure, and water permeability.

Membrane chemistry. The membranes were characterized with ATR−IR spectroscopy to verify their chemical structure. Elemental analysis was used to support the ATR−IR results. Basically, after all modifications, observable changes in IR−spectra were identified. Figure 4.30 shows an example of IR spectra for unmodified and PEGMA−modified PES-050H membranes.

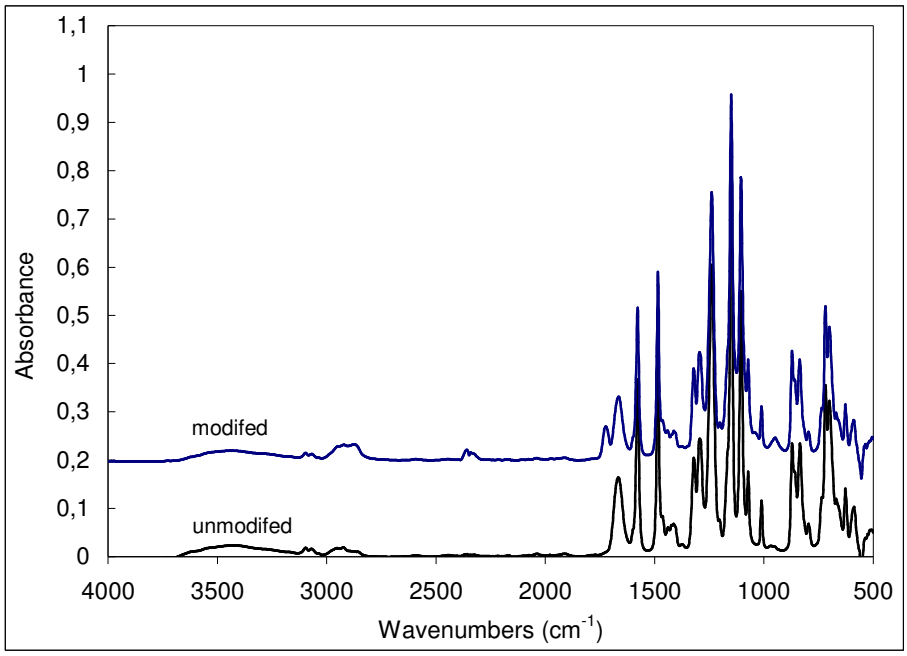

Figure 4.30. ATR−IR spectra of unmodified and PEGMA−modified PES-050H membrane.

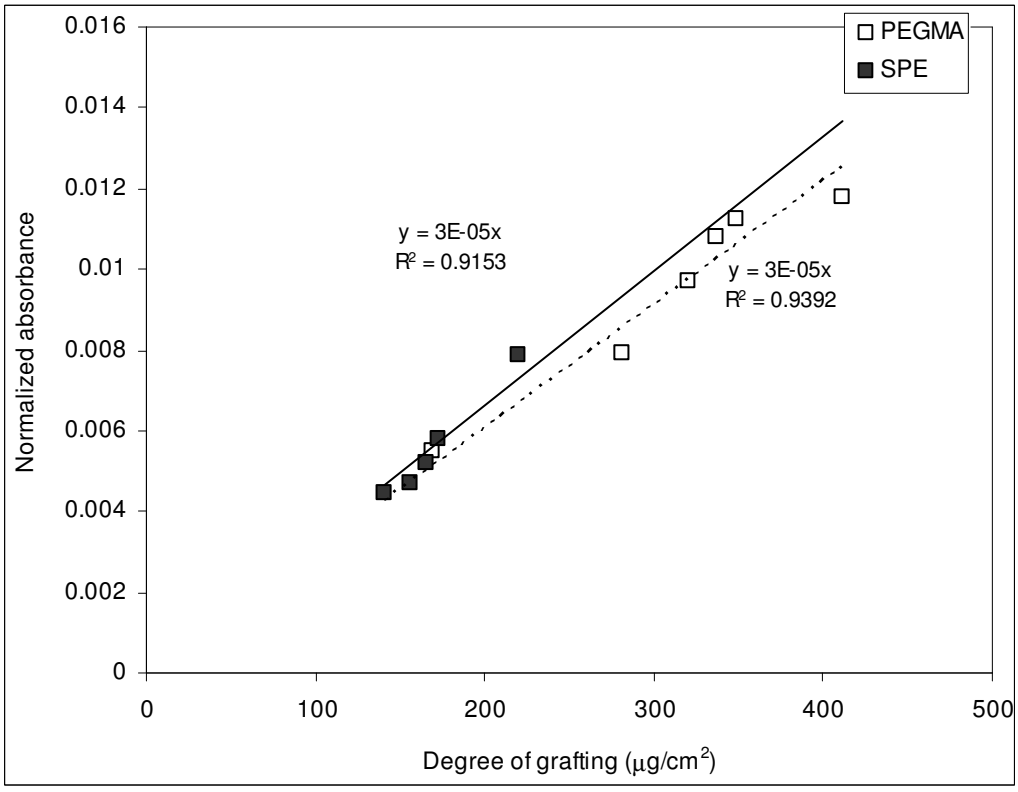

Figure 4.31. Normalized absorbance intensity (by subtracting the absorbance of the base membrane) at wavenumber of ~1725 cm^{-1} for PEGMA and ~1727 cm^{-1} for SPE as a function of DG.

Similar results were obtained from both modifications. Additional peak in the IR spectrum were the appearance of C=O vibration from the ester group of methacrylate at ~1725 cm^{-1} and ~1727 cm^{-1} for PEGMA and SPE, respectively. In addition, aliphatic stretching at wavenumbers of ~2925 cm^{-1} and of ~2875 cm^{-1} was also found for both monomers. It is interesting to note that the intensity of those bands increased with increasing the DG (Figure 4.31). As expected, these changes of IR spectra are similar to results of the previously reported studies [40,133]. However, the characteristic absorption of PEG (ν_{CO} ~1100 cm^{-1}) and the symmetric and asymmetric vibrations of SO_3^- of SPE, which should be observed at ~1220 and ~1040-1070 cm^{-1} were not observed after modification using PEGMA and SPE, respectively. Further, no change in IR spectra was observed for membrane modified with UV irradiation (only) and addition of cross-linker in the reaction mixture did not give new observable changes as well.

The elemental analysis supports all these observations (Table 4.6). Overall, the C and H contents increased after modification. The slight increase of S contents was also observed for modified membranes using SPE (note that SO_3^- was not observed in the IR spectra).

Contact Angle. The wettability of the membranes was measured in term of contact angle using captive bubble method. As presented in Figure 4.32, from the first batch modification (using PES-050H), all CAs of functionalized membranes were lower than the unmodified (61.1 $\pm$ 1.9^o) and the UV irradiated (only) membranes (59.1 $\pm$ 1.8^o for 6 min irradiation and 62.2 $\pm$ 2.2^o for 15 min irradiation). The modified membrane prepared using 40 g/L PEGMA and 6 min UV irradiation (DG = 168 $\mu g/cm^2$) exhibited the greatest hydrophilicity. The CA of ~47^o was only slightly larger than other data for grafted polyPEGMA layers on polyacrylonitrile, PAN, membranes [40,133]. The best

functionalization efficiency – significant hydrophilization at relatively low DG – was achieved with 40 g/L and 2-3 min UV irradiation time.

Table 4.6. Elemental analysis (%) of the unmodified 100 kg/mol (PES-SG100) and the modified membranes (fresh and after equilibrating in sodium hypochlorite solution).

Membrane	C	H	N	S
Base membrane (the unmodified 100 kg/mol)	59.2	3.7	n.d.[a]	13.0
PES-g-PEGMA (DG[b] = ~320)	59.8	4.6	n.d.[a]	12.5
PES-g-PEGMA (DG = ~320) after soaking in $NaHClO_3$[c] for 2 days	59.7	4.8	n.d.[a]	12.4
PES-g-PEGMA (DG = ~320) after soaking in $NaHClO_3$[c] for 8 days	59.6	4.7	n.d.[a]	12.6
PES-g-SPE (DG = ~165)	59.5	4.6	n.d.[a]	13.3
PES-g-SPE (DG = ~165) after soaking in $NaHClO_3$[c] for 2 days	59.6	4.7	n.d.[a]	13.3
PES-g-SPE (DG = ~165) after soaking in $NaHClO_3$[c] for 8 days	59.5	4.6	n.d.[a]	13.2
PES-g-PEGMA/MBAA (40/0.4[d], DG = ~250)	59.9	4.5	n.d.[a]	12.4
PES-g-PEGMA/MBAA (40/0.4[d], DG = ~250) after soaking in $NaHClO_3$[c] for 2 days	59.7	4.7	n.d.[a]	12.4
PES-g-PEGMA/MBAA (40/0.4[d], DG = ~250) after soaking in $NaHClO_3$[c] for 8 days	59.6	4.7	n.d.[a]	12.4
PES-g-PEGMA/MBAA (40/2[d], DG = ~255)	59.8	4.4	n.d.[a]	12.5
PES-g-PEGMA/MBAA (40/2[d], DG = ~255) after soaking in $NaHClO_3$[c] for 2 days	59.6	4.6	n.d.[a]	12.4
PES-g-PEGMA/MBAA (40/2[d], DG = ~255) after soaking in $NaHClO_3$[c] for 8 days	59.7	4.6	n.d.[a]	12.5
PES-g-SPE/MBAA (40/2[d], DG = ~173)	59.4	4.5	n.d.[a]	13.2
PES-g-SPE/MBAA (40/2[d], DG = ~173) after soaking in $NaHClO_3$[c] for 2 days	59.5	4.6	n.d.[a]	13.2
PES-g-SPE/MBAA (40/2[d], DG = ~173) after soaking in $NaHClO_3$[c] for 8 days	59.5	4.6	n.d.[a]	13.2

[a] n.d. not detected; [b] degree of grafting (μg/cm^2); [c] 500 mg/L active chlorine; [d] monomer/cross-linker concentration ((g/L)/(g/L))

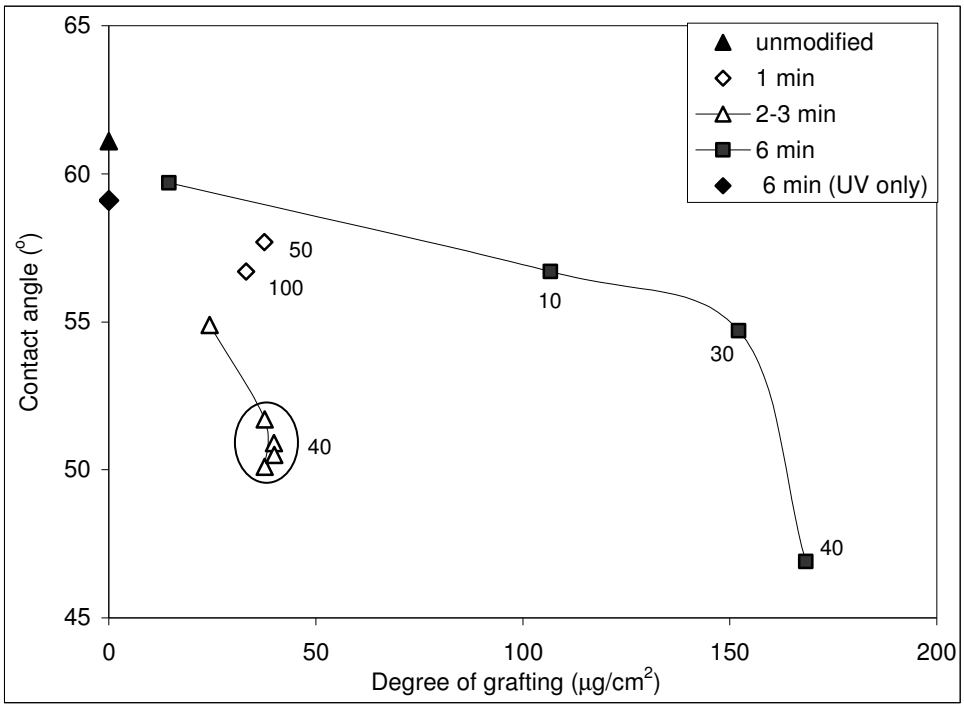

Figure 4.32. Captive bubble contact angles of unmodified and modified PES-050H membranes as a function of DG, including information about UV irradiation time used for functionalization. The numbers inside the picture indicate the monomer concentration used for modification.

For second batch modification (using PES-SG100), PEGMA–modified membranes had CA ranging from 37.8 $\pm$ 4.2° to 42.5 $\pm$ 4.3° depending on the degree of grafting (Figure 4.33). These values are somewhat smaller than for the unmodified base membrane (44.8 $\pm$ 4.2°), but much lower than for the unmodified membrane (PES-SG10) with similar nominal cut-off (61.7 $\pm$ 2.5°). These results agree well with previously reported CA of PEGMA–modified PAN membranes [133] and are somewhat smaller than lowest CA obtained in the first batch modification (~47°, cf. above). Relatively constant values of CAs were observed for SPE modified membranes (ranging from 44.1 $\pm$ 3.8° – 45.3 $\pm$ 3.0°). These values are in a good agreement with the CA of PAN–based zwitterionic polymer (similar with used in this study) blend membranes [141]. Moreover, slightly lower CA for

PEGMA–modified membranes than for SPE–modified membrane was also observed. Addition of cross-linker slightly increased the CA relative to uncross-linked modified membranes for both PEGMA and SPE.

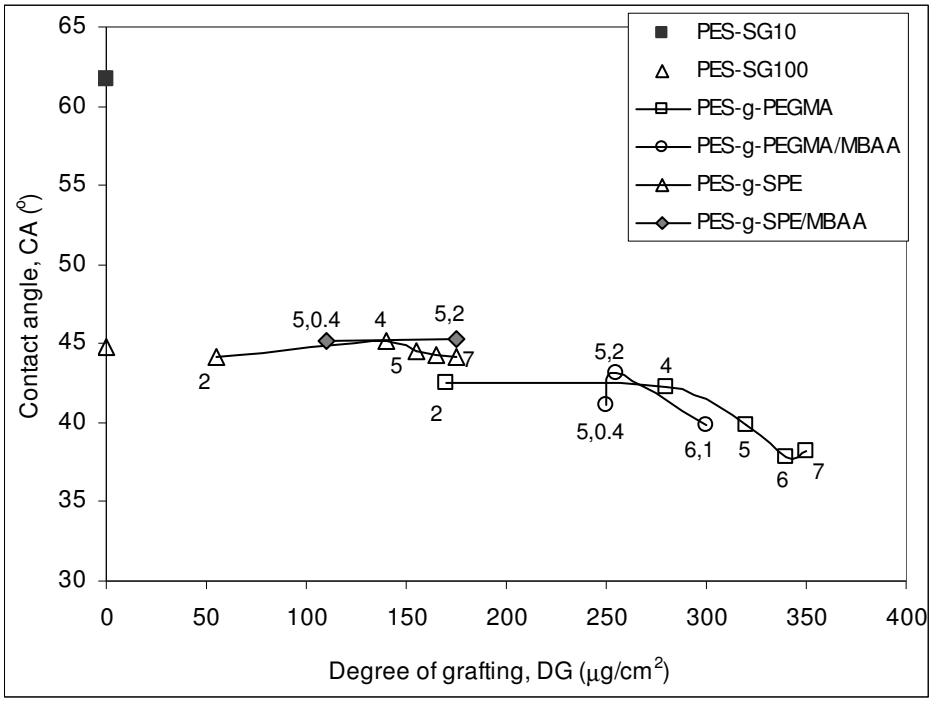

Figure 4.33. Captive bubble contact angles of unmodified and modified membranes with and without cross-linker (monomer concentration of 40 g/L) at various DGs. The numbers inside the picture indicate the UV irradiation time (for single number) and UV irradiation time and cross-linker concentration (g/L), respectively (for number couples).

Zeta potential. One of the aims of this study was to synthesis neutral polymer hydrogel composite membrane. Therefore, it is important to know the membrane surface charge. The surface charge of membrane was investigated by measuring streaming potential. Zeta potential was then calculated from streaming potential values at various pressures. Figures 4.34 and 4.35 show the zeta potential of both unmodified and modified membranes for PES-050H and PES-SG100, respectively.

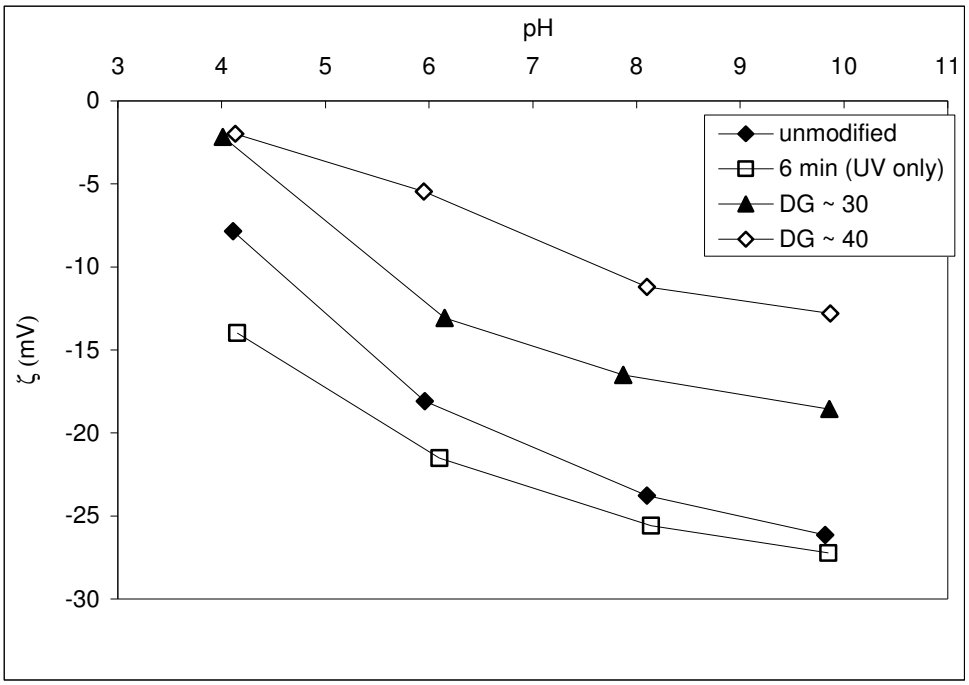

Figure 4.34. Zeta potentials, ζ, as a function of pH for unmodified and modified PES-050H membranes calculated from tangential streaming potential of outer membrane surface (0.001 mol/L KCl, 25^{o}C).

As clearly seen in those figures, the membrane surface of both unmodified membranes had negative charge over the entire pH range studied, which decreased towards acidic pH values. For membrane from the same manufacturer (PES-SG 10 and PES-SG-100), the absolute values of ZP were greater for smaller cut–off. All modification changed significantly the membrane ZP even only UV irradiation was used. The UV irradiation alone increased the negative charge of the membrane surface. By contrast, significant changing in surface ZP toward neutral values was observed for all membranes after modification using both functional monomers. The reduction of charge increased with increasing the DG, i.e. the higher DG (for the same monomer) the higher diminishing surface charge. This phenomenon agrees with previously reported ZP of self assembled alkanthiol monolayers where absolute value decreased with increasing the thickness of

PEG layers [159]. Furthermore, for similar DG, the membranes modified using SPE showed less negative charge than the membrane modified using PEGMA.

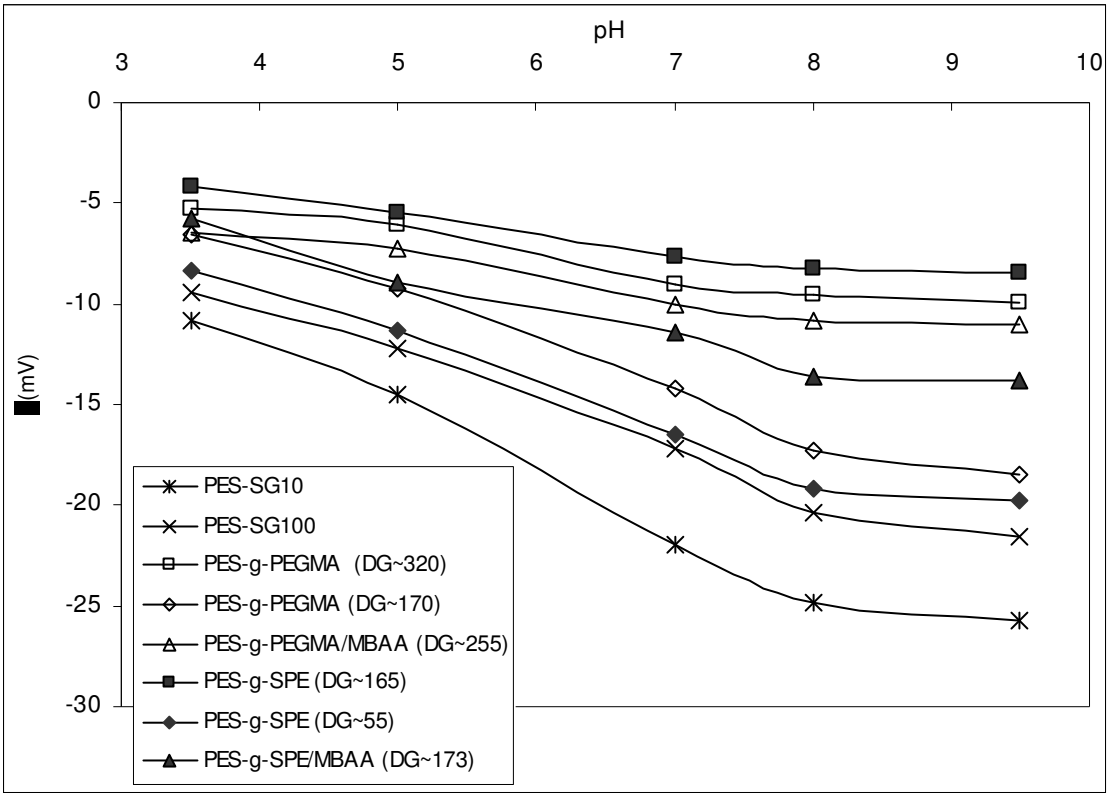

Figure 4.35. Zeta potential, ζ, of unmodified (PES-SG10 and PES SG-100) and modified PES-SG100 membranes with varying pH calculated from tangential streaming potential of outer surface (0.001 mol/L KCl, 25 ^{o}C).

Surface morphology. The changes in membrane surface morphology due to modification were visualized using SEM. Only membranes from second batch modification were investigated. As presented in Figures 4.36 and 4.37, the modification significantly changed the upper membrane surface morphology as well as pore structure except for modification using UV irradiation alone (without monomer, Figure 36 b). Unmodified membrane showed smoother surface than all modified membranes. Changing in surface morphology was more pronounced in the presence of cross-linker for both monomers used (Figure 4.37). Phase separation via insolubilization seemed to occur at

modification using cross-linker (cf. Figure 4.36 c). Agglomeration of grafted polymer was also observed on some parts of the membrane surface. This phenomenon might be responsible for the deviations observed during characterization with other techniques (e.g., contact angle). Both pore narrowing and blocking were observed as consequences of the surface modification. These effects were more pronounced for modification using SPE. Differences in structure of the grafted polymer on the membrane surface seemed to be observed between membranes modified with PEGMA and SPE. The grafted polySPE seemed to have more compact morphology.

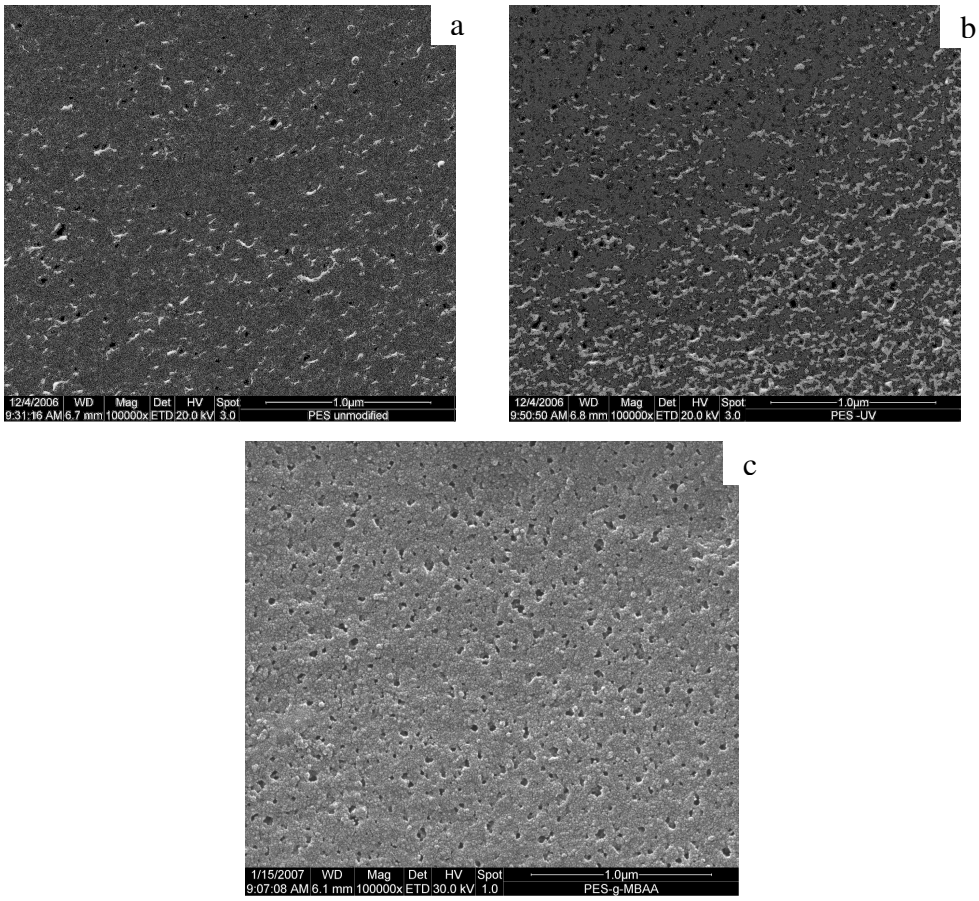

Figure 4.36. SEM images of the membrane top surface: (a) unmodified membrane, (b) irradiated (only) membrane (8 min), and (c) modified membrane using cross-linker (only) with 8 min UV irradiation.

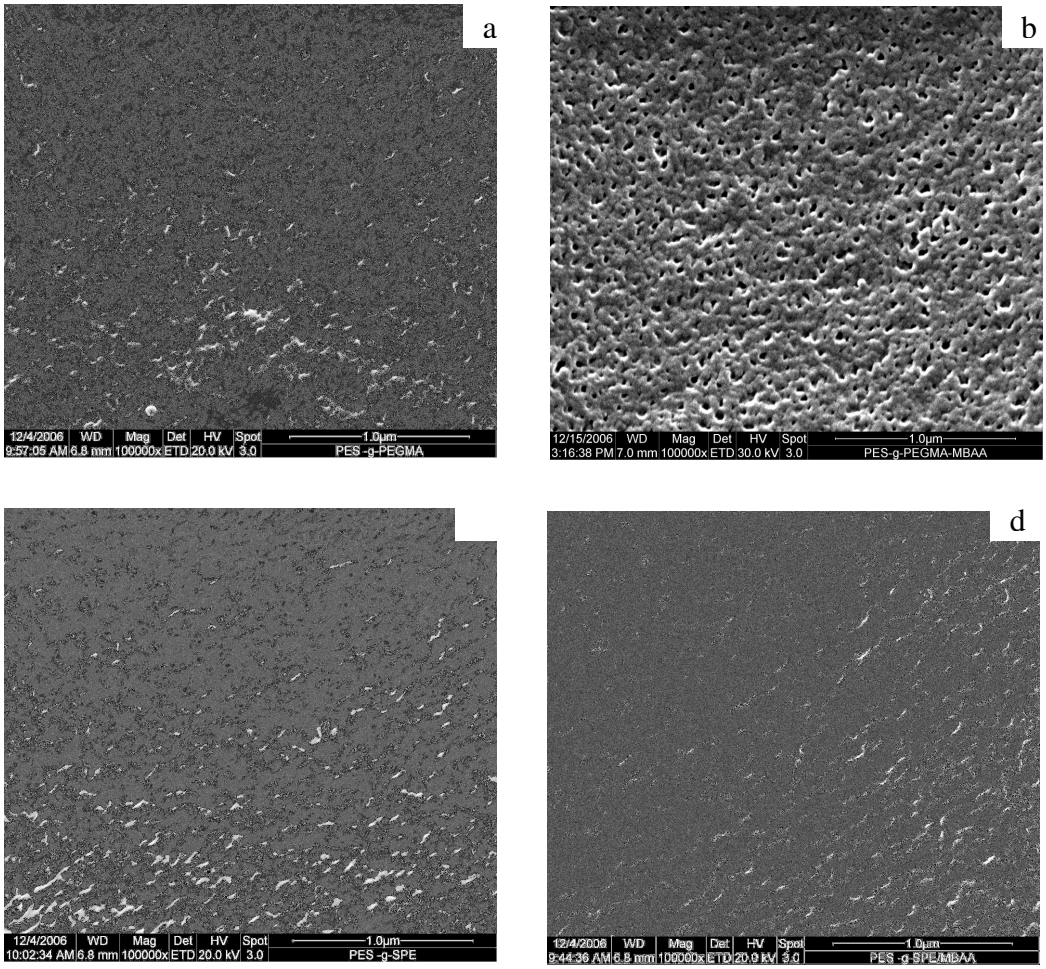

Figure 4.37. SEM images of the top surface of the modified membranes: (a) PES-g-PEGMA (5 min), (b) PES-g-PEGMA/MBAA (5 min), (c) PES-g-SPE (6 min), (d) PES-g-SPE/MBAA (5 min).

Effect of modification on membrane rejection curve. Membrane sieving or rejection is one of the important characteristics for UF membrane. This characteristic will determine selectivity of UF membrane. Rejection of polydisperse polymer (mixed dextrans for PES-050H and mixed PEGs for PES-SG100) was investigated in order to demonstrate in more detail the effect of modification on apparent pore size. Figures 4.38 and 4.39 show the rejection curve for PES-050H and PES-SG100, respectively. In general, the

modification changed the membrane apparent pore size and the nominal cut–off toward lower values for both base membranes.

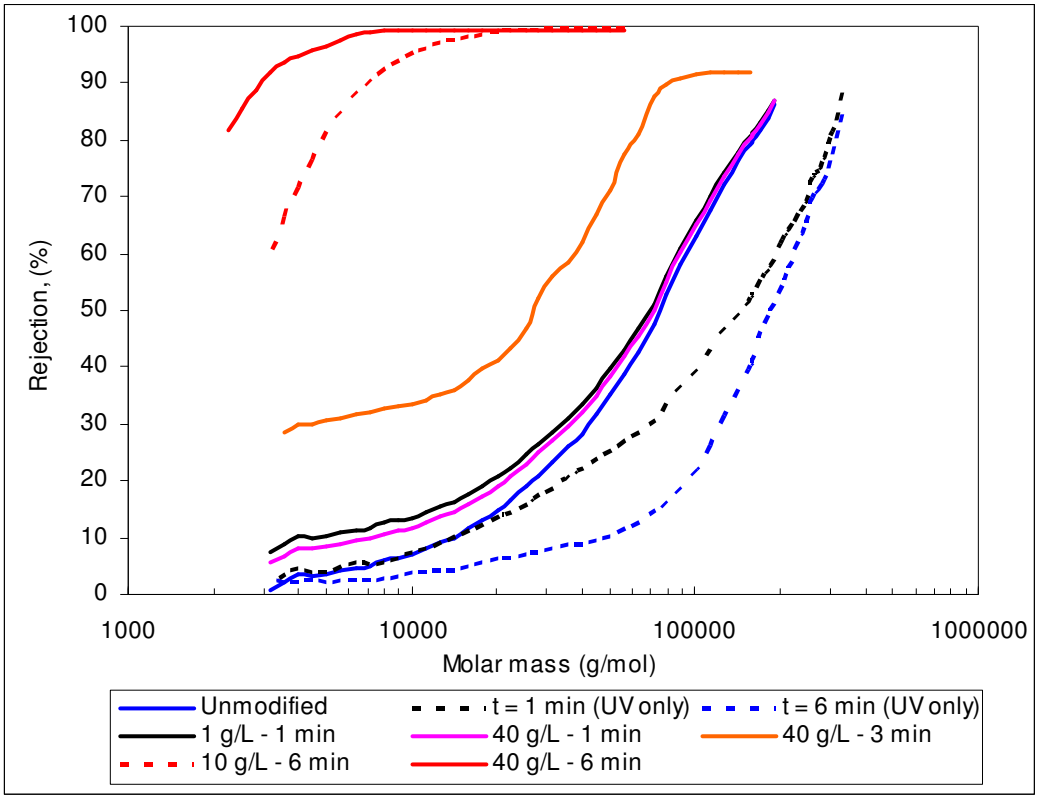

Figure 4.38. Rejection curves for unmodified, UV irradiated (only) and PEGMA–modified PES-050H membranes, determined by ultrafiltration of a dextrans mixture in water (total concentration was 1 g/L) at pressure of 20 kPa.

In the first batch modification using PES-050H, three regions based on the UV irradiation time used could be distinguished. In “period 1”, with UV irradiation up to 1 min, the modification did not change the membrane rejection. Moreover, the degradation effects of the UV irradiation alone – leading to a large shift of the sieving curve to larger values – were completely suppressed. In “period 2”, with UV irradiation times between 1.5 and 3 min, the modification changed the sieving curve towards lower values (however, the data in the MW range 100–200 kg/mol for the membrane obtained from 40 g/L PEGMA

and 3 min UV may indicate some defects in the active layer due to UV irradiation as evidenced by their constant values). In “period 3”, for UV irradiation times beyond 3 min leading to DG > 50 μg/cm^2, the grafted polyPEGMA significantly narrowed or blocked the membrane pores. This explanation is supported by the behavior of membrane hydraulic permeability after modification (cf. Chapter 4.3.3).

No effect of UV irradiation (alone) on membrane sieving was detected in second batch modifications. Both pore blocking and narrowing observed in the first modification were again observed, and with the extent was more pronounced for modification using SPE (cf. Figure 4.39). This observation is supported by visualization of membrane surface morphology by SEM (cf. Figure 4.37). The phenomenon of pore blocking was evidenced by smaller both rejection and hydraulic permeability of most of the modified membranes (M4, M5, M6, M7) than the unmodified membrane PES-SG10 (10 kg/mol) having similar cut−off (note that it is usually observed that a membrane with lower rejection would have higher hydraulic permeability). All modified membranes (except M2), regardless the DG had rejection curve as well as membrane cut−off within the range of 10 kg/mol. Comparing with unmodified membranes, the rejections of modified membranes were slightly smaller than for unmodified 10 kg/mol but significantly larger than for unmodified 100 kg/mol for all molar masses of PEGs. The presence of cross-linker increased the reduction of apparent pore size for both monomers (cf. M3, M4 and M5; M6 and M7, Figure 4.39). Furthermore, for modified membranes with similar DG (M2 and M6), modification using SPE (M6) yielded higher rejection, but lower hydraulic permeability (cf. Chapter 4.3.3) than modification using PEGMA (M2).

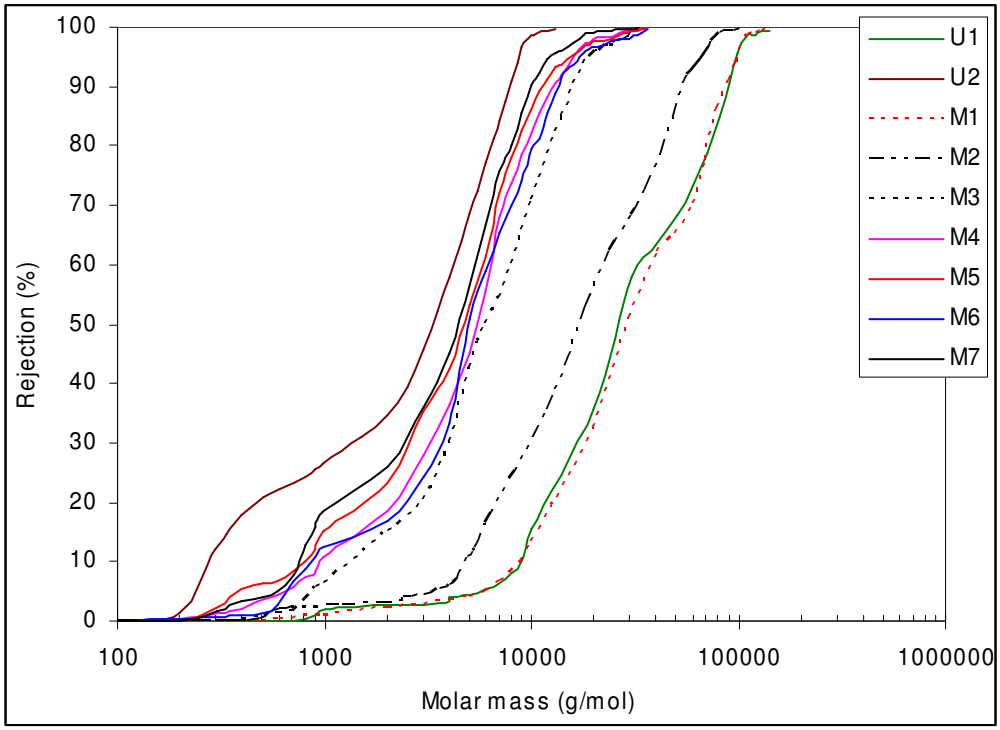

Figure 4.39. Rejection curves of unmodified PES-SG100 and modified membranes determined using PEGs mixture (1 g/L) at pressure of 100 kPa. U1 and U2 are PES-SG100 and PES-SG10 unmodified membranes, respectively, M1: modified membrane using UV (only), M2: PES-g-PEGMA (40g/L, 2 min), M3: PES-g-PEGMA (40 g/L, 5 min), M4: PES-g-PEGMA/MBAA (40/0.4 g/L, 5 min), M5: PES-g-PEGMA/MBAA (40/2 g/L, 5 min), M6: PES-g-SPE (40 g/L, 6 min), M7: PES-g-SPE/MBAA (40/2 g/L, 5 min).

Measurements of swelling degree of functional polymer used. To explain the preceding results, supporting experiment to measure the swelling degree of both polymers in water was then performed (see Section 3.4.9). It was found that the swelling degree, which is defined as the mass of the swollen polymer hydrogel relative to the mass of the dried gel, of polyPEGMA was 12.3 $\pm$ 0.3 whereas for polySPE it was 7.7 $\pm$ 0.2. This result implies that the PEGMA–based hydrogel is more swollen than SPE–base one.

4.3.3. Effect of membrane modification on membrane performance

Effect of modification on membrane permeability and membrane–solute interactions. Studies were undertaken to investigate the effect of modification on the hydraulic permeability and the membrane–solute interactions. It is important to note that BSA solution (1 g/L, pH 7.2) was used to evaluate the modified membranes obtained from first batch modification, whereas myoglobin (1 g/L, pH 7) was used for second batch modification. As presented in Figures 4.40-4.43, the results were expressed in terms of hydraulic permeability ratio (Eq. (3.6)) and relative water flux reduction due to solute adsorption (Eq. (3.1)).

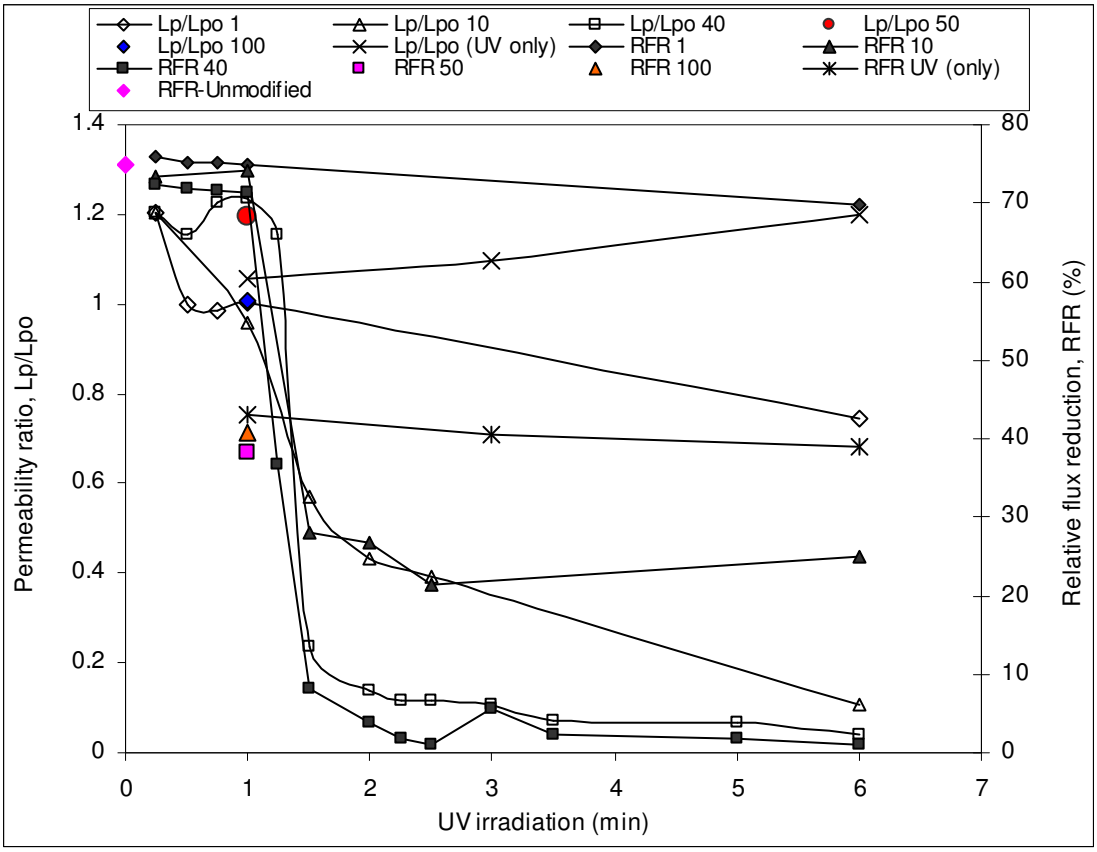

Figure 4.40. Effect of UV irradiation (only) and modification (using PEGMA) on the membrane hydraulic permeability and adsorptive fouling by BSA (1 g/L, pH 7, 2.5 h exposure) for PES-050H (first batch modification). The numbers in the legend indicate monomer concentration (g/L).

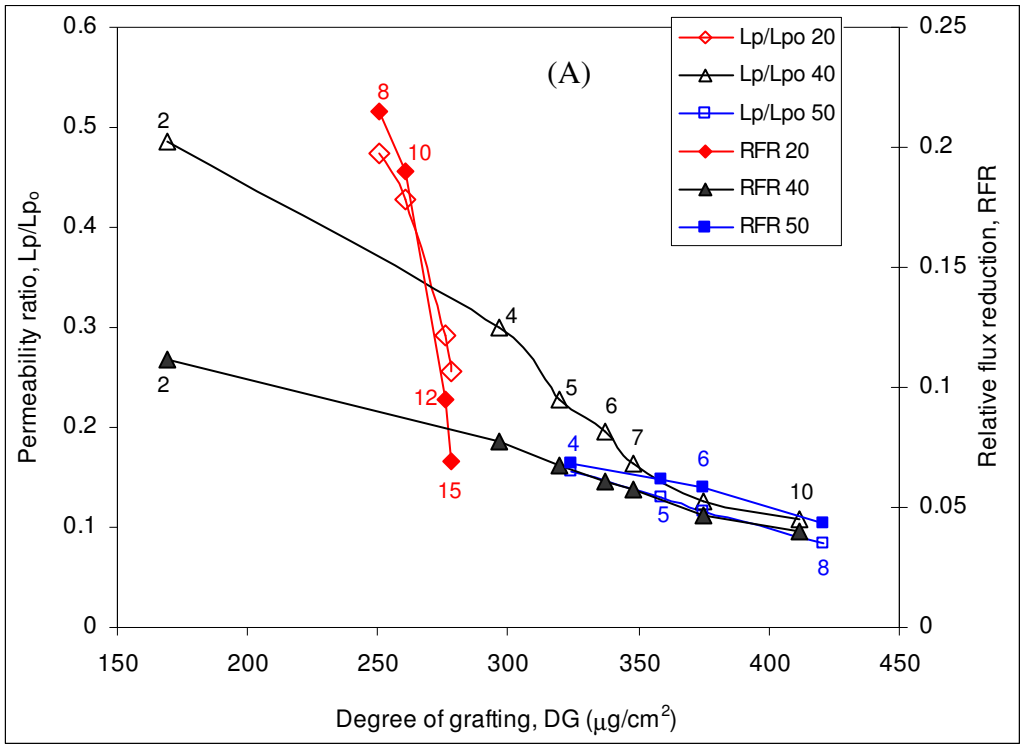

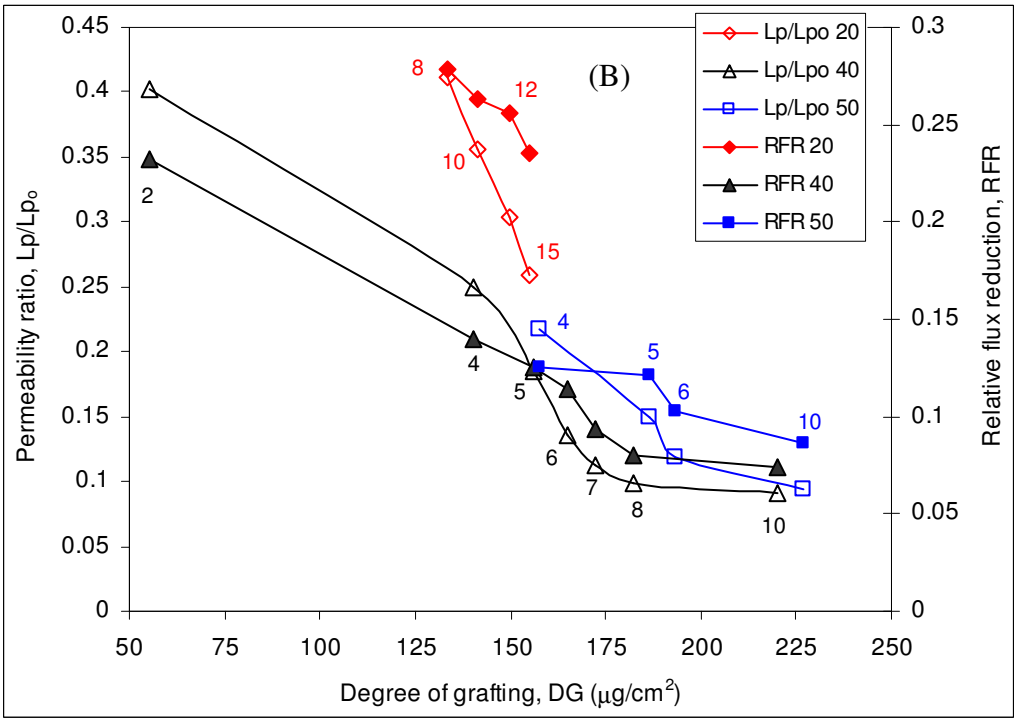

Figure 4.41. Effect of modification (without cross-linker) on the membrane hydraulic permeability and adsorptive fouling by myoglobin (1 g/L, pH 7, 2 h exposure) for PES-SG100 (second batch modification): (A) using PEGMA, (B) using SPE. The numbers inside the picture indicate the UV irradiation time whereas numbers in the legend indicate the monomer concentration (g/L).

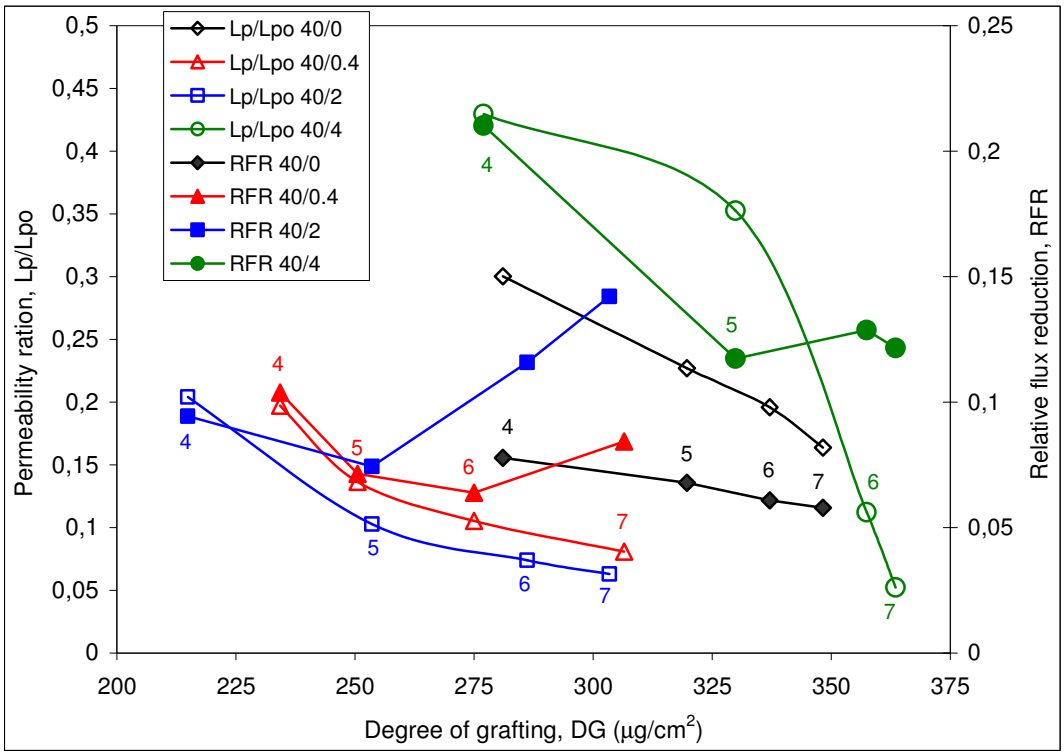

Figure 4.42. Effect of modification (using PEGMA and cross-linker) on membrane hydraulic permeability and adsorptive fouling by myoglobin (1 g/L, pH 7, 2 h exposure) for PES-SG100 (second batch modification): The numbers inside the picture indicate the UV irradiation time whereas numbers in the legend indicate the monomer and cross-linker concentrations.

For modification without cross-linker both in first and second batch modifications (Figures 4.40 and 4.41), as the DG was increased, both hydraulic permeability ratio and relative flux reduction would decrease indicating that modified membranes had lower flux, but had less solute adsorption.

Looking at Figure 4.40 more carefully, it is observed that at irradiation of the membranes for short time (~1 min), an increase of monomer concentration yielded either constant or slightly increased water fluxes. Even using a monomer concentration of 100 g/L, it gave still the same water flux as for the unmodified membrane. It was clear from DG (cf. Section 4.3.2, *Degree of grafting*), ATR–IR and CA data (cf. Section 4.3.2,

Membrane characterization) that all these membranes have been modified, and the fluxes were larger than expected due to the pure UV irradiation effect (cf. Figure 4.23). Completely different results were obtained at longer irradiation times (6 min). Large and systematic reductions of water fluxes with the tendency to level off at low values beyond 30 g/L monomer concentration were observed. Again, as mentioned for the rejection curve results (cf. Figure 4.38), three periods could be identified, i.e. in "period 1" with UV irradiation ~1 min, the water fluxes and rejection increased for monomer concentration of 40 g/L whereas the fluxes and rejection were relatively constant for monomer concentrations of 10 and 1 g/L. In "period 2" (1.5–3 min irradiation) and "period 3" the water fluxes was significantly decreased and the rejection was increased by modification.

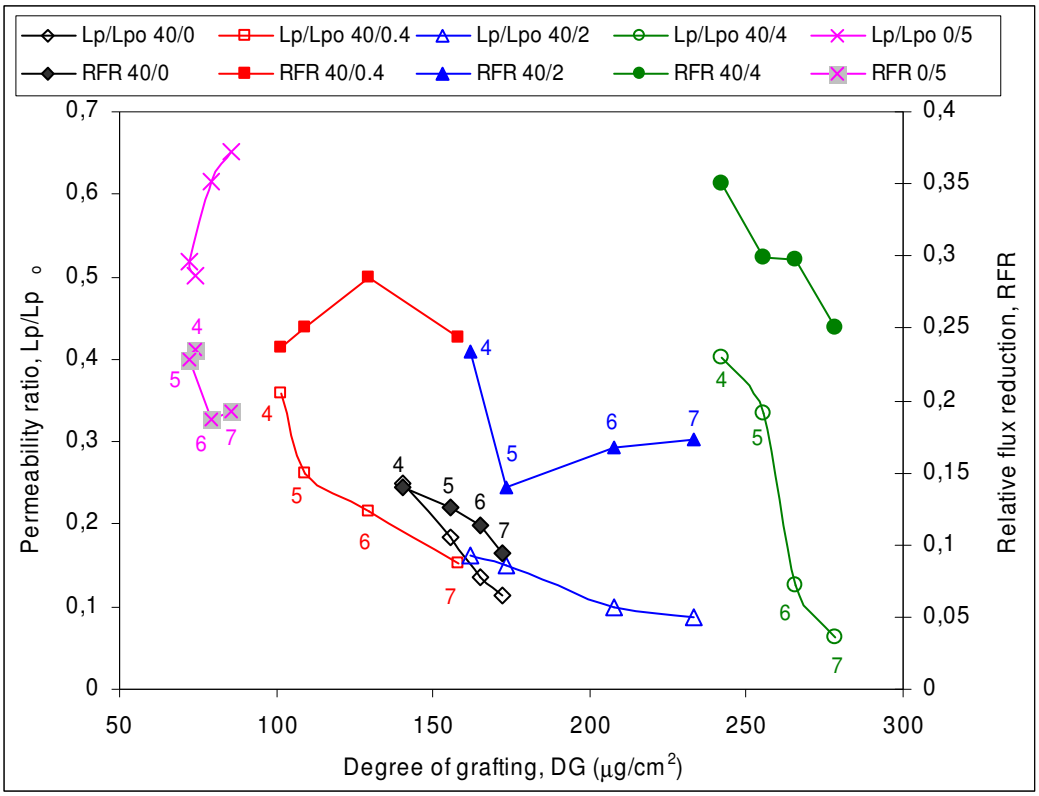

Figure 4.43. Effect of modification using (SPE and cross-linker) on membrane hydraulic permeability and adsorptive fouling by myoglobin (1 g/L, pH 7, 2 h exposure) for PES-SG100 (second batch modification). The number inside the picture indicates the UV irradiation time whereas in the legend indicates the monomer and cross-linker concentrations.

The unmodified membrane showed strong fouling (RFR = 75%). This result agrees well with previously reported studies (e.g., [35,131]). Exposing the UV-irradiated membranes to the BSA solution yielded significantly less fouling (RFR~40%) than unmodified membrane. All PES-050H grafted polyPEGMA membranes showed lower interaction with BSA as evidenced by lower RFR values (cf. Figure 4.40). Clearly, all membranes functionalized using short irradiation time ("period 1") had high or moderate RFR even though high monomer concentration has been used. Also for membranes modified with low monomer concentration (1 g/L) an increase in irradiation time did not change the RFR. On the other hand, increased monomer concentration and longer irradiation time decreased the RFR. The best results were observed for membranes functionalized using high monomer concentration (40 g/L) and moderate irradiation time (2–3 min, i.e. "period 2"), where RFR values of only 1–3% were obtained (i.e. about 35 times less than for unmodified membrane). Further increase in irradiation time (towards "period 3") could not decrease the RFR anymore.

In the second batch modification, it was found that for similar DG, modification using PEGMA yielded membranes with higher hydraulic permeability as well as RFR than modification using SPE, whereas modification with the same monomer concentration and UV irradiation time yielded membranes having higher permeability and lower RFR for PEGMA than for SPE. Further, no modified membrane, which is absolutely inert toward protein adsorption, was obtained. Overall, the presence of cross-linker caused decreasing in the membrane permeability (Figures 4.42 and 4.43). The RFR achieved by cross-linked modified membranes was slightly higher for PEGMA but significantly higher for SPE than for the respective uncross-linked modified membranes. However, for both monomers, it was observed that the presence of cross-linker could either increase or decrease the RFR.

Membrane performance based on permeability–adsorptive fouling resistance analysis. Hydraulic permeability and adsorptive fouling resistance (Eq. (3.7)) were used to evaluate the performance of modified membranes and then finally to select those, which show a better performance than commercial membranes. According to the definition, a fouling resistance value of 1 means that no adsorptive fouling occurs. The ideal functionalized membrane should have a high fouling resistance as well as a high flux.

It is obviously seen in Figures 4.44 – 4.46 that all modified membranes (without cross-linker) displayed a trade-off relationship between fouling resistance and membrane permeability, i.e. membranes with higher fouling resistance had lower hydraulic permeability (cf. also Figure 4.41). Different phenomenon was observed for cross-linked modified membranes (Figures 4.45 and 4.46), i.e. as the water permeability was decreased (by increasing the UV irradiation time), the fouling resistance would rise and fall even though a more arbitrary trend was observed for modification using SPE (see also Figures 4.42 and 4.43).

For the first batch modification, no membrane would fully meet this ideal criterion with respect to protein fouling (Figure 4.44). However, when compared with a simple "trade-off curve" – assuming that the fouling resistance of the investigated PES UF membrane would approach a value of 1 if the flux would be reduced to zero (by reducing the pore size) – , the additional effects of the functionalization (e.g., by shielding the porous surface towards adsorption) may be separately discussed. It should be noted that the unmodified PES UF membrane with a lower cut–off (10 kg/mol) from the same company (and presumably the same manufacturing process) had indeed a higher fouling resistance at lower permeability as compared to the base membrane used for the functionalizations, but the value was well below the simple "trade-off" curve. Membranes with medium fouling resistance (0.6–0.7) and high or moderate flux can be obtained from functionalizations

using UV times according to "period 1" (cf. Section 4.3.2). Membranes with high fouling resistance (~1) and low (but potentially still acceptable) flux can be obtained from functionalizations using medium UV times according to "period 2" (cf. Section 4.3.2). Surprisingly, all membranes functionalized with long UV times ("period 3"; cf. Section 4.3.2) had a performance below the "trade-off curve".

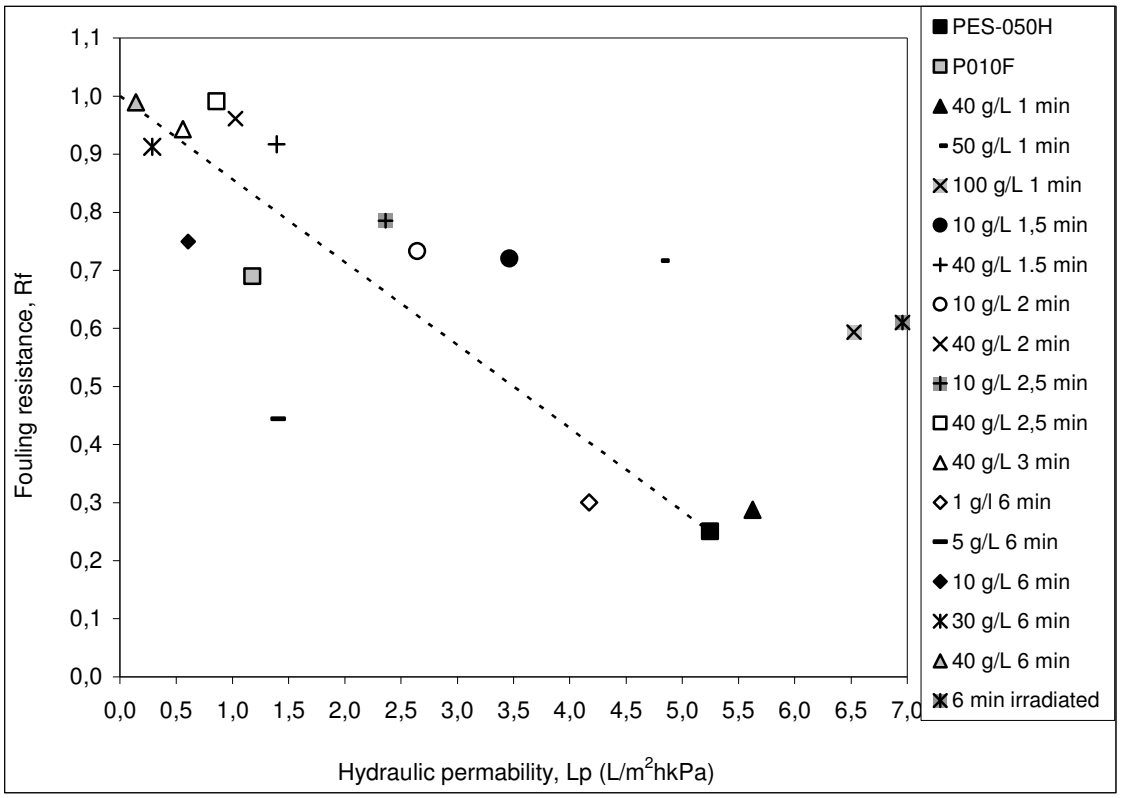

Figure 4.44. Hydraulic permeability–fouling resistance analysis of UV-irradiated and PEGMA–modified membranes (PES-050H first batch modification). Membrane fouling resistance was evaluated using BSA (1 g/L, pH 7.2, 2.5 h exposure). PES-050H and P010F are 50 and 10 kg/mol unmodified membranes, respectively.

In order to get really meaningful evaluation of membrane performance, a more detailed analysis was done for the second batch modification. It is of interest to compare and contrast between modified membranes (having their cut–off around 10 kg/mol, cf. Figure 4.43) and 10 kg/mol unmodified PES membrane (cf. the target of this study). The

modified membrane should have comparable water permeability with 10 kg/mol unmodified membrane, but should have higher fouling resistance. The performance indicators were then defined, i.e. the hydraulic permeability should be more than 0.75 L/m^{2}hkPa and fouling resistance should be higher than 0.9.

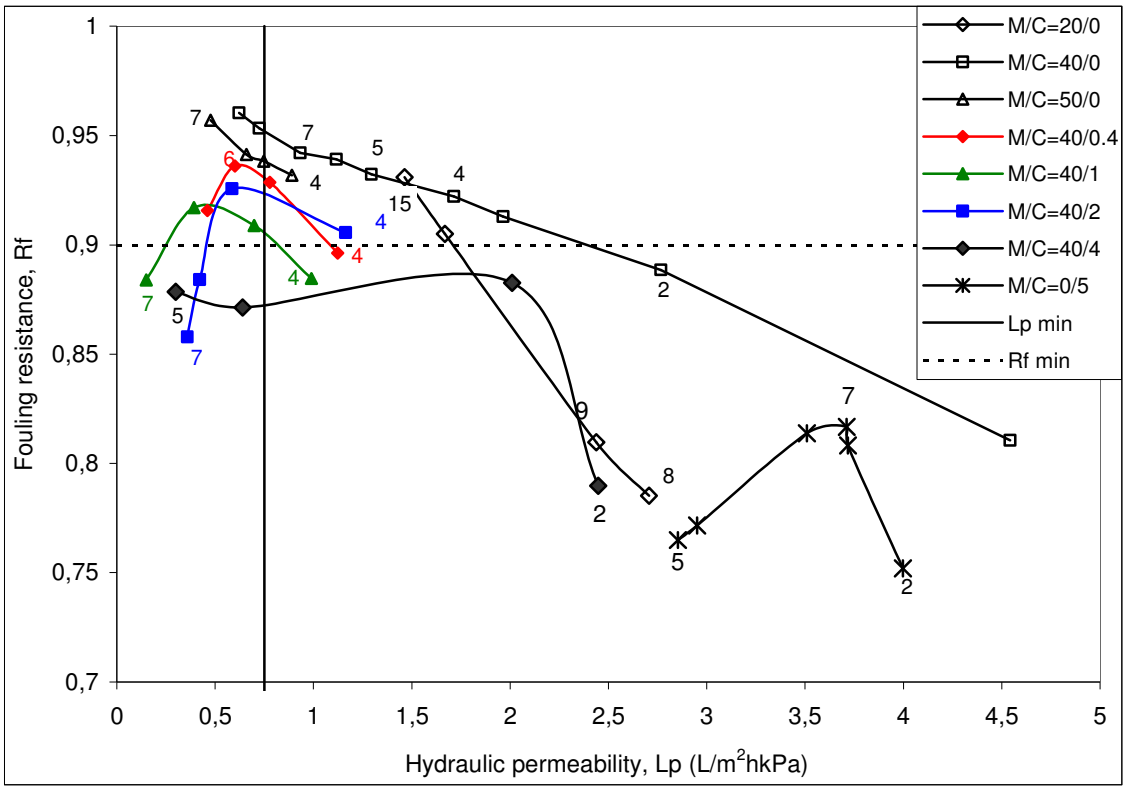

Figure 4.45. Hydraulic permeability–fouling resistance analysis of PEGMA–modified and cross-linker (alone)–modified membranes (PES-SG100 second batch modification). Membrane fouling resistance was evaluated using myoglobin (1 g/L, pH 7, 2 h exposure). The numbers inside the picture indicate the UV irradiation time whereas in the legend indicate the monomer (M) and cross-linker (C) concentrations (g/L).

It is clearly seen in Figures 4.45 and 4.46 that although all unmodified membranes had high hydraulic permeability, their fouling resistance was very low indicating strong fouling tendency. Interestingly, many membranes modified using uncross-linked PEGMA had fully achieved both criteria (Figure 4.45). Examples are modified membranes prepared

with monomer concentration of 40 g/L with UV irradiation time ranging from 3 to 7 min, which yielded hydraulic permeability range from 2.0 to 0.9 L/m^{2}hkPa and fouling resistance ranging from 0.91 to 0.94. Increasing the monomer concentration (50 g/L) did not yield a better performance whereas decreasing the monomer concentration to 20 g/L resulted in membranes that meet the criteria, but only for preparation with long UV irradiation time. Again, this result implies that 40 g/L was an "optimum" monomer concentration.

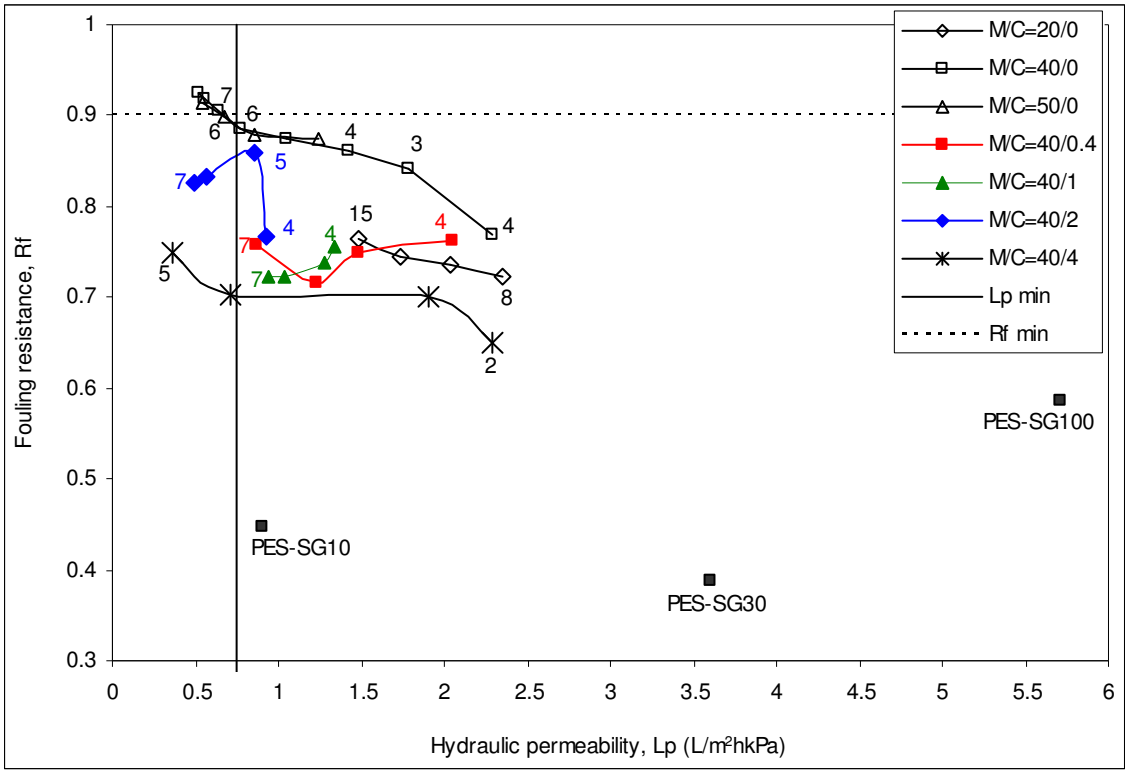

Figure 4.46. Hydraulic permeability–fouling resistance analysis of unmodified and SPE–modified membranes (PES-SG100 second batch modification). PES-SG10, PES-SG30 and PES-SG100 are 10, 30 and 100 kg/mol, unmodified membranes respectively. Membrane fouling resistance was evaluated using myoglobin (1 g/L, pH 7, 2 h exposure). The numbers inside the picture indicate the UV irradiation time whereas in the legend indicate the monomer (M) and cross-linker (C) concentrations (g/L).

The presence of cross-linker in the reaction mixture did not improve the adsorptive fouling resistance and the hydraulic permeability of uncross-linked modified membranes. Nevertheless, two cross-linked–modified membranes using the monomer/cross-linker concentrations ratio of 40/0.4 (5 min irradiation) and of 40/2 (4 min irradiation) could fulfill the criteria. Surprisingly, no SPE–modified membrane (both cross-linked and uncross-linked) would achieve the criteria (Figure 4.46). However, when compared to the unmodified membranes, some of them still had promising performance. Therefore, it is still reasonable to include some SPE–modified membranes in further evaluation (ultrafiltration). Eventually, the following modified membranes seemed to be feasible to be evaluated with respect to the stability as well as ultrafiltration performance: PES-g-PEGMA (40 g/L, 5 min), PES-g-PEGMA/MBAA (40/0.4 g/L, 5 min), PES-g-PEGMA/MBAA (40/2 g/L, 4 min), PES-g-SPE (40 g/L, 6 min) and PES-g-SPE/MBAA (40/2 g/L, 5 min); (cf. Figure 4.39).

4.3.4. Evaluation of the stability of grafted polymer layer

The stability of grafted polymer layer in sodium hypochlorite solution, which is usually used for membrane cleaning, was evaluated (only for second batch modification) as the performance alone is insufficient for commercial application. The results are presented in Figures 4.47 and 4.48.

Interestingly, it was observed that both ATR–IR absorbance and contact angle did not change after incubating for various incubating times. These results are supported by the elemental analysis (cf. Table 4.6). The elements composition did not change after incubating. This observation is in general agreement with similar study of stability of ultrathin grafted PEG films by Sharma *et al*. [135]. They found no change in CA of PEG films during 4 weeks exposing to phosphate–buffered saline solution.

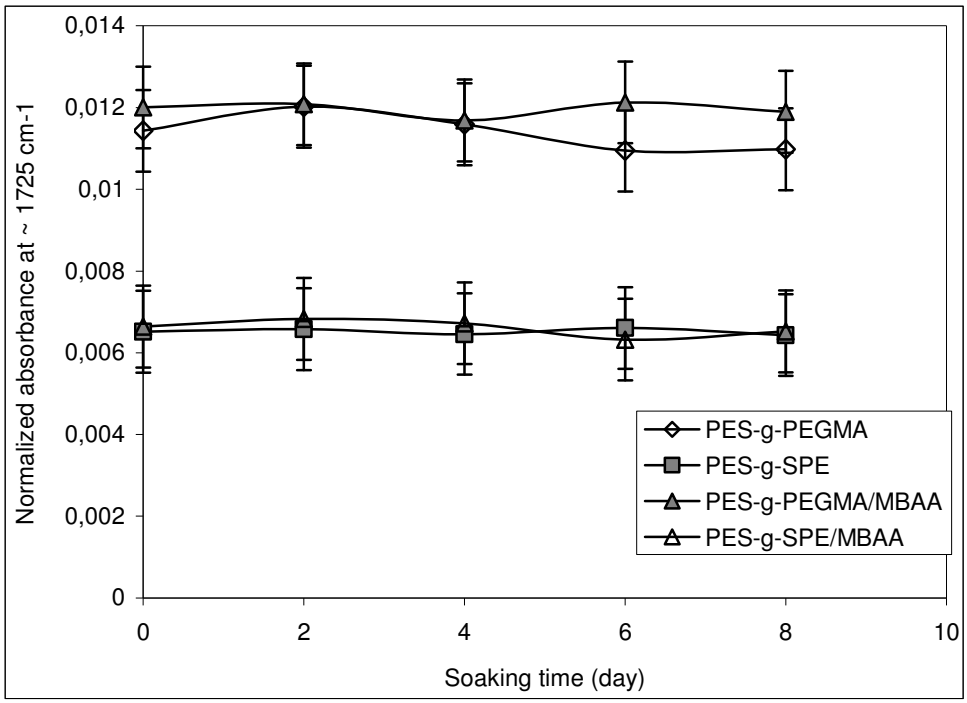

Figure 4.47. Normalized absorbance intensity (by subtracting the absorbance of the base membrane) at wavenumber of ~1725 cm^{-1} and ~1727 cm^{-1} for PEGMA– and SPE–modified membranes, respectively, after soaking in sodium hypochlorite solution.

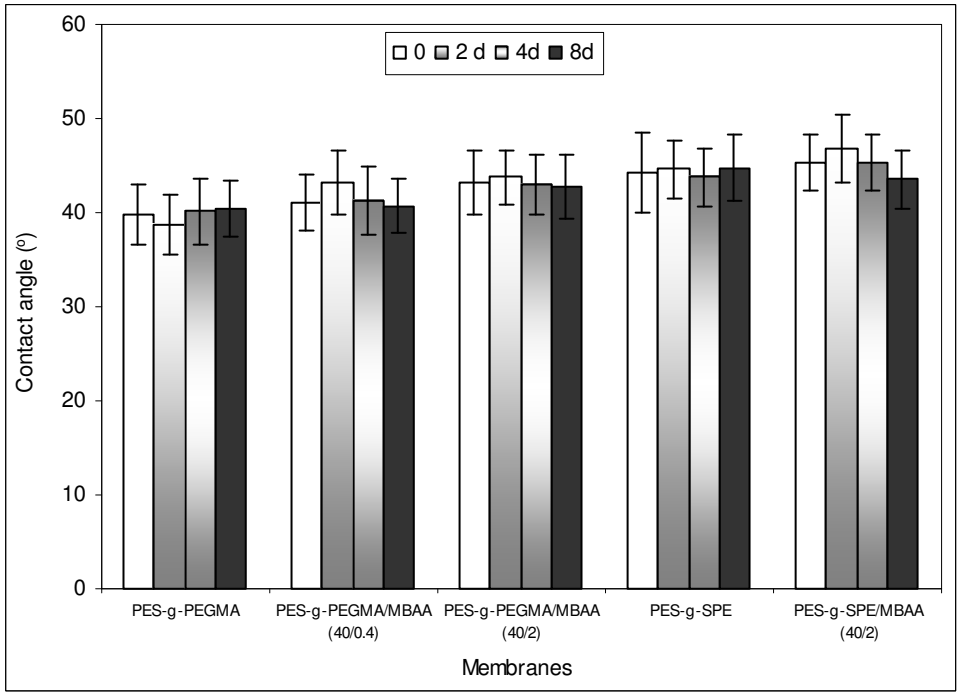

Figure 4.48. Captive bubble contact angle of modified membranes after soaking in sodium hypochlorite solution.

4.4. Evaluation of Modified Membranes Performance Based on Ultrafiltration

Ultrafiltration experiments were conducted to know the performance of modified membrane from a practical application point of view. The membrane performance was expressed in terms of permeate flux/initial water flux ratio and protein rejection. Protein (BSA solution) and sugarcane juice polysaccharide (SJP) were used as the test solution for modified membranes obtained from the first batch modification whereas protein (myoglobin solution), polysaccharide (dextran solution) and natural organic matter (humic acid solution) were used for modified membranes obtained from the second batch modification. To minimize the effect of flux–rejection trade-off, unmodified PES UF membranes having similar nominal cut–off (10 kg/mol) were included in evaluation study, i.e. P010F for the first batch modification and PES-SG10 for the second batch modification.

4.4.1. Evaluation of membrane performance for ultrafiltration of protein

Modified membranes obtained from the first batch modification with improved adsorptive fouling resistance as detected in static fouling experiments (cf. Section 4.3.3) were selected and compared with the unmodified membrane with respect to UF flux and observed protein rejection.

As obviously seen in Table 4.7, a flux versus rejection “trade-off” was also observed during UF for the series of different membranes. Membranes with high flux yielded lower rejection and membranes with high rejection had lower flux. The unmodified base membrane (50 kg/mol) had a relatively high flux, but the lowest rejection and the lowest UF flux ratio (indicating that this membrane had the highest fouling tendency). With the exception of the functionalized membrane #1 (prepared using “period 1” conditions; cf. Section 4.3.2), all modified membranes yielded lower flux than the unmodified membrane

(#0), and all membranes (#1–5) had higher rejection than the unmodified membrane. Furthermore, the rejection increased systematically with decreasing flux. Interestingly, all functionalized membranes also had higher UF flux ratio than unmodified base membranes. Nevertheless, only modified membranes prepared using periods 2 and 3 had higher flux ratio than 10 kg/mol unmodified membrane.

Table 4.7. Filtrate flux, solute rejection and flux ratio during ultrafiltration[a] of modified membrane obtained from the first batch modification

No	Membrane	Flux (L/m^2h)[b]	Rejection (%)	Flux ratio[c]
#0	Unmodified 50 kg/mol	138	56	0.21
#1	100 g/L, 1 min (~8[d])	142	62	0.24
#2	50 g/L, 1 min (~33[d])	135	59	0.22
#3	40 g/L, 1.5 min (~38[d])	112	71	0.65
#4	40 g/L, 3 min (~40[d])	70	80	0.73
#5	40 g/L, 6 min (~170[d])	29	96	0.92
#6	Unmodified 10 kg/mol	58	91	0.52

[a]Filtration was performed at a constant pressure of 100 kPa up to ~ 10 mL of permeate (from 60 mL of sample) was collected.
[b]Permeate flux; [c]UF flux ratio is the ratio between filtrate flux and the initial water flux.
[d]Degree of grafting ($\mu g/cm^2$).

Modified membranes obtained from the second batch modification having improved adsorptive fouling resistance (cf. Section 4.3.3) were initially tested with myoglobin. Figure 4.49 and Table 4.8 show the flux profile over time and apparent myoglobin rejection, respectively. Interestingly, all modified membranes had much higher flux ratio than both unmodified membranes. The unmodified membranes had permeate flux only ~20 % (for 100 kg/mol) and ~30 % (for 10 kg/mol) relative to initial water flux whereas modified membranes had more than 60% for SPE–modified membranes and more than 80% for PEGMA–modified membranes. A common phenomenon during fouling study was also observed in this work, i.e. membrane with larger pore size leading to high flux

yielded more severe fouling (higher flux loss relative to the initial water flux) than membrane with smaller pore size (cf. PES-SG10 and PES-SG100) even though it had smaller flux loss in the beginning of operation. Table 4.8 shows that the unmodified membrane (10 kg/mol) had the highest protein rejection (~70%) whereas 100 kg/mol unmodified membrane had the lowest rejection. All modified membranes had slightly lower protein rejection than 10 kg/mol unmodified membranes. Furthermore cross-linked modified membranes displayed higher rejection than uncross-linked. This rejection result agrees well with membrane rejection curves measured using PEGs presented in Figure 4.39.

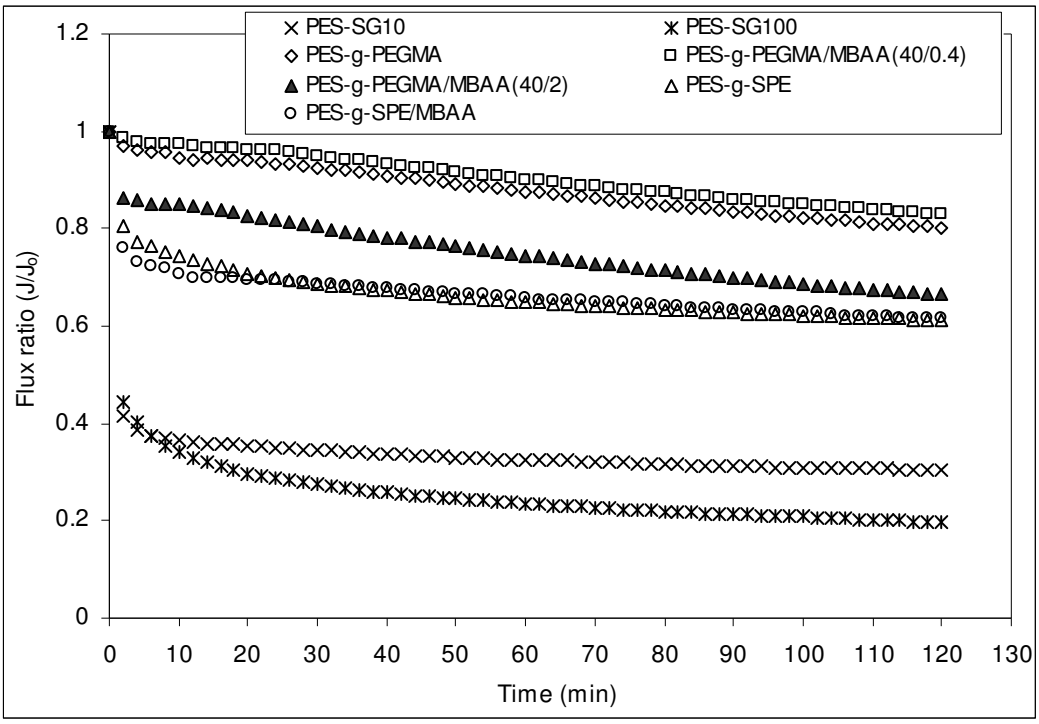

Figure 4.49. Flux profile as a function of time for various modified membranes (obtained from the second batch modification) during ultrafiltration of myoglobin solution (1 g/L, pH 7) at transmembrane pressure of 100 kPa. J_o is the initial water flux (L/m^2h). PES-SG10 and PES-SG100 are 10 and 100 kg/mol unmodified membranes, respectively.

Table 4.8. Initial water flux, water flux after external cleaning and apparent protein (myoglobin) rejection during ultrafiltration.

No	Membrane	Initial water flux (Jo), L/m^2h	Water flux after ext. cleaning L/m^2h	Myoglobin rejection (%)*
1	PES-SG10	95.2	42.5	69.4 ± 1.2
2	PES-SG100	525	248.7	15.7 ± 1.3
3	PES-g-PEGMA	93.5	83.2	57.5 ± 1.0
4	PES-g-PEGMA/MBAA (40/0.4)	84.2	76.8	61.3 ± 0.9
5	PES-g-PEGMA/MBAA (40/2)	71.2	56.4	66.0 ± 1.1
6	PES-g-SPE	87.2	68.	59.1 ± 1.3
7	PES-g-SPE/MBAA (40/2)	80.1	57.7	64.6 ± 1.4

*average value from time filtration of 20, 60, 90 and 120 min

4.4.2. Evaluation of modified membranes performance for ultrafiltration of sugarcane juice polysaccharides (SJP)

Since more than two decades, UF has been proposed as a promising alternative technology to replace the conventional sugarcane juice clarification [168-170]. However, fouling is still a big problem in this application [171-173] and consequently it will have an adverse impact on the economy and efficiency of the UF process. Thus, study was undertaken in order to know the potential of modified membrane for sugarcane juice clarification. Sugarcane juice polysaccharides (SJP) were used as the feed and only modified membranes produced from the first batch modification were tested. This SJP contains mainly polysaccharides, which also contains protein moieties [19]. In addition, phenolics compounds were also identified. Figures 4.50 and 4.51 show the results of adsorptive fouling study.

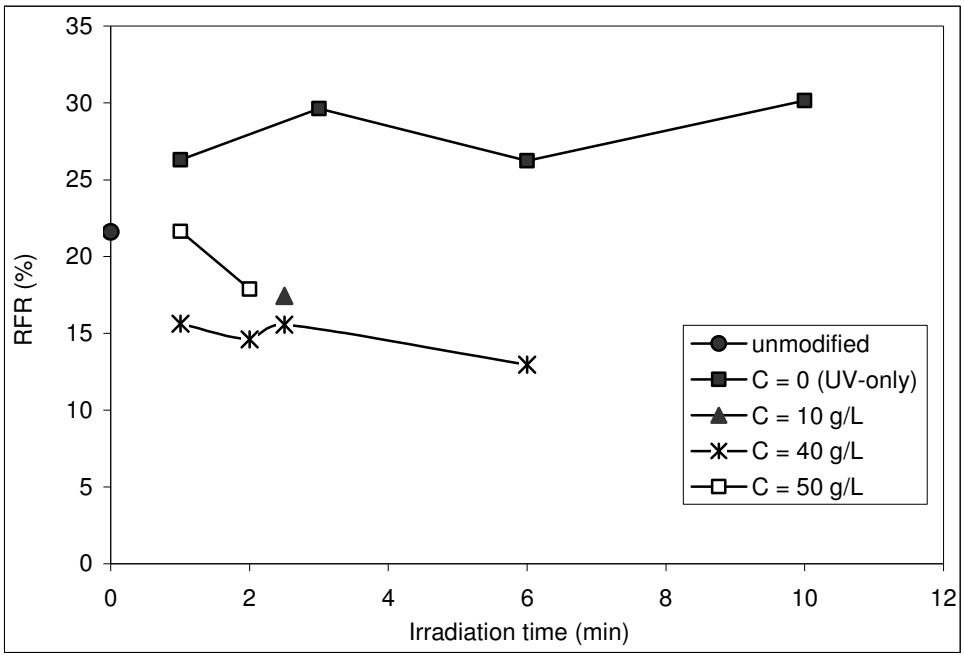

Figure 4.50. Relative water flux reduction for unmodified, UV irradiated and PEGMA–functionalized PES-050H membranes (first batch modification) after static adsorption with "reconstituted" SJP for 2.5 h exposure.

As presented in Figure 4.52, it is observed that the reconstituted SJP solution caused less RFR (22%) than BSA for the unmodified membrane (cf. Figure 4.40 for BSA). An opposite results as compared to the BSA data were found for the UV-irradiated membranes. They showed higher RFR (~25–30%) than the unmodified membrane. All PEGMA–functionalized membranes had significantly lower RFR than the unmodified membranes. All modified membranes had fouling resistance above 0.7 (Figure 4.51). However, when evaluating the effects of the photograft functionalization with PEGMA, it becomes clear that all modified membranes have a performance below the simple "trade-off curve". Then, similar results with BSA ultrafiltration, i.e. flux–rejection trade-off, were also observed upon ultrafiltration of SJP (Table 4.9). The unmodified membrane had higher flux, but lower rejection as well as flux ratio. Further, during UF of SJP, it was clearly seen that the high molecular weight fraction (molar mass ~300-80 kg/mol) was

only partly rejected by the unmodified membrane, while the rejection was significantly larger for the PEGMA–functionalized membrane with DG = 40 μg/cm^2, and complete rejection was observed for the PEGMA–functionalized membrane with DG = 170 μg/cm^2 (cf. Figure 5.52). The PEGMA functionalized membranes showed partial rejection even for the fraction with smaller size (molar mass ~15.5 kg/mol), and this is in agreement with the dextran rejection curves for these membranes (cf. Figure 4.38). It should be noted that lower nominal rejection of SJP than protein with the same membranes is due to the selection of a lower molar mass range of SJP used for the calculations (cf. Table 4.7).

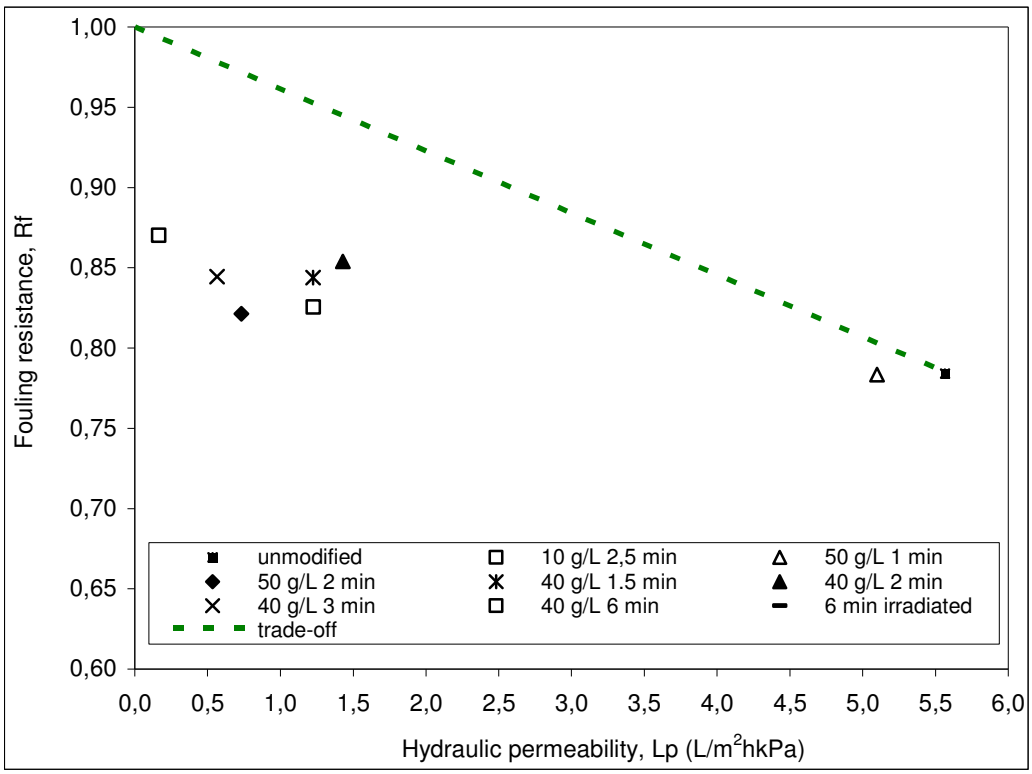

Figure 4.51. Performance analysis for unmodified, UV irradiated and PEGMA–functionalized PES-050H membranes (first batch modification) with respect to adsorptive fouling of SJP solution.

Table 4.9. Filtrate flux, solute rejection and flux ratio during SJP ultrafiltration[a]

No	Membrane	Flux (L/m^{2}h)[b]	Rejection (%)[c]	Flux ratio[d]
#0	Unmodified 50 kg/mol	120	~11	0.17
#1	100 g/L, 1 min (~8[e])	125	n.d	0.24
#2	50 g/L, 1 min (~33[e])	119	n.d	0.18
#3	40 g/L, 1.5 min (~38[e])	107	n.d	0.61
#4	40 g/L, 3 min (~40[e])	68	~20	0.72
#5	40 g/L, 6 min (~170[e])	29	~75	0.88

[a]Filtration was performed at a constant pressure of 100 kPa up to ~ 10 mL of permeate (from 60 mL of sample) was collected; [b]Permeate flux; [c]Rejection of molar mass fraction 10-30 kg/mol, calculated by are ration; [d]UF flux ratio is the ratio between filtrate flux and the initial water flux; [e]Degree of grafting (µg/cm^2).
n.d.: not done

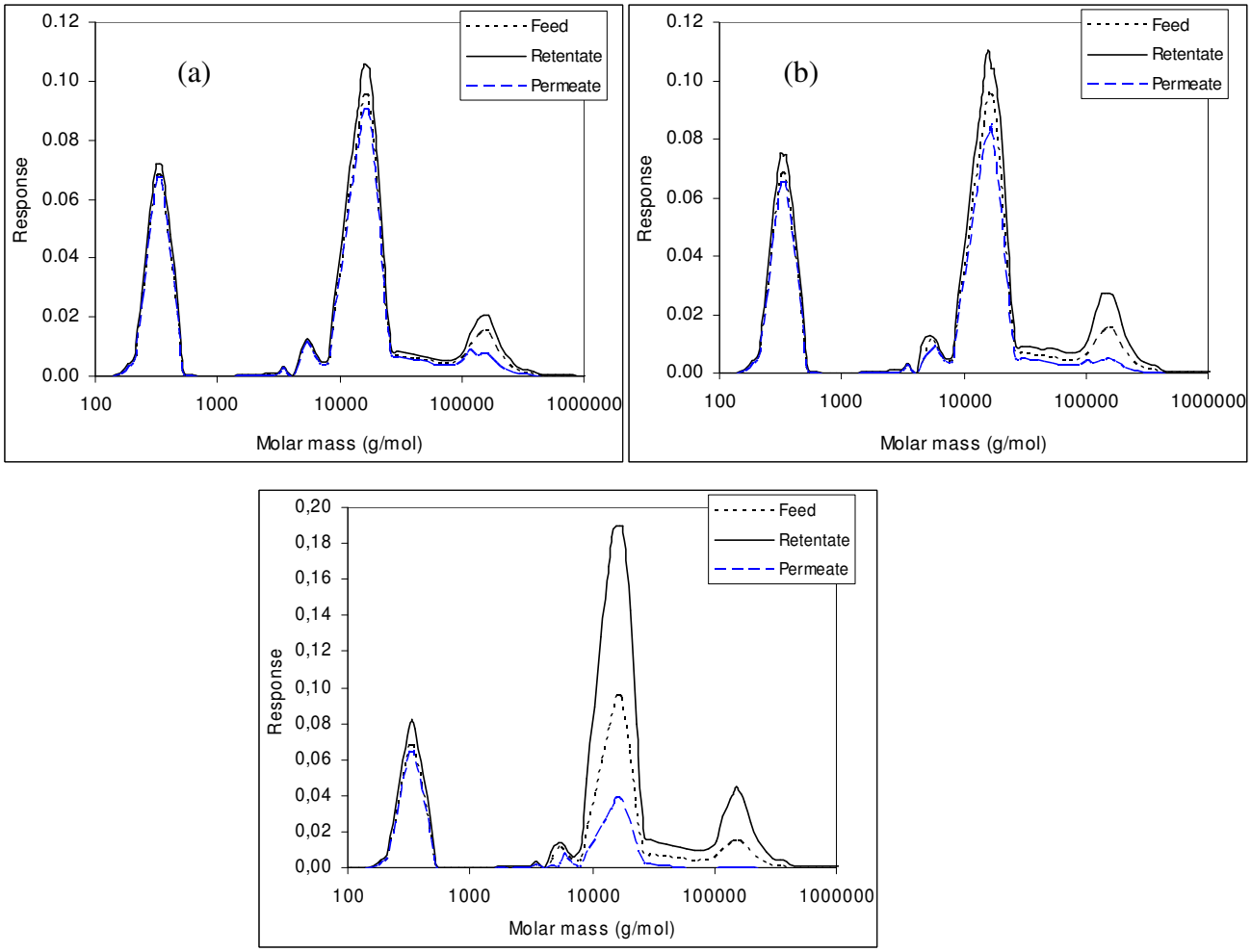

Figure 4.52. Fractionation of reconstituted SJP during UF: (a) unmodified PES-050H membrane, (b) PEGMA–functionalized (40 g/L and 3 min; DG≈40 µg/cm^2) (c) PEGMA–functionalized (40 g/L, 6 min; DG≈170 µg/cm^2); molar mass had been calculated from GPC data with dextrans as standards.

4.4.3. Evaluation of modified membranes performance for UF of dextran

As clearly observed in Section 4.2, dextran can foul the PES membrane; therefore, dextran solution was also used as the test solution to evaluate the modified membrane performance. Modified membranes obtained from the second batch modification were used in this study. The results are presented in Figures 4.53 and 4.54.

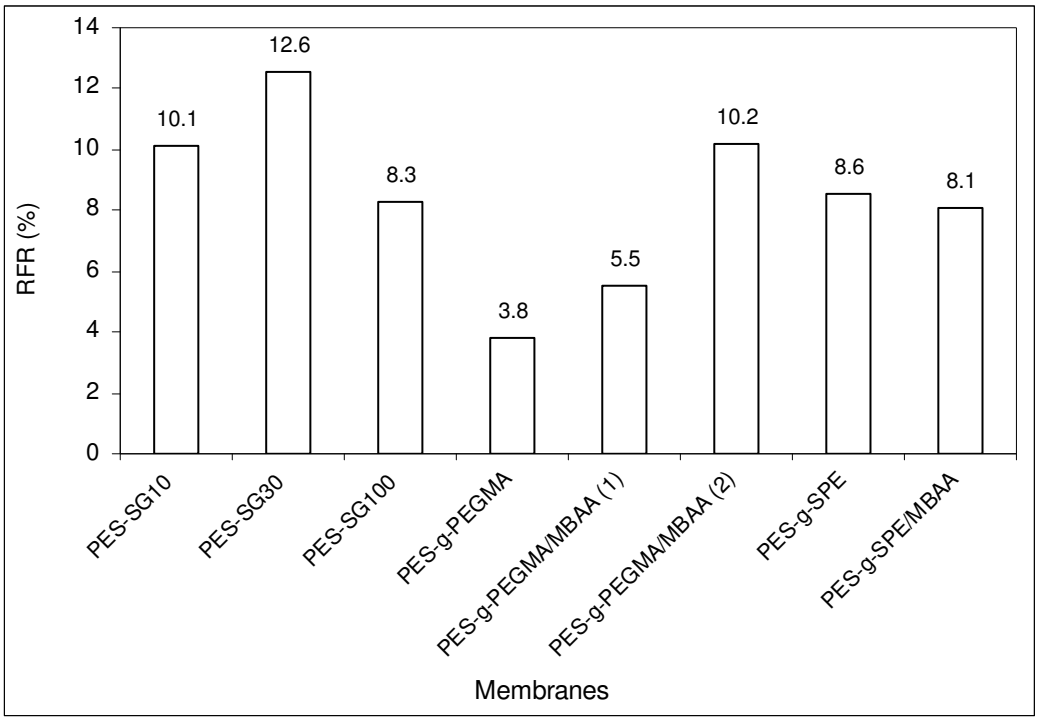

Figure 4.53. RFR of unmodified and modified PES-SG100 membranes (second batch modification) after static adsorption (3 hour) with dextran T-10 (10 g/L)

In general, all modified membranes showed lower RFR than unmodified membrane with similar membrane cut−off (PES-SG10). However, if compared to the base membrane, only PEGMA−modified membranes showed lower RFR whereas SPE−modified membranes showed similar RFR. More interestingly, the ultrafiltration data displayed that all modified membranes (except for PES-g-PEGMA/MBAA (40/2)) showed higher relative flux ratio (permeate flux/initial water flux) than PES-SG10 unmodified. The increase in flux ratio were ~10% for PES-g-PEGMA as well as PES-g-PEGMA/MBAA

with small concentration of cross-linker (0.4 g/L) and 3-5% for modification using SPE. However, modification using PEGMA with relatively high concentration of cross-linker (2 g/L) did not improve the flux ratio. These results agree well with static adsorption results (cf. Figure 4.53). It is important to note that all modified membranes had similar rejection of dextran T-10 with unmodified PES-SG 10 (74-82 %; Table 4.10). Further, the ratio of flux after external rinsing with water and initial water flux were higher for all modified membranes than for unmodified membrane.

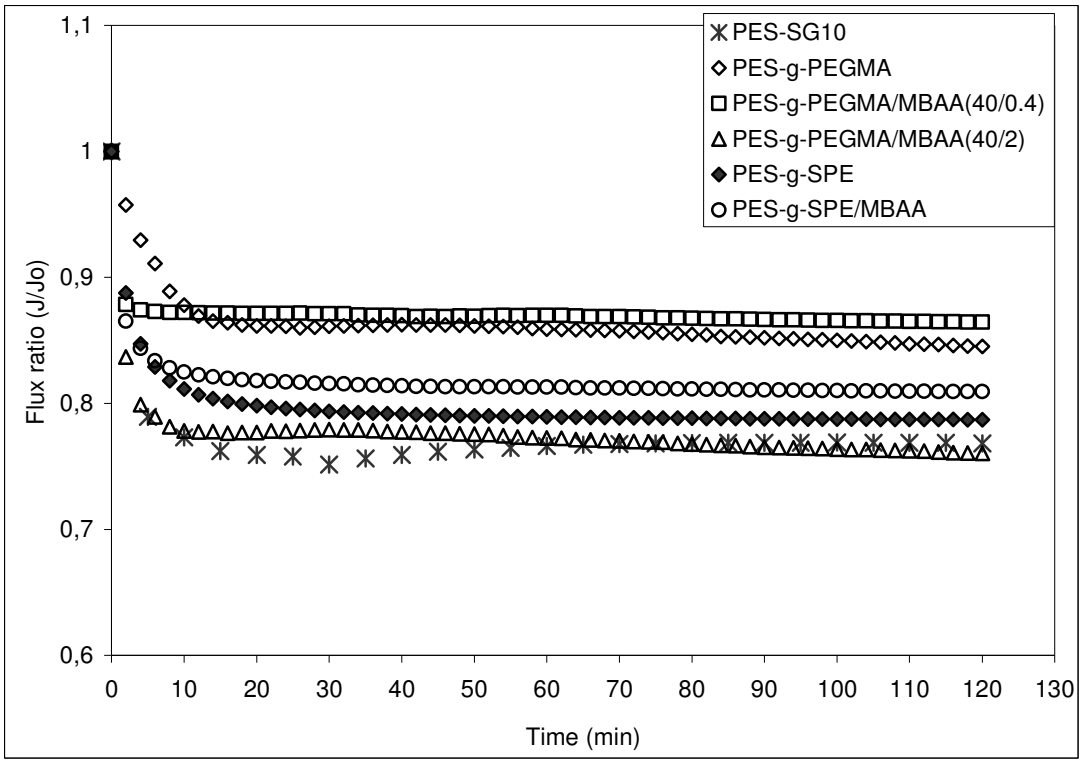

Figure 4.54. Flux profile as a function of time for unmodified (PES-SG10) and modified membranes during ultrafiltration of dextran T-10 (1 g/L) at transmembrane pressure of 100 kPa. J_o is the initial water flux (L/m^2h).

4.4.4. Evaluation of membrane performance for UF of natural organic matter (NOM)

In this study, humic acid (HA) – well known as strong foulant in surface water treatment [13,174-177] – was used as the test solution. One of the major limitations in working with

commercial humic acids is their varied properties [178]. Consequently, results obtained from one case can not immediately be applied for other case with different humic substance. Therefore, the characteristics of HA used was first investigated.

Table 4.10. Initial water flux, water flux after external cleaning and apparent dextran rejection during ultrafiltration.

No	Membrane	Initial water flux (Jo), L/m^{2}h	Water flux after ext. cleaning, L/m^{2}h	Rejection of dextran T-10 (%)*
1	PES-U10	93.2	77.2	82.6
2	PES-g-PEGMA	90.8	87.1	74.9
3	PES-g-PEGMA/MBAA (40/0.4)	88.4	83.1	77.3
4	PES-g-PEGMA/MBAA (40/2)	81.3	69.9	79.1
5	PES-g-SPE	76.6	69.1	79.6
6	PES-g-SPE/MBAA (40/2)	81	73.7	80.3

*average value from time filtration of 20, 60, 90 and 120 min

Figure 4.55 shows the NMR spectrum of humic acid used. It is observed that the HA is mainly composed of aliphatic and aromatic groups as evidenced by appearance of peaks at 0-50 and 60-96 ppm, respectively. This indicates that the HA consists of both hydrophilic and hydrophobic fractions. However, the hydrophilic fraction was much larger than the hydrophobic fraction. In addition to the aliphatic and aromatic groups, carbohydrate and aromatic C-O were also observed at 60-96 ppm and 145-162 ppm, respectively. Overall, even though the heterogeneity of HA is a common problem, this result agrees well with previous data reported by Mao *et al*. [179].

Figures 4.56 and 4.57 show the results obtained from adsorptive fouling study and ultrafiltration, respectively. In order to obtain severe fouling, calcium ions were added to the humic acid solution during ultrafiltration experiment. It is generally known that as calcium ions were added, the humic acid fouling would increase due to complexation of

Ca^{++} with the carboxyl groups in the humic acid leading to more compact character of humic acid solutes [15,175,180,181].

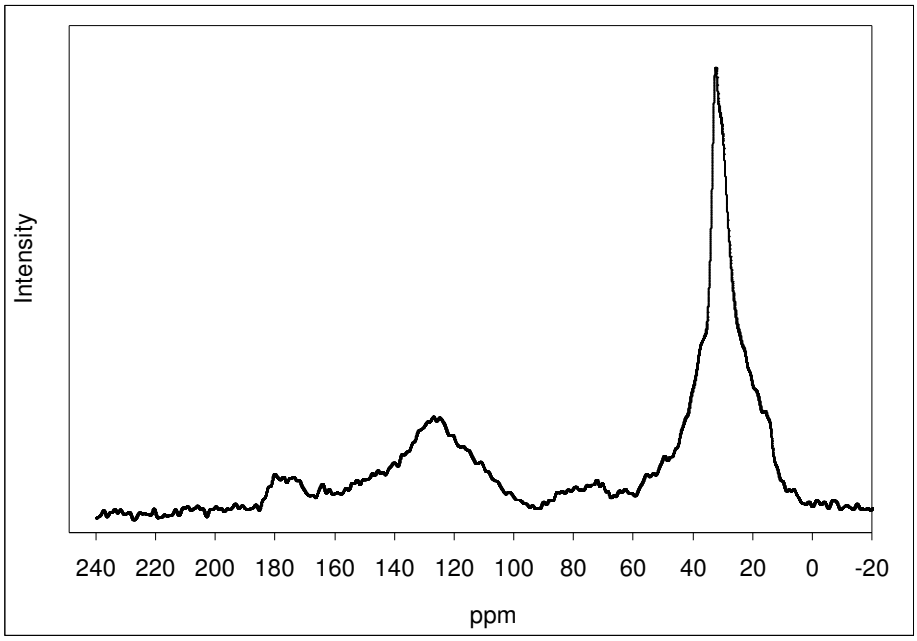

Figure 4.55. CP MAS 13C NMR spectrum of humic acid used

The results in Figure 4.56 show the effect of adsorptive fouling on RFR of various membranes at alkaline and acidic conditions and in the presence of calcium ions. It is observed that exposing the membrane in acidic and alkaline pH solutions reduced the water flux. As also found in previous literature (e.g., [13,175,177]), the fouling was larger in acidic pH than in alkaline pH. However, it is important to note that increasing water flux after exposing to the alkaline HA solution was also observed in the beginning of water flux measurements. Interestingly, all modified membranes showed significantly lower RFR than unmodified membrane with similar membrane cut–off even if compared to the base membrane (except for PES-g-SPE). Further, the membrane pore size influenced the extent of adsorptive fouling, i.e. membrane with smaller pore size showed higher adsorptive fouling as evidenced by higher RFR. However, this observation is in contrast with the result from ultrafiltration (cf. Figure 4.58).

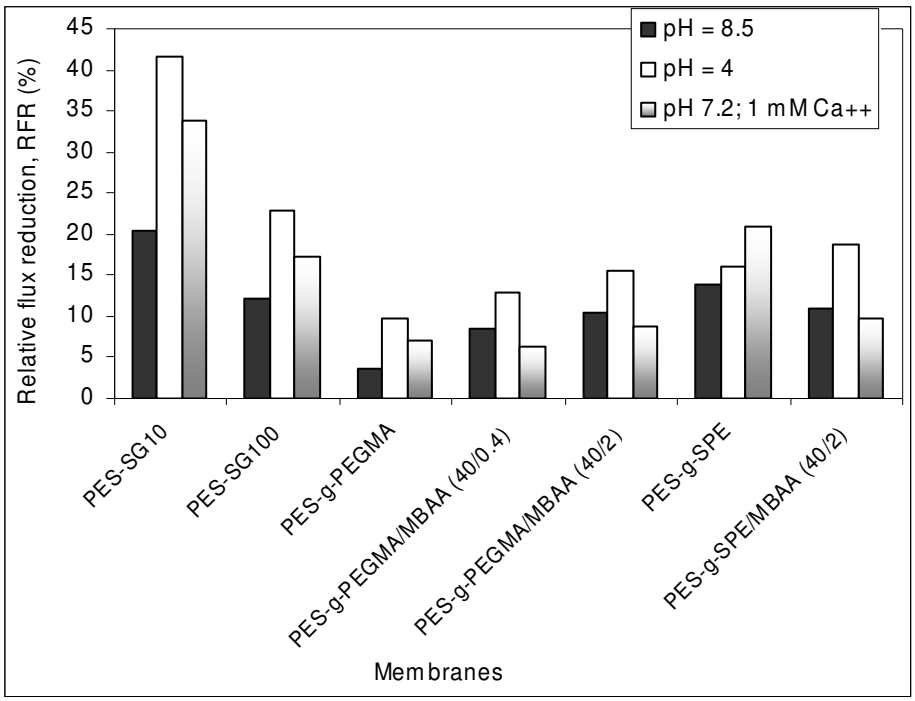

Figure 4.56. RFR after static adsorption (18 hours exposure) of various HA solutions (100 mg/L) on unmodified and modified (obtained from second batch modification) membranes. PES-SG10 and PES-SG100 are 10 and 100 kg/mol unmodified membranes respectively.

As depicted in Figure 4.57, again similar results are obviously seen, i.e. all modified membranes had higher permeate flux than unmodified membrane. For example, the PES-g-PEGMA and PES-g-PEGMA/MBAA showed permeate fluxes approximately 80% and 72% of their initial water flux, respectively. By contrast, the unmodified membranes showed permeate fluxes only approximately 51% and 39% for PES-SG10 and PES-SG100 membranes, respectively. Even though UF was done at similar initial water flux (~92 L/m^2h) in order to minimize effects of hydrodynamic conditions, membrane with larger pore sizes showed more severe fouling (cf. PES-SG10 and PES-SG100). The apparent rejections were similar for all membranes (cf. Table 4.11).

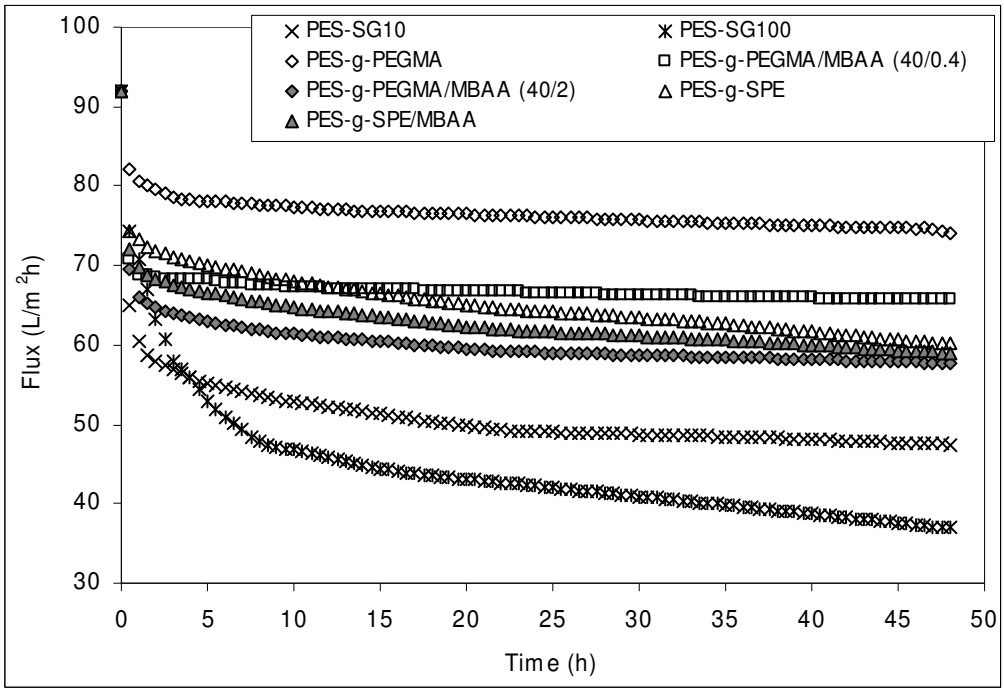

Figure 4.57. Flux profile as a function of time during ultrafiltration of humic acid (50 mg/L, pH 7.2, 1 mM Ca^{++}, conductivity 1100 μS/cm) at similar initial water flux (~92 L/m^2h). PES-SG10 and PES-SG100 are 10 and 100 kg/mol unmodified membranes, respectively.

It was also observed that the water fluxes after external rinsing were significantly higher for modified membranes than unmodified membrane (cf. Table 4.11). External rinsing by pure water and shaking could recover the initial water fluxes to approximately 90% and 86% for PES-g-PEGMA and PES-g-PEGMA/MBAA, respectively. By contrast, the same cleaning procedure for unmodified membranes yielded ~65% and ~47% recovery for PES-SG10 and PES-SG100, respectively. This observation agrees well with previous studies [15,182]. Further, Figure 4.58 shows snapshots of the membrane surfaces taken after external rinsing and shaking. Significant difference in fouling layer was observed between modified and unmodified membranes. No significant difference was observed after cleaning for both unmodified membranes. Surprisingly, similar results with unmodified membranes (even worse, cf. PES-g-SPE and PES-SG10) were obtained for

modified membranes grafted with polySPE. By contrast, significant HA layer removal from the membrane surface was obtained for PES-g-PEGMA and PES-g-PEGMA/MBAA (40/0.4) modified membranes.

Table 4.11. Initial water flux, permeate flux, water flux after external rinsing and apparent humic acid rejection during ultrafiltration.

No	Membrane	Initial water flux[a]	Permeate flux at 48 h filtration[b]	Water flux after rinsing[c]	HA rejection (%)[d]
1	PES-SG10 (unmodified)	91.7	47.3	59.3	95.4 $\pm$ 2.1
2	PES-SG100 (unmodified)	93.6	36.9	44.2	86.5 $\pm$ 3.1
3	PES-g-PEGMA	92.5	74.1	83.3	91.5 $\pm$ 2.3
4	PES-g-PEGMA/MBAA (40/0.4)	91.6	65.6	78.9	92.3 $\pm$ 2.4
5	PES-g-PEGMA/MBAA (40/2)	91	57.6	72.3	93.1 $\pm$ 2.5
6	PES-g-SPE	92.	60.1	70.3	93.3 $\pm$ 2.6
7	PES-g-SPE/MBAA (40/2)	93.1	58.9	75.2	94.1 $\pm$ 2.4

[a,b,c] Flux in L/m^2h

[c] membrane was externally rinsed with pure water and shaking

[d] average value from time filtration of 12, 24, 36 and 48 h

Overall, with respect to the all potential foulants used, modified membranes showed much better performances than unmodified membranes. Further, modified membranes prepared with PEGMA showed better performances than modified membranes prepared with zwitterionic SPE.

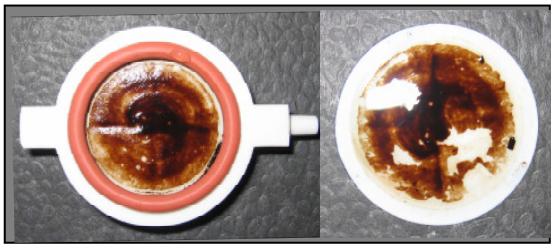

PES-SG10

PES-SG100

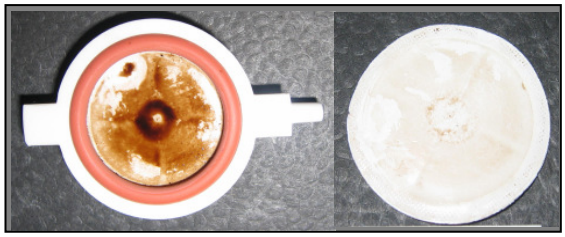

PES-g-PEGMA

PES-g-PEGMA/MBAA (40/0.4)

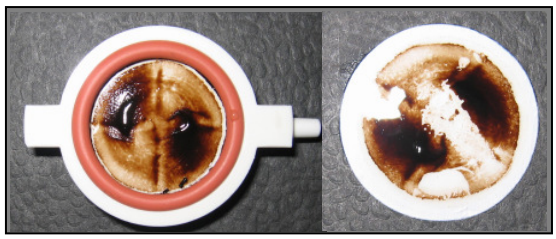

PES-g-PEGMA/MBAA (40/2)

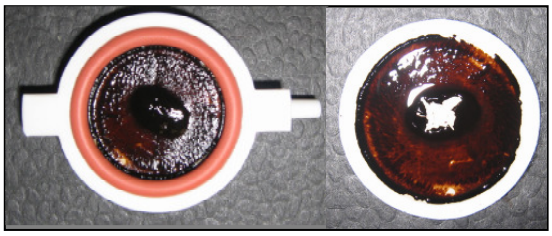

PES-g-SPE

PES-g-SPE/MBAA

Figure 4.58. Snapshots of the HA (50 mg/L, 1 mM Ca^{++}, pH 7.2)–fouled membranes: the left sides are images after ultrafiltration whereas the images on the right side taken after external cleaning (by pure water and shaking).

Chapter 5
DISCUSSION

5.1. Membrane Characterization

The differences in observed membrane characteristics among commercial UF membranes with identical nominal cut–off can be explained by differences in one or more of the following aspects: membrane material, membrane formation conditions and resulting membrane structure as well as characterization methods used by the manufacturer.

Significantly different characteristics were observed between the two PES membranes with similar cut–off. The difference in sieving curve behavior, however, is not fully surprising. Presumably, different test substances and test conditions are used by the membrane manufacturers during nominal cut–off determination. AFM data revealed that the PES-SG10 membrane had a much greater pore density (number of pores per unit area of surface) as well as a higher surface porosity than the PES-GR10 membrane (cf. Table 4.1 and Figure 4.1). In addition, pore variations in both size and shape were also observed for both membranes. Those characteristics support the much higher water permeability for the PES-SG10 than for the PES-SG10 membrane. These results agree well with the observed membrane cut–off (cf. Figure 4.7) and dextran rejection (Table 4.1) where the PES-SG10 membrane had higher values of those parameters than PES-GR10. The higher effective diffusion coefficient for the dextran T10 through the PES-SG10 membranes (cf. Table 4.4) is another consequence. Further, both membranes showed different contact angle. This difference in CA could also be caused by the differences in surface pore size and porosity [25,127], surface roughness [183] and additives used in the membrane preparation [184]. Gekas *et al.* [25] had reported that there is interdependence between

contact angle and the pore size. Ulbricht and Belfort [127] had also observed that with increasing pore size of UF membranes from the same material and manufacturing process, the contact angle values decreased due to a higher porosity. Zhang and Hallström [184] obtained significant different CA of two commercial polysulfone membranes. They reported that the difference in chemical composition of the casting solution was the most possible reason. However, in this work, similar surface chemistry of native PES membrane and only slight difference after washing imply that the effect of additive on CA should not be involved. Therefore, the probable reason for this different CA is difference in porosity. As can be seen in the preceding results, the PES-SG10 membrane had larger porosity (Table 4.1 and Figure 4.1), larger permeability (cf. Table 4.1) and larger cut−off from sieving curve (cf. Table 4.1 and Figure 4.7) as compared to the PES-GR10 membrane. This explanation is supported by results of other PES membranes with larger cut−off (from the same manufacturer, PES-SG30 and PES-SG100). These membranes had larger pore size and presumably also porosity (cf. Figure 4.2) than PES-SG10 and as consequences they had larger water permeability and smaller contact angle (cf. Table 4.1).

Similar water permeability obtained from membranes having different cut−off was observed for PES-SG100 and PES-050H. This phenomenon is due to difference in pore density, it is believed that the PES-050H membrane had lower pore density than PES-SG-10 membrane (it should be noted that the water permeability is influenced not only by pore size but also by pore density).

All PES membranes had negative charge over the entire pH range, which decreased towards acidic pH values. This result could be explained as follows: because the PES membranes should not contain anionic groups, which would be protonated below a pH 7 (this would occur for carboxyl, but not for sulfonic acid), the dissociation of surface functional groups would not be the reason for this behavior. Hence, the zeta potential will

presumably be caused by the adsorption of anions (preferential adsorption of hydroxide ions as compared with other ions [185]), at lower pH values suppressed by their reduced concentration.

By contrast, the water permeabilities, sieving curves and dextran rejections of the two cellulose–based membranes were similar (cf. Table 4.1, Figure 4.7). Presumably, both membranes had been formed via phase separation of cellulose acetate and subsequent hydrolysis. The appearance of –CH stretching and C–O single bond stretching and the absence of bands for ester proved this hypothesis (cf. Figure 4.13). The difference in intensity was presumably due to the different process used for manufacturing (cellulose regeneration and stabilization of the pore structure). Further, this caused difference in CA for the two cellulose–based membranes.

AFM data indicated a much different surface morphology between SC-10 and PES-SG10 membranes, i.e. lower pore density, larger pore size, and (consequently) larger surface roughness (Figure 4.1). However, the SC-10 membrane had lower cut–off from PEG sieving as well as dextran diffusion coefficient and higher dextran rejection (cf. Table 4.1, Table 4.4) than the PES-SG10 membrane. Therefore, the conclusions from the AFM topography images of the (dry) membranes as received from manufacturer could not directly be used for interpretation of other results. Due to the pronounced hydrophilicity of the membrane material cellulose, the surface morphology under wet conditions will be swollen (and flexible), and it will hence differ considerably from the dry condition. This explanation is supported by its low negative zeta potentials, which indicates that the outer membrane surface has much more hydrogel than solid character (as it is the case with PES; cf. above). Other possible reason behind this phenomenon is larger change (polymer collapse and agglomeration) upon drying. Therefore, in contrast to PES, the quantification of surface porosity of cellulose–based membranes seems more difficult. The data in Table

4.1 should be considered with great care, and the surface porosity (for SC-10) in swollen state is presumably lower.

Overall, the two PES membranes with nominal cut−off (NMWCO) of 10 kg/mol from different manufacturers showed different characteristics. The PES-SG10 membrane had much higher permeability, larger cut−off value, larger surface porosity and lower contact angle than the PES-GR10 membrane. By contrast, the two cellulose−based membranes were rather similar, except for difference in wettability. The different membrane material caused significant differences in surface structure (i.e. wettabilty and charge) and morphology (permanent pore structure for PES vs. swollen hydrogel for cellulose).

5.2. Study on Dextran Fouling of UF Membranes

5.2.1 Membrane−solute and membrane−solute−solute interactions

All data obtained from the different experiments with the PES UF membranes in contact with dextran and protein solutions indicate that there was solute binding to the membranes while the cellulose−based membranes showed no evidences for strong solute binding (except for the solute uptake in the membrane during diffusion measurements; cf. below).

The analysis of the RFR data for a dextran and a protein of similar size (cf. Figure 4.3) indicates that this adsorptive fouling is dominated by monolayer adsorption (according to the Langmuir model) with an only small contribution of solute−solute interactions (presumably larger for protein than dextran as indicated by larger deviation from the Langmuir model) or a bimodal adsorption site distribution (detectable only at relatively high concentration, i.e. high driving force – the critical concentration was much higher for

dextran than for protein). It is interesting to note that good correlations between RFR and data from quantitative measurements of bound dextran on the same membranes have been obtained (cf. below). Thus, it is clear that the yielded–RFR is correlated with the amount of adsorbed dextran/protein on the membrane surface and as a consequence the analysis of RFR using adsorption isotherm approach is reasonable. Then, the data from the RFR isotherms (cf. Table 4.2) reveal a much higher affinity to PES for the protein, but the affinity of dextran is also considerable. It should be noted that protein adsorption was performed at the isoelectric point (IEP) of myoglobin (pH ~7). Thus, charge based interactions should not be involved. It was frequently reported that at a pH close to the IEP, protein–membrane interactions had the strongest consequences. While this is mainly for hydrophobic interactions, the mechanisms for dextran–PES interactions will be discussed below.

Adsorption kinetic study (cf. Figure 4.4.) showed that the rate–controlling step and the reason for a more complex kinetic behavior and presumably also for the shape of the "isotherm" are simultaneous adsorption on the outer membrane surface and diffusion deeper into the membrane pore structure to other accessible adsorption sites (and thus, presumably, causing even larger effects onto flux, cf. Figure 4.5). For example, Thom et al. [186] had monitored the adsorption kinetics onto spin–coated polysulfone films for an azidobenzoyl–PEG conjugate having a molar mass of 10 kg/mol from 1 g/L solutions with and without stirring. They found that the time to reach a plateau region were 1–2 hours. This time was significantly longer than what had been estimated for the diffusion through the boundary layer only, and the process had been considered surface–reaction (adsorption) controlled. Therefore, for the 10 kg/mol dextran from 10 g/L solution in this study, the significant time delay, the long times to reach a plateau region, and the slight

further increase support the above mentioned hypothesis (adsorption and diffusion into pores as the rate−determining steps).

In addition to the flux reduction, it is clearly seen that the adsorptive fouling of dextran changed the membrane surface characteristics (contact angle, zeta potential, surface morphology) and pore structure (sieving). The reduction of CA of PES UF membrane after exposing to the dextran solution indicates that the adsorption of dextran occurred on PES (cf. Table 4.3). By contrast, the adsorption of dextran on cellulose−based membrane was not observed as evidenced by no change in CA after exposing.

As presented in Figure 4.8, exposing the membranes to the dextran solution changed the PES membrane zeta potential towards lower values, but did not change the ZP of SC membrane. These results indicate clearly that the effective surface charge of the PES membranes has been reduced by the adsorption of dextran. This reduction may be caused by a competition between the adsorption of neutral dextran and of anions from the electrolyte on the membrane surface. However, the adsorbed dextran may also create a more mobile and hence less defined plane of shear which would also lead to lower absolute values of the zeta potential. A possible quantitative explanation had been described elsewhere [187]: The increase in thickness decreases the Coulomb attraction for the adsorption of hydroxide ions by increasing the distance from the ion to the surface. Such a decrease of electrostatic attraction with increasing water−swollen film thickness on a solid (polymer) surface would lead to a lower ion adsorption consistent with the decrease in zeta potential. Therefore, both a hydrophilic dextran layer on the PES surface, and the (water−swollen) surface of the cellulose−based membrane may have the same effect onto effective surface charge. Exposing to the myoglobin solution changed more significant ZP than exposing to the dextran solution. This result can be explained considering the IEP of

the myoglobin (pH ~7), i.e. an excess of positive surface charge has been introduced via the protein.

The visualization of dextran fouling using AFM supports above observations. The changes in surface morphology due to dextran adsorption were significant and much larger for PES-GR10 than for PES-SG10 membrane (cf. Figure 4.9). The ultimate reason might be the difference in the ability to disperse the dextran on the outer surface during drying (note that drying the membrane with an adsorbed hydrophilic polymer on the surface will also involve dehydration of the hydrophilic polymer and can lead to aggregation). The different behaviour is presumably caused by different surface porosities (cf. Table 4.1, Figure 4.1): the lower porosity of the GR-PES membrane leads to a smaller number of larger dextran aggregates (cf. Figure 4.9).

The adsorptive fouling of dextran also changed the membrane sieving (cf. Figure 4.7). Both pore narrowing as well as pore blocking seemed to occur. This phenomenon could be explained that for the same molar mass, dextran has a smaller hydrodynamic radius than PEG [188]. For a molar mass of 10 kg/mol, the ratio of the hydrodynamic radii between dextran and PEG is ~0.78 (calculated using data in [188]). Therefore, dextrans – having a molar mass in the range of the cut−off obtained using PEGs – can not only block the pore entrance or reduce the effective pore radius but also penetrate deeper into the pores of the active layer. This would be in line with the hypothesis to explain the more complex effects of concentration and time during adsorption (cf. above).

Quantitative data for bound dextran on membranes in contact with a solution (no convective flux through the membrane) was obtained with two different methods, i.e. ATR−IR and SDAM. The ATR−IR data showed clearly the influence of the dextran concentration on the increasing band area with a plateau value reached at dextran concentration 5 g/L (cf. Figure 4.15). This observation is similar to the dependency of the

RFR on dextran concentration (cf. Figure 4.3). Further, the increases in IR band area for fouled PES-GR10 membranes (for 10 g/L: IR ratio = 6.5; RFR = 13, cf. Figures 4.5 and 4.15) were larger than for PES-SG10 membranes (for 10 g/L: IR ratio = 2.4; RFR = 10, cf. Figures 4.5 and 4.15), i.e. the amount of dextran adsorbed on the GR-PES membrane should be higher. A further analysis was done by correlating between RFR and increasing band area as a function of dextran concentration. Good correlation between RFR from pure water measurements and increasing band area as a function of dextran concentration was obtained (Figure 5.1). The bound amounts of dextran T10 obtained from SDAM experiments were also larger for PES-GR10 (21 mg/m^2 at 3.5 h) than for SG-PES membranes (15 mg/m^2 at 3.5 h). Again, this result was in line with RFR results (cf. above). Further, the bound amounts from SDAM were much higher for myoglobin than for dextran, irrespective the smaller concentration – this was in agreement with the larger affinity (cf. above) and with results of other kinetic studies (e.g., [189]). Figure 5.2 shows – again for the PES-SG10 membrane where both time–dependent data were available – that there is a good correlation between the RFR values from pure water flux measurements and the bound dextran amounts obtained from the SDAM experiments.

Overall, reasonable correlations of the effect of dextran concentration on RFR as well as the effect of the PES membrane type were obtained. When comparing the correlation of both quantitative methods (SDAM and IR) with RFR data, larger deviations to higher values were observed for the IR method. This could be explained with the surface selectivity of the method (sampling depth into the membrane only about 2 µm); i.e. the accumulation of dextran in the active layer region is selectively detected with this method.

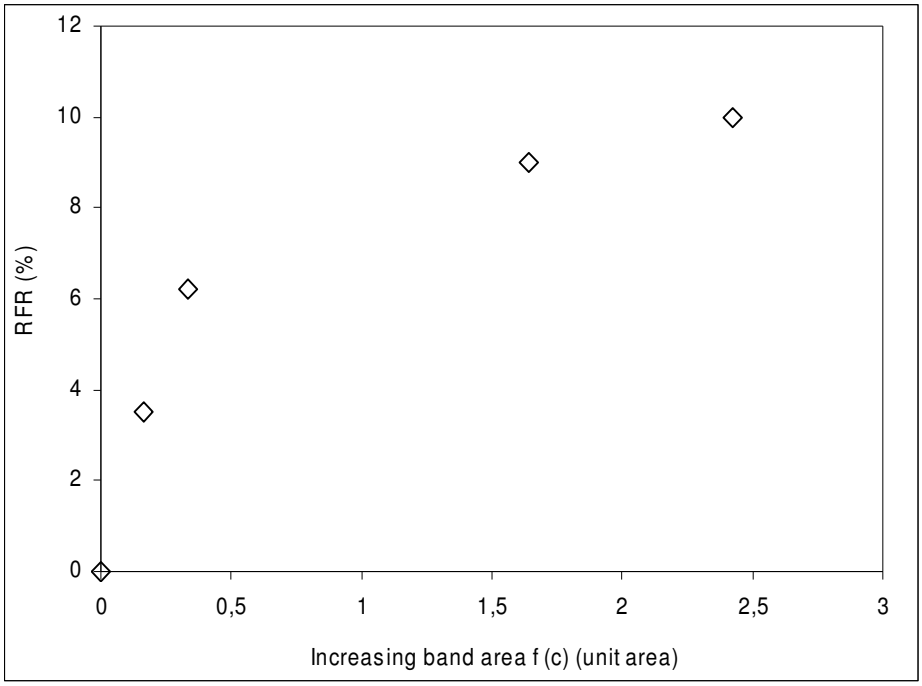

Figure 5.1. Correlation between RFR and increasing band area as a function of dextran concentration for PES-SG10.

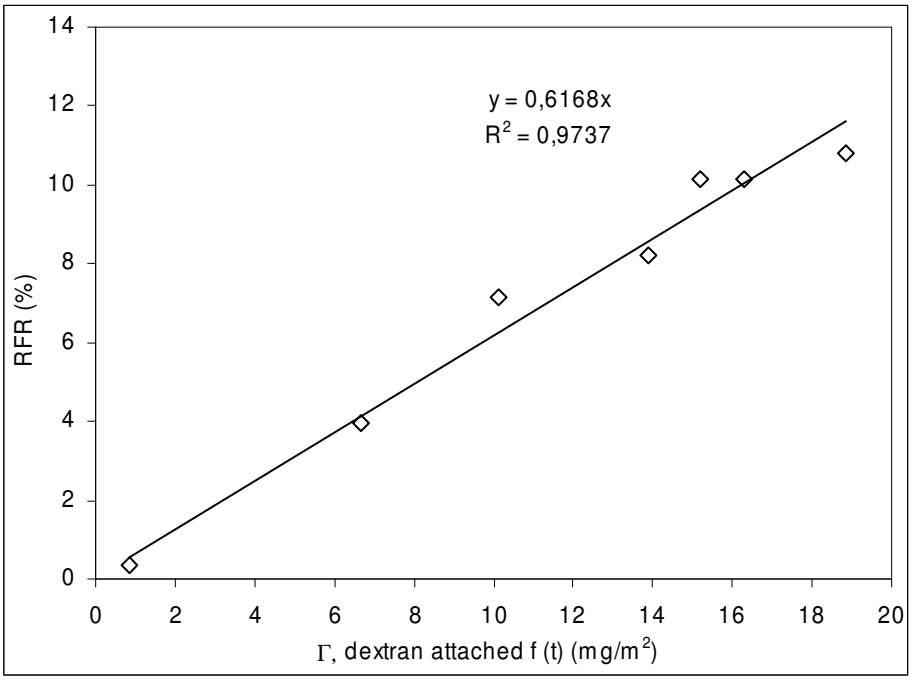

Figure 5.2. Correlation between RFR and the amount of dextran attached on membrane as a function of exposure time for PES-SG10 membranes (dextran T10, 10 g/L).

A better correlation between RFR and the SDAM data (cf. Figure 5.2) would indicate that solute binding deeper in the selective layer of the PES UF membrane is also involved in flux reduction. Because diffusion of the dextran T10 through the membranes was observed (cf. Table 4.4), this is of course possible. Surprisingly, during the SDAM experiments, uptake of dextran T10 was found also for the cellulose−based membranes, indicating a "mechanical entrapment" of dextran in these membranes because neither flux reduction nor changes in AFM has been observed (cf. above).

The complex effects of dextran molar mass on RFR by adsorption to PES membranes (cf. Figure 4.6) can then be analyzed based on the relationship between membrane pore size and dextran size. For average molar masses less than 70 kg/mol, bound dextran molecules could either narrow or completely block membrane pores. With increasing ratio between dextran size and pore size, the probability for pore blocking will increase. It should be noted that the pore blocking will yield a higher contribution to membrane resistance than pore narrowing [74]. Ye et al. [16] had found similar results during their study of crossflow filtration of alginate solution, i.e. smaller pore diameter gave a higher resistance caused by fouling. However, beyond a molar mass of 70 kg/mol, the dextran could not penetrate into the membrane pores. It should be noted that no diffusion (cf. Table 4.4) and complete rejection were observed for the dextran T100, even though previous literature showed that dextran is a flexible coil polymer and is able to deform within the membrane pores [190]. If the membrane pores are too small compared to the dextran size, penetration through the pores is not possible. As a result, the fouling was reduced with increasing the molar mass of dextran (note that penetration of dextran into the pores has been demonstrated to be involved in dextran fouling, cf. above). The differences in adsorptive fouling (extent and consequence) between the two PES membranes can again be explained with their different surface and pore morphology (cf. above), i.e. for the PES-SG

membrane with both larger surface porosity and average pore size the effects for smaller dextran size were smaller (less effects of adsorption on pore narrowing) and for larger dextran size, the effects would be larger (more effective pore blocking) than for the PES-SG10 membrane.

Irrespective the lower feed concentrations; for similar transmembrane pressure (300 kPa) used for water flux measurement and dextran filtration (cf. Figure 4.5 and 4.20), the fouling effects after UF were larger than after static adsorption. The increasing membrane rejection due to the increase in dextran molar mass can account for the increasing fouling with higher dextran molar mass; the mechanism will be accumulation of dextran on the membrane surface already containing adsorbed dextran which already partially blocks membrane pores. It is interesting to note that the mass transfer coefficient will be smaller and thus the extent of concentration polarization will be larger with increasing solute molar mass [27]. No fouling after UF was observed for the cellulose–based membranes, which also did not show a significant indication of fouling after static adsorption. Hence, in this context, the RFR test (caused by static adsorption) is most useful for the evaluation of the fouling potential of certain solutes in combination with different membranes. Note, that – different from the UF for sieving curve analysis which was performed at the same initial water flux for all membranes – in this case, the dextran UF was conducted at the same transmembrane pressure. Hence, the larger RFR after UF for the PES-SG10 membranes – a result which is different from the static data (cf. Figure 4.5) – can be explained by the higher fluxes due to higher permeability (cf. Table 4.1), and thus larger concentration polarization during dextran filtration.

The much lower UF permeate fluxes as compared to the water fluxes during ultrafiltration indicate that the concentration polarization at the membrane surface is significant (cf. Figure 4.22). However, the small flux decline for the SC-10 membrane

indicates that concentration polarization was less for this membrane. A smaller concentration polarization for SC-10 than for PES-SG10 membrane was mainly due to its smaller porosity (cf. above). Hence, a higher flux decline for PES-SG10 membrane is caused not only by concentration polarization but also by fouling. The accessibility of the pores for the dextran seemed to contribute as well. Furthermore, the additional slight decrease of flux for dextran T70 and myoglobin (myoglobin > T70) implies that the adsorption fouling contributed to the flux reduction. With the increase in molar mass of solute the membrane rejection also increased. In addition, the partial accessibility of the internal pore structure for dextran evoked above has also been confirmed with these results.

In order to rule out effects of solute entrapment in a porous structure, additional experiments with non−porous PES film have been performed (cf. Figures 4.18 and 4.19). The results agree well with results obtained using (porous) PES UF membranes. The significant changes of PES surface structure upon contact with dextran solution can only be explained by binding (adsorption) of the solute to the polymer surface. Overall, experiments of membrane−solute interactions (static adsorption) and membrane solute−solute interactions (UF) as well as SDAMs clearly showed that dextrans foul the PES membranes.

While for the cellulose−based membranes, the interaction between solutes (dextran and protein) and membrane was not significant (as evidenced no significant flux reduction), the interactions between PES and both solutes were significant. Pore narrowing and blocking were much more severe after protein adsorption than after dextran adsorption, and this can be explained with a higher coverage of the (accessible) membrane surface by the protein (>5 times higher than for dextran). Due to the higher affinity, this high surface coverage is also reached at lower solute concentration (20 times lower than

for dextran). Because membrane pores and adsorbed molecules have similar dimension, the surface coverage of PES membrane by dextran and protein could be described (Figure 5.3).

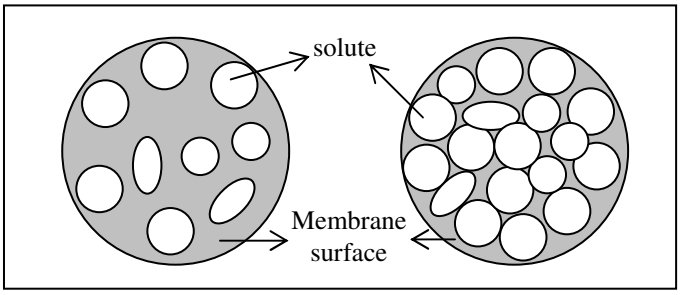

Figure 5.3. Schematic of proposed surface coverage of PES UF membrane by dextran (left cartoon) and by protein (right cartoon).

5.2.2 Mechanism of interactions

Based on the preceding results, it was reasonable to deduce that the difference in membrane surface coverage caused by different mechanisms of interaction were the reason for different fouling behavior of the two different solutes (dextran vs. myoglobin) with the two different membranes (PES vs. cellulose–based). The low binding properties of cellulose–based materials are well known (e.g., [1]), and the new information from this study is that solute uptake can take place in the membrane barrier but the consequences for permeability are still low, presumably due to the swollen, hydrogel–like morphology of this UF–selective barrier layer. Mechanisms for the interactions between the membrane polymer PES and proteins had been discussed in many phenomenological or mechanistic studies (see, for example [68,74]). The main driving force at a pH around IEP is hydrophobic attraction between PES and protein. However, in contrast, an attractive interaction between the relatively hydrophobic PES and the hydrophilic dextran is counter–intuitive.

Experiment using non porous PES film, where an additive such as PVP was not involved, confirmed that the dextran–PES membrane interactions were caused by PES material itself. Hence, two possible mechanisms are proposed to contribute to this phenomenon (Figure 5.4). First, the binding of dextran to PES can be due to hydrogen bonding between free hydroxyl groups in the dextran (as donor) and oxygen atoms projecting from the SO_2 group in PES (as acceptor). Multiple hydrogen bonds can be formed between one dextran molecule and the membrane polymer surface, and this could provide a significant enthalpy contribution to a negative free enthalpy for adsorption (Figure 5.4 (A)). Second, water structure and reactivity at solid surfaces should also be considered. While binding of water to hydrophilic surface is too strong to be displaced by a solute [191], the binding of water to hydrophobic surfaces is weaker. The adsorption to hydrophobic surfaces is mainly driven by the increase of entropy via replacement of water molecules at the surface by adsorbed solute ("surface dehydration") [192]. This process would also provide a contribution to a negative free enthalpy for adsorption of a hydrophilic polysaccharide on a hydrophobic polymer surface (Figure 5.4 (B)).

In conclusion, it was clearly seen that PES membrane has significant propensity to foul even with hydrophilic solute (e.g., dextran). Therefore, surface modification in order to obtain tailored low–fouling surface of PES UF membrane via surface hydrophilization is strongly needed. The following sections discuss the surface modification of PES UF membranes.

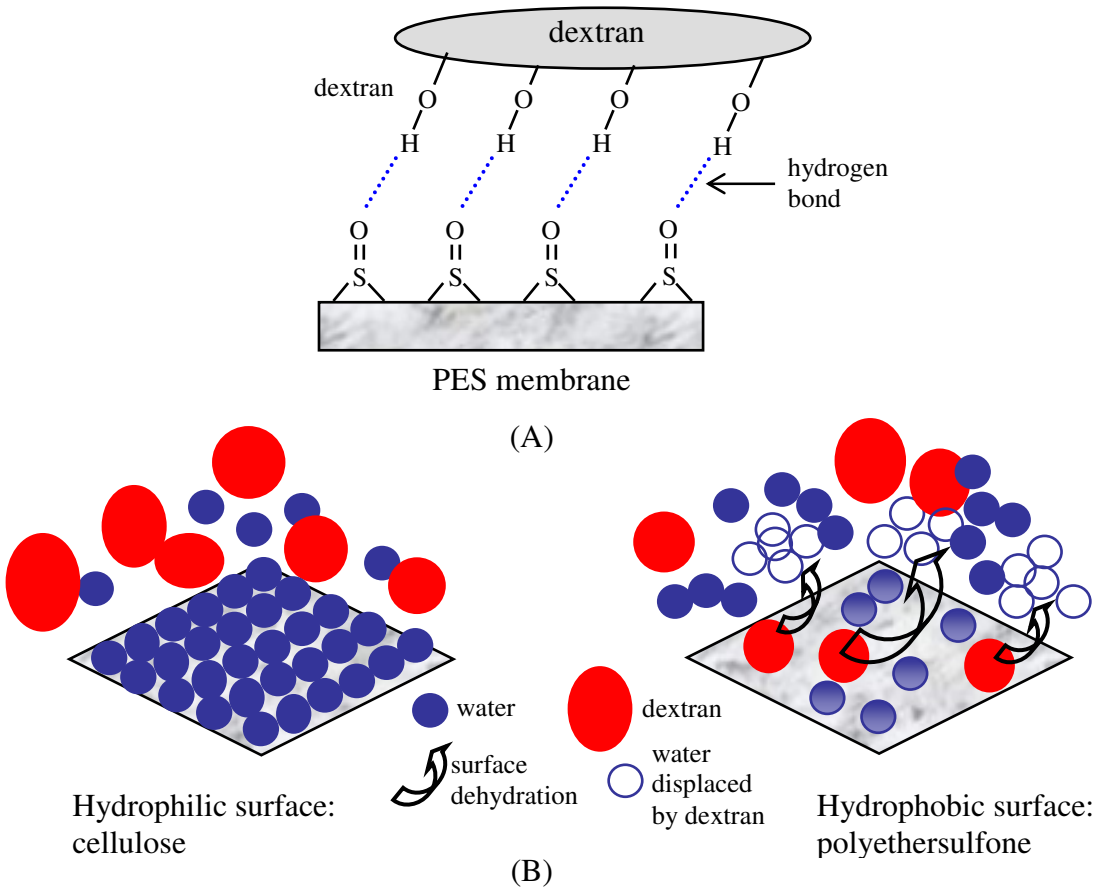

Figure 5.4. Schematic representation of proposed mechanism of PES membrane–dextran interactions: (A) via multiple hydrogen bonding, (B) displacement via dehydration process.

5.3. Surface Modification

First of all, it is important to note that, modifications of two batches were performed. Both batches had differences in pore morphology of the base membranes used, UV intensity and UV filter (cf. Sections 3.4.3 and 4.3 for more detail in surface modification conditions).

5.3.1. Effect of UV irradiation

Irradiation of membrane by UV light with increasing dose would first increase and then decrease the membrane hydraulic permeability as well as membrane cut–off. These

phenomena could be explained based on the mechanism of photodegradation of PES as reported by Kuroda et al. [193]: UV irradiation of PES causes simultaneously polymer chain scission and cross-linking processes; all main reactions proceed via PES radicals. Figure 5.5 describes the effect of UV irradiation on effective pore size of PES membrane in photograft modification. Hydroxyl and sulfonic acid groups are formed as products of chain scission in the presence of oxygen. The zeta potential data support the formation of sulfonic acid groups as consequence of chain scission (cf. Figure 4.36). Chain scission is dominant at low temperature whereas cross-linking is dominant at high temperature. It should be noted that during UV irradiation, an increase of sample temperature could not be avoided. Hence, the cross-linking process will be favored with increasing irradiation time (Figure 5.5 (B)), while chain scission would be more pronounced for short irradiation times (Figure 5.5. (A)). Nevertheless, it should be kept in mind that there is no direct relationship between the chemical reactions of the membrane polymer and the pore dimensions of the solid membrane made thereof. It is reasonable that a pore structure with characteristic dimensions in the lower nanometer range will respond with a size increase as consequence of chain scission and a size decrease as consequence of cross-linking. However, suppression of pore degradation (Figure 5.5 (C) and (D)) was observed in the presence of monomer (even with low concentration) during UV irradiation (cf. Section 5.3.3 in more detail). This, however, can only be expected if the UV energy and dose will not exceed the critical values where extensive degradation along with polymer dissolution is the consequence. In this work, such conditions have been ensured by using selective UV irradiation (>300 nm) and carefully adjusting the dose via UV irradiation time. A competition between chain scission and cross-linking had also been used for discussion of UV effects on modification by other authors [36,90,162]. We believe that different results reported by many reputable authors are due to the difference in both characteristics of the

UV light (wave length and intensity) and the PES base membrane (cut–off, thickness, additive) used for modification.

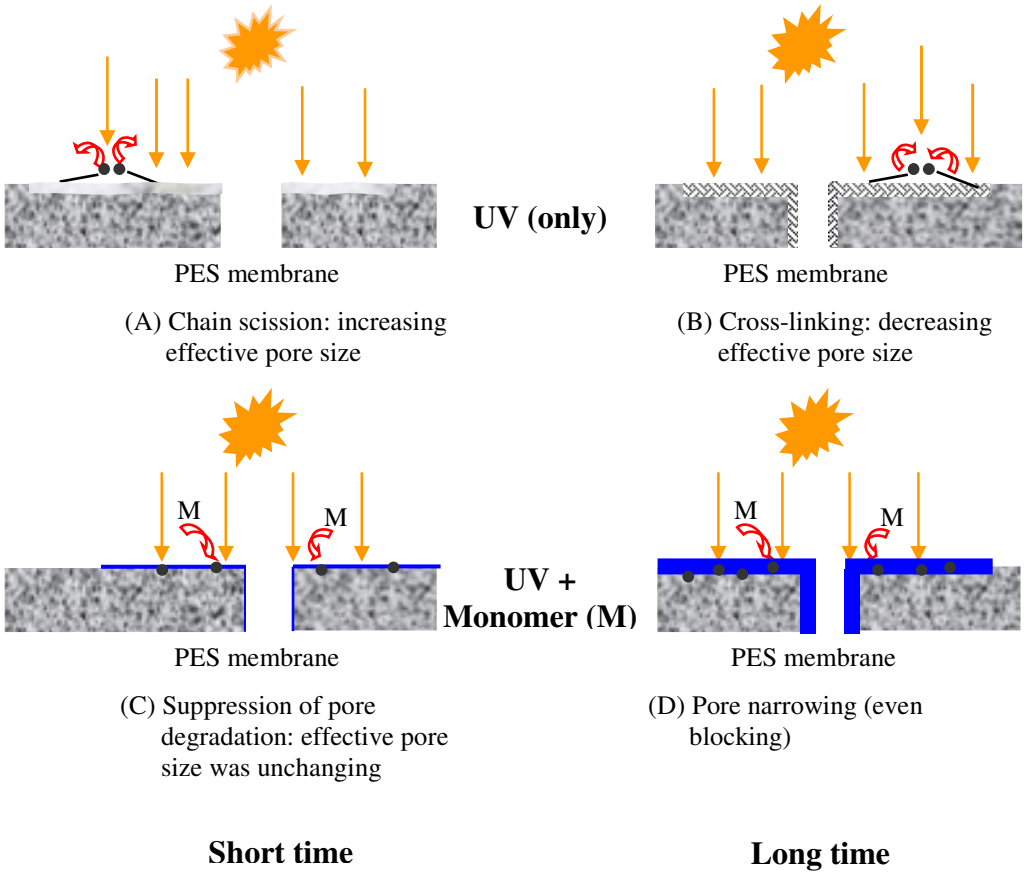

Figure 5.5. Proposed mechanism of the effect of UV irradiation on the PES (effective) membrane pore size in photograft modification.

5.3.2. Grafting efficiency

Observable changes in IR spectra and elemental analysis confirmed that the functional monomer has been photochemically grafted onto the based membrane even though some characteristics of IR adsorption of functional monomers were not observed after modification. Overlapping bands with those of PES base material could be the reason for this condition. Such overlapping band is supported by previous study by Belfer et al. [68]. Thereafter, grafting efficiency was then investigated.

DG was influenced by the amounts of monomer as well as of free radicals in grafting zone. In this context, we believe that the amounts of monomer and free radicals in the grafting zone increased with increasing the monomer concentration in the bulk and the UV irradiation time, respectively. The initial time delay during first batch modifications (cf. Figure 4.25) may be due to the presence of inhibitors (e.g., monomer stabilizator or residual oxygen) in the reaction mixtures so that termination reactions will control the functionalization. Those will be consumed in termination reactions. For longer irradiation times (6 min irradiation), the increase in DG caused by an increasing of the monomer concentration was larger in the range of 1–10 g/L than in the range of 10–40 g/L (Figure 4.26). This may be interpreted by the control of the polymer chain growth reactions from the membrane surface by the monomer transport from the bulk of the reaction mixture. The increase in graft chain length could diminish the reactivity of the radicals which can be "buried" in grafted layer and retard the transport of monomer into the grafting region. As a result, the rate of grafting was higher at lower irradiation time (Figure 4.27).

The difference in monomer characteristics such as molar mass, viscosity, polarity, solubility and swelling (in the solvent used) yielded different grafting efficiency as well as grafting behavior (Figure 4.27). Viewing from the perspective of molar mass, the efficiency of grafting (given by DG) should be lower with increasing the molar mass due to lower mobility (diffusion) as well as reactivity (addition) as reported by Ulbricht *et al.* [40]. However, the efficiency of grafting is influenced not only by molar mass but also by other characteristics. Yang and Rånby [194] reported that the reactivity of monomer in polymerization was influenced by monomer affinity (polarity) and methyl groups content. We believe that the solubility of the functional monomer in water was dominant parameter in this modification. In this context, PEGMA had higher solubility than SPE (cf. swelling experiment). In addition, slight difference in the UV absorbance spectra of both monomers

as presented in Figure 3.2 causing (slightly) difference in UV energy received by PES membrane surface might also contribute.

The presence of cross-linker in the reaction mixture could restrict the diffusion of monomer into the grafting zone, where radical is available and grafting reaction takes place. The amount of monomer in the grafting zone may decrease, many radicals might decay and therefore DG will be smaller. This restriction would be larger with increasing the cross-linking density. On the other hand, the presence of cross-linker could add sites for growing the chain (polyfunctional) and then branching reaction might occur, therefore the DG would increase. Again, the net effect of cross-linker on grafting would strongly depend on the monomer characteristics. Both those effects could be further explained by Figure 4.29. At low concentration, the presence of cross-linker would decrease the grafting yield by restriction of monomer diffusion into the grafting zone. Afterwards, the DG increased by increasing number of polyfunctional sites provided by cross-linker. In this grafting method, it is reasonable to expect that recombination of graft growing chains by termination would not occur. This hypothesis is based on the fact that the radicals were generated only in the PES polymer backbone, and no radicals were generated from the solvent or the monomer.

5.3.3. Layer structure of the modified membranes

Considering the values of DGs, as also discussed based on all results of this study (cf. below), it should definitely not imply that the functionalization was taken place only on the outer membrane surface. It is clear from Section 5.3.2 that additional polymer should be observed on the base membrane surface after modification. SEM images support that the entire membrane surface seemed to be covered by thin layer polymer indicating the membrane surface has been evenly modified. It should be kept in mind that all the SEM

images were obtained in dry condition. Therefore, the "actual" surface morphology during filtration would be more significantly different with the unmodified membrane due to hydrogel character of both grafted polymers. Further, it is reasonable to consider the membranes resulting from these modifications as composite UF membranes (Figure 5.6). Further, the term of composite membrane will be used instead of modified membrane.

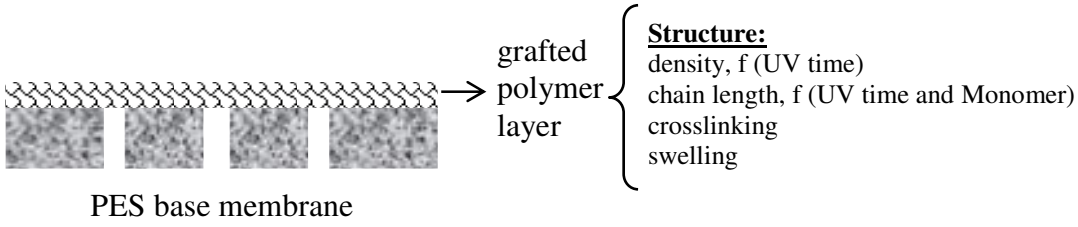

Figure 5.6. Schematic representative of resulted-composite PES UF membrane

Many previous reports had shown that sodium hypochlorite could degrade the membrane polymers PS or PES, but this study indicates clearly that the membrane surface chemistry and characteristics determined by the grafted polymeric hydrogel did not change under these cleaning conditions. Hydrophilic properties have been unchanged, but the base membrane (NMWCO 100 kg/mol) had also a similar low contact angle. However, because the ATR−IR absorbance ratio was well correlated with the DG, the data in Figure 4.47 clearly indicate that no loss or hydrolysis of the (very thin) grafted layer occurred within 8 days, proving the chemical stability study of the active layer of the photo-grafted composite membranes.

The behavior of the grafted polymer layer is influenced by grafting density, chain length, and cross-linking density. In addition, swelling degree of that polymer layer in solvent/solution used will also influence the performance. The surface characteristics of these composite membranes and the impact grafted layers on apparent membrane pore size

will be discussed in the Sections 5.3.4 and 5.3.5. Furthermore, the effect of the grafted layers on separation performance will be discussed in Section 5.4.

5.3.4. Surface characteristic of composite membranes

Overall, the modifications (both first and second batch modifications) changed the membrane surface characteristics (with respect to the chemistry, wettability, charge and morphology) and membrane pore structures.

The composite membranes were more hydrophilic than the unmodified membranes. Even though few of the CA did not correlate well with the respective DG, the overall dependency on DG was very clear (cf. Figures 4.32 and 4.33). Care should be taken to interpret these results. The CA of the composite membrane is affected by the base membrane used for modification, degree of surface coverage (DG) and structure of the grafted polymer (e.g., density and chain length). This phenomenon could be explained as follows: if the membrane surface has been completely covered by the functional polymer (in this case either polyPEGMA or polySPE), the CA angle will only depend on the CA of the polymer itself. The water CA for polyPEGMA was found in the previous literature to be 43 ± 2^{o} [195] or 44 ± 4^{o} [196]. A wider range of contact angles ($35\text{-}50^{o}$) for surfaces modified using PEGMA was also found in other reported work [197]. For incomplete surface coverage composite membrane, both the base membrane and grafted polymer would contribute to the surface CA. We believe that the high porosity of the base membrane contributed to its low contact angle whereas for composite membranes their low contact angles are mainly due to the grafted polymer on the membrane surface. This statement is supported by much higher CA of the unmodified 10 kg/mol PES membrane than the unmodified 100 kg/mol. One should be noted that during modification, decrease in surface porosity through both pore narrowing and pore blocking could not be avoided (cf.

SEM images, rejection, and hydraulic permeability reduction). The ZP data support this explanation, i.e. PEGMA–composite membranes with different DG (i.e. ~170 and ~320 μg/cm^2) showed significantly different ZP even though they had almost similar CA.

Furthermore, slightly lower CA for PEGMA–composite membranes than for SPE–composite membranes was most probably due to more swollen structure in water of polyPEGMA than polySPE. The reduction of interchain volume in the hydrogel and resulting lower water content caused by cross-linking process might also explain the slightly higher CA of cross-linked composite membranes than uncross-linked ones.

The effective surface charge of the PES base membrane has been increased by UV irradiation (alone) and diminished toward neutral by the grafted functional polymer layer. Increasing negative charge by UV irradiation was believed due to the formation of sulfonic acids groups (cf. Section 5.3.1). However, zeta potential data indicate that the shielding of the PES surface by the thin grafted polyPEGMA or polySPE layer has the dominating effect. All composite membranes were not fully neutral. It is important to note that the linear decrease in ZP with increasing the pH found for grafted polyPEGMA and polySPE reflects the typical behavior of a surface which has negative charge due to anion adsorption [133,197-199]. In addition, the ZP data also support the interpretation of CA data with respect to coverage of the outer membrane surface, i.e. PES-g-polyPEGMA membranes with different DG (e.g., ~170 and ~320 μg/cm^2) showed significantly different ZP (cf. Figure 4.35) even though they had almost the same CA (cf. above). Even though sequestering of mobile ions in the dipole layer (e.g., positive inner surface, negative outer surface) was found in previously reported ZP studies for zwitterionic micelles [200,201], the dissociation of ions should not take place in grafted polySPE in our work. Another reasonable explanation is that the charged groups of the zwitterionic polymer might be fairly evenly distributed on the entire membrane surface generating an interface that is

overall electrically neutral (but still prone to preferential anion adsorption). This hypothesis was also suggested by Holmlin et al. [137].

Overall, the characteristics of composite membranes obtained with sufficiently high DG (approximately >300 µg/cm^2 for polyPEGMA and >170 µg/cm^2 for polySPE, along with this base membrane) should be controlled by grafted polymer layer (cf. Section 5.3.5 in detail).

5.3.5. Pore structure and adsorptive fouling of composite membranes

Even though determinations of grafting density and chain lengths had been reported in some previous publications (e.g., by [202,203]), in the context of our study (with PES as the substrate and covalently grafted polyacrylates), such analyses can not be performed. With respect to the influence of the main modification parameters (UV time and monomer concentration), it is difficult to discuss separately effects onto grafting density and chain length. However, on a qualitative level this is possible for the results of this study.

The apparent pore size of composite membrane was strongly influenced by UV irradiation time (cf. Figure 4.38, first batch modification). At short irradiation (~ 1 min), modification presumably occurred only on the outer surface of the membrane, as evidenced by the increased hydrophilicity (see Figure 4.32) and pore blocking did not occur because the membrane sieving did not change. Consequently, a thin flexible polyPEGMA layer ("mushroom" regime, Figure 5.7), which does not add a resistance to the separation layer of the UF membrane, seemed to be formed. This means that surface hydrophilization was dominant, but due to the relatively low surface coverage, the hydrophilization was not complete. Moreover, the degradation effects of the UV irradiation alone – leading to a large shift of the sieving curve – were completely suppressed. This effect may only be explained when assuming that the primary radicals after UV induced

PES chain scission are not directly leading to the enlargement of the membrane pores – if those radicals are immediately "trapped" by the addition of monomer, the morphology of the solid polymer remains essentially unchanged (cf. Figure 5.5 (C)). Apparently, this mechanism seemed to be valid also for "period 2" while it is not possible making clear conclusions for "period 3" (cf. below).

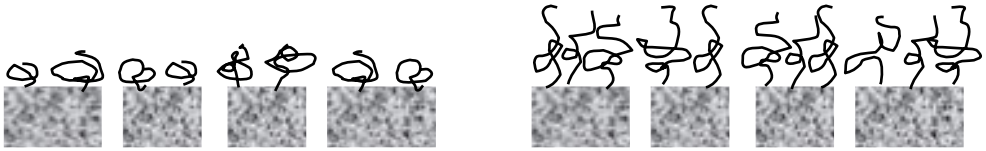

"mushroom" regime "brush" regime

Figure 5.7. Schematic model for "mushroom" and "brush" regimes

In "period 2", competition between surface hydrophilization and pore blocking was very pronounced. However, hydrophilized membranes with relatively high permeability may be obtained when precisely adjusting functionalization conditions in this "period 2". In "period 3", membrane rejection was significantly reduced by modification. An explanation is that by increasing the UV irradiation and thus polymerization time, the grafted chains were more stretched away from the solid surface and thus reduced pore size or blocked membrane pores ("brush" regime, Figure 5.7; cf. also Figure 5.5. (D)). With respect to membrane performance, the desired complete surface hydrophilization is accompanied by a severe permeability reduction. Nevertheless, such PEGMA–based composite UF membranes had also rather steep sieving curves, and they could be of interest as low–fouling membranes with low cut–off. By changing the base membrane (toward higher value of membrane cut–off) and the glass filter (toward higher absorbance) during second batch modification, obtained results support the preceding explanation (for "period 3"), i.e.

as evidenced by shifting of the rejection curve to the lower pore radii and reduction of hydraulic permeability.

Overall, for second batch modification, it is reasonable to claim that considering the high values of obtained DGs, photo-grafted polymer is formed as thin layer not only on the outer surface of membrane, but also in the pores of the UF membrane. The UV intensity at the bottom membrane surface, measured with the UVA meter (cf. Experimental), was only about 5% compared to the actual excitation intensity. Hence, due to the strong UV absorbance of PES (which is the basis for controlled photodegradation [39,133]) and light scattering, there will be a gradient of grafted polymer amount over membrane thickness, and most of the grafted polymer will be located in the upper several micrometers below the (irradiated) top surface of the membrane (i.e., also "behind" the UF active layer what has a thickness of less than 1 μm [33]).

Differences in grafting density and grafted chain length leading to different chain conformations in the grafted layer (mushroom vs. brush) are the most probable reason for different surface characteristics and membrane performance obtained for the two functional monomers in the second batch modification. An increase in (adsorptive) fouling resistance with increasing degree of grafting but also with increasing UV irradiation time and monomer concentration was convincingly observed (cf. Figures 4.27 and 4.45). Comparing the membranes with similar DG and fouling resistance, but prepared at different UV irradiation times (e.g., PEGMA–composite membranes from 20 g/L at 15 min irradiation and from 40 g/L at 4 min irradiation; cf. Figure 4.45), it is reasonable to explain that membranes modified at longer irradiation time (but lower monomer concentration) had higher grafting density but shorter chain length than membranes obtained from short irradiation time (but higher monomer concentration). This suggests that there is no need to have a high grafting density to obtain high fouling resistance when

a large enough chain length has already been achieved. Above a critical value, the grafting density did not seem to influence the fouling resistance anymore. This is supported by the fact that no significant difference has been observed between membranes obtained from 50 g/L and 40 g/L at the same irradiation time (cf. Figure 4.45). The identification of such trends is somewhat more complicated for the SPE−based composite membranes (cf. Figure 4.46), but overall similar influences can be discussed.

The following general conclusion is then made for the linear grafted copolymers: at DG values above the critical value (which may slightly depend on UV time or monomer concentration), the PES surface is completely covered by the grafted polymer layer, so that the resistance to fouling by biomacromolecules is high. Even when the polymer chains will not necessarily be in the brush regime, the internal layer structure will have influence on flux, rejection and fouling resistance. We believe that the degree of swelling of this layer is also an important parameter: At the same (mass−based) degree of modification, polyPEGMA−based layers will be more swollen than polySPE−based ones, leading to a thicker but less dense structure (Figure 5.8). This assumption can then help to understand the higher permeability and lower rejection as well as the higher fouling resistance of PEGMA−based composite membranes (cf. Figures 4.39, 4.41 and 4.45).

For grafting in the presence of cross-linker, the cross-linked grafted layer structure causing a reduction of swelling lead to a decrease water flux and an increased membrane rejection at similar DG values (observed for PEGs and the protein myoglobin). This shows that the internal structure of the grafted polymeric hydrogel has significant influence onto membrane selectivity and its size exclusion, and can be explained by solute sieving through a swollen hydrogel network with a mesh size which is adjustable by the cross-linker content (cf., e.g., [151]).

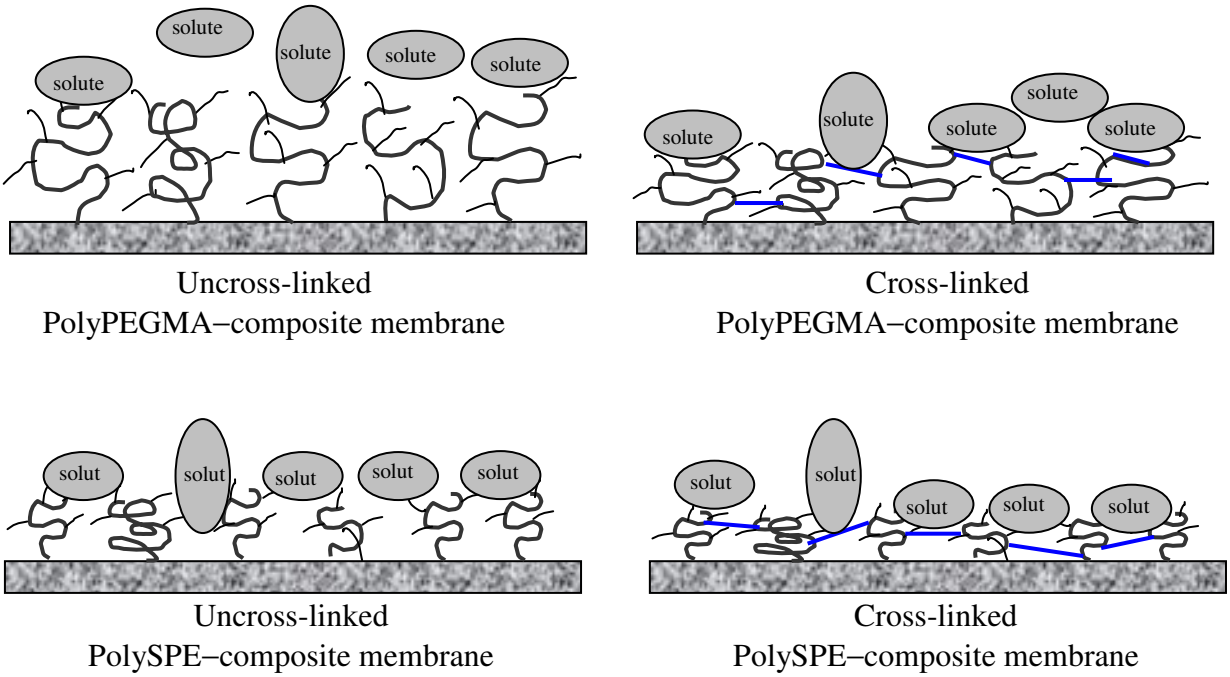

Uncross-linked
PolyPEGMA–composite membrane

Cross-linked
PolyPEGMA–composite membrane

Uncross-linked
PolySPE–composite membrane

Cross-linked
PolySPE–composite membrane

Figure 5.8. Proposed schematic of chain grafted polyPEGMA and polySPE onto composite membranes.

Basically, the proposed–mechanism of the effect of cross-linker on the membrane performance might be drawn as followed: as the degree of cross-linking was increased (by increasing the UV irradiation time), the membrane hydraulic permeability would decreased whereas the membrane fouling resistance would first increase and then decrease. Increasing the degree of cross-linking might increase the size exclusion of solute from the membrane surface. However, phase separation through insolubilization might occur at high degree of cross-linking and thus the heterogeneity of layer structure of grafted polymer might be formed. Eventually, this structure heterogeneity increased the membrane–solute interaction. Such insoluble layer was also identified during photo-initiated grafting of polymer [204]. In addition, contribution of both 3D grafted chain structure and cross-linker (alone)–solute interaction might be possible. The cross-linked structure might also

contribute to the increasing in RFR by giving higher possibility for solute to be mechanically entrapped onto membrane surface.

Overall, surface modification caused simultaneously both membrane pore narrowing (even blocking), which decreased the hydraulic permeability, and surface hydrophilization, which increased the membrane fouling resistance. In addition, reduction of effective negative charge was also observed. However, it is important to note that the reduction of pore size could also contribute to less interaction of membrane with solute. Basically, the performance of composite membranes is influenced by the characteristic of the functional monomer as well as the base membrane used, degree of surface coverage, grafted chain structure and pore structure.

A higher (adsorptive) fouling resistance for UV-irradiated (only) membrane than unmodified (cf. Figure 4.44) could be explained by electrostatic repulsion between membrane and protein. The UV-irradiated membrane is negatively charged due to sulfonic acids groups (cf. Figure 4.34). An opposite result as compared to the protein (BSA) result was obtained for exposing to sugar cane juice polysaccharides (cf. Figure 4.50), whereas no effect was observed for dextran.

A higher fouling resistance for PEGMA/SPE−based composite membranes is mainly due to the increased hydrophilicity (cf. Figure 4.33 and 4.34). However, for some functionalization conditions the effects on RFR were much larger than the relative changes of CA. Therefore, the relationship between hydrophilization and DG/pore blocking must be considered as well. Comparison study using unmodified membrane with comparable pore size proved that membrane with smaller average pore size yielded higher fouling resistance on the one hand (cf. Figures 4.44 and 4.46). On the other hand, a high fouling resistance ($R_f > 0.9$; Figures 4.44, 4.45 and 4.46) was not mainly caused by smaller pore size but by reduced membrane–solute interactions.

5.4. Evaluation of Separation Performance of Composite Membranes

5.4.1. Flux–rejection trade-off analysis for composite membrane selection

It was indicated in Section 5.3.5 that a trade-off relationship between hydraulic permeability and fouling resistance was observed. Therefore, such trade-off was first investigated during ultrafiltration experiment. As expected, a flux versus rejection trade-off was also observed during ultrafiltration. Such flux–rejection trade-off is a general phenomenon in UF as analyzed recently by Mehta and Zydney [205]. Looking at ultrafiltration using composite membranes synthesized from first batch modification, the degree of grafting and functionalization conditions had a pronounced influence (cf. Table 4.7). Membrane #1 showed a better UF performance than the unmodified membrane (#0) with respect to *all* criteria (flux, rejection, fouling resistance), but the improvements were not very large (and the long–term UF performance is uncertain). This may be related to an incomplete shielding of the PES surface with grafted polyPEGMA (cf. Figure 5.7; "mushroom" regime). Membrane #5 (prepared under "period 3" conditions; cf. Section 4.3.2) with a fully developed grafted polyPEGMA layer had the highest fouling resistance as well as rejection, but a severely reduced flux (cf. Figure 5.7; "brush" regime). The functionalization using "period 2" conditions (cf. membranes #3 and #4, Section 4.3.2) seemed to represent an optimum, i.e. membranes with a high rejection and an acceptable flux, which is also more stable over time due to relatively high fouling resistance. That the UF performance has indeed been improved by reduction of adsorptive fouling via grafting functionalization is also supported by the comparison with the unmodified PES membrane with lower cut–off (#6). With respect to UF flux and rejection, the performance of membrane #6 is between the functionalized membranes #4 and #5, but the UF flux ratio is much lower than for both modified membranes. Therefore, only composite membranes that had similar pore structure (as evidenced by similar rejection curve as well as hydraulic

permeability) with 10 kg/mol unmodified PES membrane but having higher fouling resistance were considered as membrane with improved performance.

5.4.2. Ultrafiltration of potential foulant solutions

The unmodified PES membrane (NMWCO 10 kg/mol) was included to consider the effect of flux−rejection trade-off. Then, the UF flux ratio between filtrate flux and initial water flux could be used as an additional parameter to evaluate the membrane performance (note that this parameter would be proportional to the fouling resistance during UF). In addition, solute rejections were also investigated. It is important to note that different potential foulants were used for evaluation to explore the applicability of the new composite membranes. Composite membranes made of first batch modification were evaluated by using BSA (cf. Section 5.4.1) and sugarcane juice polysaccharides (SJP) solutions. Myoglobin, dextran and humic acid were used to evaluate composite membranes obtained from second batch modification.

"Batch one" composite membranes. Upon evaluation using SJP for composite membranes obtained from first batch modification, it was observed that composite membranes showed much better fouling resistance than unmodified membrane even though fouling was still observed. The less pronounced fouling of SJP compared to protein during adsorptive fouling evaluation (cf. Figures 4.40 and 4.50) might be due to the fact that the main component in the SJP solution is the polysaccharide fraction, which is a macromolecule with a large fraction of very high molar mass and having hydrophilic character and that the content of components that could cause more severe fouling, e.g., protein and phenols, was low [19]. UV irradiated (only) membranes showed slightly higher RFR than unmodified membrane, indicating that electrostatic attraction may be responsible for an increased amount of foulant on the membrane surface. Nevertheless, for all

membranes, which have not been functionalized with PEGMA, the SJP–membrane interactions were weaker than the protein–membrane interactions. Even though all composite membranes had significantly lower RFR than unmodified membrane, the adsorptive fouling of the composite membranes with SJP (RFR ~15%) was considerably higher than with BSA (RFR 1–3%). That means that the membrane modification with PEGMA seemed to eliminate the attractive interactions observed as consequence of UV irradiation but was less efficient than for the well–known "strong foulant" BSA. This surprising phenomenon might be due to the complexity of sugarcane juice polysaccharides contents. One probable reason is that the sugarcane juice polysaccharides are composed of high and low molar mass compounds (cf. Figure 4.52). The latter may penetrate into the grafted polyPEGMA layers and yield a flux reduction. This observation did not occur for unmodified membrane. Surprisingly, ultrafiltration of SJP seemed to yield stronger fouling than BSA as evidenced by lower flux ratio. While a good correlation between static adsorption and UF tests with respect to protein fouling has been observed, for the sugar cane juice both the fouling of the unmodified membrane and the improvement of fouling resistance by polyPEGMA functionalization observed in UF have been underestimated in the static adsorption tests. This result indicates again that the UF of sugarcane juice polysaccharides seems to be more complex than UF of BSA alone.

"Batch two" composite membranes. The evaluation for composite membranes obtained from the second batch was performed and compared more precisely to commercial 10 kg/mol unmodified membrane. Evaluation using myoglobin clearly showed that composite membranes had much higher permeate flux than unmodified membranes. Even in cases where the addition of cross-linker did not improve the adsorptive fouling resistance relative to the uncross-linked composite membranes, it improved both permeate flux and rejection in the UF experiments.

Even though no composite membrane, which is absolutely inert toward dextran adsorption has been obtained, composite membranes had higher adsorptive fouling resistance than unmodified membranes having similar or slightly higher cut-off (PES-SG10 and PES-SG30) as evidenced by their lower RFR. On the one hand, this result indicates that the grafted polymer changed the surface character of the membrane leading to a smaller RFR of the composite membranes; on the other hand, the ratio of solute size to the membrane pores also determined the fouling extent (cf. Figure 4.53, PES-SG10, 30 and 100). In agreement with adsorptive fouling results, the UF data showed that the composite membrane had higher fouling resistance as evidenced by higher flux ratio. Addition of "low concentration" cross-linker could slightly increase the flux ratio of the uncross-linked composite membrane.

Similar results were obtained upon evaluation using humic acid solution, i.e. all composite membranes showed higher fouling resistance than unmodified membranes (except for PES-g-SPE in the adsorptive fouling study). The higher adsorptive fouling at lower pH might be addressed to the more compact character of humic acid at low pH and more hydrophobic [13,15,177]. It should be noted that at low pH the (modified) membrane surface charges were close to neutral (cf. Figure 4.35). Therefore, electrostatic interaction should be neglected. As mentioned in the previous studies, the membrane pore structure also determined the role of fouling. The higher fouling for the larger pore size membrane is likely due to the higher accessibility of the membrane pores to the humic acid particles. As a result, fouling occurred not only on the outer membrane surface but also within the membrane pores. Then, different behaviour of fouling layer after cleaning indicates different fouling characteristics.

5.4.3. Mechanism of fouling reduction of composite membranes

Overall, the increase in hydrophilicity via grafting of hydrogel chains from the monomers PEGMA and SPE onto UF membrane surface created protein–resistant character (note that for these grafted polymers, the charge based interactions should not exist). The same property is also much useful to reduce the adsorption of many other foulants (sugarcane juice, humic acid, and dextran). Therefore, the PEGMA– and SPE–based composite membranes were much less prone to fouling than the unmodified membranes with respect to the adsorptive fouling as well as dynamic fouling. The protein–resistant behavior for PEGMA/SPE–modified membranes was very clear, but the mechanism itself has not exactly been understood.

Possible explanations can be drawn from existing theories [99,192,206], supported by recent additional experimental studies [97,207,208]. Binding of water on a hydrophilic surface is too strong to be displaced by a solute, while the adsorption of solutes to hydrophobic solid surfaces is mainly driven by increasing the system's entropy via replacement of water molecules at the surface by adsorbed solute ("surface dehydration") [192] (cf. Section 5.2.2). As a consequence, much weaker interactions result between protein molecules and hydrophilized surfaces in general. Recently, it had been proposed that "kosmotropes" as functional groups at surfaces form a general basis for protein–resistant surfaces. Both oligoethyleneglycol (as in PEGMA) and zwitterionic groups (as in SPE) are non-ionic "kosmotropes". However, when linked to polyacrylate chains, the three–dimensional structure of the layer (content of other groups, thickness, flexibility) can not be ignored. The "protein–resistance" of PEGylated surface is often explained by the steric stabilization force, which is a general phenomenon for neutral, hydrophilic polymers in water, and the chain mobility effect [135,206]. When a solute

molecule (e.g., a protein) approaches a PEGylated surface in water, the available volume for solute to approach the surface is reduced due to a large excluded volume of the PEG chains. Consequently, a repulsive force is generated by the loss of conformational entropy of the PEG chains. From this point of view, the differences in protein–resistance, water permeability and rejection between PEGMA– and SPE–based hydrogel layers would be supported by the results of the swelling experiments (cf. Figure 5.8). The excluded volume and, consequently, the repulsion force should be larger for grafted polyPEGMA than for grafted polySPE (at same mass-based surface coverage of PES). Consequently, the results indicate that even though contribution of membrane pore structure on fouling formation was observed, the three–dimensional structure of the photo-grafted polymer hydrogel layers is of main importance for the low–fouling properties of the composite membranes.

Chapter 6
CONCLUSIONS

Studies on fouling mechanism and control of fouling via membrane surface modification of ultrafiltration have been conducted. Characterization of commercial membranes used was firstly done. Fouling mechanism study was done by studying membrane–solute (adsorptive fouling) and membrane–solute–solute (ultrafiltration) interactions whereas surface modification was performed via photograft copolymerization.

The differences in membrane material, membrane formation conditions, resulting membrane structure and characterization used by manufacturer caused different observed characteristics among commercial UF membranes from the same or different manufacturer even at identical specifications (e.g., NMWCO).

Membrane fouling mechanism study supported by a comprehensive membrane characterization and an analysis of the impact of membrane characteristics on polysaccharide and protein fouling in UF showed that the membrane–solute interactions were strongly influenced by the membrane characteristics (cellulose–based vs. PES, pore structure) and solute properties (polysaccharide vs. protein, solute molecular mass, solute concentration). No dextran binding and only very little effects of protein binding were observed to cellulose–based membranes. It was clearly observed that both proteins (BSA and myoglobin) and polysaccharides (dextran) were bound to the PES membranes and caused significant fouling. The PES membrane surface coverage by protein was much greater than by polysaccharides, and as a consequence fouling caused by protein was also more severe. The experiments using non–porous PES films confirmed that dextran was adsorbed on the PES surface with a surface coverage that was lower than for protein myoglobin. The hydrophobic interaction was the main driving force for PES–protein

interactions in this study. Two possible mechanisms, i.e. multiple hydrogen bonding and changes in water structure at the membrane polymer surface, were proposed to explain the attractive PES−dextran interactions. Nevertheless, the pore structure of the membrane skin layer in relation to the average size of the dextran also contributed to the extent of pore narrowing or blocking due to adsorptive fouling. Overall, this work provides fundamental information about a previously overlooked or underestimated problem, and it makes a significant contribution to a better understanding of polysaccharide fouling in general.

Two different commercial base membranes and slightly different UV conditions (selected based on first batch modification) were used during membrane surface modification. Photochemically initiated grafting of functional monomer was confirmed by observable change in ATR−IR spectra after modification as well as changing in elements contents and supported by SEM images. Thus, the modified membranes should be considered as composite membrane. Overall, the modifications changed the membrane characteristics with respect to the membrane chemistry, surface hydrophilicity, surface charge, surface morphology and pore structure. The surface characteristics as well as the performance of composite membranes would be influenced by the property of the base membrane itself (e.g., membrane chemistry, pore structure), the property of grafted polymer (e.g., hydrophilicity, charge, swelling degree in the solvent used) and the grafted chain structure (e.g., mushroom vs. brush like regimes, grafting density and chain length represented by degree of grafting). All composite membranes were more hydrophilic and less negatively charged than unmodified membranes. Hydrophilization and pore narrowing (even blocking) were identified during modification. Results obtained from the first batch modification suggest that photodegradation of PES by selective UV irradiation was essential to start the heterogeneous graft copolymerization. Under controlled conditions it was possible to overcompensate the degradation of the separation layer pore structure –

due to PES chain scission and cross-linking – by the growth of the grafted copolymer. Further, the results for shorter UV irradiation times suggest that if the primary radicals after UV induced PES chain scission can react with monomer (irrespective the achieved polymer chain length), the morphology of the solid membrane polymer remains essentially unchanged. All photograft copolymer composite membranes showed lower fouling tendencies with protein as well as higher rejection than the unmodified PES membrane used for functionalization. However, reduction of membrane permeability had to be considered. The UV irradiation time was the most important parameter in order to adjust the degree of functionalization. Three regimes for the photografting with respect to the relationship between hydrophilization (shielding of the PES by grafted hydrophilic polyPEGMA) and pore constriction and blocking could be identified in terms of short, medium and long irradiation time ("periods 1, 2 and 3", respectively). In combination with the monomer concentration, the degree of grafting could be adjusted to yield the desired membrane specification. The functionalization using "period 2" conditions seemed to represent an optimum because composite membranes with a high rejection and an acceptable flux, which is also more stable due to relatively high fouling resistance, could be obtained. By changing the base membrane to a membrane having greater nominal cut−off and conditions with lower UV intensity, results of second batch modification suggests that similar with the first batch modification, the grafting efficiency was influenced by UV irradiation time, monomer concentration and monomer characteristics. Addition of cross-linker could either increase (for PEGMA) or decrease (for SPE) the DG relative to the uncross-linked modification depending on the monomer characteristics. All the composite membranes showed much higher adsorptive fouling resistance than the unmodified membrane (10 kg/mol) with a hydraulic permeability that could be higher or lower depending on DG. In addition, much higher permeate flux with slightly lower

protein rejection was also observed during UF experiments. Even though the adsorptive fouling resistance was not improved by addition of cross-linker, it could improve the permeate flux as well as protein rejection via solute sieving or size exclusion. The composite membranes prepared with an "old generation" non fouling material (PEGMA) showed a better performance than composite membrane prepared with a "new generation" non fouling material (zwitterionic, SPE). Further, the differences in characteristics and performance between PEGMA– and SPE–based composite membranes could be well explained by their difference in excluded volume of chains from the surface in water as evidenced by their difference in degree of swelling. The surface chemistry as well as surface hydrophilicity of grafted monomer on the membrane surface did not change after incubating in sodium hypochlorite solution for 8 days.

Further explorations of composite membranes for UF of sugarcane juice polysaccharides (SJP), dextran and humic acid solution suggest that the composite membranes showed significantly higher fouling resistance than both unmodified membranes (PES-SG 10 and PES-SG 100). However, contribution of membrane pore structure on membrane–solute interactions was still clearly observed. Furthermore, PEGMA–based composite membranes prepared using "period 2" for the first batch and using PEGMA (PES-g-PEGMA) and PEGMA with small concentration of cross-linker (PES-g-PEGMA/MBAA (40/0.4)) for second batch showed the best performance during evaluation using different types of test solution. Finally, their combined high fouling resistance and relatively high flux and high rejection (comparable with 10 kg/mol unmodified membrane) suggest that the resulting composite membranes are very attractive as a new generation of thin layer composite low fouling UF membranes.

References

[1] M. Cheryan, Ultrafiltration and microfiltration handbook, Technomic Publishing Company Inc., Pennsylvania, 1998.

[2] L.J. Zeman, A.L. Zydney, Microfiltration and ultrafiltration: principles and applications, Marcel Dekker Inc., New York, 1996.

[3] B. Girard, L.R. Fukumoto, Membrane processing of fruit juices and beverages: A review, Crit. Rev. Biotechnol. 20 (2000) 109.

[4] R. van Reis, A.L. Zydney, Membrane separations in biotechnology, Curr. Opin. Biotechnol. 12 (2001) 208.

[5] A.-S. Jönsson, G. Trägårdh, Ultrafiltration applications, Desalination 77 (1990) 135.

[6] J.G. Jacangelo, R.R. Trussell, M. Watson, Role of membrane technology in drinking water treatment in the United States, Desalination 113 (1997) 119.

[7] E. Matthiasson, The role of macromolecular adsorption in fouling of ultrafiltration membranes, J. Membr. Sci. 16 (1983) 23.

[8] K.J. Jim, A.G. Fane, C.J.D. Fell, D.C. Joy, Fouling mechanisms of membranes during protein ultrafiltration, J. Membr. Sci. 68 (1992) 79.

[9] J.A. Koehler, M. Ulbricht, G. Belfort, Intermolecular forces between proteins and polymer films with relevance to filtration, Langmuir 13 (1997) 4162.

[10] I.H. Huisman, P. Prádanos, A. Hernández, The effect of protein-protein and protein-membrane interactions on membrane fouling in ultrafiltration, J. Membr. Sci. 179 (2000) 79.

[11] K.L. Jones, C.R. O'Melia, Ultrafiltration of protein and humic substances: effect of solution chemistry on fouling and flux decline, J. Membr. Sci. 193 (2001) 163.

[12] B. Kwon, J. Cho, N. Park, J. Pellegrino, Organic nanocolloid fouling in UF membranes, J. Membr. Sci. 279 (2006) 209.

[13] C. Jucker, M.M. Clark, Adsorption of aquatic humic substances on hydrophobic ultrafiltration membranes, J. Membr. Sci. 97 (1994) 37.

[14] A. Maartens, P. Swart, E.P. Jacobs, Removal of natural organic matter by ultrafiltration: characterization, fouling and cleaning, Wat. Sci. Technol. 40 (1999) 113.

[15] W. Yuan, A.L. Zydney, Humic Acid fouling during ultrafiltration, Environ. Sci. Technol. 34 (2000) 5043.

[16] Y. Ye, P.L. Clech, V. Chen, A.G. Fane, Evolution of fouling during crossflow filtration of model EPS solutions, J. Membr. Sci. 264 (2005) 190.

[17] B.P. Frank, G. Belfort, Polysaccharides and sticky membrane surfaces: critical ionic effects, J. Membr. Sci. 212 (2003) 205.

[18] A. Vernhet, M. Moutounet, Fouling of organic microfiltration membranes by wine constituents: importance, relative impact of wine polysaccharides and polyphenols and incidence of membrane properties, J. Membr. Sci. 201 (2002) 103.

[19] N.K. Saha, M. Balakrishnan, M. Ulbricht, Polymeric membrane fouling in sugarcane juice ultrafiltration: role of juice polysaccharides, Desalination 189 (2005) 59.

[20] V. Singleton, Review article: advances in techniques of dextran analysis – a modern day perspective, Int. Sugar J. 104 (1239) (2002) 132.

[21] J.D. Steels, R.M. Schoth, J.P. Jensen, A simple, quick enzymatic spectrophotometric assay for dextran, Zuckerindustrie 126 (2001) 264.

[22] P.E. Barker, R.M. Alsop, G.J. Vlachogiannis, Fractionation, purification and concentration of dextran solutions by ultrafiltration, J. Membrane Sci. 20 (1984) 79.

[23] H. de Balmann, R. Nobrega, The deformation of dextran molecules. Causes and consequences in ultrafiltration, J. Membr. Sci. 40 (1989) 311.

[24] R. Nobrega, H.D. Balmann, P. Aimar, V. Sanchez, Transfer of dextran through ultrafiltration membranes: a study of rejection data analysed by gel permeation chromatography, J. Membr. Sci. 45 (1989) 17.

[25] V. Gekas, K.M. Persson, M. Wahlgren, B. Sivik, Contact angles of ultrafiltration membranes and their possible correlation to membrane performance, J. Membr. Sci. 72 (1992) 293.

[26] A.V.R. Reddy, D.J. Mohan, A. Bhattacharya, V.J. Shah, P.K. Ghosh, Surface modification of ultrafiltration membranes by preadsorption of a negatively charged polymer: I. Permeation of water soluble polymers and inorganic salt solutions and fouling resistance properties, J. Membr. Sci. 214 (2003) 211.

[27] S. Mochizuki, A.L. Zydney, Dextran transport through asymmetric ultrafiltration membranes: Comparison with hydrodynamic models, J. Membr. Sci. 68 (1992) 21.

[28] P. Mulherkar, R. van Reis, Flex test: a fluorescent dextran test for UF membrane characterization, J. Membr. Sci. 236 (2004) 171.

[29] J.H. Kweon, D.F. Lawler, Investigation of membrane fouling in ultrafiltration using organic compounds, Wat. Sci. Technol. 51 (2005) 101.

[30] J.H. Kweon, D.F. Lawler, Investigation of membrane fouling by synthetic and natural particles, Wat. Sci. Technol. 50 (2005) 279.

[31] Y.-Q. Wang, T. Wang, Y.-L. Su, F.-B. Peng, H. Wu, Z.-Y. Jiang, Remarkable reduction of irreversible fouling and improvement of the permeation properties of poly(ether sulfone) ultrafiltration membranes by blending with Pluronic F127, Langmuir 21 (2005) 11856.

[32] Y.-Q. Wang, Y.-L. Su, X.-L. Ma, Q. Sun, Z.-Y. Jiang, Pluronic polymers and polyethersulfone blend membranes with improved fouling-resistant ability and ultrafiltration performance, J. Membr. Sci. 283 (2006) 440.

[33] M. Ulbricht, Advanced functional polymer membranes, Polymer 47 (2006) 2217.

[34] H. Yamagishi, J.V. Crivello, G. Belfort, Development of a novel photochemical technique for modifying poly(arylsulfone) ultrafiltration membranes, J. Membr. Sci. 105 (1995) 237.

[35] M. Taniguchi, G. Belfort, Low protein fouling synthetic membranes by UV-assisted surface grafting modification: varying monomer type, J. Membr. Sci. 231 (2004) 147.

[36] M. Taniguchi, J. Pieracci, W.A. Samsonoff, G. Belfort, UV-assisted graft polymerization of synthetic membranes: mechanistic studies, Chem. Mater. 15 (2003) 3805.

[37] J. Pieracci, J.V. Crivello, G. Belfort, UV-assisted graft polymerization of N-vinyl-2-pyrrolidinone onto poly(ether sulfone) ultrafiltration membranes using selective UV wavelengths, Chem. Mater. 14 (2002) 256.

[38] J. Pieracci, J.V. Crivello G. Belfort, Increasing membrane permeability of UV-modified poly(ether sulfone) ultrafiltration membranes, J. Membr. Sci. 202 (2002) 1.

[39] M. Ulbricht, M. Riedel, U. Marx, Novel photochemical surface functionalization of polysulfone ultrafiltration membranes for covalent immobilization of biomolecules, J. Membr. Sci. 120 (1996) 239.

[40] M. Ulbricht, H. Matuschewski, A. Oechel, H.-G. Hicke, Photo-induced graft polymerization surface modifications for the preparation of hydrophilic and low-protein–adsorbing ultrafiltration membranes, J. Membr. Sci. 115 (1996) 31.

[41] S. Rouaix, C. Causserand, P. Aimar, Experimental study of the effect of hypochlorite on polysulfone membrane properties, J. Membr. Sci. 277 (2006) 137.

[42] W.J. Koros, Y.H. Ma, T. Shimidzu, Terminology for membranes and membrane processes, J. Membr. Sci. 120 (1996) 149.

[43] W.S. Winston Ho, K.K. Sirkar, Membrane Handbook, Van Nostrand Reinhold, New York. 1992.

[44] V. Thom, Membrane-solute interaction in microporous polymer membranes, PhD Thesis, Tekst og Tryk A/S, Vedbaek, Denmark, 1996.

[45] G. Jonsson, Transport phenomena in ultrafiltration: membrane selectivity and boundary layer phenomena, Pure Appl. Chem. 58 (1986) 1647.

[46] G. Jonsson, C.E. Boesen, Water and solute transport trough cellulose acetate reverse osmosis membranes, Desalination 17 (1975) 145.

[47] K.S. Spiegler, O. Kedem, Thermodynamics of hyperfiltration (reverse osmosis): criteria for efficient membranes, Desalination 1 (1966) 311.

[48] J.A. Howell, O. Velicangil, Theoretical considerations of membrane fouling and its treatment with immobilized enzymes for protein ultrafiltration, J. Appl. Polym. Sci. 27 (1982) 21.

[49] V.L. Vilker, C.K. Colton, K.A. Smith, The osmotic pressure of concentrated protein solutions: Effect of concentration and pH in saline solutions of bovine serum albumin, J. Colloid Interface Sci. 79 (1981) 548.

[50] G. Jonsson, Boundary layer phenomena during ultrafiltration of dextran and whey protein solutions, Desalination 51 (1984) 61.

[51] G.B. van den Berg, C.A. Smolders, Flux decline in ultrafiltration processes, Desalination 77 (1990) 101.

[52] G.A. Denisov, Theory of concentration polarization in cross-flow ultrafiltration: gel-layer model and osmotic-pressure model, J. Membr. Sci. 91 (1994) 173.

[53] W.S. Opong, A.L. Zydney, Diffusive and convective protein transport trough asymmetric membranes, AIChE J. 37 (1991) 1497.

[54] S. Bhattacharjee, A. Sharma, P.K. Bhattacharya, Surface interactions in osmotic pressure controlled flux decline during ultrafiltration, Langmuir 10 (1994) 4710.

[55] J.A. Koehler, M. Ulbricht, G. Belfort, Intermolecular forces between a protein and a hydrophilic modified polysulfone film with relevance to filtration, Langmuir 16 (2000) 10419.

[56] P. Bacchin, P. Aimar, R.W. Field, Critical and sustainable fluxes: Theory, experiments and applications, J. Membr. Sci. 281 (2006) 42.

[57] G. Belfort, J.M. Pimbley, A. Greiner, K.Y. Chung, Diagnosis of membrane fouling a rotating annular filter.1. Cell culture media, J. Membr. Sci. 77 (1993) 1.

[58] G. Bolton, D. LaCasse, R. Kuriyel, Combined models of membrane fouling: Development and application to microfiltration and ultrafiltration of biological fluids, J. Membr. Sci. 277 (2006) 75.

[59] C.-C. Ho, A.L. Zydney, A combined pore blockage and cake filtration model for protein fouling during microfiltration, J. Colloid Interface Sci. 232 (2000) 389.

[60] L. Song, Flux decline in crossflow microfiltration and ultrafiltration: mechanism and modeling of membrane fouling, J. Membr. Sci. 139 (1998) 183.

[61] A.D. Marshall, P.A. Munro, G. Trägårdh, The effect of protein fouling in microfiltration and ultrafiltration on permeate flux, protein retention and selectivity: a literature review, Desalination 91 (1993) 65.

[62] S. De, J.M. Dias, P.K. Bhattacharya, Short and long term flux decline analysis in Ultrafiltration, Chem. Eng. Commun. 159 (1997) 67.

[63] Hermia, Constant pressure blocking filtration laws−application to power law non-Newtonian fluids, Trans. Inst. Chem. Eng. 60 (1982) 183.

[64] W.R. Bowen, J.I. Calvo, A. Hernández, Steps of membrane blocking in flux decline during protein microfiltration, J. Membr. Sci. 101 (1995) 153.

[65] M. Taniguchi, J.E. Kilduff, G. Belfort, Modes of natural organic matter fouling during ultrafiltration, Environ. Sci. Technol. 37 (2003) 1676.

[66] K. Khatib, K. Rose, O. Barres, W. Stone, J.Y. Bottero, C. Anselme, Physico-chemical study of fouling mechanisms of ultrafiltration membrane on Biwa lake (Japan), J. Membr. Sci. 130 (1997) 53.

[67] T. Murayama, S. Katoh, M. Nakajima, H. Nabetani, T.P. Abbott, A. Shono, K. Satoh, FT−IR analysis of BSA fouled on ultrafiltration and microfiltration membranes, J. Membr. Sci. 192 (2001) 201.

[68] S. Belfer, R. Fainchtain, Y. Purinson, O. Kedem, Surface characterization by FTIR-ATR spectroscopy of polyethersulfone membranes − unmodified, modified and protein fouled, J. Membr. Sci. 172 (2000) 113.

[69] L. Gourley, M. Britten, S.F. Gauthier, Y. Pouliot, Chracterization of adsorptive fouling on ultrafiltration membranes by peptides mixtures using contact angle measurements, J. Membr. Sci. 97 (1994) 283.

[70] L. Palacio, J.I. Calvo, P. Prádanos, A. Hernández, P. Väisänen, M. Nyström, Contact angles and external protein adsorption onto UF membranes, J. Membr. Sci. 152 (1999) 189.

[71] W.R. Bowen, N. Hilal, R.W. Lovitt, C.J. Wright, Characterization of membrane surfaces: direct measurement of biological adhesion using an atomic force microscope, J. Membr. Sci. 154 (1999) 205.

[72] T.J. Su, J.R. Lu, Z.F. Cui, R.K. Thomas, Fouling of ceramic membranes by albumins under dynamic filtration conditions, J. Membr. Sci. 173 (2000) 167.

[73] R. Chan, V. Chen, Characterization of protein fouling on membranes: opportunities and challenges, J. Membr. Sci. 242 (2004) 169.

[74] G. Belfort, R.H. Davis, A.L. Zydney, The behavior of suspensions and macromolecular solutions in crossflow microfiltration, J. Membr. Sci. 96 (1994) 1.

[75] C.-C. Ho, A.L. Zydney, Effect of membrane morphology on the initial rate of protein fouling during microfiltration, J. Membr. Sci. 155 (1999) 261.

[76] P.R. Babu, V.G. Gaikar, Membrane characteristics as determinant in fouling of UF membranes, Sep. Purif. Technol. 24 (2001) 23.

[77] K.L. Jones, C.R. O'Melia, Protein and humic acid adsorption onto hydrophilic membrane surfaces: effect of pH and ionic strength, J. Membr. Sci. 165 (2000) 31.

[78] D.B. Burns, A.L. Zydney, Effect of solution pH on protein transport trough ultrafiltration membranes, Biotechnol. Bioeng. 64 (1999) 27.

[79] K.-J. Kim, V. Chen, A.G. Fane, Ultrafiltration of colloidal silver particles: flux, rejection, and fouling, J. Colloid Interface Sci. 155 (1993) 347.

[80] M.R. Mackley, N.E. Sherman, Cross-flow cake filtration mechanisms and kinetics, Chem. Eng. Sci. 47 (1992) 3067.

[81] D.A. Drew, J.A. Schonberg, G. Belfort, Lateral inertial migration of a small sphere in fast laminar flow through a membrane duct, Chem. Eng. Sci. 46 (1991) 3219.

[82] H.B. Winzeler, G. Belfort, Enhanced performance for pressure-driven membrane processes: the argument for fluid instabilities, J. Membr. Sci. 80 (1993) 35.

[83] K. Stamatakis, C. Tian, A simple model of cross-flow filtration based on particle adhesion, AIChE J. 39 (1993) 1292.

[84] J. de Bruijn, A. Vanegas, R. Borquez, Influence of crossflow ultrafiltration on membrane fouling and apple juice quality, Desalination 148 (2002) 131.

[85] S.T.D. de Baros, C.M.G. Andrade, E.S. Mendes, L. Peres, Study of fouling mechanism in pineapple juice clarification by ultrafiltration, J. Membr. Sci. 215 (2003) 213.

[86] S.N. Jagannadh, H.S. Muralidhara, Electrokinetics methods to control membrane fouling, Ind. Eng. Chem. Res. 35 (1996) 1133.

[87] C.W. Robinson, M.H. Siegel, A. Condemine, C. Fee, T.Z. Fahidy, B.R. Glick, Pulsed-electric-field crossflow ultrafiltration of bovine serum albumin, J. Membr. Sci. 80 (1993) 209.

[88] W.R. Bowen in “Chromatographic and membrane processes in biotechnology”, C.A. Costa and J.S. Cebral (Eds.), Kluwer Academic Publisher, The Netherlands, 1991, 207.

[89] M.J. Steuck, Porous membrane having hydrophilic surface and process, US Patent 4618533, 1984.

[90] M. Nyström, P. Järvinem, Modification of polysulfone ultrafiltration membranes with UV irradiation and hydrophilicity increasing agents, J. Membr. Sci. 60 (1991) 275.

[91] P.W. Kramer, Y.S. Yeh, H. Yasuda, Low temperature plasma for preparation of separation membranes, J. Membr. Sci. 46 (1989) 1.

[92] K.J. Kim, A.G. Fane, C.J.D. Fell, The performance of ultrafiltration membranes pretreated by polymers, Desalination 70 (1988) 229.

[93] N. Hilal, O.O. Ogunbiyi, N.J. Miles, R. Nigmatullin, Methods employed for control of fouling in MF and UF membranes: A comprehensive review, Sep. Sci. Technol. 40 (2005) 1957.

[94] A. Mehta, A.L. Zydney, Effect of membrane charge on flow and protein transport during ultrafiltration, Biotechnol. Prog. 22 (2006) 484.

[95] K.-J. Kim, A.G. Fane, Performance evaluation of surface hydrophilized novel ultrafiltration membranes using aqueous proteins, J. Membr. Sci. 99 (1995) 149.

[96] M.K. Ko, J.J. Pellegrino, R. Nassimbene, P. Marko, Characterization of the adsorption-fouling layer using globular proteins on ultrafiltration membranes, J. Membr. Sci. 76 (1993) 101.

[97] E. Ostuni, R.G. Chapman, R.E. Holmin, S. Takayama, G.M. Whitesides, A survey of the structure-property relationships of surfaces that resist the adsorption of protein, Langmuir 17 (2001) 5605.

[98] R.G. Chapman, E. Ostuni, M.N. Liang, G. Meluleni, E. Kim, L. Yan, G. Pier, H.S. Warren, G.M. Whitesides, Polymeric thin films that resist the adsorption of protein and the adhesion of bacteria, Langmuir 17 (2001) 1225.

[99] R.S. Kane, P. Deschatelets, G.M. Whitesides, Kosmotropes form the basis of protein-resistant surfaces, Langmuir 19 (2003) 2388.

[100] K. Kato, E. Uchida, E.T. Kang, Y. Uyama, Y. Ikada, Polymer surface with graft chains, Prog. Polym. Sci. 28 (2003) 209.

[101] A. Dimov, M.A. Islam, Hydrophilization of polyethylene membranes, J. Membr. Sci. 50 (1990) 97.

[102] V. Chen, A.G. Fane, C.J.D. Fell, The use of anionic surfactants for reducing fouling of ultrafiltration membranes: their effects and optimization, J. Membr. Sci. 67 (1992) 249.

[103] L.E.S. Brink, S.J.G. Elbers, T. Robbertsen, P. Both, The anti-fouling action of polymers preadsorbed on ultrafiltration and microfiltration membranes, J. Membr. Sci. 76 (1993) 281.

[104] K.B. Hvid, P. Nielsen, F. Stengaard, Preparation and characterization of a new ultrafiltration membrane, J. Membr. Sci. 53 (1990) 189.

[105] R.H. Li, T.A. Barbari, Performance of poly(vinyl alcohol) thin-gel composite ultrafiltration membrane, J. Membr. Sci. 105 (1995) 71.

[106] S.P. Nunes, M.L. Sforca, K.-V. Peinemann, Dense hydrophilic composite membranes for ultrafiltration, J. Membr. Sci. 106 (1995) 49.

[107] G. Decher, Fuzzy nano assemblies: Toward layered polymeric multicomposites, Science 277 (1997) 1232.

[108] M.L. Bruening, D.M. Sullivan, Enhancing the ion-transport selectivity of multilayer polyelectrolyte membranes, Chem. Eur. J. 8 (2002) 3833.

[109] X. Zeng, E. Ruckenstein, Membrane chromatography: preparation and applications to protein separation, Biotechnol. Prog. 15 (1999) 1003.

[110] H.-G. Hicke, P. Bohme, M. Becker, H. Schulze, M. Ulbricht, Immobilization of enzymes onto modified polyacrylonitrile membranes: Application of the acyl azide method, J. Appl. Polym. Sci. 60 (1996) 1147.

[111] C. Geismann, M. Ulbricht, Photoreactive functionalization of poly(ethylene terephthalate) track-etched pore surfaces with ‘‘smart’’ polymer systems, Macromol. Chem. Phys. 206 (2005) 268.

[112] L. Breitbach, E. Hinke, E. Staude, Heterogenous functionalizing of polysulfone membranes, Angew. Makromol. Chem. 184 (1991) 183.

[113] V. Thom, K. Jankova, M. Ulbricht, J. Kops, G. Jonsson, Synthesis of photoreactive α-4-azidobenzoyl-ω-methoxy-poly(ethylene glycol)s and their end-on photo-grafting onto polysulfone ultrafiltration membranes, Macromol. Chem. Phys. 199 (1998) 2723.

[114] Z.-M. Liu, Z.-K. Xu, L.-S. Wan, J. Wu, M. Ulbricht, Surface modification of polypropylene microfiltration membranes by the immobilization of poly(*N*-vinyl-2-pyrrolidone): a facile plasma approach, J. Membr. Sci. 249 (2005) 21.

[115] S. M. C. Ritchie, L. G. Bachas, T. Olin, S. K. Sikdar, D. Bhattacharyya, Surface modification of silica- and cellulose-based microfiltration membranes with functional polyamino acids for heavy metal sorption, Langmuir 15 (1999) 6346.

[116] C.-M. Chan, Polymer surface modification and characterization, Carl Hanser Verlag, München, 1994.

[117] H. Yamagishi, J.V. Crivello, G. Belfort, Evaluation of photochemically modified poly (arylsulfone) ultrafiltration membranes, J. Membr. Sci. 105 (1995) 249.

[118] M. Taniguchi, J.E. Kilduff, G. Belfort, Low fouling synthetic membranes by UV-assisted graft polymerization: monomer selection to mitigate fouling by natural organic matter, J. Membr. Sci. 222 (2003) 59.

[119] M. Ulbricht, A. Oechel, C. Lehmann, G. Tomaschewski, H.-G. Hicke, Gas-phase photoinduced graft polymerization of acrylic acid onto polyacrylonitrile ultrafiltration membranes, J. Appl. Polym. Sci. 55 (1995) 1707.

[120] M. Ulbricht, Photograft–polymer–modified microporous membranes with environment–sensitive permeabilities, React. Funct. Polym. 31 (1996) 165.

[121] M. Ulbricht, M. Riedel, Ultrafiltration membrane surfaces with grafted polymer 'tentacles': preparation, characterization and application for covalent protein binding, Biomaterials 19 (1998) 1229.

[122] M. Ulbricht, H. Yang, Porous polypropylene membranes with different carboxyl polymer brush layers for reversible protein binding via surface-initiated graft copolymerization, Chem. Mater. 17 (2005) 2622.

[123] T.R. Dargaville, G.A. George, D.J.T. Hill, A.K. Whittaker, High energy radiation grafting of fluoropolymers, Prog. Polym. Sci. 28 (2003) 1355.

[124] M.M. Nasef, E.-S.A. Hegazy, Preparation and applications of ion exchange membranes by radiation-induced graft copolymerization of polar monomers onto non-polar films, Prog. Polym. Sci. 29 (2004) 499.

[125] S.L Lim, A.G. Fane, C.J. D. Fell, Radiation-induced grafting of regenerated cellulose hollow-fiber membranes, J. Appl. Polym. Sci. 41 (1990) 1609.

[126] S. Mok, D.J. Worsfold, A. Fouda, T. Matsuura, Surface modification of polyethersulfone hollow-fiber membranes by γ-ray irradiation, J. Appl. Polym. Sci. 51 (1994) 193.

[127] M. Ulbricht, G. Belfort, Surface modification of ultrafiltration membranes by low temperature plasma. I. Treatment of polyacrylonitrile, J. Appl. Polym. Sci. 56 (1995) 325.

[128] M. Ulbricht, G. Belfort, Surface modification of ultrafiltration membranes by low temperature plasma II. Graft polymerization onto polyacrylonitrile and polysulfone, J. Membr. Sci. 111 (1996) 193.

[129] H. Chen, G. Belfort, Surface modification of poly(ether sulfone) ultrafiltration membranes by low-temperature plasma-induced graft polymerization, J. Appl. Polym. Sci. 72 (1999) 1699.

[130] B. Kaeselev, J. Pieracci, G. Belfort, Photoinduced grafting of ultrafiltration membranes: comparison of poly(ether sulfone) and poly(sulfone), J. Membr. Sci. 194 (2001) 245.

[131] J. Pieracci, J.V. Crivello G. Belfort, Photochemical modification of 10 kDa polyethersulfone membranes for reduction of biofouling, J. Membr. Sci. 156 (1999) 223.

[132] J.E. Kilduff, S. Mattaraj, M. Zhou, G. Belfort, Kinetics of membrane flux decline: the role of natural colloids and mitigation via membrane surface modification, J. Nanopart. Res. 7 (2005) 525.

[133] M. Ulbricht, K. Richau, H. Kamusewitz, Chemically and morphologically defined ultrafiltration membrane surfaces prepared by heterogeneous photo-initiated graft polymerization, Colloids and Surf. A 138 (1998) 353.

[134] A. Akthakul, R.F. Salinaro, A.M. Mayes, Antifouling polymer membranes with subnanometer size selectivity, Macromolecules 37 (2004) 7663.

[135] S. Sharma, R.W. Johnson, T.A. Desai, Evaluation of the stability of nonfouling ultrathin poly(ethylene glycol) films for silicon-based microdevices, Langmuir 20 (2004) 348.

[136] P. Harder, G. Grunze, R. Dahint, G.M. Whitesides, P.E. Laibinis, Molecular conformation in oligo(ethylene glycol)-terminated self-assembled monolayers on gold and silver surfaces determines their ability to resist protein adsorption, J. Phys. Chem. B 102 (1998) 426.

[137] R.E. Holmlin, X. Chen, R.G. Chapman, S. Takayama, G.M. Whitesides, Zwitterionic SAMs that resist nonspecific adsorption of protein from aqueous buffer, Langmuir 17 (2001) 2841.

[138] S. Chen, L. Li, S. Jiang, Strong resistance of oligo(phosphorylchorylcholine) self-assembled monolayers to protein adsorption, Langmuir 22 (2006) 2418.

[139] S. Chen, J. Zheng, L. Li, S. Jiang, Strong resistance of phosphorylcholine self-assembled monolayers to protein adsorption: insights into nonfouling properties of zwitterionic materials, J. Am. Chem. Soc. 127 (2005) 14473.

[140] H. Kitano, A. Kawasaki, H. Kawasaki, S. Morokoshi, Resistance of zwitterionic telomers accumulated on metal surfaces against nonspecific adsorption of proteins, J. Colloid Interface Sci. 282 (2005) 340.

[141] Q. Sun, Y. Su, X. Ma, Y. Wang, Z. Jiang, Improved antifouling property of zwitterionic ultrafiltration membrane composed of acrylonitrile and sulfobetaine copolymer, J. Membr. Sci. 285 (2006) 299.

[142] T. Wang, Y.-Q. Wang, Y.-L. Su, Z.-J. Jiang, Antifouling ultrafiltration membrane composed of polyethersulfone and sulfobetaine copolymer, J. Membr. Sci. 280 (2006) 343.

[143] K. Ishihara, H. Miyazaki, T. Kurosaki, N. Nakabayashi, Improvement of blood compatibility on cellulose dialysis membrane. III. Synthesis and performance of water-soluble cellulose grafted with phospholipid polymer as coating material on cellulose dialysis membrane, J. Biomed. Mater. Res. 29 (1995) 181.

[144] Z.-K. Xu, Q.-W. Dai, J. Wu, X.-J. Huang, Q. Yang, Covalent attachment of phospholipid analogous polymers to modify a polymeric membrane surface: A novel approach, Langmuir 20 (2004) 1481.

[145] H. Yang, D. Lazos, M. Ulbricht, Thin, highly crosslinked polymer layer synthesized via photoinitiated graft copolymerization on a self assembled-monolayer-coated gold surface, J. Appl. Polym. Sci. 97 (2005) 158.

[146] Pierce: BCA protein assay reagent kit, No. 23225, 23227.

[147] L. Lebrun, G.-A. Junter, Diffusion of dextran through microporous membrane filters, J. Membr. Sci. 88 (1994) 253.

[148] W. Zhang, M. Wahlgren, B. Sivik, Membrane characterization by the contact angle technique II. Characterization of UF-membranes and comparison between the captive bubble and sessile drop as methods to obtain water contact angles, Desalination 72 (1989) 263.

[149] D. Möckel, E. Staude, M. Dal-Chin, K. Darcovich, M. Guiver, Tangential flow streaming potential measurements: Hydrodynamic cell characterization and zeta potentials of carboxylated polysulfone membranes, J. Membr. Sci. 145 (1998) 211.

[150] K.J. Kim, A.G. Fane, M. Nystrom, A. Pihlajamaki, W.R. Bowen, H. Mukhtar, Evaluation of electroosmosis and streaming potential for measurement of electric charges of polymeric membranes, J. Membr. Sci. 116 (1996) 149.

[151] C. Fänger, H. Wack, M. Ulbricht, Macroporous poly(N-isopropylacrylamide) hydrogels with adjustable size “cut-off“ for the efficient and reversible immobilization of biomolecules, Macromol. Biosci. 6 (2006) 393.

[152] A.K. Fritzsche, A.R. Arevalo, M.D. Moore, C.J. Weber, V.B. Elings, K. Kjoller, C.M. Wu, Image enhancement of polyethersulfone ultrafiltration membrane surface structure for atomic force microscopy, J. Appl. Polym. Sci. 46 (1992) 167.

[153] W.R. Bowen, N. Hilal, R.W. Lovitt, C.J. Wright, Direct measurement of interactions between adsorbed protein layers using an atomic force microscope, J. Colloid Interface Sci. 197 (1998) 348.

[154] A.W. Adamson, Physical Chemistry of Surfaces, 4th ed. John Wiley & Sons, New York, 1982.

[155] C.M. Tam, A.Y. Tremblay, Membrane pore characterization – comparison between single and multicomponent solute probe techniques, J. Membr. Sci. 57 (1991) 271.

[156] M. Nyström, M. Lindström, E. Matthiasson, Streaming potential as a tool in the characterization of ultrafiltration membranes, Colloids and Surf. 36 (1989) 297.

[157] C. Lettmann, D. Möckel, E. Staude, Permeation and tangential flow streaming potential measurements for electrokinetic characterization of track-etched microfiltration membranes, J. Membr. Sci. 159 (1999) 243.

[158] C. Causserand, M. Nyström, P. Aimar, Study of streaming potentials of clean and fouled ultrafiltration membranes, J. Membr. Sci. 88 (1994) 211.

[159] Y.-H.M. Chan, R. Schweiss, C. Werner, M. Grunze, Electrokinetic characterization of oligo - and poly(ethylene glycol)-terminated self-assembled monolayers on gold and glass surfaces, Langmuir 19 (2003) 7380.

[160] D. Lazos, S. Franzka, M. Ulbricht, Size-selective protein adsorption to polystyrene surfaces by self-assembled grafted poly(ethyleneglycols) with varied chain lengths, Langmuir 21 (2005) 8774.

[161] B. Swerdya-Krawiec, H. Devaraj, G. Jacob, J.J. Hickman, A new interpretation of serum albumin surface passivation, Langmuir 20 (2004) 2054.

[162] B. Kaeselev, P. Kingshott, G. Jonsson, Influenced of the surface structure on the filtration performace of UV-modified PES membranes, Desalination 146 (2002) 265.

[163] J. Pieracci, D.W. Wood, J.V. Crivello, G. Belfort, UV-Assisted graft polymerization of *N*-vinyl-2-pyrrolidinone onto poly(ether sulfone) ultrafiltration membranes: comparison of dip versus immersion modification techniques, Chem. Mater. 12 (2000) 2123.

[164] T. Kai, H. Goto, Y. Shimizu, T. Yamaguchi, S. Nakao, S. Kimura, Development of crosslinked plasma-graft filling polymer membranes for the reverse osmosis of organic liquid mixtures, J. Membr. Sci. 265 (2005) 101.

[165] B. Gupta, F. Büchi, G. Scherer, A. Chapiró, Crosslinked ion exchange membranes by radiation grafting of styrene/divinylbenzene into FEP films, J. Membr. Sci. 118 (1996) 231.

[166] P.A. Dworjanyn, J.L. Garnett, Synergistic effects of urea with polyfunctional acrylates for enhancing the photografting of styrene to polypropylene**,** J. Polym. Sci. C, Polym. Lett. 26 (1988) 135.

[167] A.M. Mika, R.F. Childs, J.M. Dickson, B.E. McCarry, D.R. Gagnon, Porous, polyelectrolyte-filled membranes: effect of cross-linking on flux and separation, J. Membr. Sci. 135 (1997) 81.

[168] W.K. Nielsen, S. Kristensen, R.F. Madsen, Prospects and possibilities in application of membrane filtration system within the beet and cane sugar industry, Sugar Tech. Rev. 9 (1982) 59.

[169] S. Kishihara, H. Tamaki, S. Fujii, M. Komoto, Clarification of technical sugar solutions through dynamic layer formed on a porous ceramic tube, J. Membr. Sci. 41 (1989) 103.

[170] V. Gekas, G. Trägårdh, Membrane technology in the sugar industry, Desalination 69 (1989) 9.

[171] M. Balakrishnan, M. Dua, J.J. Bhagat, Effect of operating parameters on sugarcane juice ultrafiltration: results of a field experience, Sep. Purif. Technol. 19 (2000) 209.

[172] P.K. Bhattacharya, S. Agarwal, S. De, U.V.S.R. Gopal, Ultrafiltration of sugarcane juice for recovery of sugar: analysis of flux and retention, Sep. Purif. Technol. 21 (2001) 247.

[173] M. Balakrishnan, M. Dua, P.N. Khairnar, Significance of membrane type and feed stream in the ultrafiltration of sugarcane juice, Sep. Sci. Technol. 36 (2001) 619.

[174] V. Lahoussine-Turcaud, M.R. Wiesner, J.-Y. Bottero, Fouling in tangential-flow filtration: The effect of colloid size and coagulation pretreatment, J. Membr. Sci. 52 (1990) 173.

[175] S. Hong, M. Elimelech, Chemical and physical aspects of natural organic matter (NOM) fouling of nanofiltration membranes, J. Membr. Sci. 132 (1997) 159.

[176] T. Thorsen, Membrane filtration of humic substances − state of the art, Wat. Sci. Technol. 40 (1999) 105.

[177] M. Mänttäri, L. Puro, J. Nuortila-Jokinen, M. Nyström, Fouling effects of polysaccharides and humic acid in nanofiltration, J. Membr. Sci. 165 (2000) 1.

[178] R.L. Malcolm, P. MacCarthy, Limitation in the use of commercial humic acids in water and soil research, Environ. Sci. Technol. 20 (1986) 904.

[179] J. Mao, W. Hu, G. Ding, K. Schmidt-Rohr, G. Davies, E.A. Ghabbour, B. Xing, Suitability of different ^{13}C solid-state NMR techniques in the characterization of humic acids, Inter. J. Environ. Anal. Chem. 82 (2002) 183.

[180] J. Cho, G. Amy, J. Pellegrino, Membrane filtration of natural organic matter: factors and mechanisms affecting rejection and flux decline with charged ultrafiltration (UF) membrane, J. Membr. Sci. 164 (2000) 89.

[181] A.I. Schäfer, A.G. Fane, T.D. Waite, Nanofiltration of natural organic matter: Removal, fouling and the influence of multivalent ions, Desalination 118 (1998) 109.

[182] J. Cho, G. Amy, J. Pellegrino, Membrane filtration of natural oraganic matter: initial comparison of rejection and flux decline characteristics with ultrafiltration and nanofiltration membranes, Wat. Res. 33 (1999) 2517.

[183] M. Taniguchi, G. Belfort, Correcting for surface roughness: advancing and receding contact angles, Langmuir 18 (2002) 6465.

[184] W. Zhang, B. Hallström, Membrane characterization using the contact angle technique I. Methodology of the captive bubble technique, Desalination 79 (1990) 1.

[185] R. Zimmermann, S. Dukhin, C. Werner, Electrokinetic measurements reveal interfacial charge at polymer films caused by simple electrolyte ions, J. Phys. Chem. B 105 (2001) 8544.

[186] V.H. Thom, G. Altankov, Th. Groth, K. Jankova, G. Jonsson, M. Ulbricht, Optimizing cell–surface interactions by photografting of poly(ethylene glycol), Langmuir 16 (2000) 2756.

[187] H.J. Kreuzer, R.L.C. Wang, M. Grunze, Hydroxide ion adsorption on self-assembled monolayers, J. Am. Chem. Soc. 125 (2003) 8384.

[188] C. Causserand, S. Rouaix, A. Akbari, P. Aimar, Improvement of a method for characterization of ultrafiltration membranes by measurements of tracers retention, J. Membr. Sci. 238 (2004) 177.

[189] A. Amanda, S.K. Mallapragada, Comparison of protein fouling on heat-treated poly(vinyl alcohol), poly(ether sulfone) and regenerated cellulose membranes using diffuse reflectance infrared fourier transform spectroscopy, Biotechnol. Prog. 17 (2001) 917.

[190] M.P. Bohrer, G.D. Patterson, P.J. Carroll, Hindered diffusion of dextran and ficoll in microporous membranes, Macromolecules 17 (1984) 1173.

[191] E.A. Vogler, Structure and reactivity of water at biomaterial surfaces, Adv. Colloid Interface Sci. 74 (1998) 69.

[192] E.A. Vogler, Water and the acute biological response to surfaces, J. Biomater. Sci. Polym. Ed. 10 (1999) 1015.

[193] S. Kuroda, I. Mita, K. Obata, S. Tanaka, Degradation of aromatic polymers: part IV. Effect of temperature and light intensity on the photodegradation of polyethersulfone, Polym. Degr. Stab. 27 (1990) 257.

[194] W. Yang, B. Rånby, Bulk surface photografting process and its applications. II. Principal factors affecting surface photografting, J. Appl. Polym. Sci. 62 (1996) 545.

[195] N. Singh, X. Cui, T. Boland, S.M. Husson, The role of independently variable grafting density and layer thickness of polymer nanolayers on peptide adsorption and cell adhesion, Biomaterials 28 (2007) 763.

[196] W.H. Yu, T. Kang, K.G. Neoh, S. Zhu, Controlled grafting of well-defined polymers on hydrogen-terminated silicon substrates by surface-initiated atom transfer radical polymerization, J. Phys. Chem. B 107 (2003) 10198.

[197] E. Uchida, Y. Uyama, Y. Ikada, Grafting of water-soluble chains onto a polymer surface, Langmuir 10 (1994) 481.

[198] S. Schwarz, H.-J. Jacobasch, D. Wyszynski, E. Staude, E. Electrokinetic measurements on porous polysulfone membranes, Angew. Makromol. Chem. 221 (1994) 165.

[199] C. Werner, H.J. Jacobasch, G. Reichelt, Surface characterization of hemodialysis membranes based on streaming potential measurements, J. Biomater. Sci. Polym. Ed. 7 (1995) 61.

[200] M.D. Baptista, I. Cuccovia, H. Chaimovich, M.J. Politi, W.F. Reed, Electrostatic properties of zwitterionic micelles, J. Phys. Chem. 96 (1992) 6442.

[201] K. Iso, T. Okada, Evaluation of electrostatic potential induced by anion-dominated partition into zwitterionic micelles and origin of selectivity in anion uptake, Langmuir 16 (2000) 9199.

[202] B. Zdyrko, V. Klep, I. Luzinov, Synthesis and surface morphology of high-density poly(ethylene glycol) grafted layers, Langmuir 19 (2003) 10179.

[203] S.J. Sofia, V. Premnath, E.W. Merrill, Poly(ethylene oxide) grafted to silicon surfaces: grafting density and protein adsorption, Macromolecules 31 (1998) 5059.

[204] D. Ruckert, G. Geuskens, Surface modification of polymers—IV. Grafting of acrylamide via an unexpected mechanism using a water soluble photo-initiator, Eur. Polym. J. 32 (1996) 201.

[205] A. Mehta, A.L. Zydney, Permeability and selectivity analysis for ultrafiltration membranes, J. Membr. Sci. 249 (2005) 245.

[206] J.H. Lee, H.B. Lee, J.D. Andrade, Blood compatibility of polyethylene oxide surfaces Prog. Polym. Sci. 20 (1995) 1043.

[207] A. Sethuraman, M. Han, R.S. Kane, G. Belfort, Effect of surface wettability on the adhesion of proteins, Langmuir 20 (2004) 7779.

[208] L.D. Unsworth, H. Sheardown, J.L. Brash, Effect of surface wettability on the adhesion of proteins, Langmuir 21 (2005) 1036.

Appendix-1

List of publications during doctoral study

Papers in Journals (peer-reviewed)

1. H. Susanto, M. Ulbricht, Influence of ultrafiltration membrane characteristics on adsorptive fouling with dextrans, *J. Membr. Sci.* **2005**, 266, 132.
2. H. Susanto, M. Ulbricht, Performance of surface modified polyethersulfone membranes for ultrafiltration of aquatic humic substances, *Desalination* **2006**, 199, 384.
3. H. Susanto, M. Ulbricht, Insights into polysaccharide fouling of ultrafiltration membranes, *Desalination* **2006**, 200, 181.
4. H. Susanto, M. Balakrishnan, M. Ulbricht, Via surface functionalization by photograft copolymerization to low−fouling polyethersulfone−based ultrafiltration membranes, *J. Membr. Sci.* **2007**, 288, 157.
5. H. Susanto, S. Franzka, M. Ulbricht, Dextran fouling of polyethersulfone ultrafiltration membranes–Causes, extent and consequences*, J. Membr. Sci.* **2007**, 296, 147.
6. H. Susanto, M. Ulbricht, Photo-grafted thin polymer hydrogel layers on PES ultrafiltration membranes: Characterization, stability and influence on separation performance, *Langmuir* **2007**, 23, 7818.
7. H. Susanto, M. Ulbricht, Highly fouling resistant ultrafiltration membrane for water and wastewater treatments, *Wat. Sci. Technol*. **2007**, submitted.
8. H. Susanto, M. Ulbricht, Novel type of hydrogel composite membrane for low fouling ultrafiltration of natural organic matter, *Environ. Sci. Technol.* **2007,** submitted.

Oral Papers in International Conferences

2007 **2nd IWA National Young Water Professionals Conference, Berlin, Germany.**

"Highly fouling resistant ultrafiltration membranes for water and wastewater treatments"

2006 Euromembrane 2006, Giardini Naxos, Italy.

"Performance of surface modified polyethersulfone membranes for ultrafiltration of aquatic humic substances"

North American Membrane Society (NAMS) 2006, Chicago, United States.

"Impact of membrane characteristics on polysaccharide fouling in ultrafiltration"

2005 **International Conference on Membrane and Membrane Processes 2005, Seoul, Korea.**

"Mechanisms for Polysaccharide Fouling of Ultrafiltration Membranes"

Network Young Membrains Meeting, 2005, Twente, the Netherlands

"Control of non protein fouling for ultrafiltration via resposive polymer surface functionalization"

Poster Papers in International Conferences

2006 Euromembrane 2006, Giardini Naxos, Italy.

"Insights into polysaccharide fouling of ultrafiltration membranes"

2005 **10th Aachen Membrane Colloquium, 2005, Aachen, Germany.**

"Fouling study and membrane surface modification in polysaccharide ultrafiltration"

2004 International conference on alternative and conventional anti-fouling strategies, IBBS, 2005, Mülheim, Germany.

"Mechanism of polysaccharides fouling and control strategy in ultrafiltration membrane"

Appendix-2

Curriculum Vitae

Name : Heru Susanto

Place/Date of Birth : Semarang, Indonesia / 29 May 1975

Education

1993-1997 (B. Eng) : Dept. of Chem. Eng., Universitas Diponegoro, Indonesia

1999-2001 (M. Eng) : Dept. of Chem. Eng., Institut Teknologi Bandung, Indonesia, with field of the research was membrane technology

April, 2004–July, 2007 : Dr. rer. net — Institute of Technical Chemistry (Lehrstuhl für Technische Chemie II), Department of Chemistry, Universität Duisburg-Essen, Germany, with field of the research is membrane technology

Workshop

1. 2nd ITB-UNESCO International Workshop on Membranes, Membrane Technology for Industry and Environmental Protection, February 8-9, 2000
2. Pre-congress Workshops, Membranes for liquid separations, including fouling issues (MF. UF, NF, RO), ICOM, Seoul, Korea, 2005
3. Workshops, Membrane for food processing, North American Membrane Society (NAMS), Chicago, United States, 2006

Research Experience

- Development of liquid-liquid membrane contactor for pure water production (Master thesis 2000-2001)
- Application of reverse osmosis for soluble starch recovery (2002)
- Application of ultrafiltration for sugarcane juice clarification (2002)
- Construction of combination of reverse osmosis and ion exchange processes for pure water production (2003)
- Membrane contactor for flue gas cleaning (2003-2004)